



Australian Rainfall & Runoff

---

A GUIDE TO  
FLOOD ESTIMATION

---

BOOK 3 - PEAK FLOW ESTIMATION

Version 4.2



Australian Government



ENGINEERS  
AUSTRALIA



The Australian Rainfall and Runoff: A guide to flood estimation (ARR) is licensed under the Creative Commons Attribution 4.0 International Licence, unless otherwise indicated or marked.

**Please give attribution to:** © Commonwealth of Australia (Geoscience Australia) 2019.

### **Third-Party Material**

The Commonwealth of Australia and the ARR's contributing authors (through Engineers Australia) have taken steps to both identify third-party material and secure permission for its reproduction and reuse. However, please note that where these materials are not licensed under a Creative Commons licence or similar terms of use, you should obtain permission from the relevant third-party to reuse their material beyond the ways you are legally permitted to use them under the fair dealing provisions of the Copyright Act 1968.

### **Acknowledgement of Country**

We acknowledge the Traditional Owners of Country throughout Australia and recognise their continuing connection to land, waters and culture. We pay our respects to their Elders past and present.

If you have any questions about the copyright of the ARR, please contact:

[hazards@ga.gov.au](mailto:hazards@ga.gov.au) or [admin@arr-software.org](mailto:admin@arr-software.org)

c/o 11 National Circuit,  
Barton, ACT

ISBN 978-1-925848-36-6

How to reference:

Ball J, Babister M, Nathan R, Weeks W, Weinmann E, Retallick M, Testoni I, (Editors)  
Australian Rainfall and Runoff: A Guide to Flood Estimation, © Commonwealth of Australia  
(Geoscience Australia), Version 4.2, 2019.

How to reference Book 9: Runoff in Urban Areas:

Coombes, P., and Roso, S. (Editors), 2019 Runoff in Urban Areas, Book 9 in Australian  
Rainfall and Runoff - A Guide to Flood Estimation, Commonwealth of Australia, ©  
Commonwealth of Australia (Geoscience Australia), Version 4.2, 2019.

## **PREFACE**

Since its first publication in 1958, Australian Rainfall and Runoff (ARR) has remained one of the most influential and widely used guidelines published by Engineers Australia (EA). The 3<sup>rd</sup> edition, published in 1987, retained the same level of national and international acclaim as its predecessors.

With nationwide applicability, balancing the varied climates of Australia, the information and the approaches presented in Australian Rainfall and Runoff are essential for policy decisions and projects involving:

- infrastructure such as roads, rail, airports, bridges, dams, stormwater and sewer systems;
- town planning;
- mining;
- developing flood management plans for urban and rural communities;
- flood warnings and flood emergency management;
- operation of regulated river systems; and
- prediction of extreme flood levels.

However, many of the practices recommended in the 1987 edition of ARR have become outdated, and no longer represent industry best practice. This fact, coupled with the greater understanding of climate and flood hydrology derived from the larger data sets now available to us, has provided the primary impetus for revising these guidelines. It is hoped that this revision will lead to improved design practice, which will allow better management, policy and planning decisions to be made.

One of the major responsibilities of the National Committee on Water Engineering of Engineers Australia is the periodic revision of ARR. While the NCWE had long identified the need to update ARR it had become apparent by 2002 that even with a piecemeal approach the task could not be carried out without significant financial support. In 2008 the revision of ARR was identified as a priority in the National Adaptation Framework for Climate Change which was endorsed by the Council of Australian Governments.

In addition to the update, 21 projects were identified with the aim of filling knowledge gaps. Funding for Stages 1 and 2 of the ARR revision projects were provided by the now Department of the Environment. Stage 3 was funded by Geoscience Australia. Funding for Stages 2 and 3 of Project 1 (Development of Intensity-Frequency-Duration information across Australia) has been provided by the Bureau of Meteorology. The outcomes of the projects assisted the ARR Editorial Team with the compiling and writing of chapters in the revised ARR. Steering and Technical Committees were established to assist the ARR Editorial Team in guiding the projects to achieve desired outcomes.

**Assoc Prof James Ball**  
ARR Editor

**Mark Babister**  
Chair Technical Committee for  
ARR Revision Projects

**ARR Technical Committee:**

*Chair:* Mark Babister

*Members:*

Associate Professor James Ball  
Professor George Kuczera  
Professor Martin Lambert  
Associate Professor Rory Nathan  
Dr Bill Weeks  
Associate Professor Ashish Sharma  
Dr Bryson Bates  
Steve Finlay

Related Appointments:

ARR Project Engineer:

Monique Retallick

ARR Admin Support:

Isabelle Testoni

Assisting TC on Technical Matters:

Erwin Weinmann, Dr Michael Leonard

**ARR Editorial Team:**

*Editors:* James Ball

Mark Babister

Rory Nathan

Bill Weeks

Erwin Weinmann

Monique Retallick

Isabelle Testoni

Associate Editors for Book 9 - Runoff in Urban Areas

Peter Coombes

Steve Roso

Editorial assistance: Mikayla Ward

## **Status of this document**

This document is a living document and will be regularly updated in the future.

In development of this guidance, and discussed in Book 1 of ARR 1987, it was recognised that knowledge and information availability is not fixed and that future research and applications will develop new techniques and information. This is particularly relevant in applications where techniques have been extrapolated from the region of their development to other regions and where efforts should be made to reduce large uncertainties in current estimates of design flood characteristics.

Therefore, where circumstances warrant, designers have a duty to use other procedures and design information more appropriate for their design flood problem. The Editorial team of this edition of Australian Rainfall and Runoff believe that the use of new or improved procedures should be encouraged, especially where these are more appropriate than the methods described in this publication.

Care should be taken when combining inputs derived using ARR 1987 and methods described in this document.

## **Change Log**

### **Version 4.2 - Climate Change Chapter Update**

In late 2022 the Australian Government Department of Climate Change, Energy, the Environment and Water in partnership with Engineers Australia commenced an 18 month project to update the climate change considerations chapter of the Australian Rainfall and Runoff guidelines (Chapter 6, Book 1) to incorporate the most recent and relevant climate science and projections. The project involved the undertaking of a rigorous literature review of hydroclimatology under climate change relevant to design flood estimation, which was peer reviewed and published in a leading international journal. The findings were used to draft practical flood guidance which was finalised after an extensive process of review and feedback by industry. Funding for this project was received from National Emergency Management Agency under the Disaster Risk Reduction Package. The project report was adapted to replace Book 1 chapter 6.

#### *Climate Change Update Project Control Group:*

Leanne Haupt  
Simon Koger  
Andrew Dyer  
Karl Braganza  
Duncan McLuckie  
Monique Retallick  
Euan Brown  
Andrew Gissing  
Martyn Hazelwood  
Professor Rory Nathan

#### *Climate Change Update Technical Working Group:*

Dr Conrad Wasko  
Professor Seth Westra  
Dr Dörte Jakob  
Chris Nielsen  
Professor Jason Evans  
Simon Rodgers  
Mark Babister  
Dr Andrew Dowdy  
Dr Wendy Sharples  
Dr Ramona Dalla Pozza  
Dr Michelle Ho

This version updates Book 1 Chapter 6 to reflect updates in climate science as discussed above. While no other chapters have been updated some minor amendments were made to remove inconsistencies with the new chapter. FAQs relating to the update are available <https://arr.ga.gov.au/contact-us>.

## Key updates in Version 4.2

Update	Version 4.2
Book 1	Book 1 Chapter 6 Climate change updated
Guideline formats	PDF Web-based version Epub version
User experience	FAQs added to Geoscience Australia Website
Climate change	Reflected best practice as of 2024 and IPCC 6
Other Minor Changes	List the minor changes to the following chapters for consistency Book 1 Chapter 4 Section 15.1 Book 1 Chapter 4 Section 16.1 Book 1 Chapter 5 Section 10.4 Book 2 Chapter 1 Section 3 Book 2 Chapter 3 Section 3 Book 6 Chapter 5 Section 5 Book 8 Chapter 7 Section 7 Book 9 Chapter 6 Section 4.2 Book 9 Chapter 6 Section 4.6

---

## ARR 2019 (now Version 4.1)

Geoscience Australia, on behalf of the Australian Government, asked the National Committee on Water Engineers (NCWE) - a specialist committee of Engineers Australia - to continue overseeing the technical direction of ARR. ARR's success comes from practitioners and researchers driving its development; and the NCWE is the appropriate organisation to oversee this work. The NCWE has formed a sub-committee to lead the ongoing management and development of ARR for the benefit of the Australian community and the profession. The current membership of the ARR management subcommittee includes Mark Babister, Robin Connolly, Rory Nathan and Bill Weeks.

The ARR team have been working hard on finalising ARR since it was released in 2016. The team has received a lot of feedback from industry and practitioners, ranging from substantial feedback to minor typographical errors. Much of this feedback has now been addressed. Where a decision has been made not to address the feedback, advice has been provided as to why this was the case.

A new version of ARR is now available. ARR 2019 is a result of extensive consultation and feedback from practitioners. Noteworthy updates include the completion of Book 9, reflection of current climate change practice and improvements to user experience, including the availability of the document as a PDF.

## Key updates in ARR 2019

Update	ARR 2016	ARR 2019
Book 9	Available as “rough” draft	Peer reviewed and completed
Guideline formats	Epub version Web-based version	Following practitioner feedback, a pdf version of ARR 2019 is now available
User experience	Limited functionality in web-based version	Additional pdf format available
Climate change	Reflected best practice as of 2016 Climate Change policies	Updated to reflect current practice
PMF chapter	Updated from the guidance provided in 1998 to include current best practice	Minor edits and reflects differences required for use in dam studies and floodplain management
Examples		Examples included for Book 9
Figures		Updated reflecting practitioner feedback

As of May 2019, this version was considered to be final.

### **ARR 2016 (now Version 4.0)**

Released July 2016



BOOK 3

# Peak Flow Estimation

---

## Peak Flow Estimation

---

---

# Table of Contents

1. Introduction .....	1
1.1. Why Estimate Peak Discharges? .....	1
1.2. Book Contents .....	1
1.3. Selection of Method .....	2
1.4. Scope .....	2
1.5. Terminology .....	3
1.6. References .....	3
2. At-Site Flood Frequency Analysis .....	5
2.1. Introduction .....	5
2.2. Conceptual Framework .....	5
2.2.1. Definition of Flood Probability Model .....	5
2.2.2. Annual Maximum and Peak-Over-Threshold Perspectives .....	6
2.2.3. Advantages and Disadvantages of Flood Frequency Analysis .....	11
2.2.4. Range of Application .....	12
2.3. Selection and Preparation of Data .....	13
2.3.1. Requirements of Data for Valid Analysis .....	13
2.3.2. Types of Flood Data .....	14
2.3.3. Annual Maximum Flood Gauged Series .....	15
2.3.4. Peak-Over-Threshold Gauged Series .....	16
2.3.5. Monthly and Seasonal Gauged Series .....	17
2.3.6. Extension of Gauged Records .....	18
2.3.7. Rating Curve Error in Gauged Discharges .....	19
2.3.8. Historical and Paleo Flood Information .....	21
2.3.9. Data Characterising Long-Term Climate Persistence .....	22
2.3.10. Regional Flood Information .....	24
2.3.11. Missing Records .....	24
2.4. Choice of Flood Probability Model .....	25
2.4.1. General .....	25
2.4.2. Choice of Distribution Family for Annual Maximum Series .....	26
2.4.3. Choice of Distribution for Peak-Over-Threshold Series .....	31
2.5. Choice of Flood Quantile Estimator .....	31
2.5.1. Expected Parameter Quantiles .....	32
2.5.2. Expected AEP Quantiles .....	33
2.5.3. Selection of Flood Quantile Estimator .....	34
2.6. Fitting Flood Probability Models to Annual Maxima Series .....	34
2.6.1. Overview of Methods .....	34
2.6.2. Probability Plots .....	35
2.6.3. Bayesian Calibration .....	37
2.6.4. L-moments Approach .....	45
2.6.5. Method of Moments Approach .....	51
2.7. Fitting Flood Probability Models to Peak Over Threshold Series .....	51
2.7.1. Probability Plots .....	51
2.7.2. Fitting Peak-Over-Thresholds Models .....	52
2.8. Supplementary Information .....	52
2.8.1. Example 1: Extrapolation and Process Understanding .....	52
2.8.2. Example 2: Accuracy of Daily Gauged Discharges .....	54
2.8.3. Example 3: Fitting a probability model to gauged data .....	55
2.8.4. Example 4: Use of binomial censored historical data .....	69
2.8.5. Example 5: Use of regional information .....	73
2.8.6. Example 6: Censoring PILFs using multiple Grubbs-Beck test .....	78

2.8.7. Example 7: Improving poor fits using censoring of low flow data .....	85
2.8.8. Example 8: A Non-Homogeneous Flood Probability Model .....	88
2.8.9. Example 9: L-moments fit to gauged data .....	92
2.8.10. Example 10: Improving poor fits using LH-moments .....	94
2.8.11. Example 11: Fitting a probability model to POT data .....	98
2.9. References .....	99
3. Regional Flood Methods .....	105
3.1. Introduction .....	105
3.2. Conceptual Framework .....	106
3.2.1. Definition of Regional Flood Frequency Estimation .....	106
3.2.2. Formation of Regions .....	106
3.2.3. Development of Regional Flood Frequency Estimation Technique .....	107
3.2.4. Data Required to Develop Regional Flood Frequency Estimation Technique .....	108
3.2.5. Accuracy Considerations .....	109
3.3. Statistical Framework .....	110
3.3.1. Region Of Influence (ROI) Approach .....	110
3.3.2. Parameter Regression Technique .....	110
3.3.3. Generalised Least Squares Regression .....	111
3.3.4. Development of Confidence Limits for the Estimated Flood Quantiles ....	112
3.4. RFFE Techniques for Humid Coastal Areas .....	112
3.4.1. Data Used to Develop RFFE Technique .....	112
3.4.2. Adopted RFFE Regions .....	115
3.4.3. Adopted Estimation Equations .....	116
3.5. RFFE Techniques for Arid/Semi-Arid Areas .....	116
3.5.1. Data Used to Develop RFFE Technique .....	116
3.5.2. Adopted Regions .....	117
3.5.3. Adopted Estimation Equations .....	118
3.6. Fringe Zones .....	118
3.7. Relative Accuracy of the RFFE Technique .....	119
3.8. Bias Correction .....	121
3.9. Combining Regional and At-Site Quantile Estimates .....	122
3.10. Impact of Climate Change .....	122
3.11. Progressive Improvement of RFFE Model 2015 v1 .....	122
3.12. RFFE Implementation and Limitations .....	123
3.12.1. Overview of RFFE Accuracy .....	123
3.12.2. RFFE Implementation .....	124
3.13. Practical Considerations for Application of the RFFE Technique .....	125
3.13.1. Urban Catchments .....	125
3.13.2. Catchments Containing Dams and Other Artificial Storage .....	126
3.13.3. Catchments Affected by Mining .....	126
3.13.4. Catchments with Intensive Agricultural Activity .....	126
3.13.5. Catchment Size .....	127
3.13.6. Catchment Shape .....	127
3.13.7. Atypical Catchment Types .....	127
3.13.8. Catchment Location .....	128
3.13.9. Arid and Semi-arid Areas .....	128
3.13.10. Baseflow .....	129
3.14. RFFE Model 2015 .....	129
3.15. Worked Examples .....	133

3.15.1. Application of RFFE Model 2015 to the Wollomombi River at Coinside, NSW (Region 1) (A Catchment Having No Major Regulation, No Major Natural or Artificial Storage and No Major Land Use Change) .....	133
3.15.2. Application for the Four Mile Brook at Netic Rd, SW Western Australia (Region 5) (a Catchment Having No Major Regulation, No Major Natural or Artificial Storage and no Major Land Use Change) .....	135
3.15.3. Application for the Morass Creek at Uplands, VIC (Region 1) (a Catchment Having Significant Natural Floodplain Storage Where RFFE Model 2015 Output is Not Directly Applicable) .....	138
3.16. Further Information on the Development and Testing of RFFE Technique 2015 .....	141
3.17. References .....	143

---

## List of Figures

3.2.1. Peak Over Threshold series .....	8
3.2.2. Annual Exceedance Probability (AEP) - Exceedances per Year (EY) Relationship ..	11
3.2.3. Hydrograph for a 1000 km <sup>2</sup> Catchment Illustrating Difficulty of Assessing Independence of Floods .....	13
3.2.4. Depiction of Censored and Gauged Flow Time Series Data .....	15
3.2.5. Rating Curve Extension by Fitting to an Indirect Discharge Estimate .....	20
3.2.6. Rating Curve Extension by Slope-Conveyance Method .....	21
3.2.7. Annual Average Interdecadal Pacific Oscillation Time Series .....	23
3.2.8. NSW Regional Flood Index Frequency Curves for Positive and Negative Interdecadal Pacific Oscillation epochs (Kiem et al., 2003) .....	24
3.2.9. Rating error multiplier space diagram for rating curve .....	39
3.2.10. Bilinear channel storage-discharge relationship .....	53
3.2.11. Simulated rainfall and flood frequency curves with major floodplain storage activated at a threshold discharge of 3500 m <sup>3</sup> /s .....	54
3.2.12. Comparison between true peak flow and 9:00 am flow for Goulburn River at Coggan	55
3.2.13. Comparison between true peak flow and 9:00 am flow for Hunter River at Singleton .....	55
3.2.14. TUFLOW Flike Splash Screen .....	56
3.2.15. Create New .fld file .....	57
3.2.16. Flike Editor Screen .....	58
3.2.17. Observed Values Screen .....	59
3.2.18. Import Gauged Values Screen .....	60
3.2.19. View Gauged Values in Text Editor .....	61
3.2.20. Observed Values screen with Imported Data .....	62
3.2.21. Rank Data Screen .....	63
3.2.22. General Screen – After Data Import .....	64
3.2.23. Blank TUFLOW-Flike Screen .....	65
3.2.24. Probability Plot .....	66
3.2.25. Results File .....	67
3.2.26. Probability Plot using Gumbel Scale .....	68
3.2.27. Censoring observed values tab .....	70
3.2.28. Configured Flike Editor .....	71
3.2.29. Probability plot of the Singleton data with historic information .....	72
3.2.30. Probability plot of the Singleton data with historic information .....	73
3.2.31. Gaussian prior distributions .....	75
3.2.32. Prior for Log-Pearson III window .....	75

3.2.33. Probability plot of with prior regional information .....	76
3.2.34. Comparison between the results from Example 3 and Example 5 .....	77
3.2.35. TUFLOW Flike editor window with Wimmera data .....	79
3.2.36. Initial probability plot for Wimmera data with GEV .....	80
3.2.37. Results of the multiple Grubbs-Beck test .....	81
3.2.38. Excluded gauged values .....	82
3.2.39. Censoring of observed values .....	83
3.2.40. GEV fit - 56 years AM of gauged discharge - Using multiple Grubbs-Beck test .....	84
3.2.41. Bayesian fit to all gauged data Gumbel probability plot .....	85
3.2.42. Bayesian fit with 5 low outliers censored after application of multiple Grubbs-Beck test .....	86
3.2.43. Bayesian fit with floods below 250 m <sup>3</sup> /s threshold treated as censored observations .....	88
3.2.44. Histogram of IPO- and IPO+ flood ratios .....	89
3.2.45. Log-Normal fit to 43 years of IPO+ data for the Clarence river at Lilydale (units ML/day). .....	90
3.2.46. Log-Normal fit to 33 years of IPO- data for the Clarence river at Lilydale (units ML/day). .....	90
3.2.47. Log-Normal fit to 76 years of data for the Clarence river at Lilydale (units ML/day). .....	91
3.2.48. Marginal, IPO+ and IPO+ log-Normal distributions for the Clarence River at Lilydale .....	92
3.2.49. Flike Editor configured for L-moments .....	93
3.2.50. Configured Flike Editor .....	95
3.2.51. L-moment fit - Albert River at Broomfleet .....	96
3.2.52. LH-moment fit with shift H=4 .....	97
3.2.53. Plot of the fitted POT exponential model against the observed POT series .....	99
3.3.1. Geographical Distribution of the Adopted 798 Catchments from Humid Coastal Areas of Australia and 55 Catchments from Arid/Semi-arid Areas .....	113
3.3.2. Adopted Regions for RFFE Technique in Australia .....	115
3.3.3. Standardised Residuals vs. Normal Scores for Region 1 Based on Leave One Out Validation for AEPs of 10% and 5% .....	120
3.3.4. Screen Shot of RFFE Model 2015 (Landing Page) .....	130
3.3.5. RFFE Model 2015 Screen Shot for Data Input for the Wollomombi River at Coinside, NSW .....	131
3.3.6. RFFE Model 2015 Screen Shot for Model Output for the Wollomombi River at Coinside, NSW (Region 1) .....	132
3.3.7. RFFE Model 2015 vs. At-site FFA Flood Estimates for the Wollomombi River at Coinside, NSW (Region 1) .....	134

3.3.8. RFFE Model 2015 Screen Shot for Data Input for Four Mile Brook at Netic Rd, SW WA (Region 5) .....	136
3.3.9. RFFE Model 2015 Screen Shot for Model Output for Four Mile Brook at Netic Rd, SW WA (Region 5) .....	137
3.3.10. RFFE Model 2015 vs. At-site FFA Flood Estimates for Four Mile Brook at Netic Rd, SW WA (Region 5) .....	138
3.3.11. RFFE Model 2015 Screen Shot for Data Input for the Morass Creek at Uplands, VIC (Region 1) .....	139
3.3.12. RFFE Model 2015 Screen Shot for Model Output for the Morass Creek at Uplands, VIC (Region 1) .....	140
3.3.13. RFFE Model 2015 vs. At-site FFA Flood Estimates (for the Morass Creek at Uplands, VIC) (Region 1) .....	141
3.3.14. Standardised Residuals vs. Normal Scores for Region 1 Based on Leave-one-out Validation for AEPs of 50%, 20%, 2% and 1% .....	142
3.3.15. Standardised Residuals vs. Normal Scores for Region 1 Based on Leave-one-out Validation for AEPs of 2% and 1% .....	143



---

## List of Tables

3.2.1. Selected Homogeneous Probability Models Families for use in Flood Frequency Analysis .....	27
3.2.2. Frequency factors for standard normal distribution. ....	29
3.2.3. L-moments for several distributions (from Stedinger et al. (1993)) .....	46
3.2.4. LH-moments for GEV and Gumbel distributions (from Wang (1997)) .....	48
3.2.5. Polynomial coefficients for use with Equation (3.2.73) .....	49
3.2.6. Selected Results .....	68
3.2.7. Gauged flows on the Hunter River at Singleton .....	69
3.2.8. Posterior Mean, Standard Deviation and Correlation for the LP III .....	72
3.2.9. Comparison of Selected Quantiles with 90% Confidence Limits .....	72
3.2.10. Comparison of LP III Parameters with and without prior information .....	77
3.2.11. Selected Results .....	77
3.2.12. Selected Results .....	84
3.2.13. L-moment and GEV Parameter Estimates .....	93
3.2.14. Comparison of Quantiles using a Bayesian and LH-moments Inference Methods .	98
3.3.1. Summary of Adopted Catchments from Humid Coastal Areas of Australia .....	114
3.3.2. Distribution of Shape Factors for the Selected Catchments .....	115
3.3.3. Details of RFFE Technique for Humid Coastal Areas of Australia .....	115
3.3.4. Summary of adopted stations from arid/semi-arid areas of Australia .....	117
3.3.5. Details of RFFE technique for arid/semi-arid regions .....	118
3.3.6. Upper bound on (absolute) median relative error (RE) from leave-one-out validation of the RFFE technique (without considering bias correction) .....	121
3.3.7. Region Names for Application of the RFFE Model 2015 (see Figure 3.3.2 for the Extent of the Regions) .....	129
3.3.8. Application Data for the Wollomombi River at Coinside, NSW (Region 1) (Basic Input Data) .....	134
3.3.9. Fifteen Gauged Catchments (Used in the Development of RFFE Model 2015) Located Closest to Wollomombi River at Coinside, NSW .....	135
3.3.10. Application Data for Four Mile Brook at Netic Rd, SW Western Australia (Region 5) (Basic Input Data) .....	136
3.3.11. Application Data for the Morass Creek at Uplands, VIC (Region 1) (Basic Input Data) .....	138
3.3.12. Further Information on the Development and Testing of RFFE Technique 2015 ..	141

---

# Chapter 1. Introduction

James Ball, Erwin Weinmann, George Kuczera

Chapter Status	Final
Date last updated	14/5/2019

## 1.1. Why Estimate Peak Discharges?

As outlined in earlier books, there are many alternative forms of design flood problems and hence there are many alternative flood characteristics requiring estimation of a design flood quantile. For many fluvial design flood problems (i.e. problems associated with estimating design flood quantiles at a riverine location), estimation of the quantile of the peak discharge is the critical flood characteristic. This estimation is required as part of the design process for many structures in rural and urban environments (for example culverts and small to medium bridges) and particularly so for small and medium sized catchments. In many of these discharge dominated design problems, an estimation of the full hydrograph and other flood characteristics is not necessary and hence only the peak characteristics of the flood hydrograph require estimation. Where estimation of the full flood hydrograph is required, techniques outlined in other sections of ARR are required in preference to the approaches presented in this book.

Following the concepts outlined in [Book 1](#) for estimation of design flood parameters, where adequate data of sufficient quality are available, it is recommended that an at-site Flood Frequency Analysis (FFA) be used for estimation of the design peak flood discharges quantiles. Details of suitable approaches are outlined in [Book 3, Chapter 2](#).

For many other situations no observed data of a suitable quality for at-site Flood Frequency Analysis are available for estimation of the desired flood quantiles. It is recommended that in these situations, Regional Flood Frequency Estimation (RFFE) techniques be applied. Details of suitable approaches are outlined in [Book 3, Chapter 3](#).

While a consistent methodology for Regional Flood Frequency Estimation for any region in Australia is outlined in [Book 3, Chapter 3](#), designers are reminded of the guidance provided in [Book 1, Chapter 1, Section 1](#); namely, where circumstances warrant, flood engineers have a duty to use other procedures and data that are more appropriate for their design flood problem than those recommended in this Edition of Australian Rainfall and Runoff. This guidance is particularly relevant where approaches have been developed for limited regions of the country without the aim of these approaches being suitable for application across the whole country or being subject to same development testing as the RFFE model proposed herein. An example of this situation is the Pilbara Region of Western Australia where independent studies by [Davies and Yip \(2014\)](#) and [Flavell \(2012\)](#) have developed Regional Flood Frequency Estimation techniques for this region.

## 1.2. Book Contents

This book contains three chapters with the final two chapters dealing with alternative approaches to the estimation of the peak flood discharge for design purposes. Provided in the this chapter is a general introduction to the contents of this book. Following this introduction, at-site Flood Frequency Analysis is presented in [Book 3, Chapter 2](#). While these analysis techniques are applicable only to catchments where gauged information is

available, the philosophy of Flood Frequency Analysis and its application underpin many of the approaches presented in Book 3, Chapter 3 for rural ungauged catchments. It is considered, therefore, to be a fundamental component of the estimation of peak flood quantiles.

Presented in Book 3, Chapter 3 is a range of regional flood methods for estimation of peak flood discharge quantiles in ungauged catchments. These techniques use the results of at-site flood frequency analyses at gauged sites to derive peak discharge estimation procedures for ungauged locations in the same hydrologic region. As the flood characteristics vary considerably between different regions, a range of methods (similar philosophical development but differing in parameter values) have been developed to suit the specific conditions and requirements in different regions.

Different to previous versions of Australian Rainfall and Runoff, in the development of this edition of Australian Rainfall and Runoff there has been an assumption that users will have computing resources available. The techniques presented in the following sections therefore require computing resources for their implementation. Therefore, the discussion in the following sections focusses on both the theoretical basis of the techniques and their implementation.

### **1.3. Selection of Method**

Following the discussion in Book 1, the primary criterion for the selection of the methods recommended in ARR is that the methods should be based on observed flood data in the region of interest and have been peer reviewed by the profession.

In early editions of Australian Rainfall and Runoff, application of this criterion was not always possible because of the paucity of observed flood data technology limitations and the limited analysis of the available data. Hence it was necessary to recommend many arbitrary methods based purely on engineering judgement. The previous approaches towards estimation of the Rational Method runoff coefficient ("C") for urban catchments is an example of this necessity. As discussed by Hicks et al. (2009), the approach for estimation of the urban runoff coefficient presented by O'Loughlin and Robinson (1987) did not have a scientific foundation but was included to provide the necessary guidance in the application of this method.

For significant portions of Australia, this is no longer the case, and data are available for the development of techniques that have undergone review by the profession from both a scientific and a practical perspective. In these regions, the continued use of arbitrary design methods and information cannot be justified.

It is worthwhile noting that the continued collection of data is necessary to enable ongoing and continued improvements in the design methods, particularly in the robustness of predictions and the detection of inappropriate flood quantile estimates.

### **1.4. Scope**

This book has been prepared as a guide or manual, rather than a mandatory code of practice. Rules and methods appropriate to various situations are presented, together with relevant background information. Since catchments and the problems involved are diverse, and the related technology is changing, recommendations herein should not be taken as binding. They should be considered together with other information and local experience when being implemented.

The contents of this book within Australian Rainfall and Runoff are intended for a wide readership including engineers, students, technicians, surveyors and planners. Readers should be familiar with the basic concepts of catchment hydrology and hence have a basic knowledge of hydrology and hydraulics.

## 1.5. Terminology

Many terms associated with design flow estimation have been used in a loose manner, and sometimes quite incorrectly and in a misleading fashion. As outlined in Book 1, Chapter 2, the National Committee on Water Engineering of Engineers Australia had three major concerns:

- Clarity of meaning;
- Technical correctness; and
- Practicality and acceptability.

In view of the loose and frequently incorrect manner in which many terms often are used, it was considered that Australian Rainfall and Runoff should adopt terminology that is technically correct, as far as this is possible and in harmony with other objectives. Even if this terminology is not entirely popular with all users, it was considered that Engineers Australia has a responsibility to encourage and educate engineers regarding correct and consistent terminology. It was recognised also by the National Committee on Water Engineering that as well as being correct technically, the terms adopted should be relatively simple and suitable for use in practical design as this would facilitate acceptance by the profession.

The issue of terminology is particularly relevant to the usage of the term model. There are many and varied usages of this term within the field of design flood estimation. For example, the software used for implementation of a particular approach commonly is called a model by users while others refer to the model as the encapsulation of the design flood estimation approach, the calculations necessary for implementation of the approach (usually in software but could be hand calculations) and the data necessary for implementation of the approach. In the following definitions of the terms “model”, “technique” and “approach”, the explanations used are suitable for the guidance contained within this book.

While the major terminology is discussed in Book 1 of Australian Rainfall and Runoff, those terms pertinent only to the contents of this book are presented herein.

## 1.6. References

Davies, J.R. and Yip, E. (2014), Pilbara Regional Flood Frequency Analysis, Proc. Hydrology and Water Resources Symposium, Perth, February 2014, Engineers Australia, pp: 182-189.

Flavell, D. (2012), Design Flood Estimation in Western Australia, Australian Journal of Water Resources, 16(1), 1-20.

Hicks, B., Gray, S. and Ball, J.E. (2009), A Critical Review of the Urban Rational Method, Proceedings of H2009, 32nd Hydrology and Water Resources Symposium, Engineers Australia, ISBN 978-08258259461.

O'Loughlin, G.G. and Robinson, D.K., (1987), Urban stormwater drainage, Chapter 14 in Australian Rainfall and Runoff - A Guide to Flood Estimation, DH Pilgrim editor, I.E.Aust, Barton, ACT.

---

# Chapter 2. At-Site Flood Frequency Analysis

George Kuczera, Stewart Franks

Chapter Status	Final
Date last updated	14/5/2019

## 2.1. Introduction

Flood Frequency Analysis (FFA) refers to procedures that use recorded and related flood data to identify underlying probability model of flood peaks, at a particular location in the catchment, which can then be used to perform risk-based design and flood risk assessment, while providing input to regional flood estimation methods.

The primary purpose of this chapter is to present guidelines on performing Flood Frequency Analyses<sup>1</sup>. Often judgment will need to be exercised when applying these techniques. To inform such judgments, this chapter describes the key conceptual foundations that underpin Flood Frequency Analysis – the practitioner will need an understanding of elementary probability theory and statistics to get maximum benefit. In addition, a number of worked examples are provided to aid deeper insight with the implied caveat that the examples are not exhaustive in their scope. While it is expected that most practitioners will use software written by others to implement the methods described in this chapter, sufficient information is provided to enable practitioners to develop their own software applications.

## 2.2. Conceptual Framework

### 2.2.1. Definition of Flood Probability Model

In Flood Frequency Analysis flood peaks are considered to be random variables. Following convention the random variable denoting the flood peak is denoted by an upper-case symbol (e.g.  $Q$ ) whereas a specific realisation (or sample) is denoted by the lower-case symbol (e.g.  $q$ ) – where there is no ambiguity, lower-case symbols will be used.

It is assumed that each realization  $q$  is statistically independent of other realisations. This is the standard assumption in Flood Frequency Analysis and is believed to be widely applicable (e.g. [Stedinger et al. \(1993\)](#)).

In its most general form, the flood probability model can be described by its Probability Density Function (pdf)  $p(s|\theta(x))$  where  $\theta(x)$  is the vector (or list) of parameters dependent on  $x$ , a vector of exogenous or external variables such as climate indexes. The symbol ' $|$ ' is interpreted as follows: the variable to the left of ' $|$ ' is a random variable, while the variables to the right of ' $|$ ' are known values.

---

<sup>1</sup>The chapter represents a substantial revision of Chapter 10 of the 3<sup>rd</sup> Edition of Australian Rainfall and Runoff (Pilgrim and Doran, 1987). Where appropriate, original contribution by Pilgrim and Doran has been retained. Major changes include introduction of non-homogeneous probability models, replacement of product log-moments with more efficient estimation methods, use of Bayesian methods to make better use of available flood information (such as censored flow data, rating curve error and regional information), reduced prescription about the choice of flood probability model, improved identification of potentially influential low flows and guidance on fitting frequency curves to “difficult” data sets.

The distribution function of  $Q$  is defined as the non-exceedance probability  $P(Q \leq q)$  and is related to the pdf by:

$$P(Q \leq q|\theta(x)) = \int_0^q p(s|\theta(x))ds \quad (3.2.1)$$

Empirically, the pdf of  $q$  is the limiting form of the histogram of  $q$ , as the number of samples approaches infinity. Importantly, [Equation \(3.2.1\)](#) shows that the area under the pdf is interpreted as probability.

Homogeneous flood probability model:

The simplest form of flood probability model arises when the parameters  $\theta$  do not depend on an exogenous vector  $x$ . In such a case, each flood peak is considered to be a random realisation from the same probability model  $p(q|\theta)$ . Under this assumption, flood peaks form a homogeneous time series.

Non-homogeneous flood probability model:

A more complicated situation arises when flood peaks do not form a homogeneous time series. This may arise for a number of reasons including the following:

- Rainfall and flood mechanisms may be changing over time. For example, long-term climate change due to global warming, land use change and river regulation may render the flood record non-homogeneous.
- Climate may experience pseudo-periodic shifts that persist over periods lasting from several years to several decades. There is growing evidence that parts of Australia are subject to such forcing and that this significantly affects flood risk, for example, ([Franks and Kuczera, 2002](#); [Franks, 2002a](#); [Franks, 2002b](#); [Kiem et al., 2003](#); [Micevski et al., 2003](#)).

The practitioner needs to assess the significance of such factors and identify appropriate exogenous variables  $x$  to condition the flood probability model. Although this chapter will provide some guidance it is stressed that this is an area of continuing research – practitioners are therefore advised to keep abreast of new developments.

## 2.2.2. Annual Maximum and Peak-Over-Threshold Perspectives

Flood Frequency Analysis deals with the probability distribution of significant peak discharges<sup>2</sup>. Throughout the year, there are typically many flood peaks associated with individual storm events. This is demonstrated in [Figure 3.2.1](#) which illustrates a time series record of continuous streamflow discharge. Two types of flood data can be extracted from such a record. In turn, two measures of flood risk can be estimated:

- Annual Maximum (AM) Series

---

<sup>2</sup>Flood stage is typically not used in Flood Frequency Analysis for a number of reasons. Flood stage is dependent on the geometric properties of the cross-section. As a result, the probability models described in this chapter may not adequately fit peak stage data. Furthermore, the task of regionalizing flood frequency becomes more difficult because of the confounding influence of cross-sectional geometry. Finally, if the cross-section at which stage is measured changes over time, the stage time series will not be consistent over time precluding the use of frequency analysis.

- Peak-Over-Threshold Series

### 2.2.2.1. Annual Maximum (AM) Series

The AM series is formed by extracting maximum discharge in each year. This yields the series  $\{w_1, \dots, w_n\}$  where  $w_i$  is the maximum discharge in the  $i^{\text{th}}$  year of the  $n$ -year record.

The data in the AM series can be used to estimate the probability that maximum flood discharge in a year exceeds a particular magnitude  $w$ . In ARR, this probability is called the Annual Exceedance Probability AEP( $w$ ) and is formally defined as:

$$AEP(w) = P(W \leq w | \theta(x)) = \int_q^{\infty} p(s | \theta(x)) ds \quad (3.2.2)$$

where  $w$  is the maximum flood discharge in a year. Often it is convenient to express the AEP as a percentage  $X\%$  or alternatively for rare events, as a ratio 1 in  $Y$ . For example, the 1% AEP is equivalent to an AEP of 1 in 100 or 0.01.

### 2.2.2.2. Peak-Over-Threshold Series

The POT series is formed by extracting every statistically independent peak discharge (that exceeds a threshold discharge), from the record. This yields the series  $\{q_1, \dots, q_m\}$  where  $q_i$  is the peak discharge associated with the  $i^{\text{th}}$  statistically independent flood event in the  $n$ -year record. Typically the threshold discharge is selected so that  $m$  is about 2 to 3 times greater than  $n$ .

The data in the POT series can be used to estimate the probability distribution of the time to the next peak discharge that exceeds a particular magnitude:

$$P(\text{Time to next peak exceeding } q \leq t) = 1 - e^{-EY(q)t} \quad (3.2.3)$$

where  $t$  is time expressed in years and  $EY(q)$ , the number of exceedances per year, is the expected number of times in a year that the peak discharge exceeds  $q$ .



## Theory of Peak-Over-Threshold and Annual Maximum Series

### Annual Exceedance Probability AEP

The objective is to derive the distribution of the maximum flood peak within a specified interval of time. Referring to the continuous streamflow times series Figure 3.2.1, let the random variable  $q$  be a local peak discharge defined as a discharge that has lower discharge on either side of the peak. This presents an immediate problem as any bump on the hydrograph would produce a local peak. To circumvent this problem, we focus on peaks greater than some threshold defined as  $q_0$ . The threshold is selected so that the peaks above the threshold are sufficiently separated in time to be statistically independent of each other.

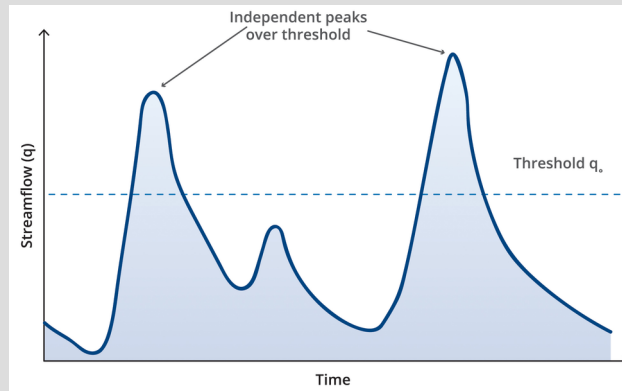


Figure 3.2.1. Peak Over Threshold series

It is assumed that all peaks above the threshold  $q_0$  are sampled from the same distribution denoted by the pdf  $p(q|q > q_0)$ .

Suppose, over a time interval of length  $t$  years, there are  $k$  peaks over the threshold  $q_0$ . This defines the POT time series  $\{q_1, \dots, q_n\}$ , which consists of  $k$  independent realisations sampled from the pdf  $p(q|q > q_0)$ .

Let  $w$  be the maximum value in the POT time series; that is,

$$w = \max\{q_1, \dots, q_k\} \quad (3.2.4)$$

For  $w$  to be the maximum value, each peak within the POT series must be less than or equal to  $w$ . In probability theory this condition is expressed by the compound event consisting of the intersection of the following  $k$  events:

$$\{(q_1 \leq w) \cap (q_2 \leq w) \cap \dots \cap (q_k \leq w)\} \quad (3.2.5)$$

Because the peaks are assumed to be statistically independent, the probability of the compound event is the product of the probabilities of the individual events. Therefore the probability that the random variable  $W \leq w$  in a POT series with  $n$  events occurring over the interval  $t$  simplifies to:

$$\begin{aligned} P(W \leq w, t) &= P[(q_1 \leq w) \cap \dots \cap (q_k \leq w)] \\ &= P(q_1 \leq w)P(q_2 \leq w) \dots P(q_k \leq w) \\ &= P(q \leq w)^k \end{aligned} \quad (3.2.6)$$

The number of POT events  $k$  occurring over an interval  $t$  is random. Suppose that the random variable  $k$  follows a Poisson distribution with  $\nu$  being the average number of POT events per year; that is:

$$P(W \leq \nu, t) = \frac{(\nu t)^n e^{-\nu t}}{n!}, n = 0, 1, 2, \dots \quad (3.2.7)$$

Application of the total probability theorem yields the distribution of the largest peak magnitude over the time interval with length  $t$ :

$$\begin{aligned} P(W \leq w, t) &= \sum_{n=0}^{\infty} P(W \leq n, t)P(W \leq \nu, t) \\ &= e^{[-(\nu t)P(q > w)]} \end{aligned} \quad (3.2.8)$$

where  $P(W \leq w, t)$  is the probability that the largest peak over time interval  $t$  is less than or equal to  $w$ . When the time interval  $t$  is set to one year, [Equation \(3.2.8\)](#) defines the distribution of the AM series.

ARR defines Annual Exceedance Probability as:

$$AEP(w) = 1 - P(W \leq w | t = 1) \quad (3.2.9)$$

where  $AEP(w)$  is the probability of the largest peak in a year exceeding magnitude  $w$ .

### Exceedances per Year (EY)

We now derive the probability distribution of the time to the next flood peak which has a magnitude in excess of  $w$ . With regard to [Equation \(3.2.8\)](#), if the largest peak during the interval  $t$  is less than or equal to  $w$ , then the time to the next peak with magnitude in excess of  $w$  must be greater than  $t$ . It therefore follows that the distribution of the time to the next peak with magnitude exceeding  $w$  is

$$\begin{aligned} P(\text{Time to next peak exceeding } w \leq t) &= 1 - e^{[-\nu P(q > w)t]} \\ &= 1 - e^{[-EY(w)t]} \end{aligned} \quad (3.2.10)$$

This is recognised as an exponential distribution with parameter  $\nu P(q > w)$  which is the expected number of peaks exceeding  $w$  per year.

ARR defines this parameter as  $EY(w)$  which stands for Exceedances per Year, but more strictly, is the expected number of peaks that exceed  $w$  in a year.

### Linking AEP and EY

If we select a particular peak magnitude  $w$ , combining [Equation \(3.2.8\)](#), [Equation \(3.2.9\)](#) and [Equation \(3.2.10\)](#) yields the following relationship between  $EY(w)$  and  $AEP(w)$ :

$$\begin{aligned} AEP(w) &= 1 - P(W \leq w | t = 1) \\ &= 1 - e^{[-vP(q > w)]} \\ &= 1 - e^{[-EY(w)]} \end{aligned} \tag{3.2.11}$$

If we express  $AEP(w)$  as  $1/Y(w)$  then [Equation \(3.2.11\)](#) can be rewritten as:

$$\begin{aligned} EY(w) &= -\log_e[1 - AEP(w)] \\ &= -\log_e\left[1 - \frac{1}{Y(w)}\right] \end{aligned} \tag{3.2.12}$$

This relationship assumes peaks in the POT series are statistically independent and that there is no seasonality in the sense that the probability density of the POT peak above a threshold  $p(q|q > q_0)$  does not change over the year. While the no-seasonality assumption appears questionable on first inspection, in practice the threshold  $q_0$  is selected so that the expected number of peaks exceeding the threshold  $q_0$  in any year is of the order of 1. This is done to ensure the POT peaks are genuine floods and statistically independent. As a consequence of the high threshold selected in practice, the impact of seasonality is diminished.

### 2.2.2.3. When to use Annual Maximum and Peak-Over-Threshold Series

The risk measures AEP and Exceedances per Year (EY) are intimately connected. The analysis presented in [Theory of Peak-Over-Threshold and Annual Maximum Series](#) shows that:

$$\begin{aligned} EY(w) &= -\log_e[1 - AEP(w)] \\ &= -\log_e\left[1 - \frac{1}{Y(w)}\right] \end{aligned} \tag{3.2.13}$$

where  $AEP(w)$  is expressed as the ratio 1 in  $Y(w)$ . This relationship is plotted in [Figure 3.2.2](#). For AEPs less than 10% (0.1 or 1 in 10 i.e. events rarer than 10% AEP), EY and AEP are numerically same, from a practical perspective. However, as the AEP increases beyond 10% (i.e. for events more frequent than 10% AEP), EY increases more rapidly than AEP. This occurs because in years with a large annual maximum peak, the smaller peaks of that year may exceed the annual maximum peak in other years.

## At-Site Flood Frequency Analysis

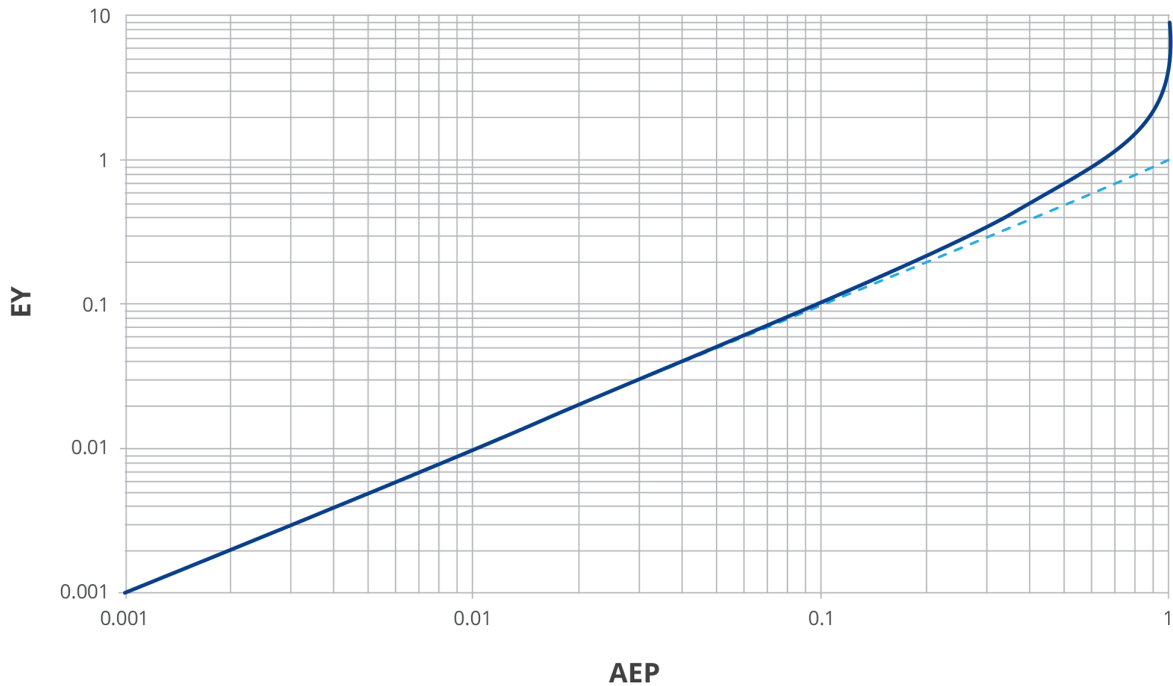


Figure 3.2.2. Annual Exceedance Probability (AEP) - Exceedances per Year (EY) Relationship

The question arises when should one use AM or POT approaches. Consistent with the guidelines provided in Book 1, the following guideline is offered:

- i. AEP of interest < 10% (i.e. events rarer than 10% AEP)

AEPs, in this range, are generally required for estimation of a design flood for a structure or works at a particular site. Use of AM series is preferred as it yields virtually identical answers to POT series in most cases, provides a more robust<sup>3</sup> estimate of low AEP floods and is easier to extract and define.

- ii. EY of interest > 0.2 events per year (i.e. events more frequent than 0.2 EY)

Use of a POT series is generally preferred because all floods are of interest in this range, whether they are the highest in the particular year of record or not. The AM series may omit many floods of interest. The POT series is appropriate for estimating design floods with a relatively high EY in urban stormwater contexts and for diversion works, coffer dams and other temporary structures. However, in practice, flow records are not often available at sites where minor works with a design EY greater than 0.1 events per year is required.

### 2.2.3. Advantages and Disadvantages of Flood Frequency Analysis

Practitioners need to be aware of the advantages and disadvantages of Flood Frequency Analysis.

<sup>3</sup>In a POT series, there are typically 2 to 3 times more peaks than in the corresponding AM series. The additional peaks are largely smaller peaks. In the case when the data is not well fitted by the chosen probability model, the fit to the upper part of the distribution may be compromised in order to obtain a good fit to the smaller peaks where the bulk of the data lies.

Flood peaks are the product of a complex joint probability process involving the interaction of many random variables associated with the rainfall event, antecedent conditions and the rainfall-runoff transformation. Peak flood records represent the integrated response of the storm event with the catchment. They provide a direct measure of flood exceedance probabilities. As a result, Flood Frequency Analysis is not subject to the potential for bias, possibly large, that can affect alternative methods based on design rainfall ([Kuczera et al., 2006](#)).

Other advantages of Flood Frequency Analysis include its comparative simplicity and capacity to quantify uncertainty arising from limited information.

Offsetting these significant advantages are several disadvantages:

- The true probability distribution family is unknown. Unfortunately, different models can fit the flood data with similar capability, yet can diverge in the right hand tail when extrapolated beyond the data.
- Short records may compromise the utility of flood estimates. Confidence limits inform the practitioner about the credibility of the estimate.
- It may be difficult or impossible to adjust the data if the catchment conditions under which the flood data were obtained have changed during the period of record, or are different to those applying to the future economic life of a structure or works being designed.

Considerable extrapolation of rating curves is necessary to convert recorded stage to discharge for the largest flood peaks at most Australian gauging stations. In addition, the probability of malfunction of recording instruments is increased during major floods. Suspect floods and the years in which they occurred may be omitted in analysis of Annual Maximum series, but this reduces the sample size and may introduce bias if the suspect floods are all major events. These problems are inherent to the calibration of all methods employing major flood peaks. At this stage it is not clear whether Flood Frequency Analysis is more sensitive to such problems than other methods.

## **2.2.4. Range of Application**

As noted the true flood probability family,  $M$ , is unknown. In practice, the choice of model is guided by goodness of fit to data. Therefore, use of the fitted frequency curve for AEPs reflected in the data is regarded as an interpolation exercise deemed reliable in the sense that confidence limits capture the uncertainty. However, when the frequency curve is extrapolated well beyond the observed data, confidence limits which quantify the effect of sampling variability on parameter uncertainty may underestimate the true uncertainty - model bias may be significant and even dominant. [Book 3, Chapter 2, Section 8](#) demonstrates the need to understand the processes affecting flood peaks beyond the observed record and illustrates the pitfall of blind extrapolation.

Large extrapolation of a flood frequency curve is not recommended. It is acknowledged that prescribing strict limits on the minimum AEP does not have a strong conceptual foundation. The limits to extrapolation should be guided by consideration of confidence limits, which are affected by the information content of the data and choice of flood model, and by judgments about model bias which cannot be quantified. In situations where the analyst is prepared to make the judgment that the processes operating in the range of the observed record continue to operate for larger floods, model bias may be deemed to be manageable – of course the effects of sampling uncertainty may be so amplified under significant extrapolation to render the frequency estimate of little value.

## 2.3. Selection and Preparation of Data

### 2.3.1. Requirements of Data for Valid Analysis

For a valid frequency analysis, the data used should constitute a random sample of independent values, ideally from a homogeneous population. Streamflow data are collected as a continuous record, and discrete values must be extracted from this record as the events to be analysed. The problem of assessing independence of events, and of selecting all independent events, is illustrated by the streamflow record for a 1000 km<sup>2</sup> catchment in [Figure 3.2.3](#). It is clear that peaks A and B are not independent of each other but are serially correlated, while peak D is independent of A and B. However, the independence of peak C in regards to A and B is open to question, as it is difficult to determine the independent peaks in the record - B and D, or B, C and D. Methods for selecting the peaks included in the analysis are described in the following subsections.

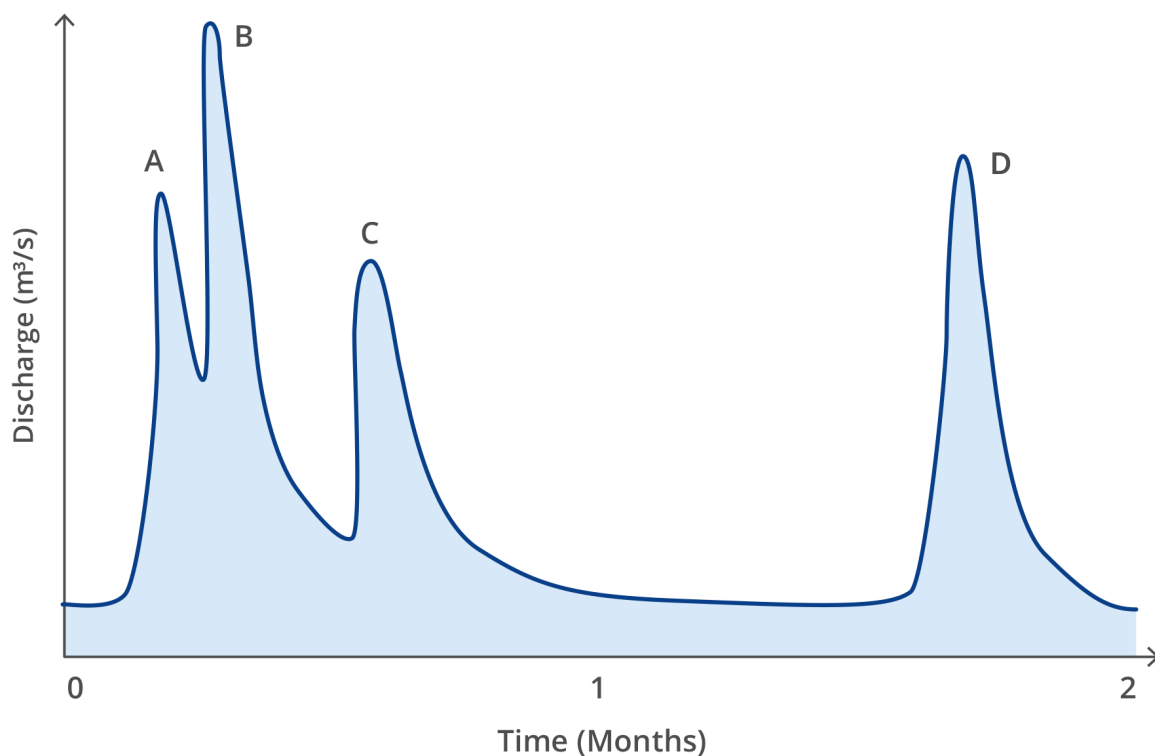


Figure 3.2.3. Hydrograph for a 1000 km<sup>2</sup> Catchment Illustrating Difficulty of Assessing Independence of Floods

Lack of homogeneity of the population of floods is another practical problem, especially if the data sample from the past is used to derive flood estimates applicable to the design life of the structure or works in future. Examples of changes in collection of data or in the nature of the catchment that lead to lack of homogeneity are:

1. Inability to allow for change of station rating curve, for example, resulting from insufficient high-stage gauging;
2. Change of gauging station site;
3. Construction of large storages, levees and channel improvements;

4. Growth in the number of farm dams on the catchment; and
5. Changes in land use such as clearing, different farming practices, soil conservation works, re-forestation, and urbanisation.

The record should be carefully examined for these and other causes of lack of homogeneity. In some cases, recorded values can be adjusted by means such as routing pre-dam floods through the storage to adjust them to equivalent present values, correcting rating errors wherever possible, or making some adjustment for urbanisation. Such decisions must be made largely by judgement. As with all methods of flood estimation, it is important that likely conditions during the design life are considered, instead of existing conditions at the time of design. Some arbitrary adjustment of derived values for likely changes in the catchment may be possible, but the recorded data must generally be accepted for analysis and design. Fortunately, the available evidence indicates that unless changes to the catchment involve large proportions of the total area or large changes in the storage on the catchment, the effects on flood magnitudes are likely to be low. In addition, the effects are likely to be larger for frequent floods than for the rare floods that are of primary interest in design.

### 2.3.2. Types of Flood Data

In the most general sense, flood peak data can be classified as either being gauged or censored.

#### 2.3.2.1. Gauged Data

Gauged data consists of a time series of flood discharge estimates. Such estimates are based on observed peak (or instantaneous) stages (or water levels). A rating curve is used to transform stage observations to discharge estimates. When extrapolated, the rating curve can introduce large systematic errors into discharge estimates.

It is important to check how the peak discharges were obtained from the gauged record. Peak discharges may be derived from daily readings, possibly with some intermediate readings during some floods, for part of the record, and continuous readings from the remainder of the record. If part of the record consists of daily readings, it is necessary to assess whether daily readings adequately approximate the instantaneous peak discharge (refer to [Book 3, Chapter 2, Section 8](#) for instances of adequate and inadequate approximations). If the daily reading is deemed as an unreliable estimate of the peak discharge during that day, the reading need not be discarded but treated as a censored discharge.

#### 2.3.2.2. Censored Data

Censored data consists of a time series of indicator values defined as:

$$I_t(q) = \begin{cases} 1 & \text{if } t^{\text{th}} \text{ flood peak} > \text{threshold } q \\ -1 & \text{if } t^{\text{th}} \text{ flood peak} \leq \text{threshold } q \end{cases} \quad (3.2.14)$$

They arise in a number of ways. For example, prior to gauging, water level records may be kept only for rare floods above some perception threshold. Therefore, all we may know is that there were  $n_a$  flood peaks above the threshold and  $n_b$  peaks below the threshold. Sometimes, frequent floods below a certain threshold may be deliberately excluded, since the overall fit gets unduly influenced by small floods.

Figure 3.2.4 presents a graphical depiction of gauged and censored time series data. In the first part of the record, all the peaks are below a threshold, while in the second part, daily readings define a lower threshold for the peak. Finally, in the third part, continuous gauging yields instantaneous peaks.

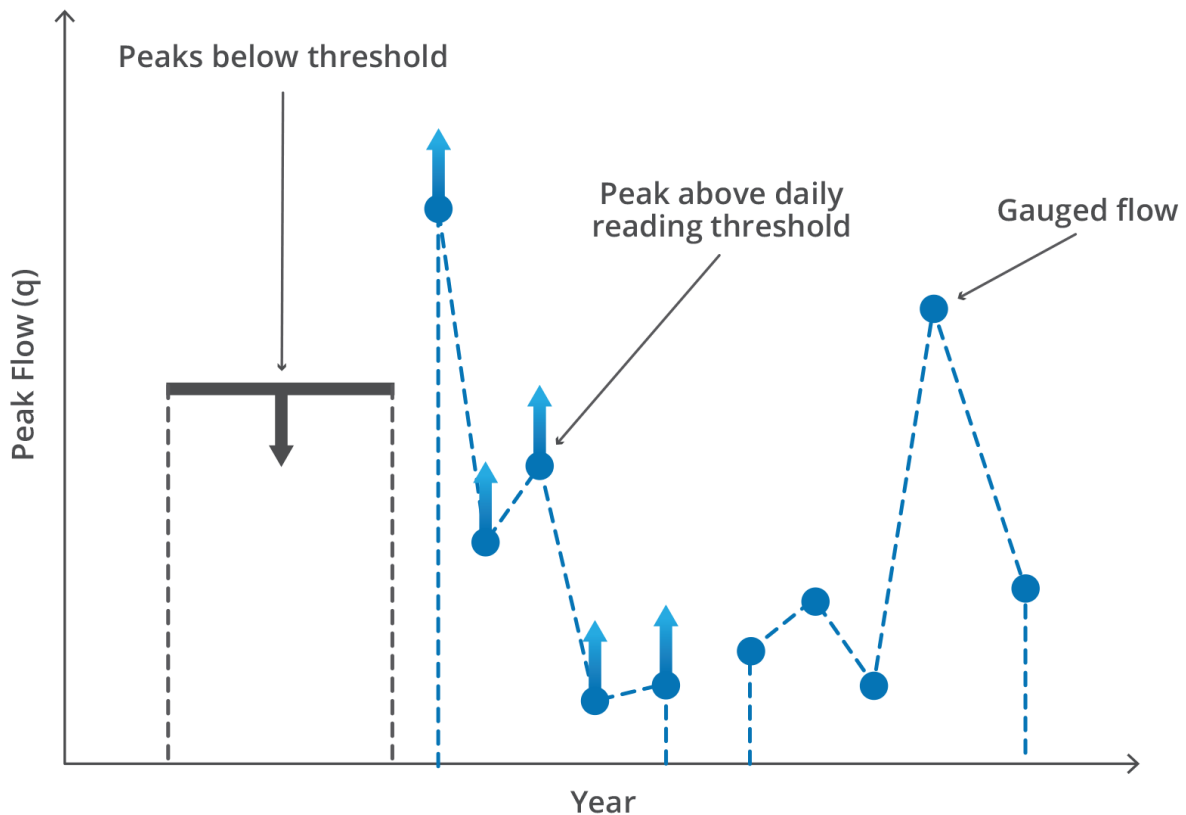


Figure 3.2.4. Depiction of Censored and Gauged Flow Time Series Data

### 2.3.3. Annual Maximum Flood Gauged Series

This is the most common method of selecting the floods to be analysed. The series comprised of the highest instantaneous rate of discharge in each year of record. The year may either be a calendar year or a water year, the latter usually commencing at the end of the period of lowest average flow during the year. Where flows are highly seasonal, especially with a wet summer, use of the water year is preferable. The highest flow in each year is selected, whether it is a major flood or not, and all other floods are neglected, even though some will be much larger than the maximum discharges selected from some other years. For  $n$  years of data, the annual flood series will consist of  $n$  values.

The Annual Maximum series has at least two advantages:

1. As the individual annual maximum discharges are likely to be separated by considerable intervals of time, it is probable that the values will be independent. Checking the dates of the annual maxima to ensure that they are likely to be independent, is a simple procedure that should be followed. If the highest annual value occurred at the start of a year and was judged to be dependent on the annual maximum at the end of the previous year, the lower of these two values should be discarded and the second highest discharge in that year substituted.
2. The series is easily and unambiguously extracted. Most data collection agencies have annual maxima on computer file and/or hard copy.



### 2.3.4. Peak-Over-Threshold Gauged Series

A POT flood series consists of all floods with peak discharges above a selected base value, regardless of the number of such floods occurring each year. The POT series is also referred to as the partial duration series or basic stage series. The number of floods  $m$  generally will be different to the number of years of record  $n$ , and will depend on the selected base discharge. ASCE (1949) recommended that the base discharge should be selected so that  $m$  is greater than  $n$ , but that there should not be more than 3 or 4 floods above the base in any one year. These two requirements can be incompatible. The U.S. Geological Survey (Dalrymple, 1960) recommended that  $m$  should equal  $3n$ . If a probability distribution is to be fitted to the POT series, the desirable base discharge and average number of floods per year selected depend on the type of distribution. These distributions are discussed further in Book 3, Chapter 2, Section 4. For the compound model using a Poisson distribution of occurrences and an exponential distribution of magnitudes, Tavares and Da Silva (1983), and Jayasuriya and Mein (1985) found that  $m$  should equal  $2n$  or greater, and the U.K Flood Studies Report (Natural Environment Research Council, 1975) recommended that  $m$  should equal  $3n$  to  $5n$ . For fitting the Log Pearson III (LP III) distribution, the values of the moments depend on the number of floods selected and the base discharge. McDermott and Pilgrim (1982) and Jayasuriya and Mein (1985) found that best results were obtained in this case when  $m$  equalled  $n$ .

An important advantage of the POT series is that when the selected base value is sufficiently high, small events that are not really floods are excluded. With the AM series, non-floods in dry years may have an undue influence on shape of the distribution. This is particularly important for Australia, where both the range of flows and the non-occurrence of floods are greater than in many other countries such as the United States and the United Kingdom. For this reason it would also be expected that the desirable ratio of  $m$  to  $n$  would be lower in Australia than in these countries (refer to Book 3, Chapter 2, Section 3).

A criterion for independence of successive peaks must also be applied in selecting events. As discussed by Laurenson (1987), statistical independence requires physical independence of the causative factors of the flood, mainly rainfall and antecedent wetness. This type of independence is necessary if the POT series is used to estimate the distribution of annual floods. On the other hand, selection of POT series floods for design flood studies should consider the consequences of the flood peaks in assessing independence of events where damages or financial penalties are the most important design variables. Factors to be considered might include duration of inundation and the time required to repair flood damage. In both cases, the size or response time of the catchment will have some effect.

The decision regarding a criterion for independence, therefore requires subjective judgement by the practitioner, designer or analyst in each case. There is often conflict that some flood effects are short-lived, perhaps only as long as inundation, while others, such as the destruction of an annual crop, may last as long as a year. It is thus not possible to recommend a simple and clear-cut criterion for independence. The circumstances and objectives of each study, and the characteristics of the catchment and flood data, should be considered in each case before a criterion is adopted. It is inevitable that the adopted criterion will be arbitrary to some extent.

While no specific criterion can be recommended, it may be helpful to consider some criteria that were used in past studies:

- Bulletin 17B of the Interagency Advisory Committee on Water Data (1982) states that no general criterion can be recommended and the decision should be based on the intended use in each case, as discussed above. However, in Appendix 14 of that document, a study

by Beard (1974) is summarised where the criterion is that it should use independent flood peaks should be separated by five days plus the natural logarithm of the square miles of drainage area, with the additional requirement that intermediate discharges must drop to below 75% of the lower of the two separate flood peaks. This may only be suitable for catchments larger than 1000 km<sup>2</sup>. Jayasuriya and Mein (1985) used this criterion.

- The UK Flood Studies Report (Natural Environment Research Council, 1975) used a criterion that flood peaks should be separated by three times the time to peak and that the flow should decrease between peaks to two-thirds of the first peak.
- McIlwraith (1953), in developing design rainfall data for flood estimation, used the following criteria, based on the rainfall causing the floods:
  - For rainfalls of short duration up to two hours, only the one highest flood within a period of 24 hours.
  - For longer rainfalls, a period of 24 hours in which no more than 5 mm of rain could occur between rain causing separate flood events.
- In a study of small catchments, Potter and Pilgrim (1971) used a criterion of three calendar days between separate flood events but lesser events could occur in the intervening period. This was the most satisfactory of five criteria tested on data from seven small catchments located throughout eastern New South Wales. It also gave the closest approximation to the above criteria used by McIlwraith (1953).
- Pilgrim and Doran (1987) and McDermott and Pilgrim (1983) adopted monthly maximum peak flows to give an effective criterion of independence in developing a design procedure for small to medium sized catchments. This was based primarily on the assumption that little additional damage would be caused by floods occurring within a month, and thus closer floods would not be independent in terms of their effects. This criterion was also used by Adams and McMahon (1985) and Adams (1987).

The criteria cited above represent a wide range and illustrate the difficult and subjective nature of the choice. It is stressed that these criteria have been described for illustrative purposes only. In each particular application the practitioner, designer or analyst should choose a criterion suitable to the analysis and relevant to all of the circumstances and objectives.

### **2.3.5. Monthly and Seasonal Gauged Series**

In some circumstances, series other than the AM or POT series may be used. The monthly and seasonal series are the most useful.

Maximum monthly flows are an approximation to the POT series in most parts of Australia, as the probability of two large independent floods occurring in the same month is low. Tropical northern Australia, the west coast of Tasmania and the south-west of Western Australia may be exceptions. It should be noted that not every monthly maximum flood will be selected, but only those large enough to exceed a selected base discharge, as is the case for the POT series. The monthly series has two important advantages over the POT series, which it approximates:

1. It is more easily extracted, as most gauging authorities have monthly maximum discharges on file.

2. It can be argued that a flood occurring within a month of a previous large flood is of little concern in design, as repairs will not have been undertaken and little additional damage will result.

With the monthly series, care is required to check any floods selected in successive months for independence. Where the dates are close, the lower value should be discarded. The second highest flood in that month could then be checked from the records, but this would generally not be worthwhile. An example of use of the monthly series is described by Pilgrim and McDermott (1982).

Seasonal flood frequencies are sometimes required. For these cases, the data are selected for the particular month or season as for the annual series, and the flood frequency analysis is carried out in a similar fashion to that for the annual series.

### **2.3.6. Extension of Gauged Records**

It may sometimes be possible to extend the recorded data by values estimated from longer records on adjacent catchments, by use of a catchment rainfall-runoff model, or by use of historical data from before the commencement of records. If this can be done validly, the effective sample size of the data will be increased and the reliability of the analysis will be greater. However, care is necessary to ensure that the extended data is valid and real information has been added. Several procedures can be used and are outlined in the following sections:

- Regression Relationship with Data from an Adjacent Catchment
- Use of a Catchment Rainfall-Runoff Model
- Station-Year Method

#### **2.3.6.1. Regression Relationship with Data from an Adjacent Catchment**

If a regression of flood peaks for the study catchment on peaks for an adjacent catchment can be established for the period of concurrent record, the relation can be used to estimate values for the study catchment for a longer period, when records are only available on the adjacent catchment. The data should first be plotted on linear and log-log scales. A regression equation can then be fitted to the values or alternatively, the graphical relation can be used directly with a smooth curve fitted by eye.

The principal shortcoming of the regression approach is that uncertainty in the transfer process is ignored resulting in an overstatement of information content. To guard against this, an approximate criterion for deciding whether the regression should be used is that the correlation coefficient of the relation should exceed 0.85 (Fiering, 1963; Matalas and Jacobs, 1964). More rigorous criteria are discussed in ARR 1987 Book 3 Section 2.6.5.

Care is needed when annual floods are used. The dates of the corresponding annual floods on the adjacent catchments should be compared. Not infrequently, the dates are different, resulting in a lack of physical basis for the relation. Although relationships of this type seem to have been used in some regional flood frequency procedures, it is recommended that regressions should only be used when the corresponding floods result from the same storm. This problem is discussed further by Potter and Pilgrim (1971).

When floods resulting from the same storm on adjacent catchments are plotted against each other, there is often a large scatter. Frequently, a large flood occurs on one catchment but

only a small flood occurs on the other. The scatter is generally greater than for the physically unrealistic relation using floods which are the maximum annual values on the two catchments but which may have occurred on different dates. The resulting relation using floods that occurred in the same storm is often so weak that it should not be used to extend records.

Wang (2001) describes a Bayesian approach that rigorously makes allowance for the noise in the transfer process. This approach is considered superior to the traditional regression transfer.

### **2.3.6.2. Use of a Catchment Rainfall-Runoff Model**

A catchment rainfall-runoff model can range from a simple rainfall-runoff regression to a catchment modelling system that simulates either continuous runoff hydrographs or single event hydrograph from rainfall data. This discussion relates primarily to the latter type of model. The calibration of such a model for a period with concurrent rainfall and runoff records and its subsequent use to extend streamflow records for the period when rainfall data are available, while an attractive approach, should only be used with great caution. Appreciable differences often occur between observed and modelled runoff, especially in periods not used in calibration and in periods with runoff not represented in the calibration. Estimation of model parameters involves considerable uncertainty. Greatest accuracy in modelling can be expected in calculating discharges around the mean value, and larger errors are likely in extreme values such as the large flood peaks required for frequency analysis. Overall, the use of catchment models to extend flood records should be adopted with caution.

### **2.3.6.3. Station-Year Method**

This method is included only to warn against its shortcomings. In this procedure, records from several adjacent catchments are joined "end-to-end" to give a single record equal in length to the sum of the lengths of the constituent records. As discussed by Clarke-Hafstead (1942) for rainfall data, spatial correlation between the records of the adjacent stations invalidates the procedure.

### **2.3.7. Rating Curve Error in Gauged Discharges**

Though it is widely accepted that discharge estimates for large floods can be in considerable error, there is limited published information on these errors and how they can be allowed for in a Flood Frequency Analysis. Rating error can arise from a number of mechanisms:

1. For large floods the rating curve typically is extrapolated or fitted to indirect discharge estimates. This can introduce a systematic but unknown bias.
2. If the gauging station is located at a site with an unstable cross-section the rating curve may shift causing a systematic but unknown bias.

The conceptual model of rating error presented in this section is based on Kuczera (1999) and is considered to be rudimentary and subject to refinement. It is assumed the cross-section is stable with the primary source of rating error arising from extension of the rating curve to large floods.

Potter and Walker (1981) and Potter and Walker (1985) observe that flood discharge is inferred from a rating curve which is subject to discontinuous measurement error. Consider Figure 3.2.5 which depicts a rating curve with two regions having different error

characteristics. The interpolation zone consists of that part of the rating curve well defined by discharge-stage measurements; typically the error Coefficient of Variation (CV) would be small, say 1 to 5%. In the extension zone the rating curve is extended by methods such as slope-conveyance, log-log extrapolation or fitting to indirect discharge estimates. Typically such extensions are smooth and, therefore, can induce systematic under- or over-estimation of the true discharge over a range of stages. The extension error CV is not well known but (Potter and Walker, 1981; Potter and Walker, 1985) suggest it may be as high as 30%.

Figure 3.2.5 and Figure 3.2.6 illustrate two cases of smooth rating curve extension wherein systematic error is introduced. In Figure 3.2.5, the estimate was below the true discharge. In the absence of any other information the rating curve is extended to pass smoothly through this point thereby introducing a systematic underestimate of large flood discharges. Even if more than one indirect discharge estimate were available, it is likely the errors will be correlated because the same biases in estimating Manning's  $n$ , conveyance and friction slope would be present

In Figure 3.2.6 the rating curve is extended using the slope-conveyance method. The method relies on extrapolating gauged estimates of the friction slope so that the friction slope asymptotes to a constant value. Depending on how well the approach to asymptotic conditions is defined by the data considerable systematic error in extrapolation may occur. Perhaps of greater concern is the assumption that Manning's  $n$  and conveyance can be reliably estimated in the overbank flow regime particularly when there are strong contrasts in roughness along the wetted perimeter.

Though Figure 3.2.5 represents an idealisation of actual rating curve extension two points of practical significance are noted:

1. The error is systematic in the sense that the extended rating curve is likely to diverge from the true rating curve as discharge increases. The error, therefore, is likely to be highly correlated- in fact, it is perfectly correlated in the idealisation of Figure 3.2.5.
2. The interpolation zone anchors the error in the extension zone. Therefore, the error in the extension zone depends on the distance from the anchor point and not from the origin. This error is termed incremental because it originates from the anchor point rather than the origin of the rating curve.

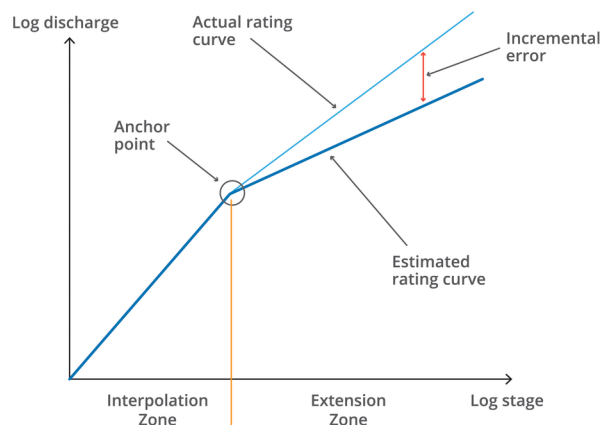


Figure 3.2.5. Rating Curve Extension by Fitting to an Indirect Discharge Estimate

## At-Site Flood Frequency Analysis

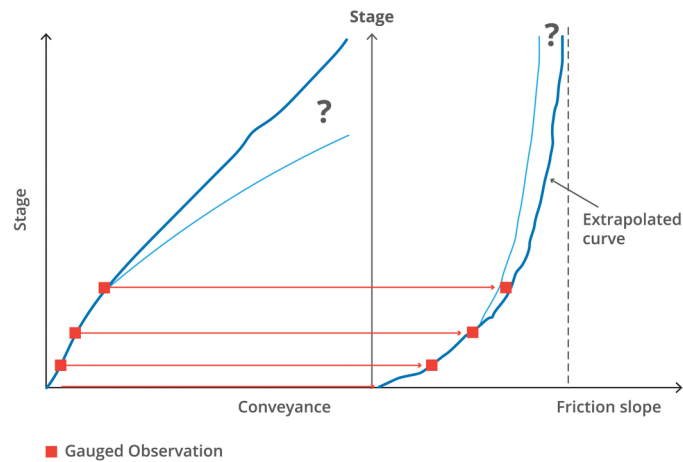


Figure 3.2.6. Rating Curve Extension by Slope-Conveyance Method

### 2.3.8. Historical and Paleo Flood Information

A flood may have occurred before the period of gauged record and known to be the largest flood, or flood of other known rank, over a period longer than that of the gauged record. Such floods can provide valuable information and should be included in the analysis if possible.

Care is needed in assessing historical floods. Only stages are usually available, and these may be determined by flood marks recorded on buildings or structures, by old newspaper reports, or from verbal evidence. Newspaper or other photographs can provide valuable information. Verbal evidence is often untrustworthy, and structures may have been moved. A further problem is that the channel morphology, and hence the stage-discharge relation of the stream, may have changed from those applying during the period of gauged record.

It is desirable to carry out Flood Frequency Analyses both by including and excluding the historical data. The analysis including the historical data should be used unless in the comparison of the two analyses, the magnitudes of the observed peaks, uncertainty regarding the accuracy of the historical peaks, or other factors, suggest that the historical peaks are not indicative of the extended period or are not accurate. All decisions made should be thoroughly documented.

Considerable work has been carried out in the United States on the assessment of paleofloods. These are major floods that have occurred outside the historical record, but which are evidenced by geological, geomorphological or botanical information. Techniques of paleohydrology have been described by [Costa \(1978\)](#), [Costa \(1983\)](#), [Costa \(1986\)](#) and [Kochel et al. \(1982\)](#) and more recently by [O'Connell et al. \(2002\)](#), and a succinct summary is given by [Stedinger and Cohn \(1986\)](#). Although high accuracy is not possible with these estimates, they may only be marginally less accurate than other estimates requiring extrapolation of rating curves, and they have the potential for greatly extending the database and providing valuable information on the tail of the underlying flood distribution. A procedure for assessing the value of paleoflood estimates of Flood Frequency Analysis is given by [Hosking and Wallis \(1986\)](#). Only a little work on this topic has been carried out in Australia, but its potential has been indicated by its use to identify the five largest floods in the last 700 years in the Finke River Gorge in central Australia ([Baker et al., 1983](#); [Baker, 1984](#)), and for more frequent floods, by identification of the six largest floods that occurred since a major flood in 1897 on the Katherine River in the Northern Territory ([Baker, 1984](#)). While the use of paleoflood data should be considered, it needs to be recognized that there

are not many sites where paleofloods can be estimated and that climate changes may have affected the homogeneity of long-term flood data.

### 2.3.9. Data Characterising Long-Term Climate Persistence

There is growing evidence that flood peaks are not identically distributed from year to year in some parts of Australia and that flood risk is dependent on long-term climate variability. The idea of alternating flood and drought dominated regimes that exist on decadal and longer timescales was first proposed by [Erskine and Warner \(1988\)](#). More recently, analyses of changes in climate state affecting flood risk have been published (refer to [Franks and Kuczera \(2002\)](#), [Franks \(2002a\)](#), and [Franks \(2002b\)](#)). The climate-dependence of flood risk is an important consideration when assessing flood risk. Most flood frequency applications will require assessment of long-term flood risk; that is, flood risk that is independent of a particular current climate state. If a flood record is sufficiently long to sample all climate states affecting flood risk, a traditional analysis assuming homogeneity will yield the long-term flood risk. Unfortunately many flood records are relatively short and may be dominated by one climate state. Blind use of such data can result in substantial bias in long-term flood risk estimates. For this reason it may be necessary to obtain climate index data which characterizes long-term persistence in climate and to investigate the homogeneity of the flood distribution.

A number of known climate phenomena impact on Australian climate variability. Most well known is the inter-annual El Niño/Southern Oscillation (ENSO). The cold ENSO phase, La Niña, results in a marked increase in flood risk across Eastern Australia, whereas El Niño years are typically without large floods ([Kiem et al., 2003](#)).

There is also mounting evidence that longer-term climate processes also have a major impact on flood risk. The Interdecadal Pacific Oscillation (IPO) is a low frequency climate process related to the variable epochs of warming and cooling in the Pacific Ocean and is described by an index derived from low pass filtering of Sea Surface Temperature (SST) anomalies in the Pacific Ocean ([Power et al., 1998](#); [Power et al., 1999](#); [Allan, 2000](#)). The IPO is similar to the Pacific Decadal Oscillation (PDO) of [Mantua et al \(1997\)](#), which is defined as the leading principal component of North Pacific monthly sea surface temperature variability.

The IPO time series from 1870 is displayed in [Figure 3.2.7](#). It reveals extended periods where the index either lies below or above zero. [Power et al. \(1999\)](#) have shown that the association between ENSO and Australian climate is modulated by the IPO- a strong association was found between the magnitude of ENSO impacts during negative IPO phases, whilst positive IPO phases showed a weaker, less predictable relationship. Additionally, [Kiem et al. \(2003\)](#) and [Kiem and Franks \(2004\)](#) analysed New South Wales flood and drought data and demonstrated that the IPO negative state magnified the impact of La Niña events. Moreover, they demonstrated that the IPO negative phase, related to mid-latitude Pacific Ocean cooling, appears to result in an increased frequency of cold La Niña events. The net effect of the dual modulation of ENSO by IPO is the occurrence of multi-decadal periods of elevated and reduced flood risk. To place this in context, [Figure 3.2.8](#) shows regional flood index curves based on about 40 NSW sites for the different IPO states ([Kiem et al., 2003](#)) – the 1% AEP flood during years with a positive IPO index corresponds to the 1 in 6 AEP flood during years with a negative IPO index. [Micevski et al. \(2003\)](#) investigating a range of sites in NSW found that floods occurring during IPO negative periods were, on average, about 1.8 times bigger than floods with the same frequency during IPO positive periods.

## At-Site Flood Frequency Analysis

A key area of current research is the spatial variability of ENSO and IPO impacts. The associations between ENSO, IPO and eastern Australian climate have been investigated from a mechanistic approach. [Folland et al. \(2002\)](#) showed that ENSO and IPO both affect the location of the South Pacific Convergence Zone (SPCZ) providing a mechanistic justification for the role of La Nina and IPO negative periods in enhancing flood risk in eastern Australia.

Whilst the work to date has primarily focused on eastern Australia, a substantial step change in climate also occurred in Western Australia around the mid-1970's, in line with the IPO and PDO indices ([Franks, 2002b](#)), however the role of ENSO is less clear and is likely to be additionally complicated by the role of the Indian Ocean.

The finding that flood risk in parts of Australia is modulated by low frequency climate variability is recent. Practitioners are reminded that this is an area of active research and therefore should keep abreast of future developments.

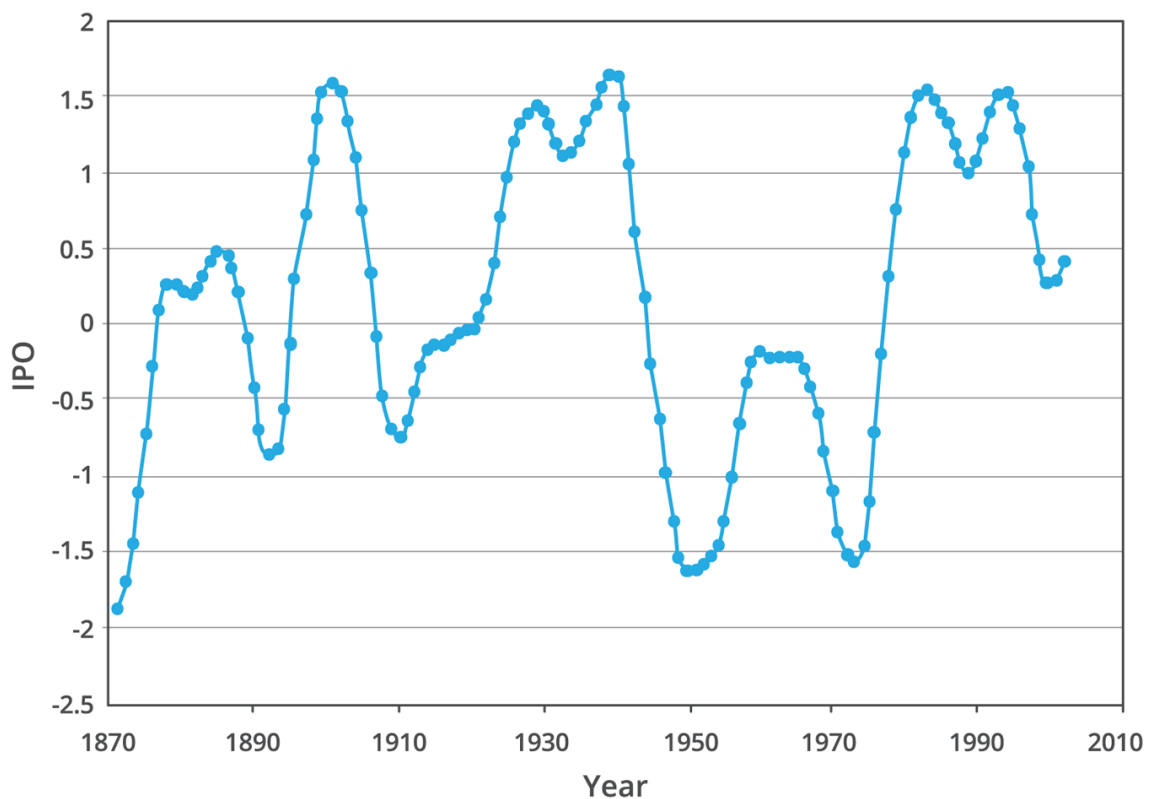


Figure 3.2.7. Annual Average Interdecadal Pacific Oscillation Time Series



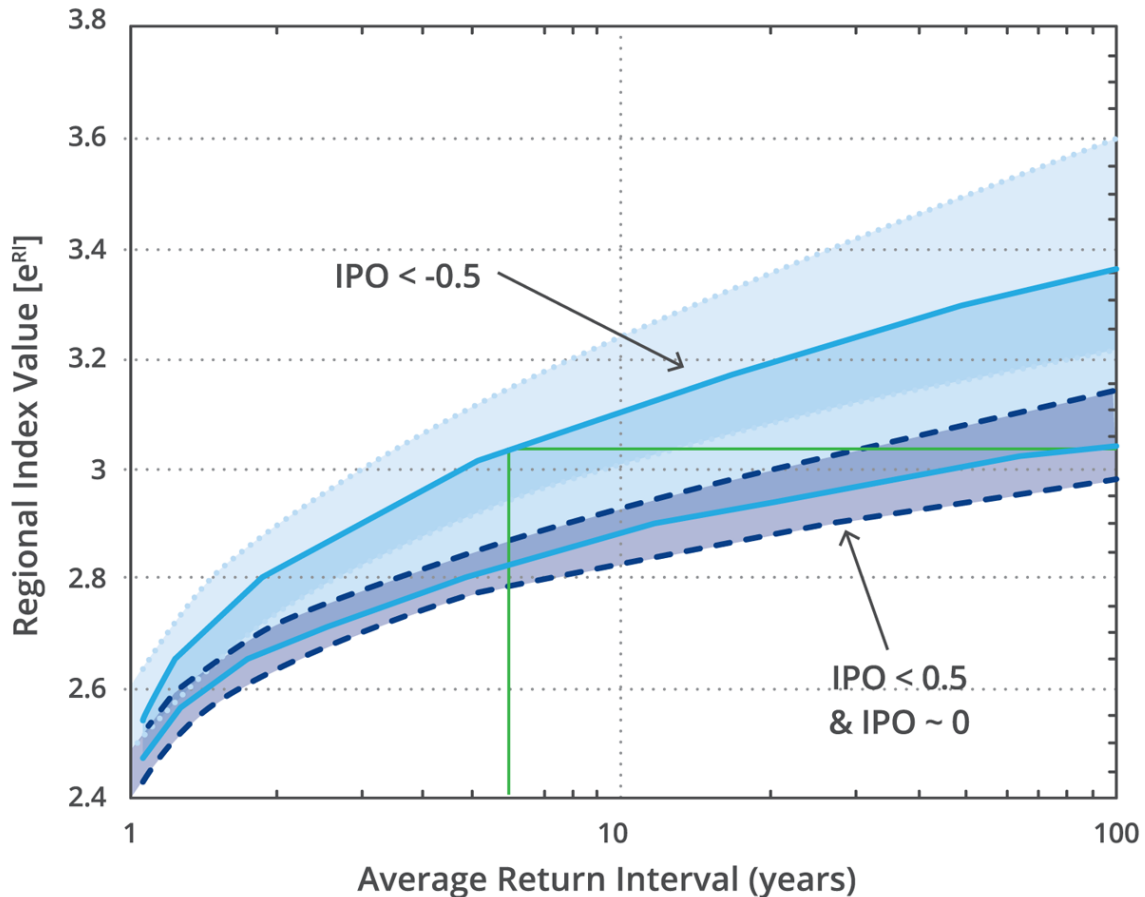


Figure 3.2.8. NSW Regional Flood Index Frequency Curves for Positive and Negative Interdecadal Pacific Oscillation epochs (Kiem et al., 2003)

### 2.3.10. Regional Flood Information

Whereas the primary focus of this chapter is Flood Frequency Analysis using at-site information, the accuracy of the frequency analysis can be improved, substantially in some cases, by augmenting at-site information with regional information. Subsequent chapters in this Book describe methods for estimating flood frequency at ungauged sites. Provided such methods also provide estimates of uncertainty, the regional information can be pooled with the at-site information to yield more accurate results. Book 3, Chapter 2, Section 6 shows how regional information on flood probability model parameters can be pooled with at-site information. When pooling at-site and regional information it is important to establish that both sources of information are consistent – that is, they yield statistically consistent results.

### 2.3.11. Missing Records

Streamflow data frequently contain gaps for a variety of reasons including the malfunction of recording equipment. Rainfall records on the catchment and streamflow data from nearby catchments may indicate the likelihood of a large flood having occurred during the gap. A regression may be able to be derived to enable a missing flood to be estimated, but as discussed in Book 3, Chapter 2, Section 3, the degree of correlation is often insufficient for a quantitative estimate.

For AM series the missing record period is of no consequence and can be included in the period of record, if it can be determined that the largest discharge for the year occurred outside the gap, or that no large rainfall occurred during the gap. However the rainfall records and streamflow on nearby catchments might indicate that a large flood could have occurred during the period of missing record. If a regression with good correlation can be derived from concurrent records, the missing flood can be estimated and used as the annual flood for the year. If the flood cannot be estimated with reasonable certainty, the whole year should be excluded from the analysis.

For POT series data, treatment of missing records is less clear. McDermott and Pilgrim (1982) tested seven methods, leading to the following recommendations based on the assumption that the periods of missing data are random occurrences and are independent of the occurrence of flood peaks.

1. Where a nearby station record exists covering the missing record period, and a good relation between the flood peaks on the two catchments can be obtained, then use this relation and the nearby station record to fill in the missing events of interest.
2. Where a nearby station record exists covering the missing record period, and the relation between the flood peaks on the two catchments is such that only the occurrence of an event can be predicted but not its magnitude, then:
  - For record lengths less than 20 years, ignore the missing data and include the missing period in the overall period of record;
  - For record lengths greater than 20 years, subtract an amount from each year with missing data proportional to the ratio of the number of peaks missed to the total number of ranked peaks in the year.
3. Where no nearby station record exists covering the missing record period, or where no relation between flood peaks on the catchment exists, then ignore the missing data and include the missing record period in the overall period of record.

## 2.4. Choice of Flood Probability Model

### 2.4.1. General

As noted in Book 3, Chapter 2, Section 2, it is assumed that each flood peak in an AM or POT series is statistically independent of other flood peaks in the series. In addition, the flood probability model, described by its probability density function (pdf)  $p(q|\theta)$ , must be specified.

There is no universally accepted flood probability model. Many types of probability distributions have been applied to Flood Frequency Analysis. Unfortunately, it is not possible to determine the true form of distribution (for example, Cunnane (1985)), and there is no rigorous analytical proof that any particular probability distribution for floods is the correct theoretical distribution. The appropriateness of these distributions can be tested by examining the fit of each distribution to observed flood data. Various empirical tests of different distributions have been carried out with recorded data from many catchments, however, conclusive evidence is not possible largely because gauged records are of insufficient length to eliminate the confounding effect of sampling variability. Examples of sampling experiments illustrating this problem are given by Alexander (1957) and Dalrymple (1960). The choice of flood probability model is further exacerbated by recent evidence that

in certain parts of Australia, the flood record is not homogeneous due to variations in long-term climate controls.

Given these considerations, it is inappropriate to be prescriptive with regard to choice of flood probability model. As a general rule, the selected probability distribution family should be consistent with available data. It is recognised that more than one probability distribution family may be consistent with the data. One approach to deal with this problem is to select the distribution family on the basis of best overall fit to a range of catchments within a region or landscape space – L-moment diagrams offer a useful tool for judging overall goodness of fit (refer to Stedinger et al. (1993), Section 18.3.3 for more details).

## 2.4.2. Choice of Distribution Family for Annual Maximum Series

Two distribution families are suggested as reasonable initial choices for AM series, namely the Generalized Extreme Value (GEV) and Log Pearson III (LP III) families. These families fit most AM flood data adequately. Nonetheless, the practitioner is reminded that there is no rigorous justification for these families, which is particularly important when extrapolating – Book 3, Chapter 2, Section 8 demonstrates the importance of understanding the mechanisms controlling flood response. The following sections describe the GEV and LP III distributions and some other distributions that may be more appropriate in certain circumstances.

### 2.4.2.1. Generalized Extreme Value (GEV) Distribution

Table 3.2.1 lists the pdf  $p(q|\theta)$  distribution function  $P(Q \leq q|\theta)$  and product moments for the GEV distribution. It has three parameters:  $\tau$ , the location parameter,  $\alpha$  the scale parameter and  $\kappa$  the shape parameter. When the shape parameter  $\kappa$  equals 0, the GEV simplifies to the Gumbel distribution, whose details are also presented in Table 3.2.1. For positive values of  $\kappa$  there exists an upper bound, while for negative  $\kappa$ , there exists a lower bound. The 1 in Y AEP quantile  $q_Y$  is given by:

$$q_Y = \begin{cases} \tau + \frac{\alpha}{\kappa} \left[ 1 - \left( -\log_e \left( 1 - \frac{1}{Y} \right) \right)^\kappa \right], & \kappa \neq 0 \\ \tau - \alpha \log_e \left( -\log_e \left( 1 - \frac{1}{Y} \right) \right), & \kappa = 0 \end{cases} \quad (3.2.15)$$

At-Site Flood Frequency  
Analysis

Table 3.2.1. Selected Homogeneous Probability Models Families for use in Flood Frequency  
Analysis

Family	Distribution	Moments
Generalized Extreme Value (GEV)	$p(q \theta) = \frac{1}{\alpha} e^{\left\{ -\left[1 - \frac{\kappa(q-\tau)}{\alpha}\right]^{\frac{1}{\kappa}} \right\} \left[1 - \frac{\kappa(q-\tau)}{\alpha}\right]^{\frac{1}{\kappa} - 1}}$ $P(Q \leq q \theta) = e^{\left\{ -\left[1 - \frac{\kappa(q-\tau)}{\alpha}\right]^{\frac{1}{\kappa}} \right\}}$ <p>when <math>\kappa &gt; 0, q &lt; \tau + \frac{\alpha}{\kappa}</math>; when <math>\kappa &lt; 0, q &gt; \tau + \frac{\alpha}{\kappa}</math></p>	$\text{Mean}(q) = \tau + \frac{\alpha}{\kappa} [1 - \Gamma(1 + \kappa)]$ <p>for <math>\kappa &gt; -1</math></p> $\text{Variance}(q) = \frac{\alpha^2}{\kappa^2} [\Gamma(1 + 2\kappa) - [\Gamma(1 + \kappa)]^2]$ <p>for <math>\kappa &gt; -\frac{1}{2}</math></p> <p>where <math>\Gamma(\ )</math> is the gamma function</p>
Gumbel	$p(q \theta) = \frac{1}{\alpha} e^{-\frac{(q-\tau)}{\alpha}} e^{-e^{-\frac{(q-\tau)}{\alpha}}}$ $P(Q \leq q \theta) = e^{-e^{-\frac{(q-\tau)}{\alpha}}}$	$\text{Mean}(q) = \tau + 0.5772\alpha$ $\text{Variance}(q) = \frac{\pi^2 \alpha^2}{6}$ $\text{Skew}(q) = 1.1396$
Log Pearson III (LP III)	$p(q \theta) = \frac{ \beta }{q\Gamma(\alpha)} [\beta(\log_e q - \tau)]^{\alpha-1} e^{-\beta(\log_e q - \tau)}$ <p><math>\alpha &gt; 0</math> when <math>\beta &gt; 0, \log_e q &gt; \tau</math>; when <math>\beta &lt; 0, \log_e q &lt; \tau</math></p>	$\text{Mean}(\log_e q) = m = \tau + \frac{\alpha}{\beta}$ $\text{Variance}(\log_e q) = s^2 = \frac{\alpha}{\beta^2}$ $\text{Skew}(\log_e q) = g = \begin{cases} \frac{2}{\sqrt{\alpha}} & \text{if } \beta > 0 \\ -\frac{2}{\sqrt{\alpha}} & \text{if } \beta < 0 \end{cases}$
log-Normal	$p(q \theta) = \frac{1}{q\sqrt{2\pi s^2}} e^{\left[ -\frac{1}{2s^2} (\log_e q - m)^2 \right]}$ <p><math>q &gt; 0, s &gt; 0</math></p>	$\text{Mean}(\log_e q) = m$ $\text{Variance}(\log_e q) = s^2$
Generalized Pareto	$p(q \theta) = \frac{1}{\beta} \left(1 - \frac{\kappa(q-q_*)}{\beta}\right)^{\frac{1}{\kappa} - 1}$ $P(Q \leq q \theta) = 1 - \left(1 - \frac{\kappa(q-q_*)}{\beta}\right)^{\frac{1}{\kappa}}$ <p>when <math>\kappa &lt; 0, q_* \leq q &lt; \infty</math>; when <math>\kappa &gt; 0, q_* \leq q \leq \frac{\beta}{\kappa}</math></p>	$\text{Mean}(q) = q_* + \frac{\beta}{1 + \kappa}$ $\text{Variance}(q) = \frac{\beta^2}{(1 + \kappa)^2 (1 + 2\kappa)}$ $\text{Skew}(q) = \frac{2(1 - \kappa)(1 + 2\kappa)^{\frac{1}{2}}}{(1 + 3\kappa)} \cdot \kappa > -1/3$
Exponential	$p(q \theta) = \frac{1}{\beta} e^{\left(-\frac{q-q_*}{\beta}\right)}$ $P(Q \leq q \theta) = 1 - e^{\left(-\frac{q-q_*}{\beta}\right)}, q \geq q_*$	$\text{Mean}(q) = q_* + \beta$ $\text{Variance}(q) = \beta^2$ $\text{Skew}(q) = 2$

Of the widely used distribution families, the GEV distribution has the strongest theoretical appeal as it is the asymptotic distribution of extreme values for a wide range of underlying parent distributions. In the context of flood frequency, suppose there are  $N$  flood peaks in a year. Provided  $N$  is large and the flood peaks are identically and independently distributed, the distribution of the largest peak discharge in the year approaches the GEV under quite general conditions. However, it is questionable whether these assumptions are satisfied in practice.

The number of independent flood peaks in any year may not be sufficient to ensure asymptotic behaviour particularly for catchments that tend to aridity. Moreover, in strongly seasonal climates, it is unlikely that the within-year independent flood peaks are random realisations from the same probability distribution.

The GEV has gained widespread acceptance (for example, Natural Environment Research Council (1975), Wallis and Wood (1985), and (Stedinger et al., 1993)).

### 2.4.2.2. Log Pearson III Distribution

Table 3.2.1 lists the pdf  $p(q|\theta)$  and product moments for Log Pearson III (LP III) distribution. It has three parameters:  $\tau$ , the location parameter,  $\alpha$  the scale parameter and  $\beta$  the shape parameter. When the skew of  $\log q$  is zero, the distribution simplifies to the log-Normal, whose details are provided in Table 3.2.1.

The LP III distribution is widely accepted in practice as it consistently fits flood data as well, if not better than other probability families. It has performed best of those that have been tested on data for Australian catchments (Conway, 1970; Kopittke et al., 1976; McMahon, 1979; McMahon and Srikanthan, 1981). It is the recommended distribution for the United States in Bulletin 17B of the Interagency Advisory Committee on Water Data (1982).

The distribution, however, is not well-behaved from an inference perspective. Direct inference of the parameters  $\alpha, \beta$  and  $\tau$  can cause numerical problems. For example, when the skew of  $\log q$  is close to zero, the shape parameter  $\alpha$  tends to infinity. Experience indicates it is preferable to fit the first three moments of  $\log q$  rather than  $\alpha, \beta$  and  $\tau$ . Note that  $\tau$  is a lower bound for positive skew and an upper bound for negative skew.

A problem arises when the absolute value of the skew of  $\log q$  exceeds 2; that is, when  $\alpha \geq 1$ . When  $\alpha < 1$ , the LP III has a gamma-shaped density. However, when  $\alpha \geq 1$ , the density changes to a J-shaped function. Indeed when  $\alpha = 1$ , the pdf degenerates to that of an exponential distribution with scale parameter  $\beta$  and location parameter  $\tau$ . For  $\alpha \geq 1$ , the J-shaped density seems to be over-parameterised with three parameters. In such circumstances, it is pointless to use the LP III. It is suggested that either the GEV or the Generalized Pareto (GP) Distributions should be used as a substitute.

An analytical form of the distribution function is not available for the LP III and log-Normal distributions. To compute the quantile  $q_Y$  (that is, the discharge with a 1 in  $Y$  AEP) the following equation may be used:

$$\log(q_Y) = m + K_Y(g)s \quad (3.2.16)$$

where  $m$ ,  $s$  and  $g$  are the mean, standard deviation and skewness of the log discharge and  $K_Y$  is a frequency factor well-approximated by the Wilson-Hilferty transformation:

$$K_Y(g) = \begin{cases} \frac{2}{g} \left[ \left\{ \frac{g}{6} \left( Z_Y - \frac{g}{6} \right) + 1 \right\}^3 - 1 \right] & \text{if } |g| > 0 \\ 0 & \text{if } g = 0 \end{cases} \quad (3.2.17)$$

for  $|g| < 2$  and AEPs ranging from 99% to 1% AEP. The term  $Z_Y$  is the frequency factor for the standard normal distribution which has a mean of zero and standard deviation of 1;  $Z_Y$  is the value of the standard normal deviate with exceedance probability  $1/Y$ . [Table 3.2.2](#) lists  $Z_Y$  for selected exceedance probabilities. Comprehensive tables of  $K_Y$  can be found in ([Pilgrim, 1987](#)).

Table 3.2.2. Frequency factors for standard normal distribution.

AEP (%)	Y in AEP of 1 in Y	$Z_Y$
50	2	0.0000
20	5	0.8416
10	10	1.2816
5	20	1.6449
2	50	2.0537
1	100	2.3263
0.5	200	2.5758
0.2	500	2.8782
0.1	1000	3.0902

### 2.4.2.3. Generalized Pareto Distribution

In POT modelling, the GP distribution is often found to satisfactorily fit the data. [Table 3.2.1](#) lists the pdf  $p(q|\theta)$ , distribution function  $P(Q \leq q|\theta)$  and product moments for the GP distribution. It has three parameters:  $q_*$ , the location parameter,  $\beta$ , the scale parameter and  $\kappa$ , the shape parameter. When  $\kappa$  equals zero, the distribution simplifies to the exponential distribution, also described in [Table 3.2.1](#).

$$q_Y = \begin{cases} q_* + \frac{\beta}{\kappa} \left[ 1 - \left( \frac{1}{Y} \right)^\kappa \right], & \kappa \neq 0 \\ q_* - \beta \log_e \left( \frac{1}{Y} \right), & \kappa = 0 \end{cases} \quad (3.2.18)$$

The GP distribution has an intimate relationship with the GEV. If the GP describes the distribution of peaks over a threshold, then for Poisson arrivals of the POT peaks with  $\nu$  being the average number of arrivals per year, it can be shown that the distribution of Annual Maximum peaks is GEV with shape parameter  $\kappa$ , scale parameter and location parameter:

$$\alpha = \beta \nu^{-\kappa} \quad (3.2.19)$$

and location parameter

$$\tau = q_* + \frac{\beta}{\kappa} \quad (3.2.20)$$

#### 2.4.2.4. Zero-threshold mixture model

In certain parts of Australia, the AM flood series may contain one or more years of zero or virtually zero flow. In such cases, the flood probability model is best described by a two-component mixture model. In any year, there are two possibilities:

1. There is a (fixed) probability  $P_0$  that the peak flow equals the zero-threshold flow  $q_0$ , which may be zero or a near-zero flow; and
2. There is a probability  $1 - P_0$  that the peak flow exceeds the threshold. In that case the distribution of the peak flow follows a standard probability model.

A formal definition of this model can be found in [Formal Definition of Zero-Threshold Mixture Distribution](#).

##### Formal Definition of Zero-Threshold Mixture Distribution

The zero-threshold mixture model has a distribution function:

$$P(Q \leq q|\theta) = \begin{cases} P_0 & \text{if } q = q_0 \\ P_0 + (1 - P_0) \frac{P(Q \leq q|\theta) - P(Q \leq q_0|\theta)}{P(Q > q_0|\theta)} & \text{if } q > q_0 \end{cases} \quad (3.2.21)$$

where  $q_0$  is the zero-threshold flow,  $P_0$  is the probability of the AM peak equaling  $q_0$  and  $P(Q \leq q|\theta)$  is a probability model such as described in [Table 3.2.1](#).

The pdf of the mixture model can be expressed using the generalized probability density which allows the random variable to take discrete values as well as continuous values:

$$p(q|\theta) = \begin{cases} P_0 & \text{if } q = q_0 \\ \frac{1 - P_0}{P(Q > q_0|\theta)} p(q|\theta) & \text{if } q > q_0 \end{cases} \quad (3.2.22)$$

#### 2.4.2.5. Multi-Component or Mixture Models

In some areas, flooding may be affected by different types of meteorological events (for example, intense tropical cyclones and storms characterised by more usual synoptic conditions) or by changing hydraulic controls (e.g., see [Book 3, Chapter 2, Section 8](#)), causing abnormal slope changes in the frequency curve. In such cases, the GEV or LP III families may not adequately fit the data. This type of problem may be of particular importance in northern Australia, and an example is described by [Ashkanasy and Weeks \(1975\)](#). It may be desirable to separate the data by cause and analyse each set separately. The above reference describes a procedure using a combination of two log-Normal distributions. A two-component extreme value distribution has been described by [Rossi et al. \(1984\)](#) and [Fiorentino et al. \(1985\)](#), and developed and applied to U.K. data by [Beran et al. \(1986\)](#). Alternatively, the four or five parameter Wakeby distribution may be used to fit such data ([Houghton, 1978](#)).

### 2.4.2.6. Non-Homogeneous Models

If the evidence suggests that flood risk is affected by multi-decadal climate persistence, the use of non-homogeneous probability models may need to be investigated. The concern is that ignoring the non-homogeneity of the flood record may lead to biased estimates of long-term flood risk.

If a non-homogeneous probability model with pdf  $p(q|\theta(x))$  is identified, this cannot be used to estimate long-term or marginal flood risk. This is because flood risk is dependent on the exogenous variables  $x$ . To estimate long-term flood risk, the dependence on  $x$  must be removed using the total probability rule to give:

$$P(Q \leq q) = \int_x \left( \int_0^q p(z | \theta(x)) dz \right) p(x) dx \quad (3.2.23)$$

where  $p(x)$  is the pdf of the exogenous variables.

If the gauged record adequately samples the distribution of  $x$ , it is not necessary to identify a non-homogeneous model. It suffices to fit a probability model to all the record to estimate the long-term flood risk.

However, if the gauged record does not adequately sample  $x$ , significant bias in flood risk may result if only at-site data are used. In such instances, it will be necessary to employ regional frequency methods that take the non-homogeneity into account. This is an area of current research. Practitioners are advised to keep abreast of new developments.

Book 3, Chapter 2, Section 8 illustrates the impact on flood risk arising from multi-decadal persistence in climate state as represented by the IPO index. It illustrates how the exogenous variable  $x$  can be constructed, demonstrates the serious bias in flood risk that can arise if short records do not adequately sample different climate states and illustrates the use of Equation (3.2.23).

### 2.4.3. Choice of Distribution for Peak-Over-Threshold Series

In some cases, it may be desirable to analytically fit a probability distribution to POT data. Distributions that have been used to describe the flood peak above a threshold include the exponential, GP and LP III.

## 2.5. Choice of Flood Quantile Estimator

This section considers the following question: Given data  $D$ , what is the best estimate of the 1 in  $Y$  AEP flood discharge.

If the true value of  $\theta$  were known, then the pdf  $p(q|\theta)$  can be used to compute the flood quantile  $q_Y(\theta)$ . For AM series the 1 in  $Y$  AEP quantile is defined as:

$$P(Q \leq q_Y | \theta) = \frac{1}{Y} = \int_{q_Y}^{\infty} p(q | \theta) dq \quad (3.2.24)$$



However, in practice the true value of  $\theta$  (as well as the distribution family) is unknown. All that is known about  $\theta$ , given the data  $D$ , is summarized by a probability distribution with pdf  $p(\theta|D)$ . Book 3, Chapter 2, Section 6 describes how this distribution may be obtained – this distribution is the posterior distribution if performing a Bayesian analysis or the sampling distribution if performing a bootstrap analysis.

If the true value of  $\theta$  is not known, it follows that the true value of the quantile  $q_Y(\theta)$  is not known. The uncertainty about  $\theta$  described by the pdf  $p(\theta|D)$ , translates into uncertainty about the quantile, described by the quantile predictive pdf  $p(q_Y|D)$ . The question then arises, which value from the quantile predictive pdf  $p(q_Y|D)$  should be adopted as the flood quantile estimate? This section presents two approaches for determining the best estimate of a flood discharge with a 1 in  $Y$  AEP knowing the pdf  $p(\theta|D)$ .

### 2.5.1. Expected Parameter Quantiles

In general the estimation of a design quantile should be guided by the consequences of under or over-design (Slack et al., 1975). This section considers the case where the consequence of over- and under-design is expressed by some measure of the difference between the true and estimated 1 in  $Y$  AEP quantiles – this difference is called the quantile error.

The loss function  $L[q_Y(D), q_Y(\theta)]$  describes the loss or consequence when the true quantile  $q_Y(\theta)$ , which depends on  $\theta$ , is incorrectly estimated by  $q_Y(D)$ , which depends on the data  $D$ . Because the true value of  $\theta$  is uncertain, the best estimator  $q_Y(D)_{opt}$  is the one that minimises the expected loss:

$$q_Y(D)_{opt} \leftarrow \min_{\theta} \int L[q_Y(D), q_Y(\theta)] p(\theta|D) d\theta \quad (3.2.25)$$

The optimal quantile estimator depends on the choice of loss function.

#### 2.5.1.1. Quadratic loss

The quadratic loss function may be appropriate when the consequences of under or over-design are judged to be same and loss is proportional to the square of the quantile error. The loss function is expressed as:

$$L[q_Y(D), q_Y(\theta)] \propto [q_Y(D) - q_Y(\theta)]^2 \quad (3.2.26)$$

The expected value of this loss function is referred to as the Mean Squared Error (MSE), which shows that the optimal quantile estimator is the expected value of  $q_Y(D)$  (DeGroot, 1970):

$$E[q_Y|D] = \int q_Y(\theta) p(\theta|D) d\theta \quad (3.2.27)$$

Stedinger (1983) observes that this integral may not exist for some of the probability distributions used in Flood Frequency Analysis. To avoid this problem the following first-order approximation may be used:

$$E[q_Y|D] = q_Y[E(\theta|D)] \quad (3.2.28)$$

where  $E(\theta | D)$  is the expected parameter given the data D:

$$E[\theta | D] = \int \theta p(\theta | D) d\theta \quad (3.2.29)$$

The term  $q_Y [E(\theta | D)]$  is referred to as the expected parameter 1 in Y AEP quantile. When this term is used it is understood that the quantile is computed with  $\theta$  assigned  $[E(\theta | D)]$ .

### 2.5.1.2. Linear asymmetric loss

The linear asymmetric loss function may be appropriate when the consequences of under and over-design are judged to be different. The loss function is expressed as:

$$L[q_Y(D), q_Y(\theta)] = \begin{cases} \alpha(q_Y(\theta) - q_Y(D)) & \text{if } q_Y(\theta) > q_Y(D), \text{ underdesign} \\ \beta(q_Y(D) - q_Y(\theta)) & \text{if } q_Y(\theta) \leq q_Y(D), \text{ overdesign} \end{cases} \quad (3.2.30)$$

where  $\alpha$  and  $\beta$  are the loss coefficients for under and over-design respectively. It can be shown that the quantile estimator that minimises the expected asymmetric linear loss must satisfy the following (DeGroot, 1970):

$$P(Q_Y \leq q_Y(D)_{opt} | D) = \frac{\alpha}{\alpha + \beta} \quad (3.2.31)$$

When  $\alpha$  equals  $\beta$ ,  $q_Y(D)_{opt}$ , it is the median of the quantile predictive distribution. However, when  $\alpha$  equals  $4\beta$ , it implies that the consequences of under-design are four times more severe than over-design, which is the 80-percentile of the predictive distribution, a far more conservative estimate than the median.

### 2.5.2. Expected AEP Quantiles

This section considers a different perspective on selecting a quantile estimator. In the previous section the uncertainty in the quantile for a given AEP was considered. In this section the uncertainty in AEP for a given  $q$  is considered.

Stedinger (1983) showed that the dependence of the flood peak pdf on uncertain parameters can be removed using total probability to yield the design flood distribution:

$$p(q|D) = \int_{\theta} p(q|\theta)p(\theta|D)d\theta \quad (3.2.32)$$

This distribution only depends on the data D (and the assumed probability family).

The design flood quantile  $q_Y$  with X% AEP can be derived by solving:

$$p(q > q_Y | D) = \int_{\theta} \left( \int_{q_Y}^{\infty} p(q|\theta) dq \right) p(\theta|D) d\theta = \frac{1}{Y} \quad (3.2.33)$$

This quantile is greater than the expected parameter X% AEP quantile  $q_Y [E(\theta | D)]$ . To gain further insight suppose we make  $q_Y$  equal to the expected parameter X% AEP quantile and compute its design flood AEP using Equation (3.2.33). Noting the inner integral is the probability of the flood peak exceeding  $q_Y$  given a particular value of  $\theta$ , Equation (3.2.33) can be rewritten as:

$$\begin{aligned}
 p(q > q_Y|D) &= \int_{\theta} \left( \int_{q_Y}^{\infty} p(q|\theta) dq \right) p(\theta|D) d\theta \\
 &= \int_{\theta} p(q > q_Y|D) p(\theta|D) d\theta \\
 &= \frac{1}{Y}
 \end{aligned}
 \tag{3.2.34}$$

It thus follows that the expected parameter 1 in Y AEP quantile  $q_Y[E(\theta|D)]$ . Moreover, it follows that the expected parameter 1 in Y AEP quantile  $q_Y[E(\theta|D)]$  has an expected AEP given by  $P(q > q_Y|D)$  which exceeds  $1/Y$ .

### 2.5.3. Selection of Flood Quantile Estimator

The choice of flood quantile estimator depends on whether the design is being carried out for many sites or a single site, on whether risk, actual discharge or average annual damage is of primary interest in design and on whether the consequences of under and over-design are different. The choice is somewhat subjective and may be a matter of policy. As a general guide, a non-exhaustive list of recommendations is given below:

1. In situations where there is indifference to the consequences of under or over-design, either the expected parameter or expected AEP quantile can be chosen.

Expected parameter quantiles may be applicable where:

- i. Sizing of a structure for a given AEP is the primary consideration and minimizing quadratic loss, as expressed by [Equation \(3.2.26\)](#), is a reasonable criterion.
- ii. Unbiased estimates of annual flood damages are required ([Doran and Irish, 1980](#)).

Expected AEP quantiles may be applicable where:

- i. Design is required for many sites in a region, and the objective is to attain a desired AEP over all sites.
  - ii. Probability of exceedance is of primary importance for design at a single site (such as in floodplain management).
2. If there are significant differences between the consequences of under and over-design, consideration should be given to using [Equation \(3.2.31\)](#) as the flood quantile estimator.

## 2.6. Fitting Flood Probability Models to Annual Maxima Series

### 2.6.1. Overview of Methods

Fitting a flood probability model involves three steps:

1. Calibrating the model to the available data D to determine the parameter values consistent with the data D.

2. Estimation of flood quantiles and their confidence limits.
3. Evaluation of goodness of fit and consistency of model with data.

Two calibration approaches are described involving Bayesian and L-moment techniques. For each approach, the algorithms are documented and illustrated with worked examples. Implementation of the algorithms in software requires specialist skill; therefore, a typical practitioner is advised to make use of the available software. The use of the method of product-moments applied to log flows is not recommended. The choice of calibration methods depends on the type of data available (gauged and censored), the extent of measurement error associated with the rating curve and the availability of regional information about parameters.

## 2.6.2. Probability Plots

An essential part of a Flood Frequency Analysis is the construction of an empirical distribution function, better known as a probability plot. In such a plot, an estimate of AEP is plotted against the observed discharge. This enables one to draw a smooth curve as an empirical probability distribution or to visually check the adequacy of a fitted distribution.

The following steps describe the production of a probability plot for gauged Annual Maximum floods:

- Rank the gauged discharges in descending order (that is, from largest to smallest) yielding the series  $\{q_{(1)}, q_{(2)}, \dots, q_{(n)}\}$  where  $q_{(i)}$  is the rank  $i$  or the  $i^{\text{th}}$  largest flood;
- Estimate the AEP for each  $q_{(i)}$  using a suitable plotting position; and
- Using suitable scales plot the estimated AEP against  $q_{(i)}$ .

For analysis of the AM series, a general formula (Blom, 1958) for estimating the AEP of an observed flood is:

$$P_{(i)} = \frac{i - \alpha}{n + 1 - 2\alpha} \quad (3.2.35)$$

where  $i$  is the rank of the gauged flood,  $n$  is the number of years of gauged floods and  $\alpha$  is a constant whose value is selected to preserve desirable statistical properties.

There are several choices for  $\alpha$ :

- $\alpha = 0$  yields the Weibull plotting position that produces unbiased estimates of the AEP of  $q_{(i)}$ ;
- $\alpha = 0.375$  yields the Blom's plotting position that produces unbiased quantile estimates for the normal distribution; and
- $\alpha = 0.4$  yields the Cunnane (1978) plotting position that produces nearly unbiased quantile estimates for a range of probability families.

While there are arguments in favour of plotting positions that yield unbiased AEPs, usage has favoured plotting positions that yield unbiased quantiles. To maintain consistency, it is recommended that the Cunnane plotting position is used, namely:

At-Site Flood Frequency  
Analysis

---

$$P_{(i)} = \frac{i - 0.4}{n + 0.2} \quad (3.2.36)$$

A more complete discussion on plotting positions can be found in Stedinger et al. (1993).

It is stressed that plotting positions should not be used as an estimate of the actual AEP or EY of an observed flood discharge. Such estimates should be obtained from the fitted distribution.

Judicious choice of scale for the probability plot can assist the evaluation of goodness of fit. The basic idea is to select a scale so that the data plot as a straight line if the data is consistent with the assumed probability model.

This is best illustrated by an example. Suppose that floods follow an exponential distribution, then from Table 3.2.1, the distribution function is:

$$P(Q \leq q) = 1 - e^{-\frac{q - q_*}{\beta}} \quad (3.2.37)$$

Replacing  $q$  by  $q_{(i)}$  and  $1 - P(Q \leq q)$  by the plotting position of  $q_{(i)}$  gives:

$$1 - P_{(i)} = e^{-\frac{q_{(i)} - q_*}{\beta}} \quad (3.2.38)$$

Making  $q_{(i)}$  the subject of the equation yields

$$q_{(i)} = q_* - \beta \log_e P_{(i)} \quad (3.2.39)$$

If  $q_{(i)}$  is plotted against  $\log_e P_{(i)}$ , the data will plot approximately as a straight line if they are consistent with the exponential distribution.

Examples for other distributions include:

- For the Gumbel distribution plot  $q_{(i)}$  against  $-\log[-\log(1 - P_{(i)})]$ . Data following a GEV distribution will plot as a curved line.
- For the log normal distribution plot  $\log q_{(i)}$  against the standard normal deviate with exceedance probability  $P_{(i)}$ . Data following a LP III distribution will plot as a curved line.

When visually evaluating the goodness of fit care needs to be exercised in judging the significance of departures from the assumed distribution. Plotting positions are correlated. As a result, they do not scatter about the fitted distribution independently of each other. The correlation can induce “waves” or regions of systematic departure from the fitted distribution. To guard against this it is suggested that statistical tests be used to assist goodness-of-fit assessment. Stedinger et al. (1993) discuss the use of the Kolmogorov-Smirnov test, the Filiben probability plot correlation test and L-moment diagrams and ratio tests.

The estimation of plotting positions for censored and historic data is more involved and in some cases can be inaccurate refer to Stedinger et al. (1993) for more details.

## 2.6.3. Bayesian Calibration

### 2.6.3.1. Overview

The Bayesian approach is a very general approach for calibrating and identifying models. The Handbook of Hydrology [Stedinger et al. \(1993\)](#) observes that “the Bayesian approach... allows the explicit modeling of uncertainty in parameters and provides a theoretically consistent framework for integrating systematic flow records with regional and other hydrologic information”. However, it is only with the advent of new computational methods that Bayesian methods can be routinely applied to flood frequency applications.

The core of the Bayesian approach is described below – refer to [Lee \(1989\)](#) and [Gelman et al. \(1995\)](#) for general expositions. The data  $D$  is hypothesised to be a random realisation from a probability model with pdf  $p(D|\theta)$  where  $\theta$  is a vector of unknown parameters. The pdf  $p(D|\theta)$  is given two labels depending on the context. When  $p(D|\theta)$  is used to describe the probability model generating the sample data  $D$  for a given  $\theta$ , it is called the sampling distribution. However, when inference about the parameter  $\theta$  is sought,  $p(D|\theta)$  is called the likelihood function to emphasise that the data  $D$  is known and the parameter  $\theta$  is the object of attention. The same notation for the sampling distribution and likelihood function is used to emphasise its oneness.

In Bayesian inference, the parameter vector  $\theta$  is considered to be a random vector whose probability distribution describes what is known about the true value of  $\theta$ . Prior to analysing the data  $D$ , knowledge about  $\theta$ , given the probability model, is summarised by the pdf  $p(\theta)$ . This density, referred to as the prior density, can incorporate subjective belief about  $\theta$ .

Bayes theorem is then used to process the information contained in the data  $D$  by updating what is known about the true value of  $\theta$  as follows:

$$p(\theta|D) = \frac{p(D|\theta)p(\theta)}{p(D)} \propto p(D|\theta)p(\theta) \quad (3.2.40)$$

The posterior density  $p(\theta|D)$  describes what is known about the true value of  $\theta$  given the data  $D$ , prior information and the probability model. The denominator  $p(D)$  is the marginal likelihood defined as:

$$p(D) = \int p(D|\theta)p(\theta)d\theta \quad (3.2.41)$$

Usually the marginal likelihood is not computed as it does not depend on  $\theta$  and serves as a normalizing constant.

### 2.6.3.2. Likelihood Function

The key to a Bayesian analysis is the formulation of the likelihood function. In the context of flood frequency, analysis two formulations are considered. The first assumes there is no error in the flood data. The focus is on the contribution to the likelihood function made by gauged and censored data. The second case generalises the likelihood function to allow for error-in-discharge estimates.

### 2.6.3.3. Likelihood function: No-error-discharge Case

Suppose the following data are available:

1. A gauged record of  $n$  true flood peaks  $\{q_1, \dots, q_n\}$ ; and
2.  $m$  censored records in which  $a_i$  annual flood peaks in  $(a_i + b_i)$  ungauged years exceeded a threshold with true discharge  $s_i$ ,  $i=1, \dots, m$ .

This data is denoted by  $D = \{q_i, i=1, \dots, n; (a_i, b_i, s_i), i=1, \dots, m\}$ . It is shown in Likelihood function: No-error-discharge case that the likelihood function is:

$$p(D|\theta) \propto \prod_{i=1}^n p(q_i|\theta) \prod_{i=1}^m [1 - P(Q \leq s_i|\theta)]^{a_i} P(Q \leq s_i|\theta)^{b_i} \quad (3.2.42)$$

#### **Likelihood function: No-error-discharge case**

The likelihood function is, by definition, the joint pdf of the observed given the parameter vector  $\theta$ .

The likelihood function for the gauged data is the joint pdf of the  $n$  gauged floods. Given the AM flood peaks are statistically independent, the likelihood can be simplified to (Stedinger and Cohn, 1986):

$$p(q_1, \dots, q_n|\theta) = \prod_{i=1}^n p(q_i|\theta) \quad (3.2.43)$$

The likelihood of the binomial censored data relies on the fact that the probability of observing exactly  $x$  exceedances in  $n$  years is given by the binomial distribution

$$P(x|n, \pi) = {}^n C_x (1 - \pi)^{n-x} \pi^x \quad (3.2.44)$$

where  $\pi$  is the probability of an exceedance.

Provided each censoring threshold does not overlap over time with any other censoring threshold, the likelihood of the censored data becomes:

$$p(\text{censored data}|\theta) = \prod_{i=1}^m [1 - P(Q \leq s_i|\theta)]^{a_i} P(Q \leq s_i|\theta)^{b_i} = \prod_{i=1}^m P(a_i, b_i|s_i, \theta) \quad (3.2.45)$$

where  $P(a_i, b_i|s_i, \theta)$  is the binomial probability of observing exactly  $a_i$  exceedances above the threshold discharge  $s_i$  in  $(a_i+b_i)$ .

### **2.6.3.4. The Likelihood Function: Error-in-discharge Case**

The incorporation of rating errors into the likelihood function complicates matters. Likelihood function: Error-in-discharge case outlines the derivation of the likelihood function using the simple rating error model presented in Book 3, Chapter 2, Section 3. There has been limited research into the use of this likelihood and on the characterisation of rating errors. Kuczera (1996) shows that, as rating error grows for floods well in excess of the largest gauged discharge, less weight is given to high floods in the calibration. This loss of information about the right tail of the flood distribution is sensitive to the magnitude of rating errors when extrapolating beyond gauged discharges. Unfortunately, little is known about these errors and hence caution is recommended if using this advanced likelihood.

**Likelihood function: Error-in-discharge case**

Figure 3.2.9 presents a rating error space diagram. In zone 1 (Figure 3.2.9), the interpolation zone it is assumed the rating error multiplier  $e_1$  equals 1 – that is, errors within the rated part of the rating curve are deemed negligible. As a result the estimated discharge  $w$  equals the true discharge  $q$ . However, in zone 2, the extension zone, the rating error multiplier  $e_2$  is assumed to be a random variable with mean of 1. The anchor point  $(q_1, w_1)$  separates the interpolation and extension zones. The rating error model can be represented mathematically as:

$$w = \begin{cases} q & \text{if } q \leq q_1 \\ w_1 + e_2(q - q_1) & \text{if } q > q_1 \end{cases} \quad (3.2.46)$$

The rating error multiplier  $e_2$  is sampled only once at the time of extending the rating curve. Therefore, all flood discharge estimates exceeding the anchor value of  $q_1$  (which equals  $w_1$ ) are corrupted by the same rating error multiplier. It must be stressed that the error  $e_2$  is not known – at best, only its probability distribution can be estimated. For practical applications one can assume  $e_2$  is distributed as either a log-Normal or normal distribution with mean 1 and standard deviation  $\sigma_2$ .

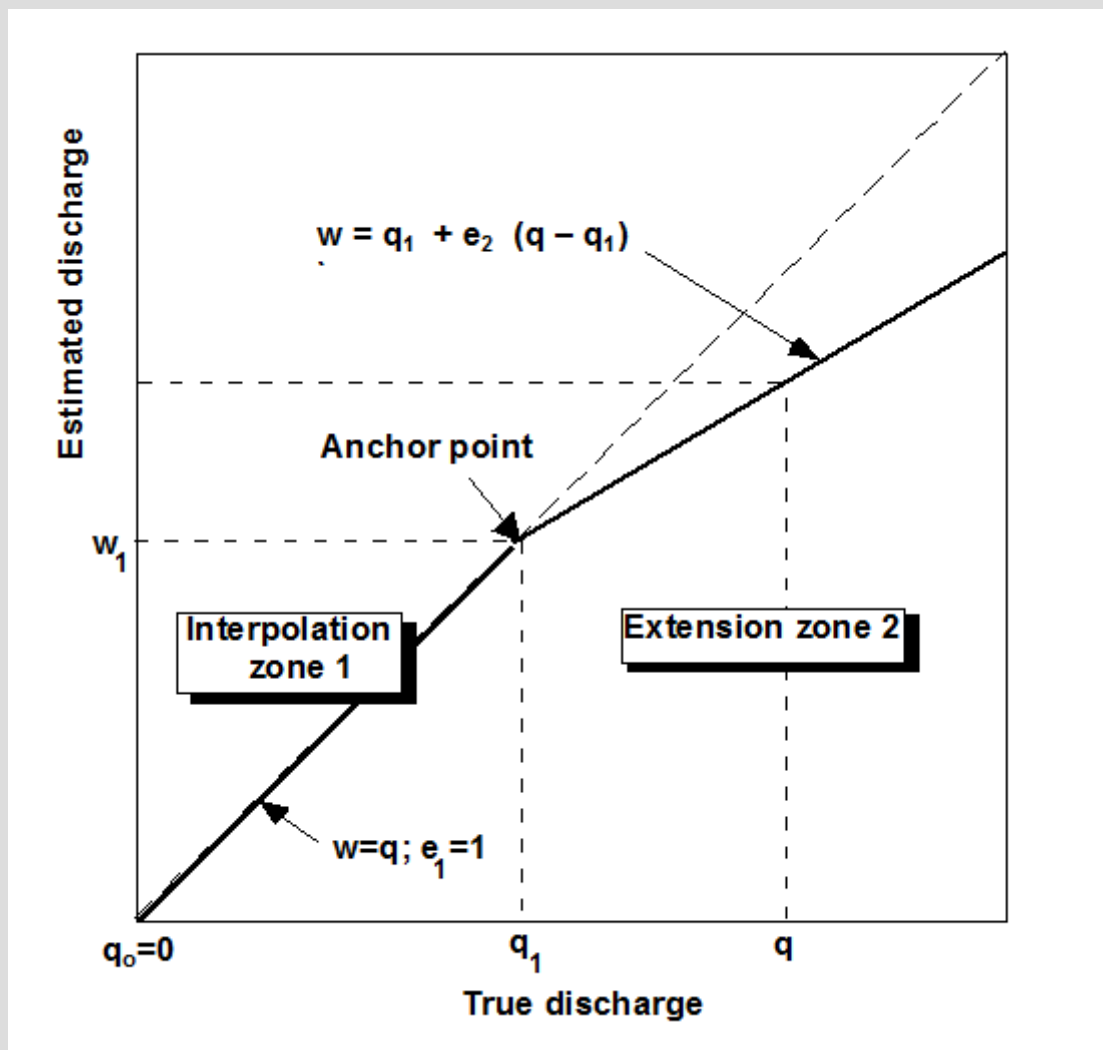


Figure 3.2.9. Rating error multiplier space diagram for rating curve



Data are assigned to each of the two zones,  $i=1,2$ , in the rating error space diagram. The rating error multiplier standard deviation for the extension zone  $\sigma_2$  is assigned a value with  $\sigma_1 = 0$ . There are  $n_i$  annual flood peak estimates  $w_{ji}$  satisfying the zone constraint  $w_{i-1} \leq w_{ji} < w_i$ ,  $j=1, \dots, n_i$  where  $w_0=0$  and  $w_2= \infty$ . In addition, there are  $m_i$  threshold discharge estimates  $w_{ji}$  for which there are  $a_{ji}$  exceedances in  $(a_{ji}+b_{ji})$  years,  $j=1, \dots, m_i$ . Collectively this data is represented as:

$$D = \{D_i, i = 1, 2\} \quad (3.2.47)$$

$$= \left\{ \left[ w_{jv} j = 1, \dots, n_i; w_{jv}, a_{jv}, b_{jv} j = 1, \dots, m_i \right], i = 1, 2 \right\}$$

Kuczera (1999) it can be shown for the two-zone rating error model of Figure 3.2.9 the likelihood reduces to:

$$p(D_1, D_2 | \theta_1, \sigma_2) = p(D_1, e_1 = 1 | \theta) \left[ \int_0^{\infty} p(D_1, e_2 | \theta) g(e_2 | \sigma_2) de_2 \right] \quad (3.2.48)$$

where

$$p(D_i, e_i | \theta_1) = \prod_{j=1}^{n_i} \frac{1}{e_i} p \left( q_{i-1} + \frac{w_{ji} - w_{i-1}}{e_i} | \theta \right) \quad (3.2.49)$$

$$= \prod_{j=1}^{m_i} P \left( a_{jv}, b_{jv} \left| q_{i-1} + \frac{w_{jv} - w_{i-1}}{e_i}, \theta \right. \right)$$

$|g(e_i | \sigma_i)$  is the rating error multiplier pdf with mean 1 and standard deviation  $\sigma_i$  and  $P(a, b | s, \theta)$  is the binomial probability of observing exactly a exceedances above the threshold discharge  $s$  in  $(a+b)$ . This is a complex expression which can only be evaluated numerically. However, it makes the fullest use of information on annual flood peaks and binomial-censored data in the presence of rating curve error. Book 3, Chapter 2, Section 3 offers limited guidance on the choice of  $\sigma_2$ .

### 2.6.3.5. Prior Distributions

The prior pdf  $p(\theta)$  reflects the worth of prior information on  $\theta$  obtained preferably from a regional analysis. A convenient distribution is the multivariate normal with mean  $\mu_p$  and covariance  $\Sigma_p$ ; that is,

$$\theta \sim N(\mu_p, \Sigma_p) \quad (3.2.50)$$

In the absence of prior information, the covariance matrix can be made non-informative as illustrated in the following equation for a three-parameter model:

$$\Sigma_p \xrightarrow{v \rightarrow \infty} \begin{pmatrix} v & 0 & 0 \\ 0 & v & 0 \\ 0 & 0 & v \end{pmatrix} \quad (3.2.51)$$

Informative prior information can be obtained from a regional analysis of flood data.

The use of an informative prior based on regional analysis is strongly recommended in all Flood Frequency Analyses involving at-site data. Even with long at-site records, the shape

parameter in the LP III and GEV distribution is subject to considerable uncertainty. Regional priors can substantially reduce the uncertainty in the shape (and even scale) parameter.

The regional procedures in Book 3, Chapter 3 are designed to express the prior information in the form of [Equation \(3.2.50\)](#) for the Log Pearson III probability model. They should be used in any Flood Frequency Analysis involving the Log Pearson III distribution unless there is evidence that the regional prior is not applicable to the catchment of interest.

#### **2.6.3.6. Monte Carlo Sampling from the Posterior Distribution**

The posterior pdf  $P(\theta|D)$  fully defines the parameter uncertainty. However, interpreting this distribution is difficult using analytical methods. Modern Monte Carlo methods for sampling from the posterior have overcome this limitation – for example, see [Gelman et al. \(1995\)](#). [Importance sampling from the posterior distribution](#) describes a particular sampling procedure called importance sampling.

### Importance sampling from the posterior distribution

Importance sampling is a widely used method [Gelman et al. \(1995\)](#) for sampling parameters from a target probability model for which there is no algorithm to draw random samples. The basic idea is to sample from a probability model for which a sampling algorithm exists – the probability model is called the importance distribution and the samples are called particles. The particles are then weighted so that they represent samples from the target distribution. The closer the importance distribution approximates the target, the more efficient the sampling.

Three steps are involved:

*Step 1:* Find most probable parameters of the target distribution

Any robust search method can be used to locate the value of  $\theta$ , which maximises the logarithm of the posterior probability density; that is,

$$\hat{\theta} \leftarrow \max_{\theta} \log p(\theta|D) \quad (3.2.52)$$

where  $\hat{\theta}$  is the most probable value of  $\theta$ . The shuffled complex evolution algorithm of [Duan et al. \(1992\)](#) is a recommended search method.

*Step 2:* Obtain the importance distribution using a multi-normal approximation to the target distribution

Almost always, the log of posterior pdf  $p(\theta|D)$  can be approximated by a second-order Taylor series expansion about the most probable parameter to yield the multivariate normal approximation

$$\theta|D \sim N(\hat{\theta}, \Sigma) \quad (3.2.53)$$

where  $\theta$  is interpreted as the mean and the posterior covariance  $\Sigma$  is defined as the inverse of the Hessian

$$\Sigma = \left( -\frac{\partial^2 \log_e p(\theta|D)}{\partial^2 \theta} \right)^{-1} \quad (3.2.54)$$

An adaptive difference scheme should be used to evaluate the Hessian. Particular care needs to be exercised when selecting finite difference perturbations for the GEV and LP III distributions when upper or lower bounds are close to the observed data.

*Step 3:* Importance sampling of target distribution

The importance sampling algorithm proceeds as follows:

1. Sample  $N$  particles according to  $\theta_i \leftarrow p_N(\theta_i), i = 1, \dots, N$  where  $p_N(\theta)$  is the pdf of the multi-normal approximation obtained in Step 2.
2. Calculate particle probability weights according to  $P(\theta_i) = \frac{p(\theta_i|D)}{p_N(\theta_i)}, i=1, \dots, N$
3. Scale the particle weights so they sum to 1.

### 2.6.3.7. Quantile Confidence Limits and Expected Probability

The posterior distribution of any function dependent on  $\theta$  can be readily approximated using Monte Carlo samples. Confidence limits describe the uncertainty about quantiles arising from uncertainty in the fitted parameters. They are used in conjunction with the probability plot to evaluate goodness-of-fit.  $100(1 - \alpha)\%$  quantile confidence limits, or more correctly probability limits. Confidence limits can be derived as follows:

1. Draw  $N$  samples from the posterior distribution  $\{\theta_i, w_i, i = 1, \dots, N\}$  where  $w_i$  is the normalized weight assigned to the sample  $\theta_i$ .
2. Rank in ascending order the  $N$  quantiles  $\{q_Y(\theta_i), i = 1, \dots, N\}$ .
3. For each ranked quantile evaluate the non-exceedance probability  $\sum_{j=1}^i w_{(j)}$  where  $W_{(j)}$  is the weight for the  $j^{\text{th}}$  ranked quantile  $q_Y(\theta_j)$ .
4. The lower and upper confidence limits are approximated by the quantiles whose non-exceedance probabilities are nearest to  $\frac{\alpha}{2}$  and  $1 - \frac{\alpha}{2}$  respectively.

The expected posterior parameters can be estimated:

$$E[\theta|D] = \sum_{i=1}^N w_i q_Y(\theta_i) \quad (3.2.55)$$

These parameters can then be used to compute the expected parameter 1 in  $Y$  AEP quantiles described in [Book 3, Chapter 2, Section 5](#).

Finally, the expected AEP probability for a flood of magnitude  $q_Y$  can be estimated:

$$E[P(q > q_Y|D)] = \sum_{i=1}^N w_i P(q > q_Y|\theta_i) \quad (3.2.56)$$

### 2.6.3.8. Treatment of Poor Fits

The standard probability models described in [Book 3, Chapter 2, Section 4](#) may sometimes poorly fit flood data. Typically the goodness-of-fit is assessed by comparing observed data against the fitted probability model and its confidence limits. A poor fit may be characterised by:

- Presence of outliers in the upper or lower tail of the distribution. Outliers in Flood Frequency Analysis represent observations that are inconsistent with the trend of the remaining data and typically would lie well outside confidence limits; and
- Systematic discrepancies between observed and fitted distributions. Caution is required in interpreting systematic departures because plotting positions are correlated. Confidence limits can help guide the interpretation.

Poor fits to the standard probability models may arise for a variety of reasons including the following:

1. Small AM peaks may not be significant floods and thus may be unrepresentative of significant flood peaks;

2. By chance, one or more observed floods may be unusually rare for the length of gauged record. Recourse to the historical flood record may be useful in resolving this issue;
3. Rating curve extensions are biased resulting in a systematic under or over-estimate of large floods (see discussion in Book 3, Chapter 2, Section 3);
4. A change in hydraulic control with discharge may affect the shape of the frequency curve as illustrated in Book 3, Chapter 2, Section 8;
5. Storm events responsible for significant flooding may be caused by different meteorological mechanisms which lead to a mixed population not amenable to three-parameter distributions. This may arise when the majority of flood-producing storms are generated by one meteorological mechanism and the minority by an atypical mechanism such as a tropical cyclone; and
6. Nonhomogeneity of the flood record.

The potential causes of a poor fit need careful investigation.

If it is decided the poor fit is due to inadequacy of the probability model, three strategies are available to deal with the problem:

1. Observations can be censored;
2. The data responsible for the unsatisfactory fit may be given less weight; and
3. A more flexible probability model can be used to fit the data.

Data in the upper part of the distribution is typically of more interest and therefore a strong case needs to be made to justify reduction in weight of such data.

### **2.6.3.9. Censoring of Potentially Influential Low Discharges**

AM series contain many Annual Maximum discharges, which are less than bank full discharge. In arid zones these low peaks may be zero or very low values, not associated with any significant storm event. These low peaks may not be representative of the physical processes driving large floods (Cohn et al., 2013; Pedruco et al., 2014). The inclusion of such data in a Flood Frequency Analysis runs the risk of low peaks unrepresentative of large floods influencing the fit to the right-hand tail of the frequency distribution, which is of most interest to the hydrologist. Therefore the identification and removal of Potentially Influential Low Flows (PILFs) is considered an important step in a Flood Frequency Analysis.

Cohn et al. (2013) developed a generalisation of the Grubbs-Beck test that was recommended in Bulletin 17B (Interagency Advisory Committee on Water Data, 1982) to identify PILFs. The multiple Grubbs-Beck test, checks if the  $k^{\text{th}}$  smallest flow is unusually low and, if it is, uses this discharge to define a threshold for censoring discharges below the threshold. The test involves two steps:

1. The outward sweep starts at the median discharge and moves towards the smallest discharge. Each flow is tested at the 0.5% significance level. If the  $k^{\text{th}}$  smallest flow is identified as a low outlier, the outward sweep stops; and
2. The inward sweep starts at the smallest discharge and moves towards the median. Each discharge is tested at the 10% significance level. If the  $m^{\text{th}}$  flow is identified as a low outlier, the inward sweep stops.

The total number of low outliers is then the maximum of  $k$  and  $m - 1$ . The flows identified as low outliers are treated as censored flows.

The multiple Grubbs-Beck test is recommended for general use but must be conducted in unison with a visual assessment of the fitted frequency curve.

### **2.6.3.10. Software**

The Bayesian approach to calibrating flood probability models is numerically complex and is best implemented in a high level programming language. The web-based software called TUFLOW FLIKE supporting the Bayesian methods described in this chapter. The reader is advised that this does not preclude use of other software if it is fit for purpose.

### **2.6.3.11. Worked Examples**

Book 3, Chapter 2, Section 8 illustrates fitting a LP III distribution to a 31-year gauged record. Although the fit is judged satisfactory, considerable uncertainty in the 1% AEP quantile is noted.

Book 3, Chapter 2, Section 8 is a continuation of Example 3 and illustrates the benefit of incorporating censored historic flood information. In the 118 years prior to gauging only one flood exceed the largest gauged flood. This information is shown to substantially reduce quantile uncertainty.

Book 3, Chapter 2, Section 8 is a continuation of Example 3. It illustrates the value of regional information in reducing uncertainty in parameters and quantiles. It is recommended that regional information be always used unless there is contrary evidence.

Book 3, Chapter 2, Section 8 illustrates the identification of PILFs using the multiple Grubbs-Beck test and fitting a LP III distribution with PILFs treated as censored discharges. It is recommended that multiple Grubbs-Beck test be performed in all Flood Frequency Analyses.

Book 3, Chapter 2, Section 8 illustrates how three-parameter distributions such as the GEV and LP III can be made to fit data exhibiting sigmoidal behaviour. Because interest is in fitting the higher discharges the low discharges are de-emphasized by treating them as censored observations. In this example the multiple Grubbs-Beck test improved the fit but a more severe manual censoring produced an even better fit to the right-hand tail.

Book 3, Chapter 2, Section 8 illustrates application of a non-homogeneous flood probability model conditioned on the IPO index. It shows how the long-term flood risk may be estimated.

## **2.6.4. L-moments Approach**

### **2.6.4.1. Overview**

L-moments were developed by Hosking (1990) to overcome the bias and sensitivity of the method of product-moments approach to fitting distributions. L-moment estimators are unbiased and are less sensitive to outliers than product-moment estimators. They have been used extensively by researchers to analyse extremes and are recommended for use in Flood Frequency Analysis in the Handbook of Hydrology (Stedinger et al., 1993).

The L-moment approach is simpler than the Bayesian approach but limited in capability. It is restricted to applications involving gauged discharge data where there is no useful regional information and rating curve errors do not require special attention.

### 2.6.4.2. L-moments for summarising distributions

Hosking (1990) developed the L-moment theory based on order statistics. The first four L-moments are defined as:

$$\lambda_1 = E[X]_{1:1} \quad (3.2.57)$$

$$\lambda_2 = \frac{1}{2} E [X_{2:2} - X_{1:2}] \quad (3.2.58)$$

$$\lambda_3 = \frac{1}{3} E [X_{3:3} - 2X_{2:3} + X_{1:3}] \quad (3.2.59)$$

$$\lambda_4 = \frac{1}{4} E [X_{4:4} - 3X_{3:4} + 3X_{2:4} - X_{1:4}] \quad (3.2.60)$$

where  $X_{j:m}$  is the  $j^{\text{th}}$  smallest variable in a sample of size  $m$  and  $E$  stands for expectation.

Wang (1996) justifies L-moments as follows: "When there is only one value in a sample, it gives a feel of the magnitude of the random variable. When there are two values in a sample, their difference gives a sense of how varied the random variable is. When there are three values in a sample, they give some indication on how asymmetric the distribution is. When there are four values in a sample, they give some clue on how peaky, roughly speaking, the distribution is."

When many such samples are considered, the expectations  $\lambda_1$  and  $\lambda_2$  give measures of location and scale. Moreover, the L-moment ratios:

$$\tau_3 = \frac{\lambda_3}{\lambda_2} \quad (3.2.61)$$

$$\tau_4 = \frac{\lambda_4}{\lambda_2} \quad (3.2.62)$$

give measures of skewness and kurtosis respectively. Hosking termed  $\tau_3$  L-skewness and  $\tau_4$  L-kurtosis. Hosking also defined the L-coefficient of variation as:

$$\tau_2 = \frac{\lambda_2}{\lambda_1} \quad (3.2.63)$$

Table 3.2.3 Summarizes L-moments for a range of distributions.

Table 3.2.3. L-moments for several distributions (from Stedinger et al. (1993))

Family	L-moments
Generalized Extreme Value (GEV)	$\lambda_1 = \tau + \frac{\alpha}{\kappa} [1 - \Gamma(1 + \kappa)]$ $\lambda_2 = \frac{\alpha}{\kappa} \Gamma(1 + \kappa) [1 - 2^{-\kappa}]$ $\tau_3 = \frac{2(1 - 3^{-\kappa})}{1 - 2^{-\kappa}} - 3$ $\tau_4 = \frac{1 - 5(4^{-\kappa}) + 10(3^{-\kappa}) - 6(2^{-\kappa})}{1 - 2^{-\kappa}}, \kappa \neq 0$

At-Site Flood Frequency  
Analysis

Family	L-moments
Gumbel	$\lambda_1 = \tau + 0.5772\alpha$ $\lambda_2 = \alpha \ln 2$ $\tau_3 = 0.1699$ $\tau_4 = 0.1504$
Generalized Pareto	$\lambda_1 = q_* + \frac{\beta}{1+\kappa}$ $\lambda_2 = \frac{\beta}{(1+\kappa)(2+\kappa)}$ $\tau_3 = \frac{1-\kappa}{3+\kappa}$ $\tau_4 = \frac{(1-\kappa)(2-\kappa)}{(3+\kappa)(4+\kappa)}$

### 2.6.4.3. L-moments estimates for gauged data sample data

The traditional L-moment estimator is based on probability weighted moments. However, Wang (1996) derived the following sample estimators directly from the definition of the first four L-moments:

$$\hat{\lambda}_1 = \frac{1}{n C_1} \sum_{i=1}^n q_{(i)} \quad (3.2.64)$$

$$\hat{\lambda}_2 = \frac{1}{2} \frac{1}{n C_2} \sum_{i=1}^n ({}^{i-1}C_1 - {}^{n-i}C_1) q_{(i)} \quad (3.2.65)$$

$$\hat{\lambda}_3 = \frac{1}{3} \frac{1}{n C_3} \sum_{i=1}^n ({}^{i-1}C_2 - 2{}^{i-1}C_1 + {}^{n-i}C_2) q_{(i)} \quad (3.2.66)$$

$$\hat{\lambda}_4 = \frac{1}{4} \frac{1}{n C_4} \sum_{i=1}^n ({}^{i-1}C_3 - 3{}^{i-1}C_2 + 3{}^{i-1}C_1 - {}^{n-i}C_3) q_{(i)} \quad (3.2.67)$$

where  $q_{(i)}$ ,  $i = 1, 2, \dots, n$  are gauged peak discharges ranked in ascending order and:

$${}^m C_k = \begin{cases} \frac{m!}{k!(m-k)!} & \text{if } k \leq m \\ 0 & \text{if } k > m \end{cases} \quad (3.2.68)$$

is the number of combinations of any k items from m items.

### 2.6.4.4. Parameter and quantile estimation

The method of L-moments involves matching theoretical and sample L-moments to estimate parameters. The L-moments in Table 3.2.3 are replaced by their sample estimates given by Equation (3.2.67). The resulting equations are then solved to obtain estimates of the parameters. These parameters are used to calculate the X% AEP quantiles.



### 2.6.4.5. LH-moments for fitting the GEV distribution

When the selected probability model does not adequately fit all the gauged data, the lower discharges may exert undue influence on the fit and give insufficient weight to the higher discharges which are the principal object of interest. To deal with this situation, [Wang \(1997\)](#) introduced a generalisation of L-moments called LH-moments. A more detailed exposition can be found in [LH-moments for fitting the GEV Distribution](#).

#### LH-moments for fitting the GEV Distribution

LH-moments are based on linear combinations of higher order-statistics. A shift parameter  $\eta = 0, 1, 2, 3, \dots$  is introduced to give more emphasis on higher ranked flows. LH-moments are defined as:

$$\lambda_1^\eta = E[X_{(\eta+1):(\eta+1)}] \quad (3.2.69)$$

$$\lambda_2^\eta = \frac{1}{2} E [X_{(\eta+2):(\eta+2)} - X_{(\eta+1):(\eta+3)}] \quad (3.2.70)$$

$$\lambda_3^\eta = \frac{1}{3} E [X_{(\eta+3):(\eta+3)} - 2X_{(\eta+2):(\eta+3)} + X_{(\eta+1):(\eta+3)}] \quad (3.2.71)$$

$$\lambda_4^\eta = \frac{1}{4} E [X_{(\eta+4):(\eta+4)} - 3X_{(\eta+3):(\eta+4)} + 3X_{(\eta+2):(\eta+4)} - X_{(\eta+1):(\eta+4)}] \quad (3.2.72)$$

[Table 3.2.4](#) presents the relationship between the first four LH-moments and the parameters of the GEV and Gumbel distributions.

Table 3.2.4. LH-moments for GEV and Gumbel distributions (from [Wang \(1997\)](#))

Family	LH-moments
Generalised extreme value (GEV)	$\lambda_1^n = \tau + \frac{\alpha}{\kappa} [1 - \Gamma(1+\kappa)(\eta+1)^{-\kappa}] \lambda_2^n = \frac{(\eta+2)\alpha\Gamma(1+\kappa)}{2!\kappa} [-(\eta+2)^{-\kappa} + (\eta+1)^{-\kappa}]$ $\lambda_3^n = \frac{(\eta+3)\alpha\Gamma(1+\kappa)}{3!\kappa} [-(\eta+4)(\eta+3)^{-\kappa} + 2(\eta+3)(\eta+2)^{-\kappa} - (\eta+2)(\eta+1)^{-\kappa}]$ $\lambda_4^n = \frac{(\eta+4)\alpha\Gamma(1+\kappa)}{4!\kappa} [-(\eta+6)(\eta+5)(\eta+4)^{-\kappa} + 3(\eta+5)(\eta+4)(\eta+3)^{-\kappa} - 3(\eta+4)(\eta+3)(\eta+2)^{-\kappa} + (\eta+3)(\eta+2)(\eta+1)^{-\kappa}]$ <p style="text-align: center;">where <math>\kappa \neq 0</math></p>

At-Site Flood Frequency  
Analysis

Family	LH-moments
Gumbel	$\lambda_1^n = \tau + \alpha [0.5772 + \ln(\eta + 1)] \lambda_2^n = \frac{(\eta + 2)\alpha}{2!} [\ln(\eta + 2) - \ln(\eta + 1)]$ $\lambda_3^n = \frac{(\eta + 3)\alpha}{3!} [(\eta + 4)\ln(\eta + 3) - 2(\eta + 3)\ln(\eta + 2) + (\eta + 2)\ln(\eta + 1)]$ $\lambda_4^n = \frac{(\eta + 4)\alpha}{4!\kappa} [(\eta + 6)(\eta + 5)\ln(\eta + 4) - 3(\eta + 5)(\eta + 4)\ln(\eta + 3) + 3(\eta + 4)(\eta + 3)\ln(\eta + 2) - (\eta + 3)(\eta + 2)\ln(\eta + 1)]$
<p>For ease of computation <u>Wang (1997)</u> derived the following approximation for the shape parameter <math>\kappa</math>:</p> $\kappa = a_0 + a_1[\tau_3^\eta] + a_2[\tau_3^\eta]^2 + a_3[\tau_3^\eta]^3 \quad (3.2.73)$ <p>where the polynomial coefficients vary with <math>\eta</math> according to <u>Table 3.2.5</u>.</p>	

Table 3.2.5. Polynomial coefficients for use with Equation (3.2.73)

$\eta$	$a_0$	$a_1$	$a_2$	$a_3$
0	0.2849	-1.8213	0.8140	-0.2835
1	0.4823	-2.1494	0.7269	-0.2103
2	0.5914	-2.3351	0.6442	-0.1616
3	0.6618	-2.4548	0.5733	-0.1273

At-Site Flood Frequency  
Analysis

$\eta$	$a_0$	$a_1$	$a_2$	$a_3$
4	0.7113	-2.5383	0.5142	-0.1027

Wang (1997) derived the following estimators for LH-moments with shift parameter  $\eta$ :

$$\lambda_1^\eta = \frac{1}{n} \sum_{i=1}^n i^{-1} C_{\eta+1} \eta^{x(i)} \quad (3.2.74)$$

$$\hat{\lambda}_2^\eta = \frac{1}{2} \frac{1}{n} \sum_{i=1}^n \left( i^{-1} C_{\eta+1} - i^{-1} C_{\eta} \right) q(i) \quad (3.2.75)$$

$$\hat{\lambda}_3^\eta = \frac{1}{3} \frac{1}{n} \sum_{i=1}^n \left( i^{-1} C_{\eta+2} - 2 i^{-1} C_{\eta+1} + i^{-1} C_{\eta} \right) q(i) \quad (3.2.76)$$

$$\begin{aligned} \hat{\lambda}_4^\eta = \frac{1}{4} \frac{1}{n} \sum_{i=1}^n & \left( i^{-1} C_{\eta+3} - 3 i^{-1} C_{\eta+2} + 3 i^{-1} C_{\eta+1} - i^{-1} C_{\eta} \right) q(i) \\ & + 3 i^{-1} C_{\eta+1} - 2 i^{-1} C_{\eta} \end{aligned} \quad (3.2.77)$$

The selection of the best shift parameter requires some form of goodness-of-fit test. Wang (1998) argued that the first three LH-moments are used to fit the GEV model leaving the fourth LH-moment available for testing the adequacy of the fit. Wang (1998) proposed the following approximate test statistic:

$$z = \frac{\hat{\tau}_4^\eta - \tau_4^\eta}{\sigma(\hat{\tau}_4^\eta | \hat{\tau}_3^\eta = \tau_3^\eta)} \quad (3.2.78)$$

where  $\hat{\tau}_4^\eta$  is the sample estimate of the LH-kurtosis,  $\tau_4^\eta$  is the LH-kurtosis derived from the GEV parameters fitted to the first three LH-moments, and  $\sigma(\hat{\tau}_4^\eta | \hat{\tau}_3^\eta = \tau_3^\eta)$  is the standard deviation of  $\hat{\tau}_4^\eta$  assuming the sample LH-skewness equals the LH-skewness derived from the GEV parameters fitted to the first three LH-moments. Under the hypothesis that the underlying distribution is GEV, the test statistic  $z$  is approximately normal distributed with mean 0 and variance 1. Wang (1998) describes a simple relationship to estimate  $\sigma(\hat{\tau}_4^\eta | \hat{\tau}_3^\eta = \tau_3^\eta)$ .

### 2.6.4.6. Parameter Uncertainty and Quantile Confidence Limits

The sampling distribution  $p(\theta|D)$  can be approximated using the Monte Carlo method known as the parametric bootstrap described in [Parametric bootstrap](#). This procedure yields  $N$  equi-weighted samples that approximate the sampling distribution  $p(\theta|D)$ . As a result, they can be used to quantify parameter uncertainty and estimate quantile confidence limits. However, because the parametric bootstrap assumes  $\theta$  is the true parameter, it underestimates the uncertainty and therefore should not be used to estimate expected probabilities.

### Parametric bootstrap

The sampling distribution of an estimator can be approximated using the Monte Carlo method known as the parametric bootstrap:

1. Fit the probability model to  $n$  years of gauged discharges using L or LH-moments to yield the parameter estimate  $\theta$ .
2. Set  $i=1$
3. Randomly sample  $n$  flows from the fitted distribution; that is,  $q_{ji} \leftarrow p(q|\hat{\theta}), j = 1, \dots, n$
4. Fit the model to the sampled flows  $\{q_{ji}, j = 1, \dots, n\}$  using L or LH-moments to yield the parameter estimate  $\theta_i$
5. Increment  $i$ . Go to step 3 if  $i$  does not exceed  $N$ .

This procedure yields  $N$  equi-weighted samples that approximate the sampling distribution  $p(\theta|D)$ . As a result, they can be used to quantify parameter uncertainty and estimate quantile confidence limits. However, because the parametric bootstrap assumes  $\hat{\theta}$  is the true parameter, it underestimates the uncertainty and therefore should not be used to estimate expected probabilities.

### 2.6.4.7. Software

Implementation of L and LH-moments requires extensive computation. The TUFLOW FLIKE software, supports the L and LH-moment estimation described in this section.

### 2.6.4.8. Worked Examples

Book 3, Chapter 2, Section 8 illustrates fitting the GEV distribution using L-moments to a 47-year gauged record. Book 3, Chapter 2, Section 8 revisits Book 3, Chapter 2, Section 8 demonstrating the search procedure for finding the optimal shift in LH-moments fitting.

## 2.6.5. Method of Moments Approach

The method of moments used in conjunction with the LP III distribution was the recommended method in Australian Rainfall and Runoff (Pilgrim, 1987). The method was simple to implement but, unlike US practice, did not use regionalised skew. Its use is no longer recommended in Australia. Both, the Bayesian and L-moment procedures, make better use of the available information.

## 2.7. Fitting Flood Probability Models to Peak Over Threshold Series

### 2.7.1. Probability Plots

As with the analysis of Annual Maximum series, it is recommended that a probability plot of the POT data series be prepared. The plot involves plotting an estimate of the observed ARI against the discharge. The ARI of a gauged flood can be estimated using:

$$T_{(i)} = \frac{n + 0.2}{i - 0.4} \quad (3.2.79)$$

where  $i$  is the rank of the gauged flood (in descending order) and  $n$  is the number of years of record.

## 2.7.2. Fitting Peak-Over-Thresholds Models

In some cases, it may be desirable to analytically fit a probability distribution to POT data. Two general approaches have been used.

In the first approach, the annual flow series distribution has been estimated from the POT series on the basis that the latter considers all of the relevant data and should thus provide a better estimate. The basis for the procedure is [Equation \(3.2.14\)](#), which links Poisson arrivals of flood peaks with a distribution of flood magnitudes above some threshold. [Jayasuriya and Mein \(1985\)](#), [Ashkar and Rousselle \(1983\)](#) and [Tavares and Da Silva \(1983\)](#) explored this approach using the exponential distribution. The approach has been fairly successful, but some results have diverged from the distribution derived directly from the annual series. Given the concern that the fit to the right tail of the annual maximum series may be compromised by the leverage exerted by the low flows, this approach cannot be recommended as a replacement for the analysis of annual series data. If possible, the base discharge for this approach should be selected so that the number of floods in the POT series  $m$  is at least 2 to 3 times the number of years of record  $n$ . However, it may be necessary to use a much lower value of  $m$  in regions with low rainfall where the number of recorded events that could be considered as floods is low.

The second approach uses a probability distribution as an arbitrary means of providing a consistent and objective fit to POT series data. For example, [McDermott and Pilgrim \(1982\)](#), [Adams and McMahon \(1985\)](#) and [Jayasuriya and Mein \(1985\)](#) used the LP III distribution – they found that selecting a threshold discharge such that  $m$  equalled  $n$  was best. [Book 3, Chapter 2, Section 8](#) illustrates this approach using L-moments to fit an exponential distribution to a POT series.

## 2.8. Supplementary Information

### 2.8.1. Example 1: Extrapolation and Process Understanding

The importance of process understanding when extrapolating beyond the observed record is illustrated by a simple Monte Carlo experiment. A Poisson rectangular pulse rainfall model is used to generate a long record of high resolution rainfall. This is routed through a rainfall-runoff model to generate runoff into the stream system. The storage-discharge relationship for the stream is depicted by the bilinear relationship shown in [Figure 3.2.10](#). A feature of this relationship is the activation of significant flood terrace storage once a threshold discharge is exceeded.

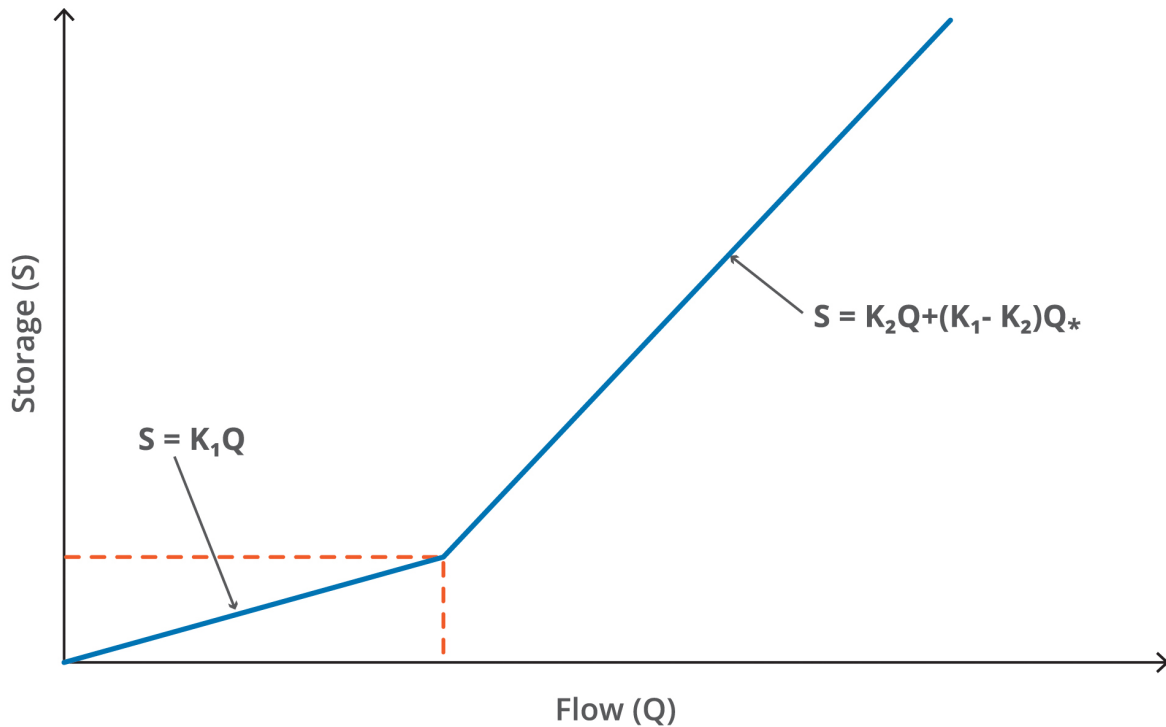


Figure 3.2.10. Bilinear channel storage-discharge relationship

The routing model parameters were selected so that major flood terrace storage is activated by floods of less than 1 in 100 AEP. This situation was chosen to represent a river with multiple flood terraces with the lowest terraces accommodating the majority of floods and the highest terrace only inundated by extreme floods.

Figure 3.2.11 presents the flood frequency curve based on 30 000 simulated years – it shows a clear break in slope around the 1 in 100 AEP corresponding to the activation of major flood terrace storage. Indeed the flood frequency curve displays downward curvature despite that the fact the rainfall frequency curve displays upward curvature in the 1 in 100 to 1 in 1000 AEP range. In contrast the flood frequency curve based on 100 years of “data” shows no evidence of downward curvature. This is because in a 100 year record there is little chance of the major flood terrace storage being activated. Indeed without knowledge of the underlying hydraulics one would be tempted to extrapolate the 100 year flood record using a straight line extrapolation. Such an extrapolation would rapidly diverge from the “true” frequency curve.

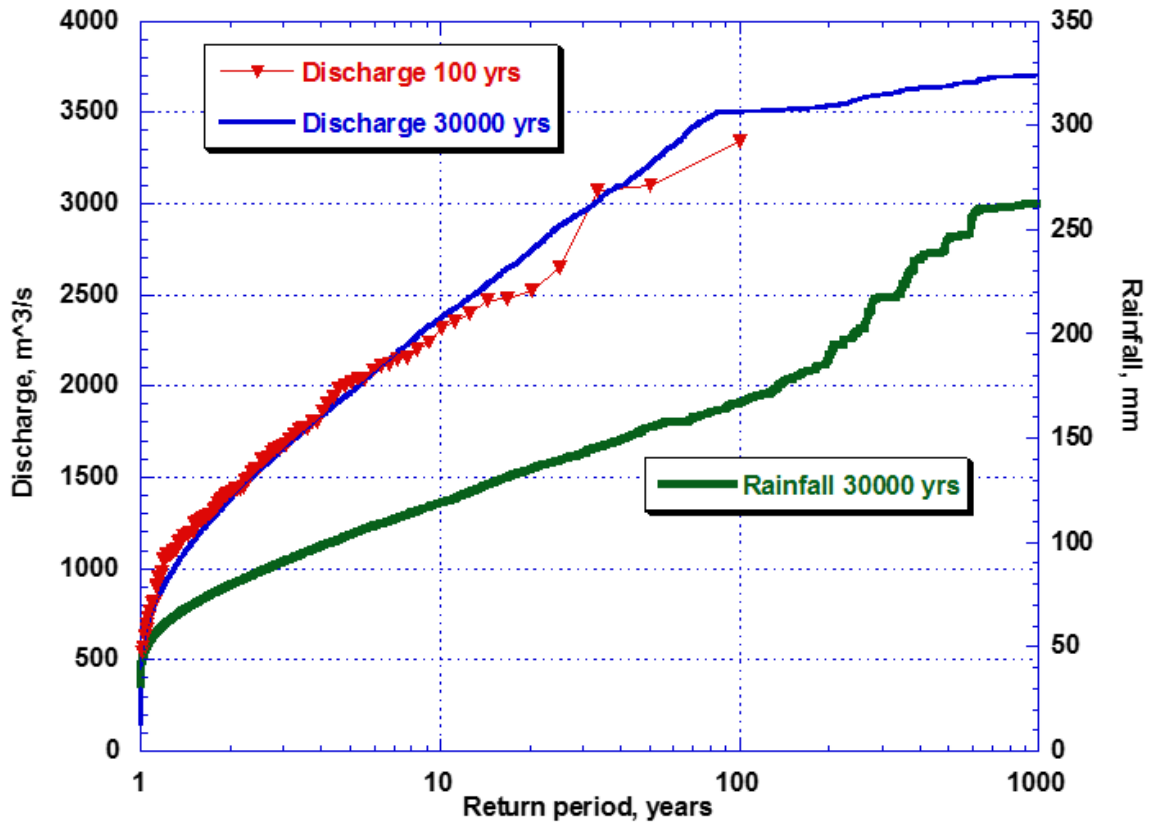


Figure 3.2.11. Simulated rainfall and flood frequency curves with major floodplain storage activated at a threshold discharge of 3500 m<sup>3</sup>/s

Although the example idealises the dominant rainfall-runoff dynamics it delivers a very strong message. Extrapolation of flood frequency curves fitted to gauged discharges records requires the exercise of hydrologic judgment backed up by appropriate modelling. The problem of extrapolation is much more general. For example, in this case, if a rainfall-runoff approach were used with the rainfall-runoff model calibrated to small events the simulated flood frequency curve is likely to be compromised in a similar way.

## 2.8.2. Example 2: Accuracy of Daily Gauged Discharges

The use of daily discharge readings in Flood Frequency Analysis is most problematic for smaller catchments, which can be “flashy” in the sense that the hydrograph can rise and subside within a twenty four hour period. This effect can be quite significant, even for reasonably large catchments.

Figure 3.2.12 and Figure 3.2.13, taken from Micevski et al. (2003), compare instantaneous annual maximum discharge against the discharge recorded at 9am on the same day for two gauging stations in the Hunter Valley: Goulburn River at Coggan with area 3340 km<sup>2</sup> and Hunter River at Singleton with area 16 400 km<sup>2</sup>. The dashed line represents equality. Figure 3.2.12 demonstrates that the true peak flow can be up to 10 times the 9:00 am flow. In contrast the estimation error is much smaller for the larger catchment shown in Figure 3.2.13.

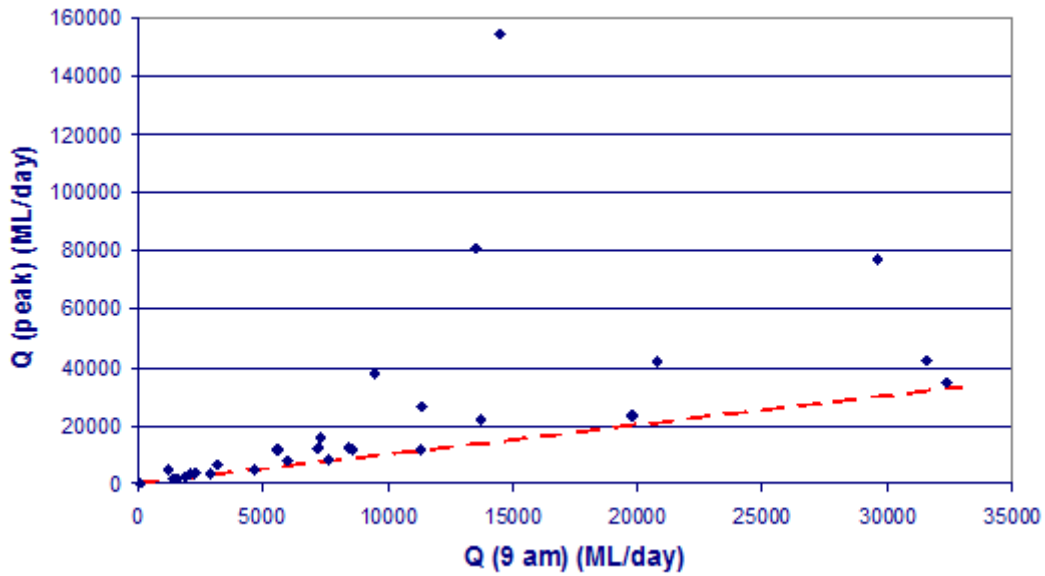


Figure 3.2.12. Comparison between true peak flow and 9:00 am flow for Goulburn River at Coggan

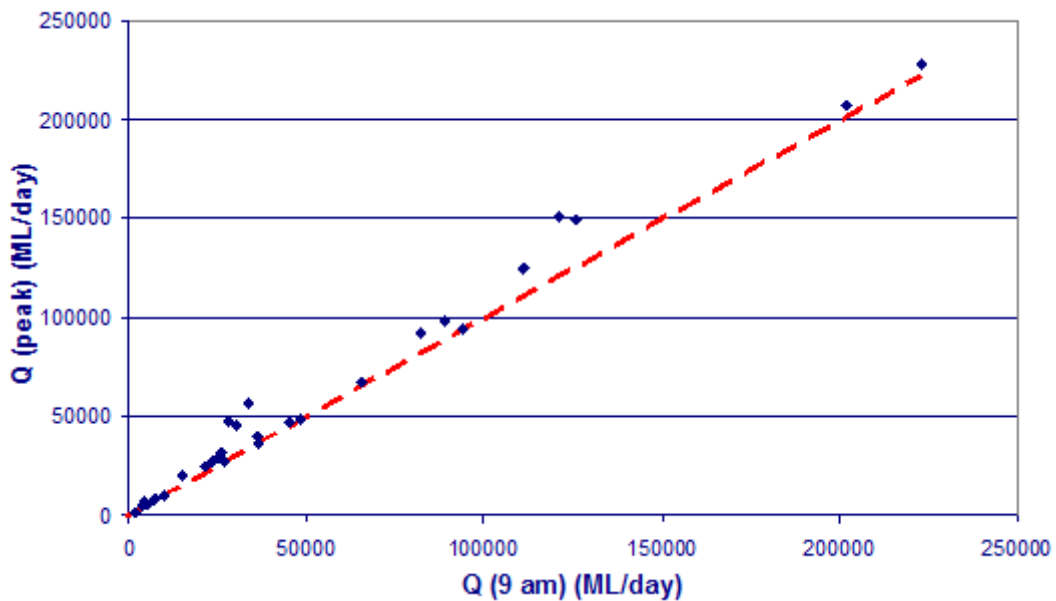


Figure 3.2.13. Comparison between true peak flow and 9:00 am flow for Hunter River at Singleton

The example demonstrates the need to check the representativeness of daily readings by comparing instantaneous peak flows against daily readings.

### 2.8.3. Example 3: Fitting a probability model to gauged data

#### 2.8.3.1. Launch TUFLOW Flike

This example demonstrates undertaking a flood frequency analysis using the procedures described in this book. Specifically, this example covers the fitting of a Log Pearson Type III



## At-Site Flood Frequency Analysis

distribution to an annual maximum series for the Hunter River at Singleton. The analysis will be undertaken using TUFLOW Flike which has been developed to undertake flood frequency analysis as described in this book, that is, it has the ability to fit a range of statistical distributions using a Bayesian Inference method.

Once TUFLOW Flike has been obtained and installed, launch **TUFLOW Flike** and the screen in [Figure 3.2.14](#) will appear.

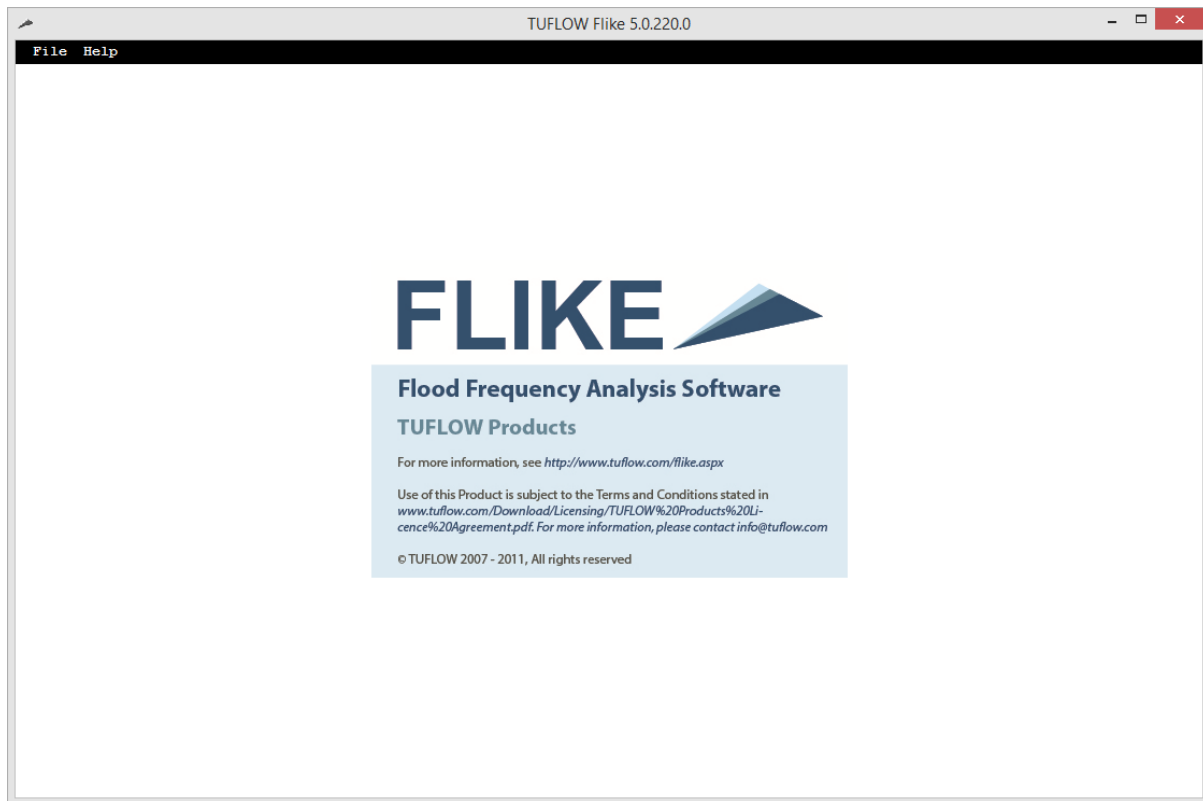


Figure 3.2.14. TUFLOW Flike Splash Screen

### 2.8.3.2. Create the .fld file

The first step will be to create the **.fld** file which contains information about the project. To create a new **.fld** file, select **New** from the **File** dropdown menu. This will open a new window called **Open** as shown in [Figure 3.2.15](#).

## At-Site Flood Frequency Analysis

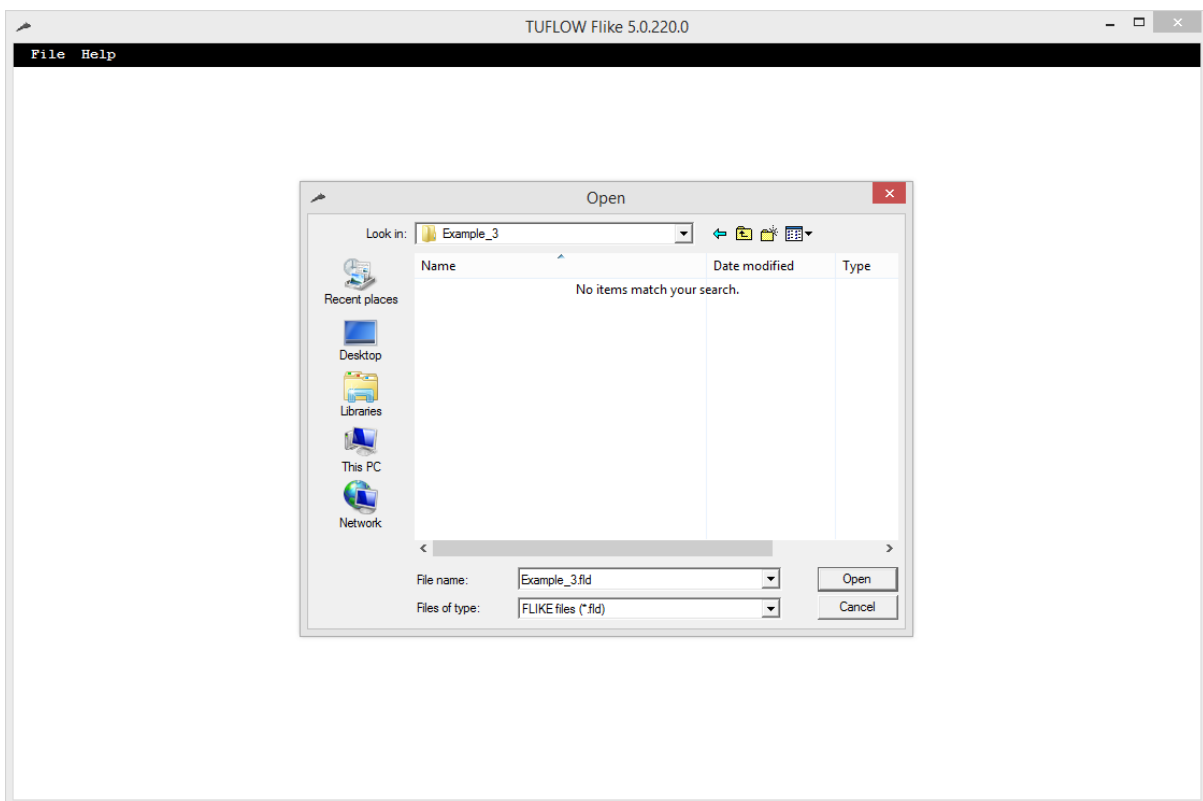


Figure 3.2.15. Create New .fld file

Create and save a new .fld file in an appropriate location, such as in a folder under the job directory, and give it a logical name, in this case **Example\_3.fld**. A message will appear asking if you want to create the file, select **Yes**. Note that the window is titled **Open**, but it works for creating new files as well. Once the .fld file has been saved, the **Flike Editor** window will open which will be used in the next step.

### 2.8.3.3. Configure the Project Details

The .fld file is used to store the project data and configuration. Once the .fld has been created the **Flike Editor** window will open automatically (see [Figure 3.2.16](#)) and the project will be configured here. The first bit of information to be completed is the project a name which is filled in the **Title** text box. The project title can go over two lines.

FLIKE Editor

General Gauged Flows Censored Data Errors

Title  
Hunter river at Singleton

Inference method

Bayesian with  No prior information  
 Gaussian prior distributions **Edit**

Zero threshold of

**Censor** low outliers above zero threshold  
using multiple Grubbs Beck test

LH moments fit to gauged flows with  
 Optimized H  
 H=0  H=1  H=2  H=3  H=4

Probability model

Log-normal  log Pearson III (LP3)  
 Gumbel  Generalized extreme value (GEV)  
 Generalized Pareto

Number of gauged data  Number of censoring thresholds   
Number of censored gauged data

Maximum AEP 1-in-Y in probability plot  years

Always display report file  Yes  No

**OK** **Cancel**

Figure 3.2.16. Flike Editor Screen

#### 2.8.3.4. Import the Data

The next step is to import the flood series to analyse. To do this select the **Observed values** tab in the **Flike Editor** as shown in [Figure 3.2.17](#). In this tab the flood series to be investigated will be imported.

At-Site Flood Frequency  
Analysis

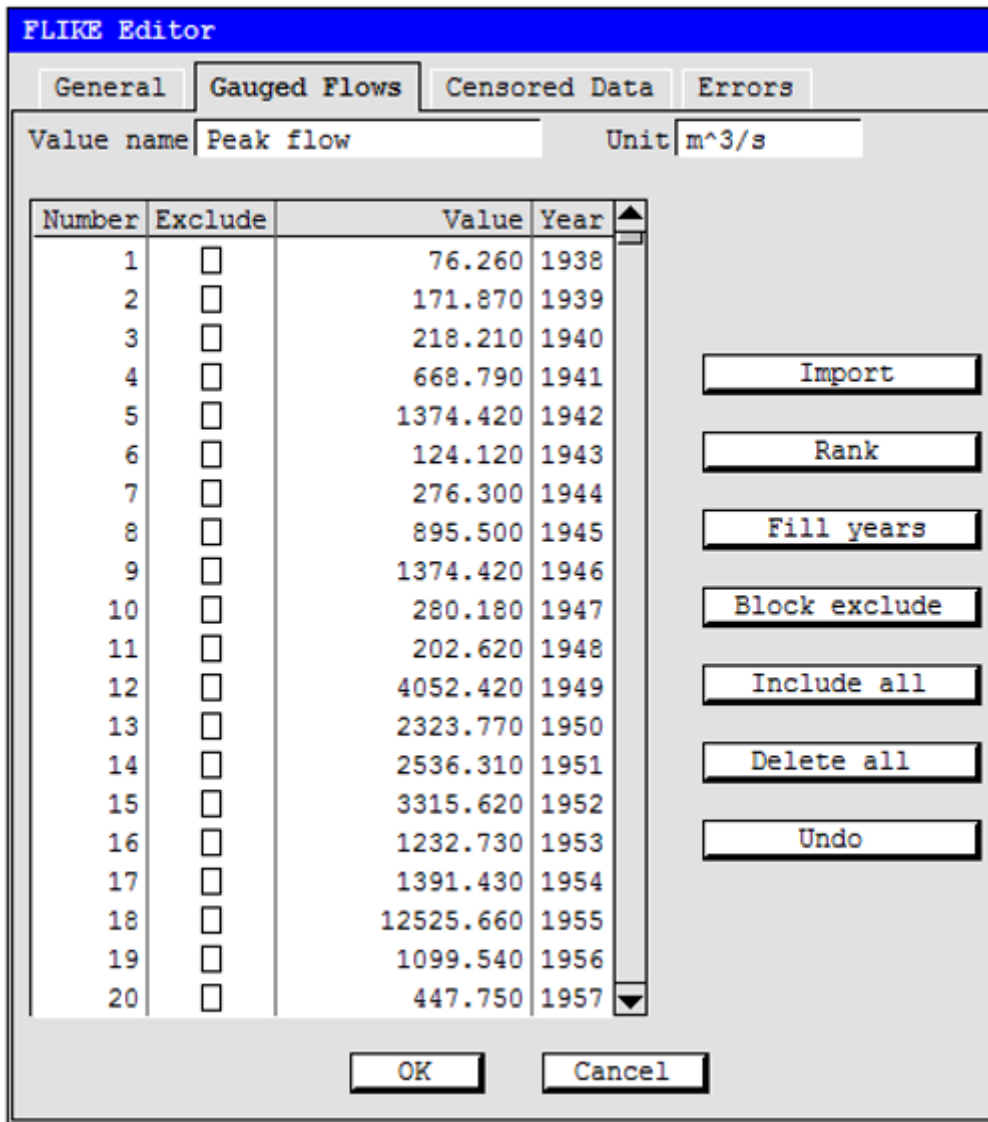


Figure 3.2.17. Observed Values Screen

To import the flood series select the **Import** button and the **Import gauged values** window opens as shown in [Figure 3.2.18](#). Now select the **Browse** button and navigate to the Singleton flood series. This example data are included in the TUFLOW Flike download, a copy of which was installed in the **data** folder in the install location of TUFLOW-Flike. By default, this location is *C:\TUFLOW Flike\data\singletonGaugedFlows.csv*. This data also appears at the end of this example.

## At-Site Flood Frequency Analysis

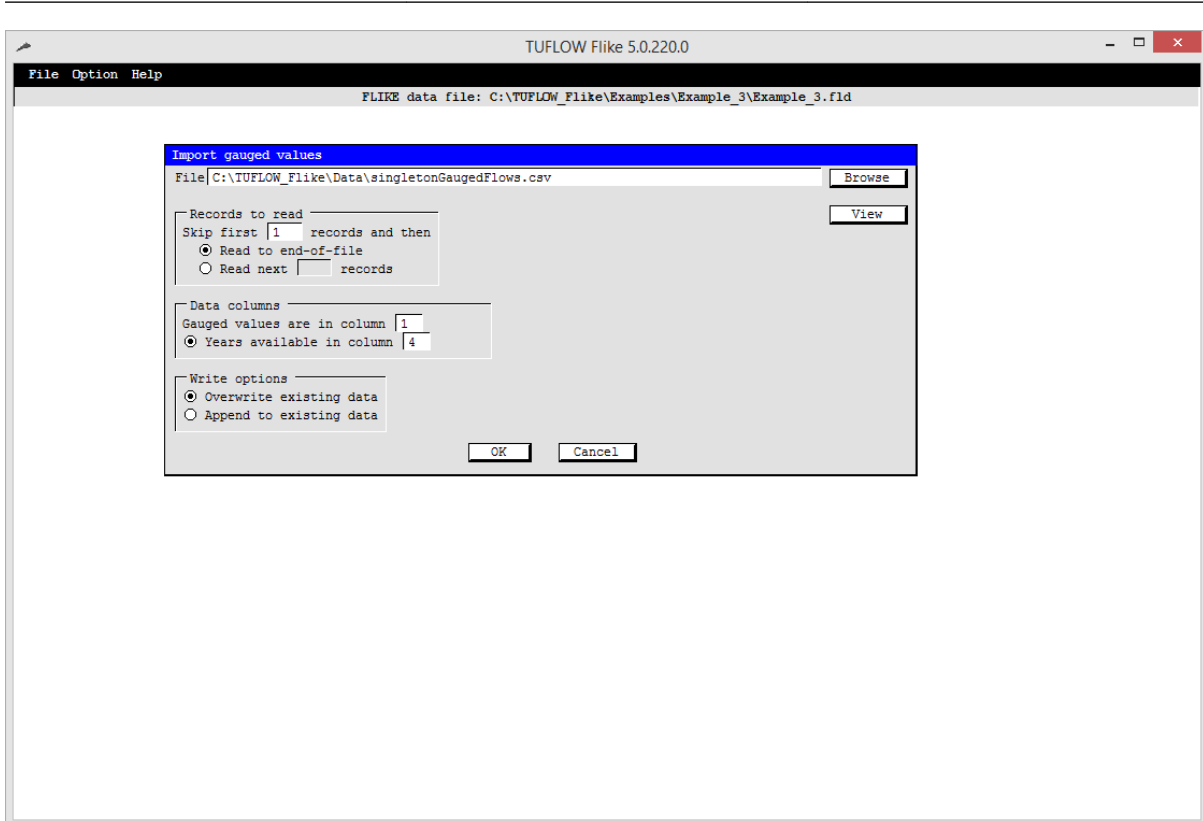


Figure 3.2.18. Import Gauged Values Screen

Once the data file has been selected, the program will return to the **Import gauged values** window. As the input data format is flexible TUFLOW Flike needs to be told how to interpret the data file. To view the format of the data, select the **View** button and the data will be open in your default text editor (see [Figure 3.2.19](#)). In the example data the first line contains a header line and the data follows this. The flow values are in the first column and the year in the fourth column. Having taken note of the data structure close the text editor and return to the **Import gauged values** window. It's a good habit to check the data in the text editor to ensure that the format of the data is known and the file has not been corrupted or includes a large number of trailing comma or whitespace. This last issue commonly occurs when deleting information from excel files, but it is easy to fix. Simply delete any trailing comma or white space in a text editor.

## At-Site Flood Frequency Analysis

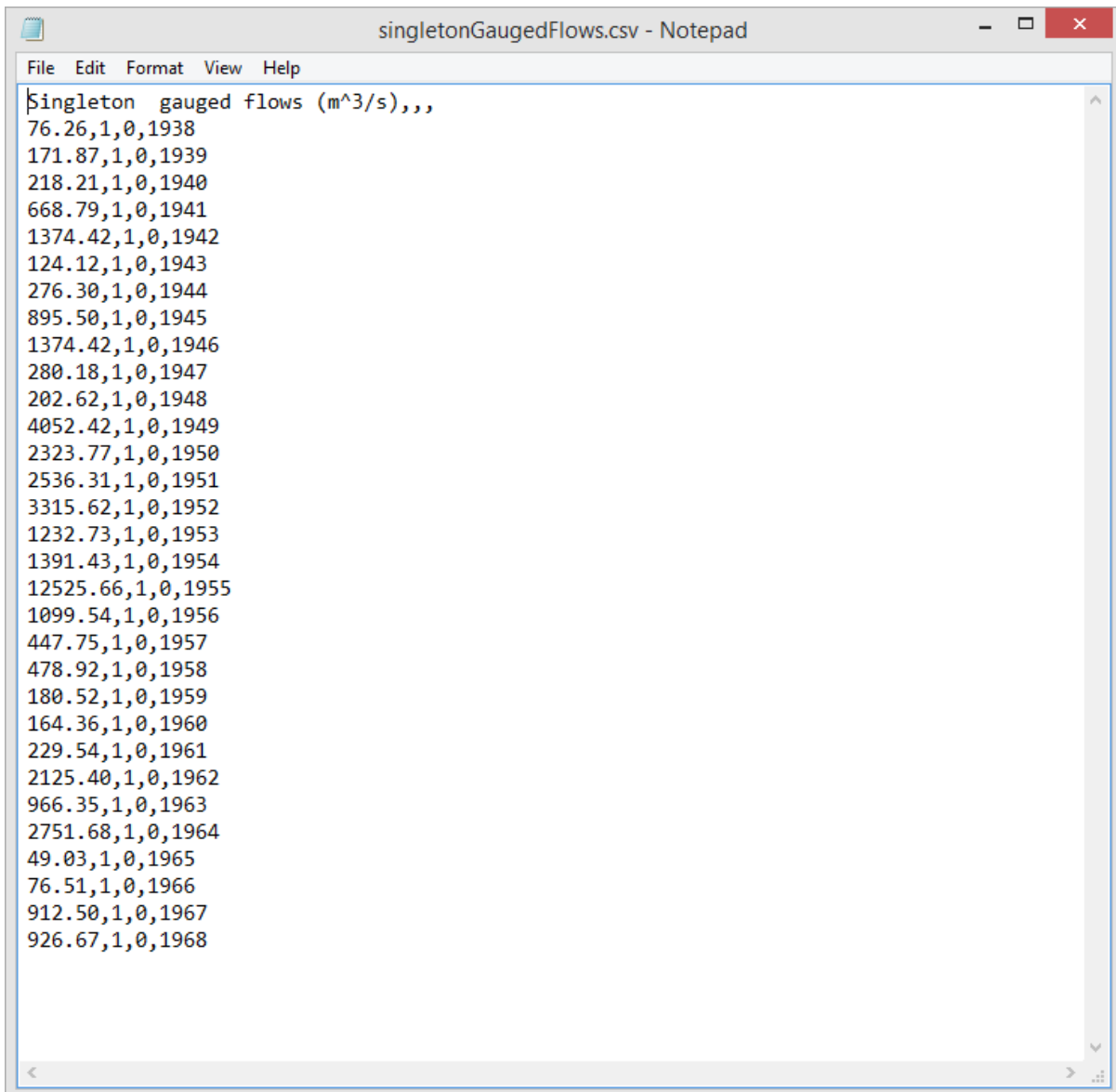


Figure 3.2.19. View Gauged Values in Text Editor

The next step is to configure the import of the data. As the example data has a header, the first line needs to be skipped. Enter **1** into the **Skip first \_\_ records and then text field**. This will skip the first line. Ensure that the **Read to the end-of-file** option is selected (this is the default). Occasionally, there may be a need to specify how many records to read, in which case this can be achieved by selecting the **Read next \_\_ records** option and entering the desired number of records to read. Next, specify which column the flood data are in, by filling the **gauged values are in column \_\_** text box, in this example data this is column 1. Next, select the **Years available in column \_\_** text box and specify the column that this data is in (column 4). Finally, select **OK** to import the data. The **Import gauged values** window should look similar to [Figure 3.2.18](#).

The **Value** and **Year** columns in the **Observed values** tab will now be filled with the data in the order that they were in the data file as shown in [Figure 3.2.20](#). The data can be sorted by value and year using the **Rank** button. Selecting this button will open a new window ([Figure 3.2.21](#)) where there are five choices to rank by, these are:

## At-Site Flood Frequency Analysis

- **Descending flow:** Ranks the data in order of values from largest to smallest
- **Ascending flow:** Ranks the data in order of values from smallest to largest
- **Descending year:** Ranks the data in order of year from largest to highest
- **Ascending year:** Ranks the data in order of year from highest to largest
- **Leave unchanged :** Leaves both the values and years unchanged

It is always a good idea to initially rank your data in descending order so you can check the largest flows. For this data series the value is 12 525.66 m<sup>3</sup>/s. Leave the data ranked in descending order for this example.

Note that the value name and units can be specified by entering values in the **Valuename** and **Unit** text boxes. These titles do not affect the computations in any way, they do, however, assist in reviewing the results, particularly when presenting results to external audiences.

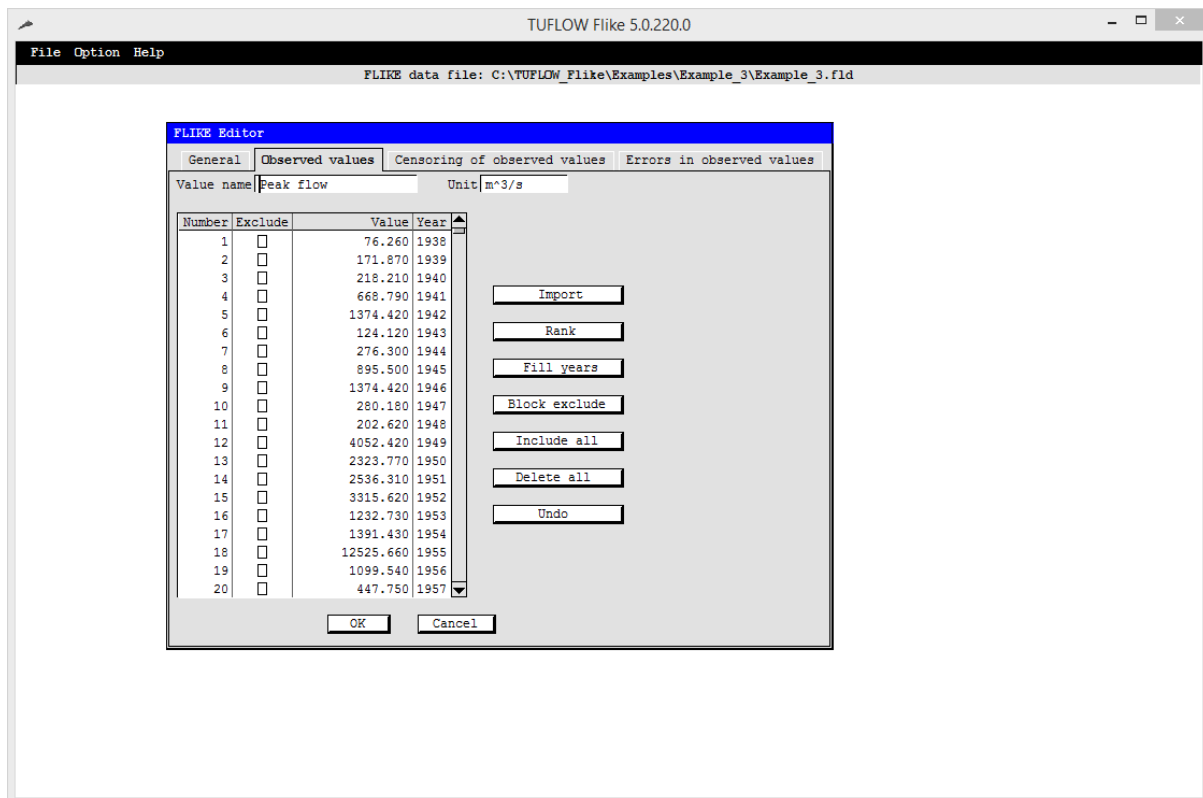


Figure 3.2.20. Observed Values screen with Imported Data

## At-Site Flood Frequency Analysis

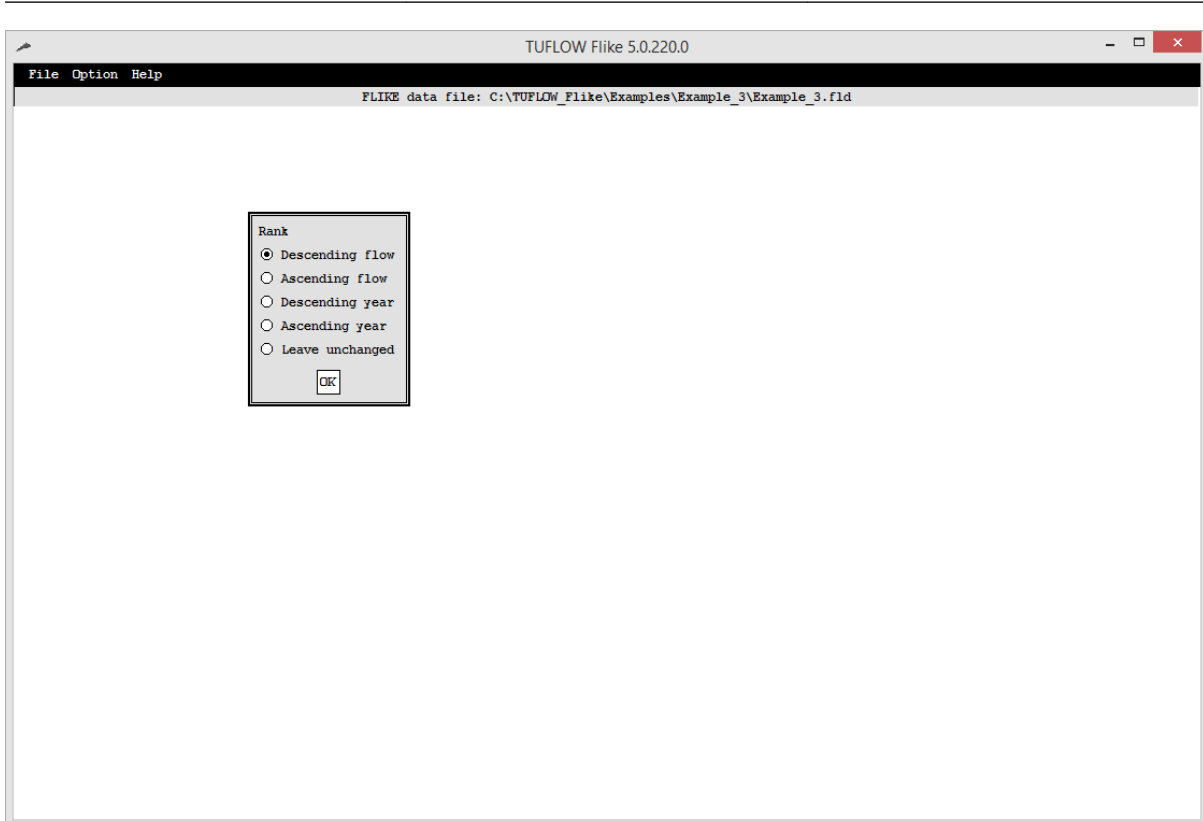


Figure 3.2.21. Rank Data Screen

### 2.8.3.5. Configure the distribution and fit method

Now that the data has been imported the statistical distribution can be fitted to the data. To do this, select the **General** tab. As noted above, for this example the Log Pearson Type III distribution will be fitted using the Bayesian Inference method.

Before configuring the model it is worthwhile checking that TUFLOW Flike has interpreted the data correctly. The number of observed data is reported in the **Number of observed data** text box. In this case the number of observations or length of the data series is 31 as shown in [Figure 3.2.22](#). Before continuing, check that this is the case.

Next, select the probability model; the Log Pearson Type III. To do this ensure that the radio button next to the text **Log Pearson Type III (LP3)** is selected (this is the default) as in [Figure 3.2.22](#).

The final task is to choose the fitting method. In this example the Bayesian Inference method will be used. To do this, ensure that the radio button next to **Bayesian with** is selected and the radio button next to **No prior information** is selected as shown in [Figure 3.2.22](#). Again, both of these are the defaults.



## At-Site Flood Frequency Analysis

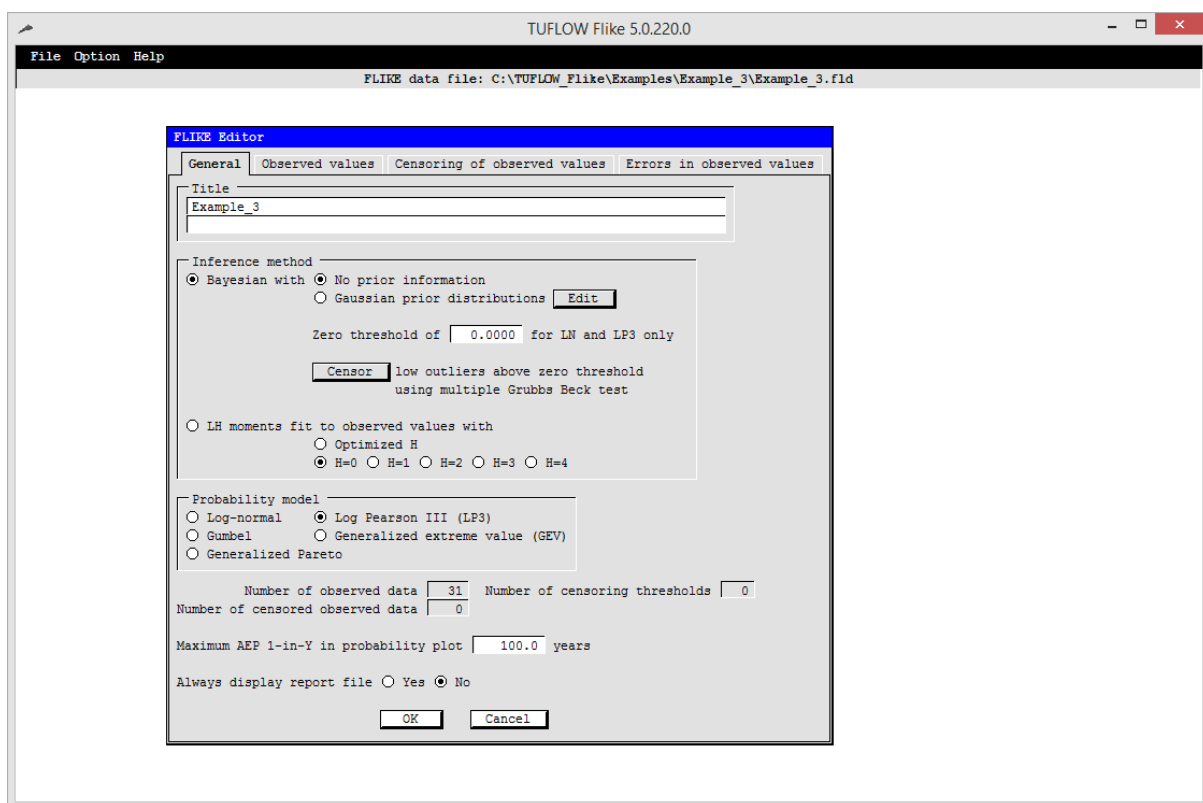


Figure 3.2.22. General Screen – After Data Import

### 2.8.3.6. Running TUFLOW Flike and accessing Results

TUFLOW Flike presents the results in two ways:

- As a visual plot; and
- In a text based report file.

Both of these will be explored in this example and both should be consulted when undertaking a Flood Frequency Analysis. Before we proceed with this example the length of the x-axis in the plot needs to be specified; that is, the lowest probability (rarest event) to be displayed. It is recommended to always enter a value greater than the 1 in Y AEP event that you are interested in. This is specified in the **Maximum AEP 1 in Y in probability plot \_\_\_ years** text box. In this example, enter the 1 in 200 year AEP event as shown in [Figure 9](http://localhost:8889/Fit.model.png) [http://localhost:8889/Fit.model.png]. By default the plot window automatically launches when a distribution is fitted.

In addition to the plot window a report file can also be automatically launched in a text editor. This can be quite helpful when you are developing a model, as it allows you to more readily compare the results. To do this select the appropriate radio button next to **Always display report file** as shown in [Figure 3.2.22](#).

### 2.8.3.7. Run TUFLOW Flike

Now that the data has been imported, the distribution selected, the fit method configured and the output configured TUFLOW Flike is ready to run. To fit the model select **OK** on the **General** tab and this will return you to the **TUFLOW Flike** window, which will look quite empty as in [Figure 3.2.23](#). In this window, select the **Option** dropdown menu and choose

## At-Site Flood Frequency Analysis

---

**Fitmodel.** This will run TUFLOW-Flike and present you with a **Probability Plot** as well as opening the **Report File** in a text editor.

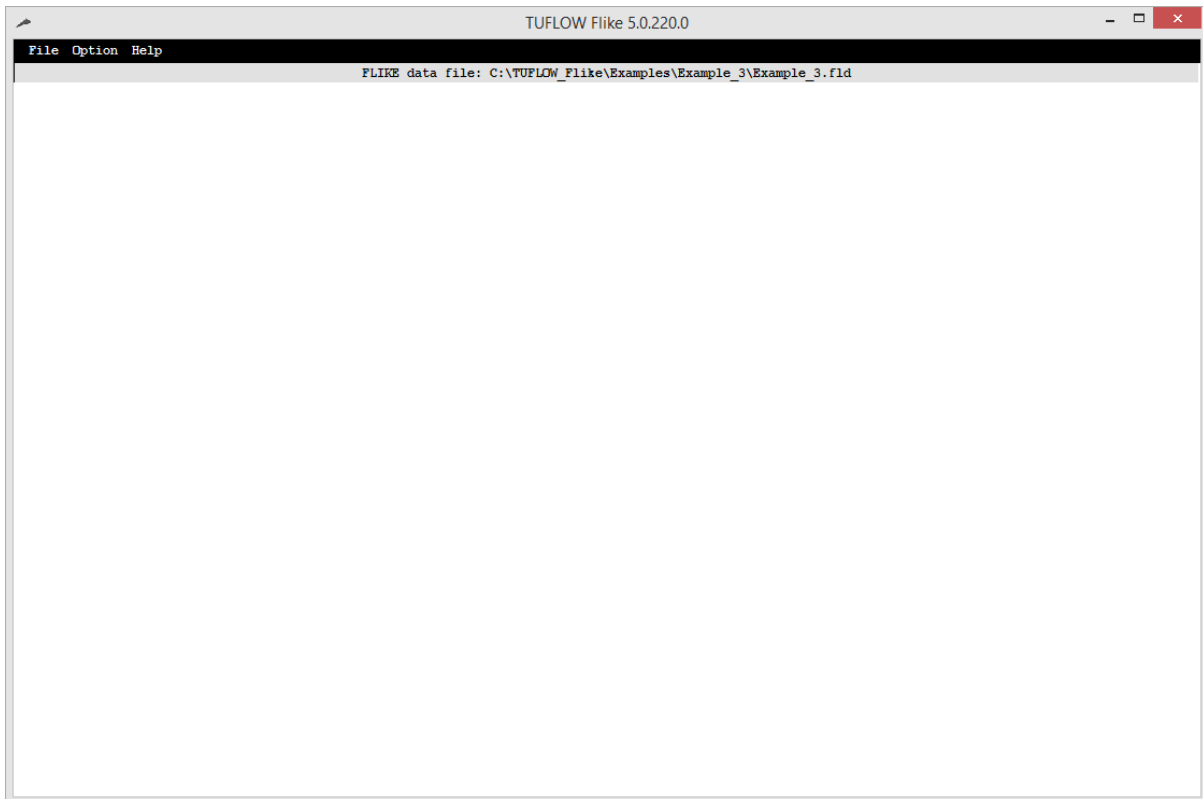


Figure 3.2.23. Blank TUFLOW-Flike Screen

### 2.8.3.8. Reviewing the results

When TUFLOW-Flike has finished fitting the distribution to the input data, a plot screen will appear similar to [Figure 3.2.24](#) and the results file will be shown in the default text editor as in [Figure 3.2.25](#).

# At-Site Flood Frequency Analysis

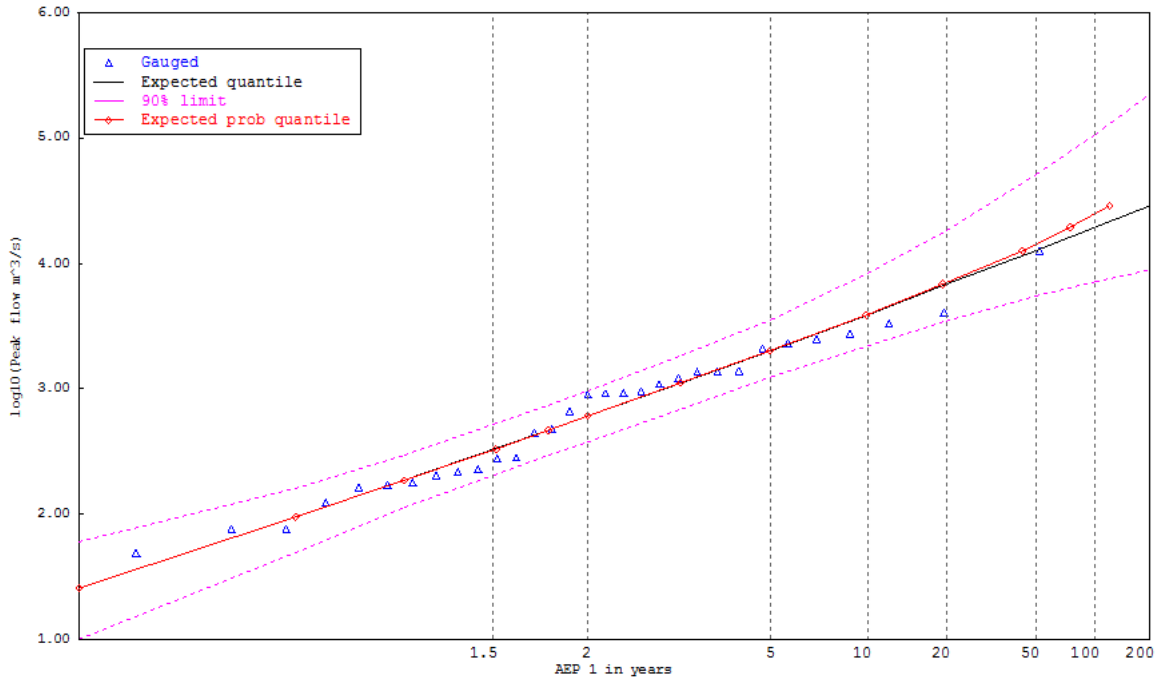


Figure 3.2.24. Probability Plot

## At-Site Flood Frequency Analysis

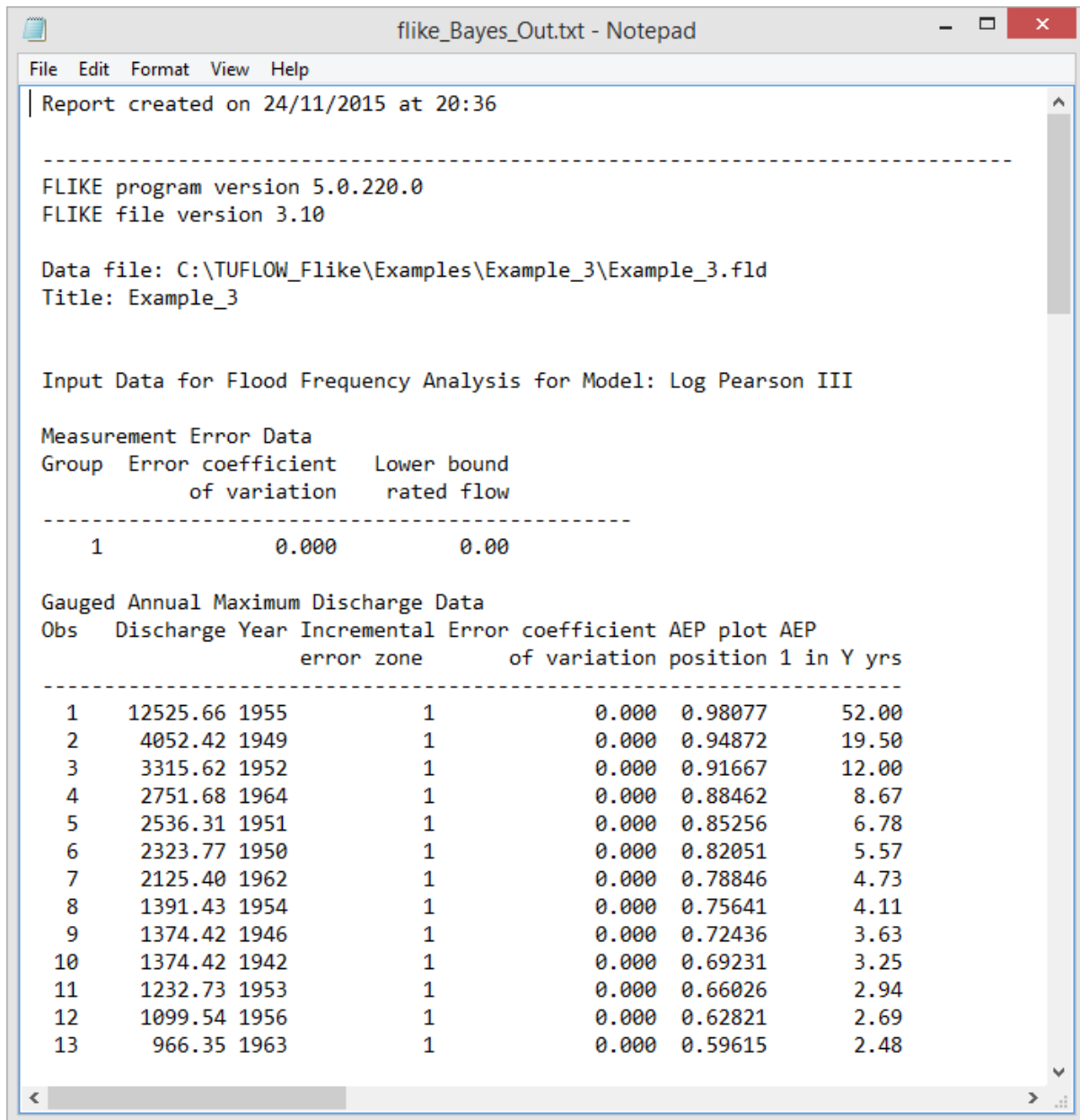


Figure 3.2.25. Results File

When fitting a flood series to a probability distribution it is essential that the results are viewed and reviewed. This is most easily achieved by first viewing the results in the **Probability Plot**. If the **Probability Plot** window has been closed, it can be reopened by selecting the **Option** dropdown menu and then **Viewplot**. The plot contains information about the fit as well as the quantile values and confidence limits. Within the plot window the y-axis contains information on discharge (or log discharge depending on the Plot scale selected) and x-axis displays the Annual Exceedance Probability (AEP) in terms of 1 in Y years. The plot displays the:

- Log-Normal probability plot of the gauged flows with plotting position determined using the Cunnane plotting position, shown as blue triangles;
- X% AEP quantile curve (derived using the posterior mean parameters), shown as a black line;

## At-Site Flood Frequency Analysis

- 90% quantile confidence limits shown as dashed pink lines; and
- The expected probability quantile, shown as a red line.

For the data contained in this example the resulting plot displays a good fit to the gauged data and appears to have tight confidence limits with all gauged data points falling within the 90% confidence limits; by default the figure plots the logarithm of the flood peaks. The plot can be rescaled to remove the log from the flow values. Select the **Plotscale** button and choose one of the non-log options, that is, either Gumble or Exponential and the uncertainty changes as in Figure 3.2.26. This will present a more sobering perspective on the model fit with the confidence limit appearing much larger for rarer flood quantiles. This can be confirmed by reviewing the results in the **Result file**. Table 3.2.6 presents a subset of the results found in the **Result file** of selected X% AEP quantiles  $q_Y$  and their 90% confidence limits. For example, for the 1% AEP flood, the 5% and 95% confidence limits are respectively 37% and 546% of the quantile  $q_Y$ ! The 0.2% AEP confidence limits are so wide as to render estimation meaningless. Note the expected AEP for the quantile  $q_Y$  consistently exceeds the nominal X% AEP. For example, the 1% (1 in 100) AEP quantile of 19 572 m<sup>3</sup>/s has an expected AEP of 1.35% (1 in 74).

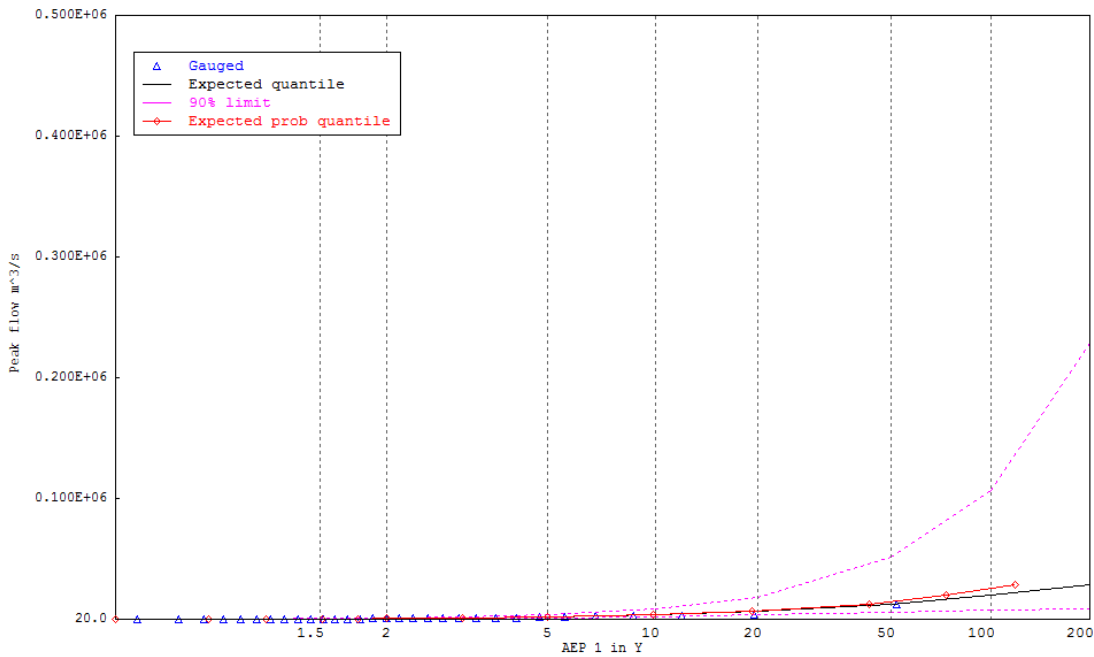


Figure 3.2.26. Probability Plot using Gumbel Scale

Table 3.2.6. Selected Results

1 in Y AEP	Quantile Estimate $q_Y$	Quantile confidence limits 5% limit	Quantile confidence limits 95% limit	Expected 1 in Y AEP for $q_Y$
10	3929	2229	8408	10.1%
50	12 786	5502	51 010	2.32%
100	19 572	7188	107 122	1.36%

At-Site Flood Frequency  
Analysis

1 in Y AEP	Quantile Estimate $q_Y$	Quantile confidence limits 5% limit	Quantile confidence limits 95% limit	Expected 1 in Y AEP for $q_Y$
500	47 034	11 507	570 635	0.48%

Table 3.2.7. Gauged flows on the Hunter River at Singleton

Year	Flow (m <sup>3</sup> /s)	Year	Flow (m <sup>3</sup> /s)	Year	Flow (m <sup>3</sup> /s)	Year	Flow (m <sup>3</sup> /s)
1938	76.26	1946	1374.42	1954	1391.43	1962	2125.4
1939	171.87	1947	280.18	1955	12525.66	1963	966.35
1940	218.21	1948	202.62	1956	1099.54	1964	2751.68
1941	668.79	1949	4052.42	1957	447.75	1965	49.03
1942	1374.42	1950	2323.77	1958	478.92	1966	76.51
1943	124.12	1951	2536.31	1959	180.52	1967	912.5
1944	276.3	1952	3315.62	1960	164.36	1968	926.67
1945	895.5	1953	1232.73	1961	229.54		

### 2.8.4. Example 4: Use of binomial censored historical data

This example is a continuation of **Example 3** and it examines the benefit of using historical flood information. In the previous example the gauged record spanned the period 1938 to 1968. The biggest flood in that record occurred in 1955 with a discharge of 12 526 m<sup>3</sup>/s. An examination of historic records indicates that during the ungauged period 1820 to 1937 there was only one flood that exceeded the 1955 flood and that this flood occurred in 1820. The information for the 1820 flood is not from a stream gauge; rather it is from a variety of sources including newspaper articles. This information is valuable, perhaps the most valuable, even though the magnitude of the 1820 flood is not reliably known. This information can be incorporated into a Bayesian approach. The way that this is done in TUFLOW Flike is through censoring data.

From the information about the flood history at Singleton we can make the following conclusions:

- Over the ungauged period 1820 to 1937 there was:
  - One flood above the 1955 flood; and
  - 117 floods below the 1955 flood.

Note that the ungauged record length is 118 years, that is, all years from 1820 to 1937 are included as it is assumed each year has an event. Also, note that the ungauged period cannot overlap with the gauged period.

#### 2.8.4.1. Launch TUFLOW-Flike

As in **Example 3** launch TUFLOW Flike; however, this time open the **.fld** file previously created: **Example\_3.fld**. This file will be used as it contains the data that are needed for this example. To do this select the File dropdown menu and then select **Open**. Navigate to the **Example\_3.fld** in the next dialogue box and open the file. The **Flike Editor** window will then appear containing all the information from Example 3.

### 2.8.4.2. Save Example\_4.fld

The next step is to save the **Example\_4.fld** file as a new file. It is best to do this immediately to ensure that no data is overwritten. To do this, select **OK** from the **Flike Editor** window which will return to the main **TUFLOW Flike** window. Select **File** again and then **Saveas**. Save the file as **Example\_4.fld** in a new folder called **Example 4**.

### 2.8.4.3. Enter Historical Flood Information

In this step the historical flood information is entered. To edit the **Example\_4.fld** data from the **TUFLOW-Flike** window select **Options** and then **Edit data**. This reopens the Flike Editor window. Now select the **Censoring of observed values** tab and this will open a window similar to [Figure 3.2.27](#) with no data.

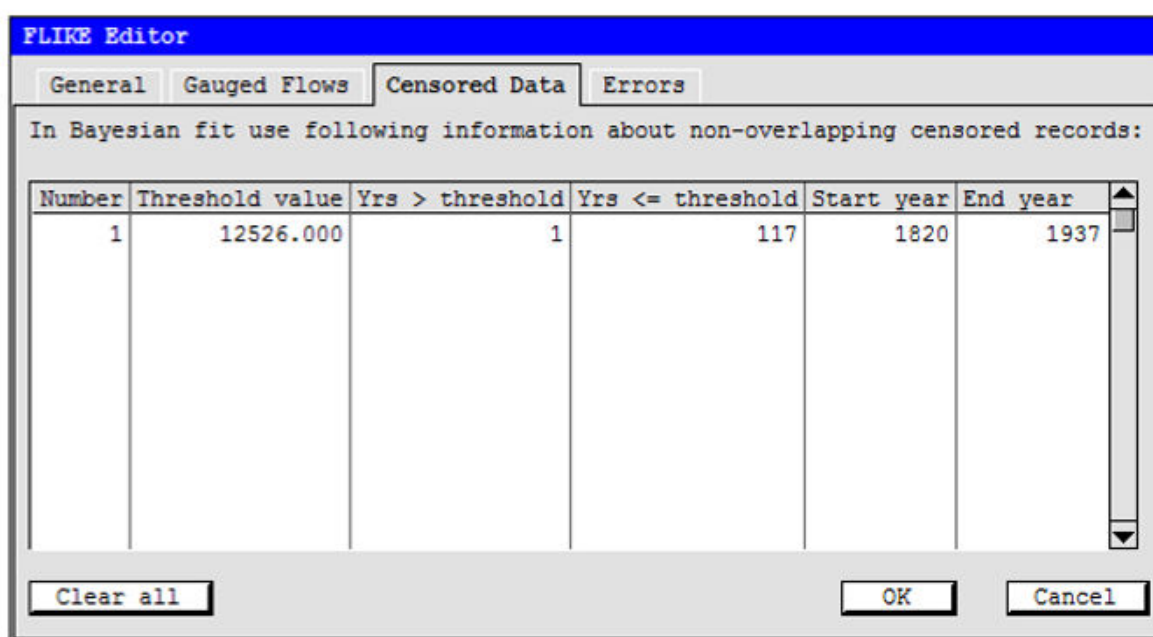


Figure 3.2.27. Censoring observed values tab

The historical data needs to be entered into the **Censoring of observed values** tab, that is, we need to let TUFLOW-Flike know that there has been one flood greater than the 1955 flood between 1820 and 1937. So:

- The **Threshold value** is  $12\,526\text{m}^3/\text{s}$  - the size of the 1955 flood.
- The Years greater than the threshold (**Yrs > threshold**) is one (1) – the 1820 flood.
- The Years less than or equal to the threshold (**Yrs <= threshold**) is 117 – there were 117 years between 1820 and 1937 with flood less than the 1820 flood.
- The **Start Year** is 1820; and  
The **End Year** is 1937.

Once the data has been entered, select **OK** which will return the main **TUFLOW-Flike** window. TUFLOW-Flike performs some checks of the data to ensure that it has been

entered correctly. However, these are only checks and it is up to the user to ensure they have correctly configured the historic censoring.

Return to the **General** tab by selecting **Options** and then **Edit data** and it should appear as in [Figure 3.2.28](#). **Note the Number of censoring thresholds** text field has been populated with the number 1, so TUFLOW-Flike has recognised that there censoring has been configured.

As with the previous example, check that the **Always display report file** radio button has been selected.

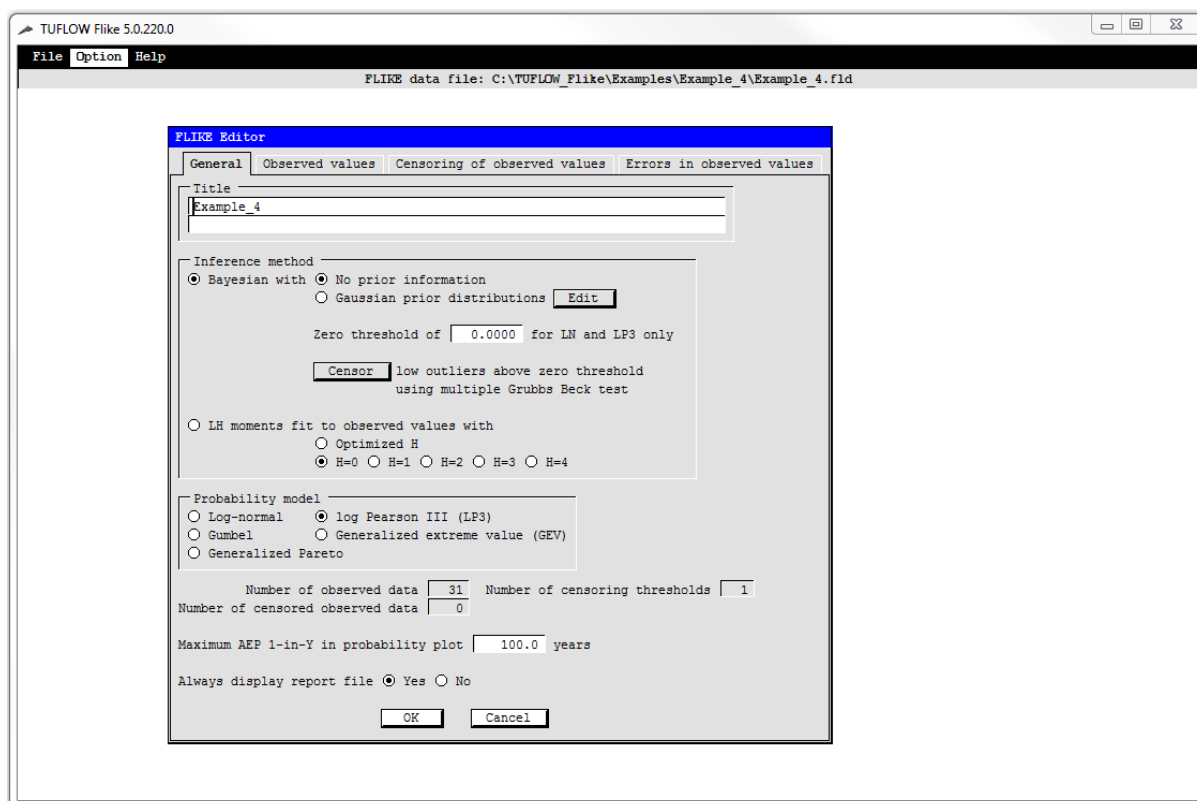


Figure 3.2.28. Configured Flike Editor

#### 2.8.4.4. Run TUFLOW-Flike with Historic Censoring Data

On the general tab select **OK** and return to the **TUFLOW-Flike** window. As in the previous exercise select **Option** and then **Fit model**. This will run TUFLOW-Flike and when the engine has finished the **Probability Plot** will open together with the **Report File**.

#### 2.8.4.5. Results

[Table 3.2.8](#) presents the posterior mean, standard deviation and correlation for the Log Pearson Type III parameters:  $m$ ,  $loges$  and  $g$  which are respectively the mean, standard deviation and skewness of  $loge(q)$  taken from the **Report File**. Comparison with Example 3 reveals the censored data have reduced by almost 17% the uncertainty in the skewness ( $g$ ) parameter. This parameter controls the shape of the distribution, particularly in the tail region where the floods of interest are.



At-Site Flood Frequency  
Analysis

Table 3.2.8. Posterior Mean, Standard Deviation and Correlation for the LP III

LP III Parameter	Mean	Std. Deviation	Correlation		
m	6.365	0.237	1.000		
log <sub>e</sub> s	0.303	0.120	-0.236	1.000	
g	-0.004	0.405	-0.227	-0.409	1.000

The resulting **Probability plot** is shown in [Figure 3.2.30](#). This figure displays on a log normal probability plot the gauged flows, the X% AEP quantile curve (derived using the posterior mean parameters), the 90% quantile confidence limits and the expected probability curve. Compared with Example 3 the tightening of the confidence limits is noticeable.

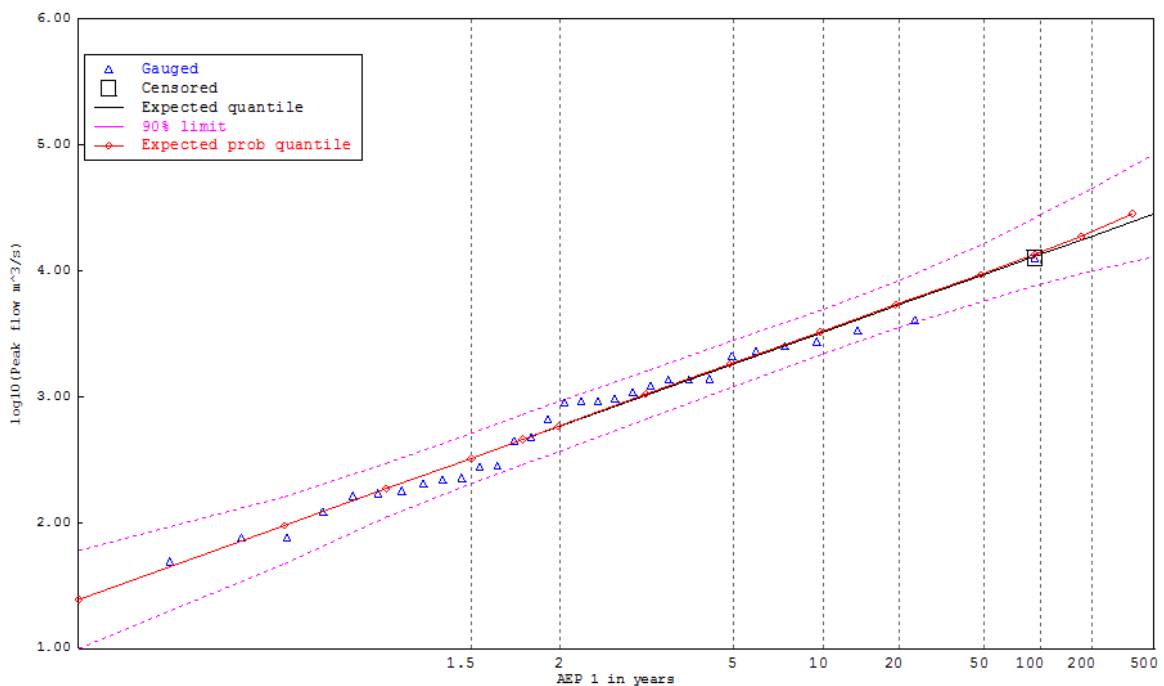


Figure 3.2.29. Probability plot of the Singleton data with historic information

The following table ([Table 3.2.9](#)) of selected 1 in Y AEP quantiles  $q_Y$  and their 90% confidence limits illustrates the benefit of the information contained in the historic data. For example, for the 1% AEP flood the 5% and 95% confidence limits are respectively 58% and 205% of the quantile  $q_Y$ ! This represents a major reduction in quantile uncertainty compared with Example 3 which yielded limits of 38% and 553%. This is illustrated in graphically [Figure 3.2.30](#).

Table 3.2.9. Comparison of Selected Quantiles with 90% Confidence Limits

1 in Y AEP	Quantile Estimate $q_Y$	Quantile Confidence Limits 5% Limit	Quantile Confidence Limits 95% Limit	Expected 1 in Y AEP for $q_Y$
10	3294	2181	4947	10.37%
50	9350	5778	16 511	2.09%

## At-Site Flood Frequency Analysis

1 in Y AEP	Quantile Estimate $q_Y$	Quantile Confidence Limits 5% Limit	Quantile Confidence Limits 95% Limit	Expected 1 in Y AEP for $q_Y$
100	13 511	7785	27 687	1.08%
500	28 542	12 966	85 583	0.28%

Note that **Report File** presents the Expected AEP in 1 in Y years whereas Table 3.2.9 presents as the Expected AEP as a percentage.

This example highlights the significant reductions in uncertainty that historical data can offer. However, care must be exercised to ensure the integrity of the historic information – see Book 3, Chapter 2, Section 3 for more details.

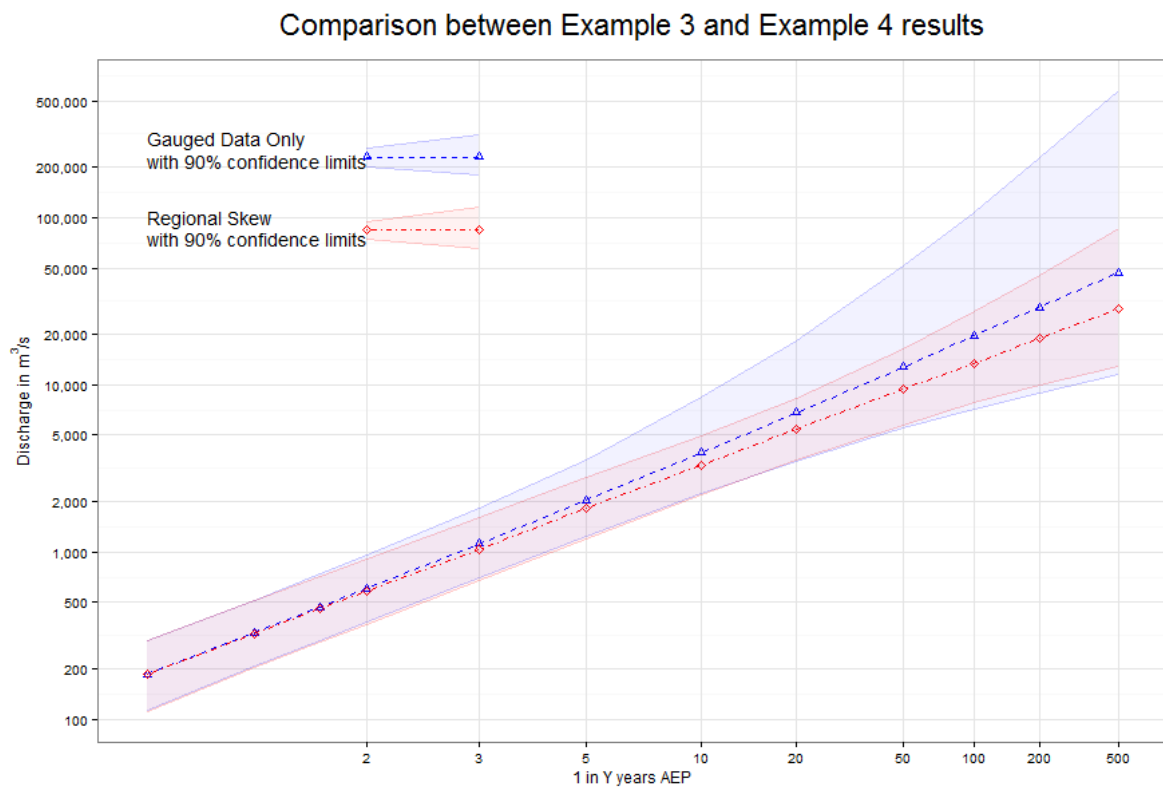


Figure 3.2.30. Probability plot of the Singleton data with historic information

### 2.8.5. Example 5: Use of regional information

In this example the use of regional parameter information is explored, building on Example 3. As was shown in Example 3, there was significant uncertainty in the skewness parameter. In that example, the posterior mean of the skewness was estimated to be 0.131 with a posterior standard deviation of 0.479. This led to significant uncertainty in the quantile estimates, for instance the 5% and 95% confidence limits for the 1% AEP quantile were 37% and 546% respectively of the 1% AEP quantile. This example shows how the use of regional information can reduce, sometimes significantly, the uncertainty of quantile estimates. Details on the use of regional information can be found in Book 3, Chapter 2, Section 3 and Book 3, Chapter 2, Section 6.

In this hypothetical example, a regional analysis of skewness has been conducted and the expected regional skew was found to be 0.00 with a standard deviation of 0.30. This information can be incorporated into the Bayesian analysis undertaken by TUFLOW Flike as shown in this example.

### 2.8.5.1. Launch TUFLOW Flike

The Singleton data from the previous examples will be used in this example, so as in Example 4 launch TUFLOW Flike and open the **.fld** file created in Example 3. Save the opened **.fld** as, say, **Example\_5.fld**.

### 2.8.5.2. Enter Prior Information

The next step will be to enter the prior information, that is the regional information on skew. To do this, select **Edit data** from the **Options** menu. As before, this opens the **Flike Editor**. To enter the prior regional information, check the **Gaussian prior distributions** radio button and then click on the Edit button as shown in [Figure 3.2.31](#). This will open the **Prior for Log-Pearson III** window as shown in [Figure 3.2.32](#).

The regional skewness (0.00) is entered into the **Mean Skew of log Q** text box and the standard deviation of the regional skew (0.300) is entered into the **Standard Deviation Skew of log Q** as shown in [Figure 3.2.32](#). Note in practice careful attention to the units being used is required.

Very large prior standard deviations are assigned to the **Mean of log Q** and **Standard deviation of log Q** parameters to ensure there is no prior information about these parameters. If the *Log Pearson III* distribution has been selected, the option to import the prior information from the ARR Regional Flood Frequency Estimation method is available ([Book 3, Chapter 3](#)).

Select **OK** to return to the **Flike editor** window.

At-Site Flood Frequency  
Analysis

**FLIKE Editor**

General   Gauged Flows   Censored Data   Errors

Title  
Hunter river at Singleton

Inference method

Bayesian with  No prior information  
 Gaussian prior distributions **Edit**

Zero threshold of

**Censor** low outliers above zero threshold  
using multiple Grubbs Beck test

LH moments fit to gauged flows with  
 Optimized H  
 H=0  H=1  H=2  H=3  H=4

Probability model

Log-normal    log Pearson III (LP3)  
 Gumbel    Generalized extreme value (GEV)  
 Generalized Pareto

Number of gauged data    Number of censoring thresholds   
 Number of censored gauged data

Maximum AEP 1-in-Y in probability plot  years

Always display report file  Yes  No

**OK**   **Cancel**

Figure 3.2.31. Gaussian prior distributions

**Prior for Log-Pearson III**

Parameter	Mean	Std dev	Correlation		
Mean of log Q	<input type="text" value="1.000"/>	<input type="text" value="100000000.000"/>	<input type="text" value="1.000"/>		
Std dev of log Q	<input type="text" value="1.000"/>	<input type="text" value="100000000.000"/>	<input type="text" value="0.000"/>	<input type="text" value="1.000"/>	
Skew of log Q	<input type="text" value="0.000"/>	<input type="text" value="0.300"/>	<input type="text" value="0.000"/>	<input type="text" value="0.000"/>	<input type="text" value="1.000"/>

**Import** prior from ARR regional frequency report file

**OK**   **Cancel**

Figure 3.2.32. Prior for Log-Pearson III window

### 2.8.5.3. Run TUFLOW Flike with Regional Information

As in the previous examples select **OK** from the **Flike Editor** window to return to the main **TUFLOW Flike** window and select **Fit model** from the **Options menu** to run TUFLOW Flike. This should result in the Probability plot as shown in [Figure 3.2.33](#).

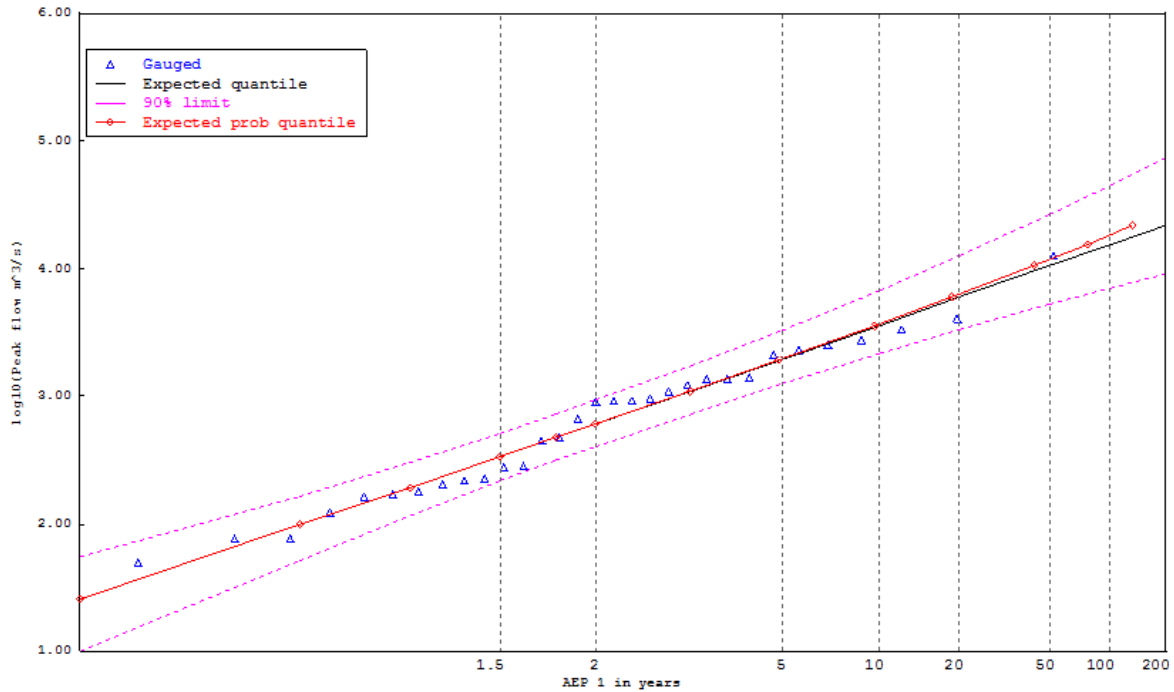


Figure 3.2.33. Probability plot of with prior regional information

[Figure 3.2.33](#) presents the probability plot for the LP III model fitted to the gauged data with prior information on the skewness. Comparison of the results from this example with the results from Example 3 (see [Figure 3.2.34](#)) reveals substantially reduced uncertainty in the right hand tail.

## At-Site Flood Frequency Analysis

Comparison between Example 1 and Example 3 results

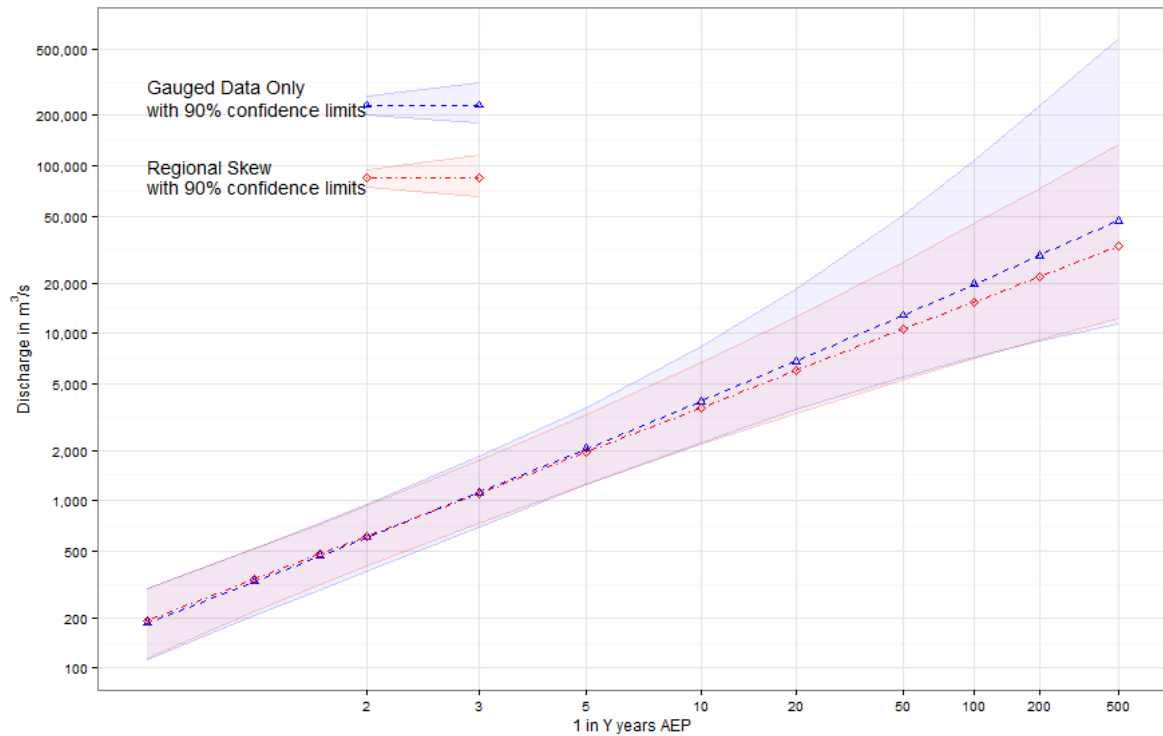


Figure 3.2.34. Comparison between the results from Example 3 and Example 5

Table 3.2.10. Comparison of LP III Parameters with and without prior information

LP III Parameter	No Prior Information		With Prior Information	
	Mean	Std. Deviation	Mean	Std. Deviation
m	6.433	0.262	6.421	0.251
log <sub>e</sub> s	0.353	0.144	0.320	0.131
g	0.131	0.479	0.019	0.261

Table 3.2.11 presents selected AEP quantiles  $q_Y$  and their 90% confidence limits. This table further illustrates the benefit of incorporating regional information. For example, for the 1% AEP flood the 5% and 95% confidence limits are respectively 37% and 546% of the quantile  $q_{1\%}$  when no prior information is used. These limits are reduced to 46% and 292%, respectively using prior regional information.

Table 3.2.11. Selected Results

AEP (%)	No Prior Information			With Prior Information		
	Quantile Estimate $q_Y$	Quantile Confidence 5% Limit	Quantile Confidence 95% Limit	Quantile Estimate $q_Y$	Quantile Confidence 5% Limit	Quantile Confidence 95% Limit
10%	3929	2229	8408	3598	2172	6702
2%	12 786	5 502	51 010	10 535	5 310	26 633
1%	19 572	7 188	107 122	15 413	7 093	45 087

At-Site Flood Frequency  
Analysis

AEP (%)	No Prior Information			With Prior Information		
	Quantile Estimate $q_Y$	Quantile Confidence 5% Limit	Quantile Confidence 95% Limit	Quantile Estimate $q_Y$	Quantile Confidence 5% Limit	Quantile Confidence 95% Limit
0.2%	47 034	11 507	570 635	33 365	12 244	134 107

### 2.8.6. Example 6: Censoring PILFs using multiple Grubbs-Beck test

In many Australian watercourses there are often years in which there are no floods. The annual maximum from those years are not representative of the population of floods and can unduly influence the fit of the distribution as discussed in [Book 3, Chapter 2, Section 6](#). The flow values are referred to as Potentially Influential Low Flows (PILFs). It is recommended that in all flood frequency analyses the removal of these flows is investigated using the multiple Grubbs-Beck test to identify PILFs. The following example is taken from [Pedruco et al. \(2014\)](#) using data provided by the Wimmera Catchment Management Authority. The table at the end of this example lists 56 years of Annual Maximum discharges for the Wimmera River at Glynwylln. This data is included in the TUFLOW Flike download and was installed in the **data** folder in the install location of TUFLOW Flike. This location will be something similar to *C:\TUFLOW Flike\data\wimmeraGaugedFlows.csv*.

This example will examine the influence of PILFs and demonstrate how to use the multiple Grubbs-Beck test to safely remove them from the flood frequency analysis.

#### 2.8.6.1. Launch TUFLOW Flike and Import Data

As in Example 3 launch TUFLOW Flike and create a new **.fld** file. Save the opened **.fld** as say, **Example\_6.fld**. Import the Wimmera River data in the same way that the Singleton data was imported, ensuring that the structure of the data has been checked using the **View** button. The **Records** start in the second row (skip the first), **Years** are in column 1 and the **Gauged values** are in column 2. Configure the import options and import the data.

Once this has been done and the **Gauged values** have been ranked in descending order the Flike Editor window should look like [Figure 3.2.35](#).

## At-Site Flood Frequency Analysis

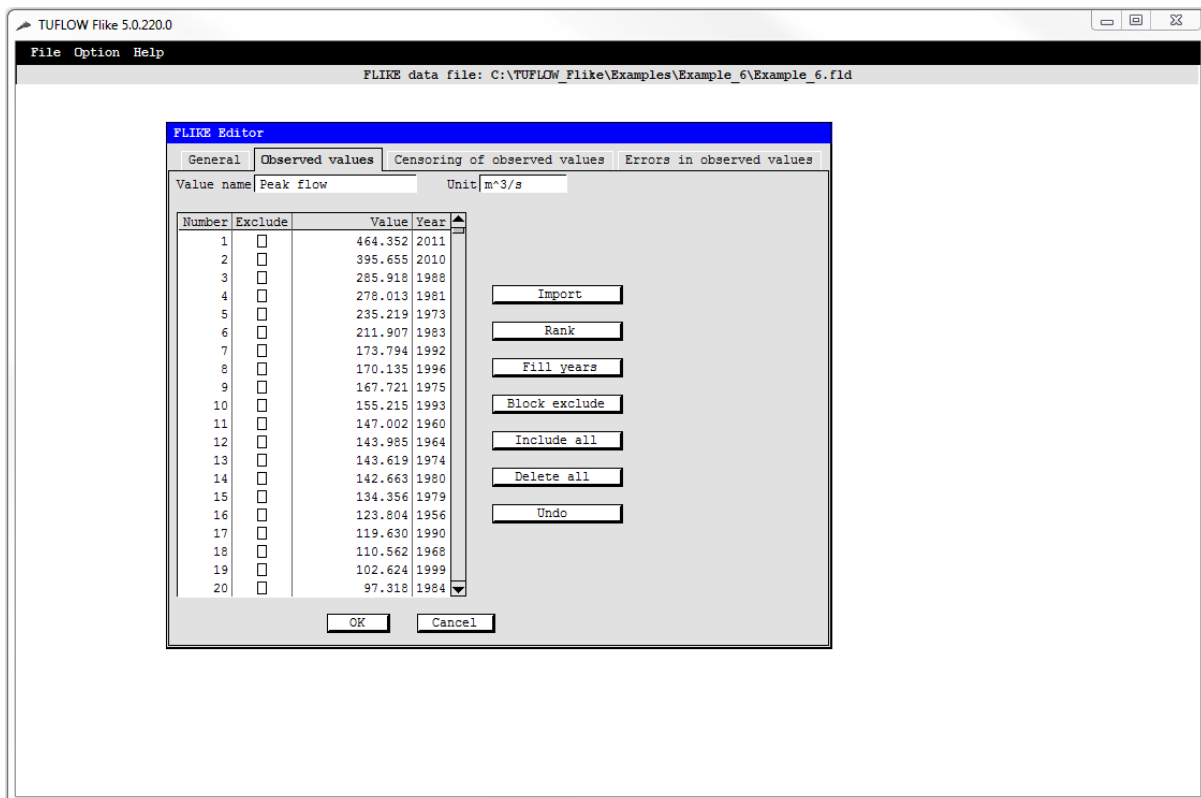


Figure 3.2.35. TUFLOW Flike editor window with Wimmera data

### 2.8.6.2. Fit Distribution

The Wimmera data will be fitted to a Generalised Extreme Value (GEV) distribution. To do this, return to the **Flike Editor General** tab and ensure that the following settings have been chosen:

- Bayesian inference method with **No prior information**;
- The **GEV** probability model; and
- The **Maximum AEP** is set to 200 years

Once these settings have been selected, select **OK** and run TUFLOW Flike in the usual way.

### 2.8.6.3. Initial Results

When TUFLOW Flike has run a new probability plot window will open. The plot will **not** look like [Figure 3.2.36](#). To expose a better view of the distributions fit, the plot scale should be changed using the **Plot Scale** button from a **Gumbel** plot scale to a **Gumbel-log** plot scale and the y-axis rescaled using the **Rescale** button to have a minimum of 0.0 and a maximum of 4.0.

In [Figure 3.2.36](#), the fit to the right-hand tail is not satisfactory. The expected quantiles are significantly greater than the gauged data, further the largest 3 data points fall outside of the lower 90% confidence limits.



## At-Site Flood Frequency Analysis

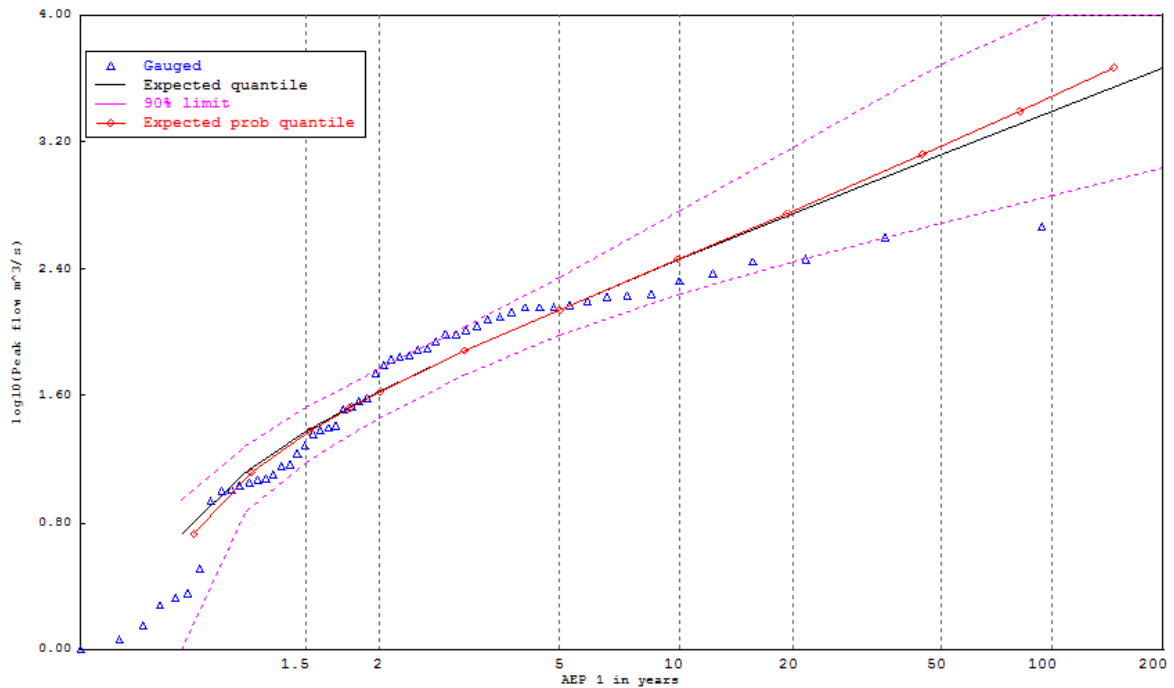


Figure 3.2.36. Initial probability plot for Wimmera data with GEV

### 2.8.6.4. Multiple Grubbs-Beck test

The fit of the distribution can be improved by removing PILFs. In TUFLOW Flike this can be done using the multiple Grubbs-Beck test, to do this, return to the **Flike Editor** window and select the **Censor** button. TUFLOW Flike will run the multiple Grubbs-Beck test on the Wimmera data and when finished it will return a window similar to the one shown in [Figure 3.2.37](#). The multiple Grubbs-Beck test has detected 27 possible PILFs, select **Yes** to censor them.

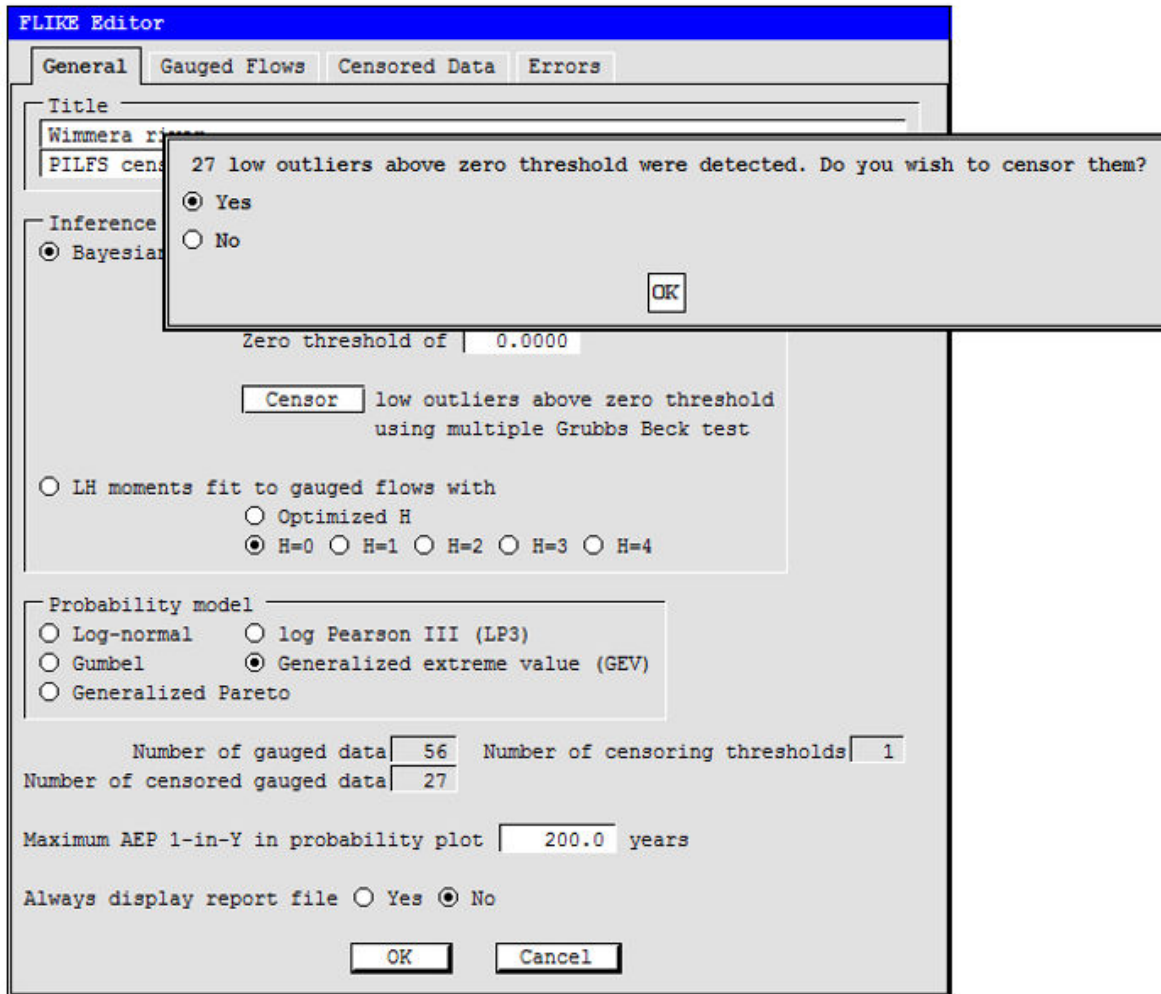


Figure 3.2.37. Results of the multiple Grubbs-Beck test

On agreeing to censor these flows, TUFLOW Flike automatically performs two changes to the inference setup:

1. The 27 lowest discharges are excluded from the calibration.
2. A censored threshold is added, with the information that there are 27 Annual Maximum discharges that lie below the threshold of 54.396m<sup>3</sup>/s which corresponds the 28th ranked discharge.

These are further explained below

#### 2.8.6.4.1. Excluded Data

The exclusion of the lowest 27 discharges can be seen in the **Observed Flows** tab of the **Flike Editor** as shown in [Figure 3.2.38](#). In this tab all the values below the threshold have the **Exclude check** box crossed, this can be seen by scrolling down the window or by re-ranking the data and selecting **Ascending**. If you have re-ranked the data in ascending order re-rank it back into **Decesending** order.

## At-Site Flood Frequency Analysis

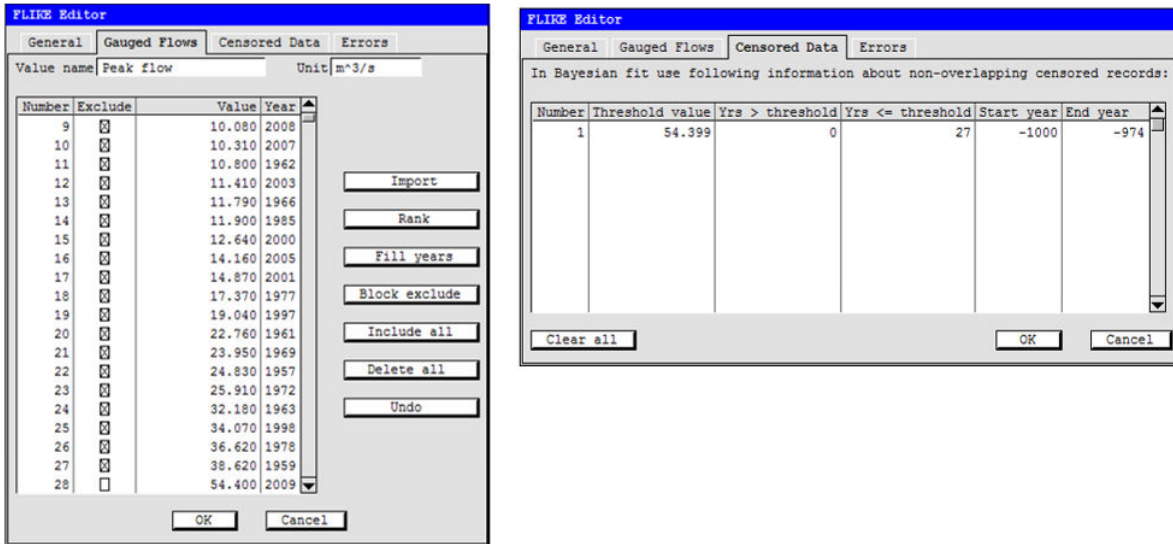


Figure 3.2.38. Excluded gauged values

### 2.8.6.4.2. Censoring Threshold

The addition of the censored threshold appears in the **Censoring of observed values** tab of the **Flike Editor** as shown in [Figure 3.2.39](#). The **Threshold** value (54.396m<sup>3</sup>/s) has been automatically populated together with the years that are greater than the threshold (0). The number of years less than the threshold (27) has also been populated. What this is telling TUFLOW Flike is that 27 years of discharges are less than the threshold are being censored; that is, gauged values are not considered but the frequency is. The **Start year** and **End year** are also populated with dummy year ranges beginning 1000BC. This is done to satisfy an automatic check in TUFLOW Flike designed to assist in the entry of historic data.

## At-Site Flood Frequency Analysis

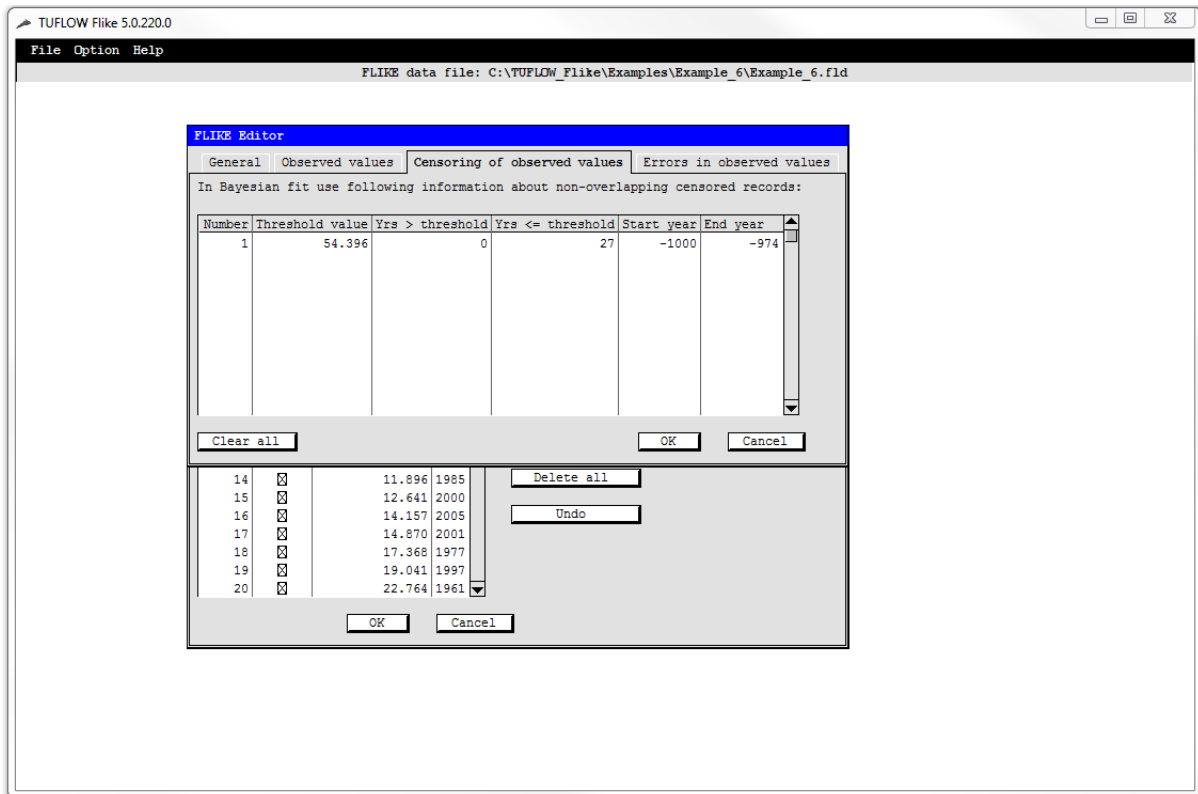


Figure 3.2.39. Censoring of observed values

### 2.8.6.5. Results using multiple Grubbs-Beck test

Return to the main **TUFLOW Flike** window and run TUFLOW FLIKE by selecting **Fit model**. As usual, a **Probability plot** window will automatically appear, as for the initial results change the plot scale to Gumbel-log and rescale the y-axis to have a minimum of 0.0 and a maximum of 4.0. The resulting plot will look like [Figure 3.2.40](#).

A comparison of [Figure 3.2.36](#) and [Figure 3.2.40](#) shows the improved fit, in [Figure 3.2.40](#) all of the gauged data points fall within the 90% confidence limits. Further, censoring the PILFs using the multiple Grubbs-Beck test has significantly altered the quantile estimates and reduced the confidence limits as shown in [Table 3.2.12](#). For instance the quantile q1% when PILFs are excluded is around 21% of the initial estimate. The lower and upper confidence limits have been considerable reduced, initially they were 30% and 500% of the quantile q1% and following the removal of PILFs they became 68% and 220% of the quantile q1%.

## At-Site Flood Frequency Analysis

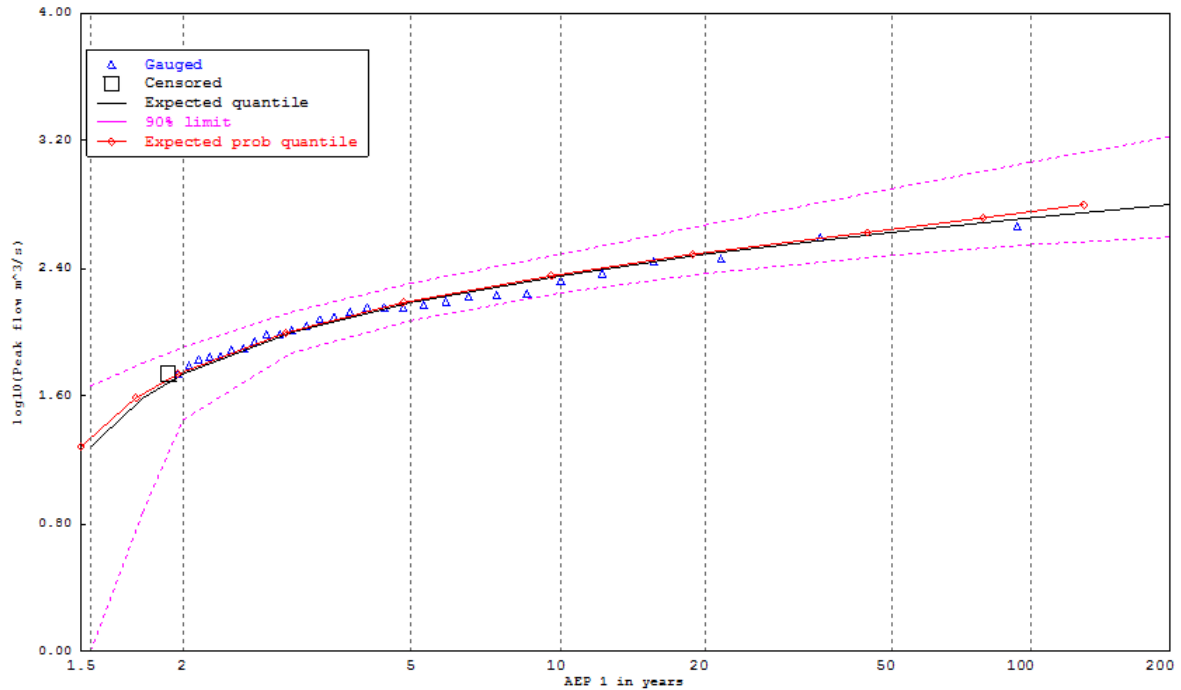


Figure 3.2.40. GEV fit - 56 years AM of gauged discharge - Using multiple Grubbs-Beck test

Table 3.2.12. Selected Results

AEP (%)	No Removal of PILFS			Removal of PILFS		
	Quantile Estimate $q_Y$	Quantile Confidence 5% Limit	Quantile Confidence 95% Limit	Quantile Estimate $q_Y$	Quantile Confidence 5% Limit	Quantile Confidence 95% Limit
10%	286	172	578	227	177	311
2%	1315	493	4975	423	304	784
1%	2481	737	12 398	521	354	145
0.2%	10696	1802	101 034	789	448	2813

### Annual Maximum data for the Wimmera River at Glynwylln

464.35	167.72	119.63	71.4	32.18	14.16	8.52
395.65	155.22	110.56	69.67	25.91	12.64	3.22
285.92	147	102.62	67.49	24.83	11.9	2.28
278.01	143.99	97.32	61.64	23.95	11.79	2.13
235.22	143.62	96.78	54.4	22.76	11.41	1.9
211.91	142.66	87.98	38.62	19.04	10.8	1.43
173.79	134.36	79.15	36.62	17.37	10.31	1.16
170.13	123.8	77.03	34.07	14.87	10.08	0.01

## 2.8.7. Example 7: Improving poor fits using censoring of low flow data

The standard probability models such as GEV and LP III may not adequately fit flood data for a variety of reasons, for example Probable Influential Low Flow Flows (PILFs). In this example the censoring of data is used to censor low discharge data and improve the fit of the distribution to the data.

Often the poor fit of a distribution is associated with a sigmoidal probability plot as illustrated in [Figure 3.2.41](#). In such cases a four or five-parameter distributions which have sufficient degrees of freedom can be used to track the data in both upper and lower tails of the sigmoidal curve. Alternatively a calibration approach that gives less weight to smaller floods can be adopted. The second approach is adopted in this example.

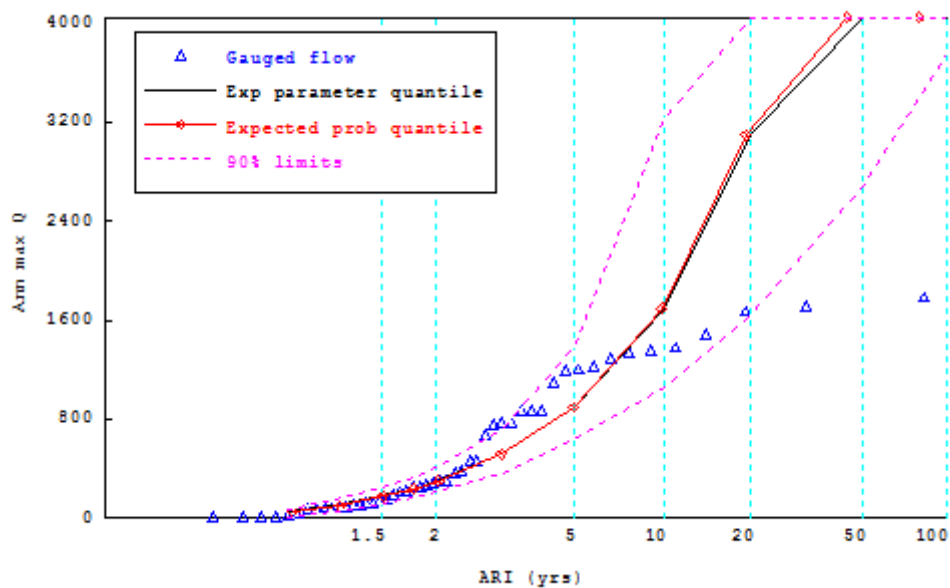


Figure 3.2.41. Bayesian fit to all gauged data Gumbel probability plot

### 2.8.7.1. Launch TUFLOW Flike and Import Data

As in previous examples launch TUFLOW Flike, create a new **.fld** file and import the Albert River at Bromfleet data (*albertRvGaugedFlows.txt*) file which was included in the TUFLOW Flike install in the **data** directory. Note the structure of this file and configure the **Import gauged values** window. The Albert River at Broomfleet data is included at the end of this example.

### 2.8.7.2. Fit GEV Distribution

To recreate [Figure 3.2.41](#) fit a GEV distribution to the Albert River data and accept the defaults in the **General** tab of the **FLIKE Editor**. The plot in [Figure 3.2.41](#) can be recreated by changing the plot scale to **Gumbel** and rescaling the y-axis to 0 and 4000.

[Figure 3.2.41](#) displays the GEV Bayesian fit on a Gumbel probability plot. Although the observed floods are largely contained within the 90% confidence limits, the fit, nonetheless, is poor – the data exhibit a sigmoidal trend with reverse curvature developing for floods with

an AEP greater than 50%. It appears that the confidence limits have been inflated because the GEV fit represents a poor compromise.

### 2.8.7.3. Use the multiple Grubbs Beck test to improve fit

The first step in improving the poor fit of this data is to use the multiple Grubbs Beck test to remove PILFs. Repeat the procedure outline in the previous example. This will result in the censoring of 5 data points with a threshold of 36.509m<sup>3</sup>/s.

Now run TUFLOW Flike and fit the model. Changing the plot scale and rescale the y-axis as above will result in [Figure 3.2.42](#).

[Figure 3.2.42](#) displays the fit after censoring the 5 low outliers identified by the multiple Grubbs-Beck test. The improvement in fit is marginal at best over [Figure 3.2.41](#).

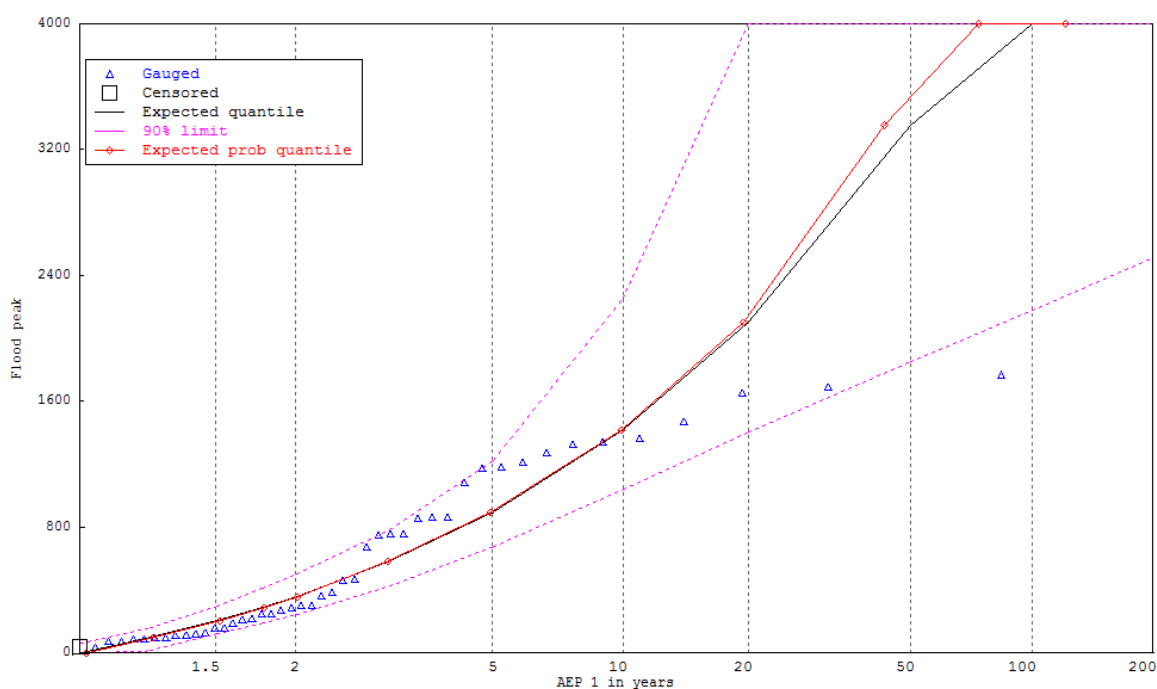


Figure 3.2.42. Bayesian fit with 5 low outliers censored after application of multiple Grubbs-Beck test

### 2.8.7.4. Trial and error approach

To deal with this poor fit, a trial-and-error approach to selecting the threshold discharge for the censoring low flows can be used to obtain a fit that favours the right hand tail of the distribution. This involves testing different threshold values until an acceptable fit is produced. [Figure 3.2.43](#) illustrates one such fit. To de-emphasise the left hand tail the floods below the threshold of 250 m<sup>3</sup>/s were censored. This means the GEV distribution was fitted to:

- A gauged record consisting of the 27 floods above 250m<sup>3</sup>/s; and
- A censored record consisting of 23 floods below the threshold of 250m<sup>3</sup>/s and 0 floods above this threshold.

To do this in TUFLOW Flike there are two steps, as in Example 6, these are:

- Exclude the flows below 250m<sup>3</sup>/s
- Create a censoring threshold

This is essentially the same process that was undertaken to exclude flows in Example 6 except it needs to be done manually. This is outlined below.

#### **2.8.7.4.1. Excluded data**

The flows below 250m<sup>3</sup>/s need to be excluded from the analysis. To do this select the **Observed values** tab of the **Flike Editor** and choose the **Block exclude** button. Enter 250 into **Value below which values are to be excluded** text box and select **OK**. This will exclude all values below 250m<sup>3</sup>/s which can be confirmed by scrolling down the table in the **Observed values** tab.

#### **2.8.7.4.2. Censoring threshold**

As in the previous example a censoring threshold needs to be entered into the Censoring of observed values tab. Populate the tab with the following information:

- **Threshold value:** 250
- Years greater than threshold (**Yrs > threshold**): 0
- Years less than or equal to threshold (**Yrs <= threshold**): 23
- **Start year:** 1000
- **End year:** 1022

#### **2.8.7.5. Results of the trial and error approach**

Run TUFLOW Flike in the usual way and a Probability plot similar to [Figure 3.2.43](#) will be obtained.

The censored record provides an anchor point for the GEV distribution – it ensures that the chance of an Annual Maximum flood being less than 250m<sup>3</sup>/s is about 23/50 without forcing the GEV to fit the peaks below the 250m<sup>3</sup>/s threshold. The fit effectively disregards floods with a greater than 50% AEP and provides a good fit to the upper tail. Another benefit is the substantially reduced 90% confidence limits which can be reviewed by examining the results files.



## At-Site Flood Frequency Analysis

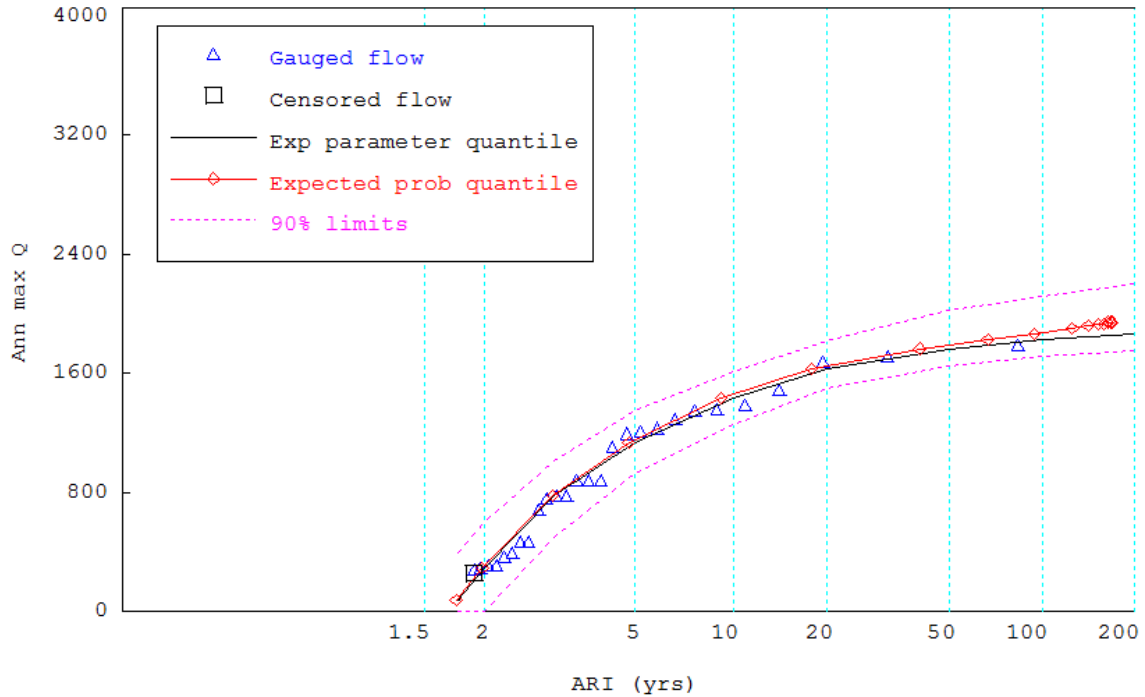


Figure 3.2.43. Bayesian fit with floods below 250 m<sup>3</sup>/s threshold treated as censored observations

### Annual Maximum data for the Albert River at Bromfleet data

1765.92	1689.51	1652.72	1468.77	1364.06	1341.42	1327.27	1273.5
1214.07	1185.77	1177.28	1086.72	865.98	863.15	860.32	761.27
761.27	752.78	676.37	466.95	461.29	384.88	362.24	305.64
302.81	285.83	271.68	294.61	249.61	220.74	210.55	190.74
156.5	156.22	131.03	124.52	116.88	113.77	99.9	95.65
88.3	87.73	78.11	72.73	36.51	22.36	16.7	15.85
15.57	13.02						

### 2.8.8. Example 8: A Non-Homogeneous Flood Probability Model

The work of Micevski et al. (2003) illustrates an example of a non-homogeneous model. An indicator time series based on the IPO time series (Figure 7) was used to create the exogenous vector  $x$

$$x = \{I_t, t = 1, \dots, n\} \quad (3.2.80)$$

where the indicator

$$I_t = \begin{cases} 1 & \text{if } IPO_t \geq IPO_{\text{thresh}} \\ 0 & \text{if } IPO_t < IPO_{\text{thresh}} \end{cases} \quad (3.2.81)$$

$IPO_t$  is the IPO index for year  $t$  and  $IPO_{\text{thresh}}$  is a threshold value equal to  $-0.125$ .

## At-Site Flood Frequency Analysis

At each of the 33 NSW sites considered by Micevski et al. the AM peak flows were stratified according to the indicator  $I_t$ . A 2-parameter log-Normal distribution was fitted to the gauged flows with indicator equal to 1 – this is the IPO+ distribution. Likewise, a 2-parameter log-Normal distribution was fitted to the gauged flows with indicator equal to 0 – this is the IPO- distribution. Figure 3.2.44 presents the histogram for the ratio of the IPO- and IPO+ floods for selected 1 in Y AEPs. If the IPO+ and IPO- distributions were homogeneous then about half of the sites should have a flood ratio < 1 – Figure 3.2.44 shows otherwise.

Figures Figure 3.2.45 and Figure 3.2.46 present log normal fits to the IPO+ and IPO- annual maximum flood data for the Clarence river at Lilydale respectively. Though the adequacy of the log normal model to fit high floods may be questioned, in the AEP range 1 in 2 to 1 in 10 years, the IPO- floods are about 2.6 times the IPO+ floods with the same AEP.

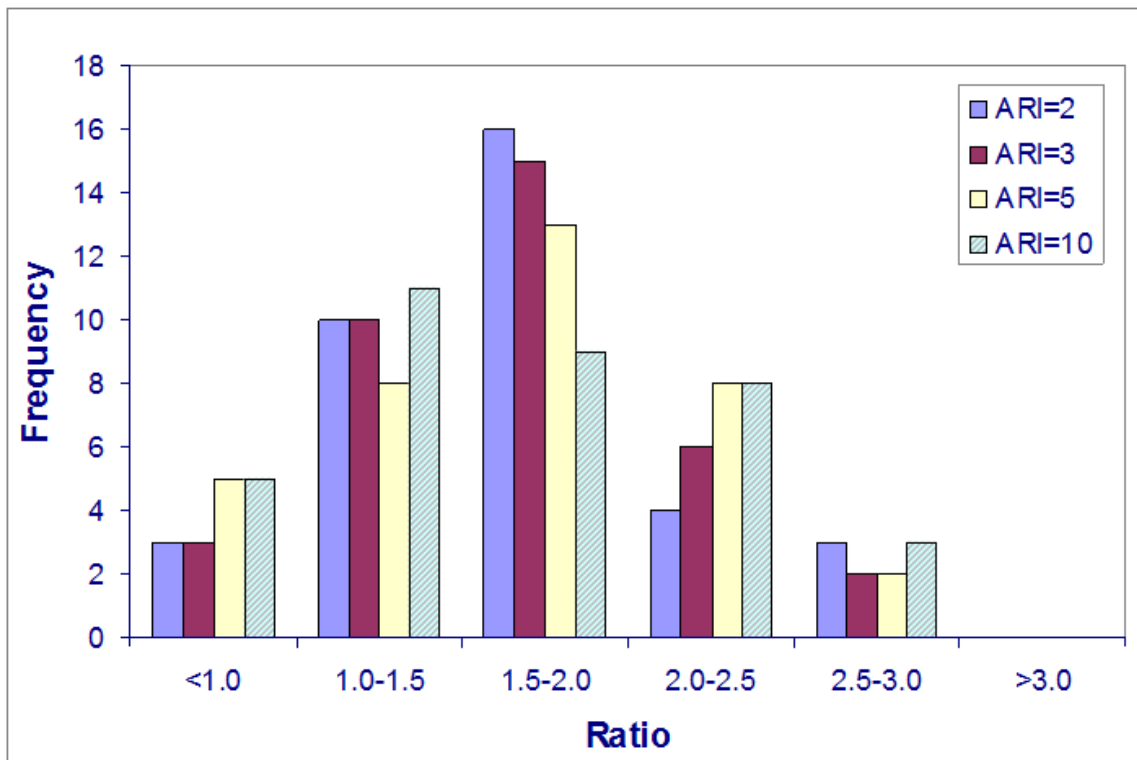


Figure 3.2.44. Histogram of IPO- and IPO+ flood ratios

### At-Site Flood Frequency Analysis

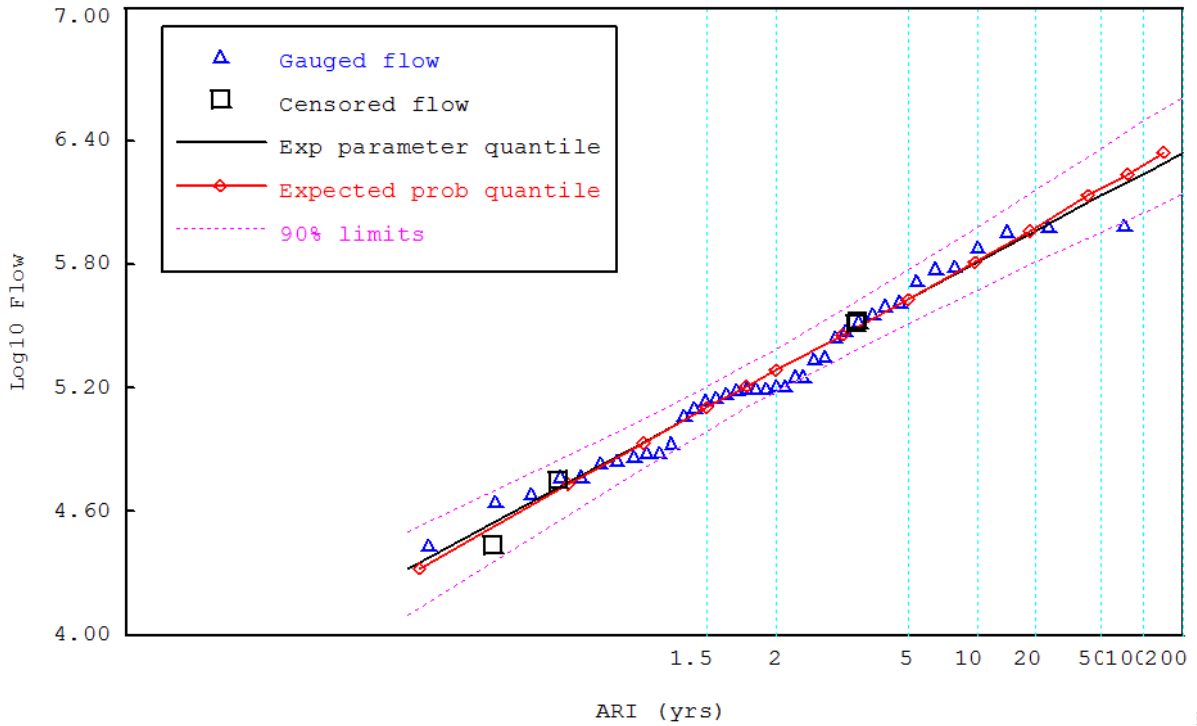


Figure 3.2.45. Log-Normal fit to 43 years of IPO+ data for the Clarence river at Lilydale (units ML/day).

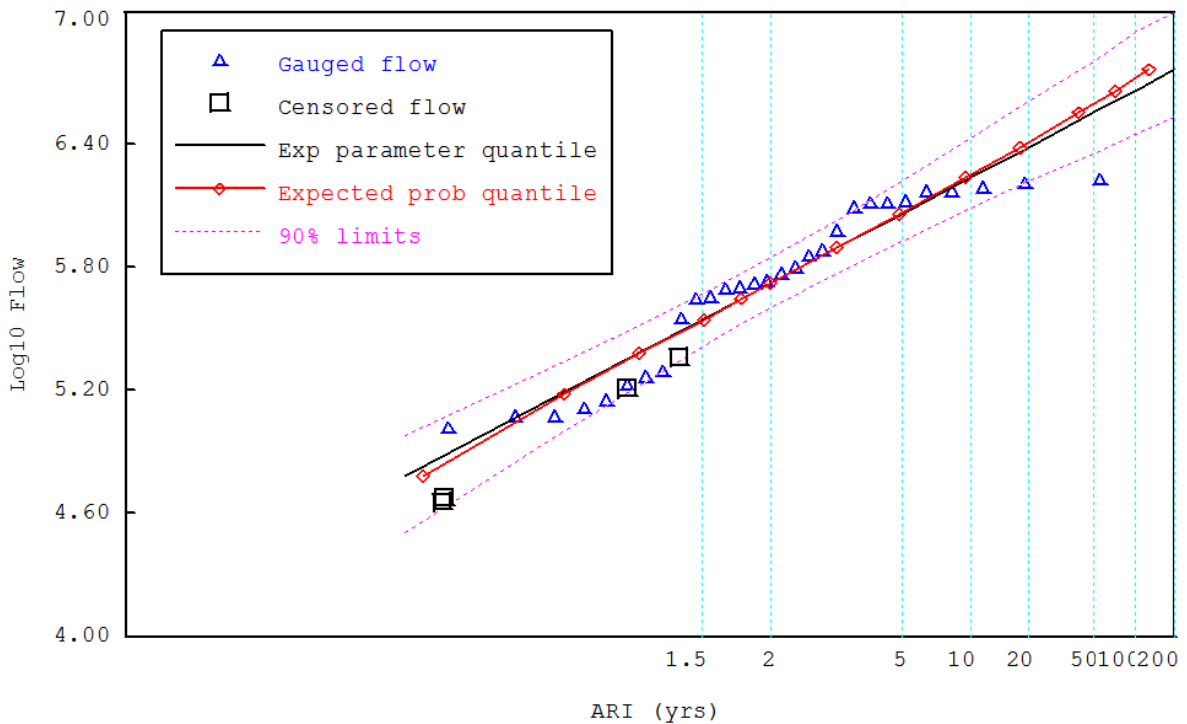


Figure 3.2.46. Log-Normal fit to 33 years of IPO- data for the Clarence river at Lilydale (units ML/day).

## At-Site Flood Frequency Analysis

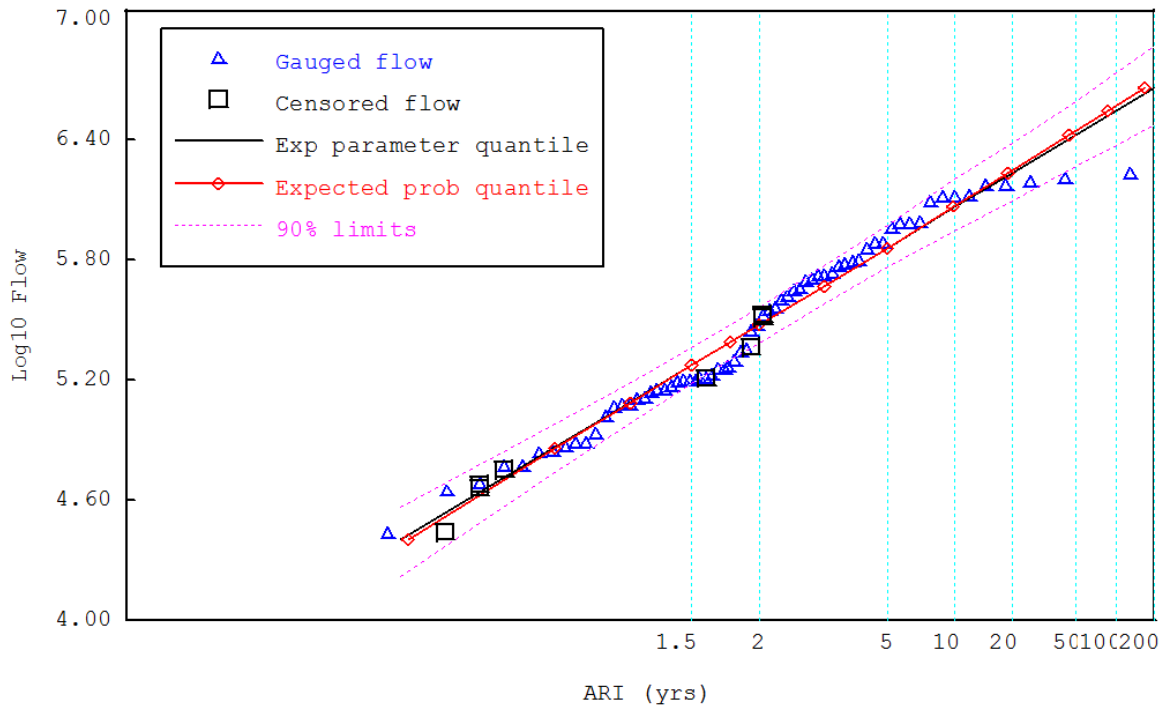


Figure 3.2.47. Log-Normal fit to 76 years of data for the Clarence river at Lilydale (units ML/day).

To avoid bias in estimating long-term flood risk it is essential that the gauged record adequately span both IPO+ and IPO- years. In this example, the IPO+ record is 43 years and the IPO- record is 33 years in length. With reference to Figure 7 this length of record appears to adequately sample both IPO epochs. This suggests that fitting to all the data will yield a largely unbiased estimate of the long-term flood risk. Figure 3.2.47 illustrates a log normal fit to all the data.

A better appreciation of the differences in flood risk can be gleaned by considering Figure 3.2.48 which presents the fitted log normal distributions to the IPO+, IPO- and total data. During an IPO+ period a flood peak of 100 m<sup>3</sup>/s has a 1 in 20 AEP while during an IPO- period it has a 1 in 4 AEP. Likewise a flood peak of 200 m<sup>3</sup> /s has 1 in 100 and 1 in 10 AEPs for IPO+ and IPO- periods respectively. The differences in flood risk are considerable. If a short gauged record falling largely in the IPO+ period was used, a standard flood frequency analysis could seriously underestimate the long-term or marginal flood risk.

The marginal flood risk can be derived by combining the IPO+ and IPO- distribution using Equation (3.2.23) to give

$$P(Q \leq q) = P(x = 0) \int_0^q p(z|\theta(x=0))dz + P(x=1) \int_0^q p(z|\theta(x=1))dz \quad (3.2.82)$$

The exogenous variable  $x$  can take two values, 0 or 1, depending on the IPO epoch.  $P(x=0)$ , the probability of being in an IPO- epoch, is assigned the value 33/76 based on the observation that 33 of the 76 years of record were in the IPO- epoch. Likewise  $P(x=1)$ , the probability of being in an IPO+ epoch, is assigned the value 43/76. It follows that  $p(z|\theta, x=0)$  and  $p(z|\theta, x=1)$  are the log normal pdfs fitted to IOP- and IPO+ data respectively.

The derived marginal distribution is plotted in [Figure 3.2.48](#). It almost exactly matches the log normal distribution fitted to all the data.

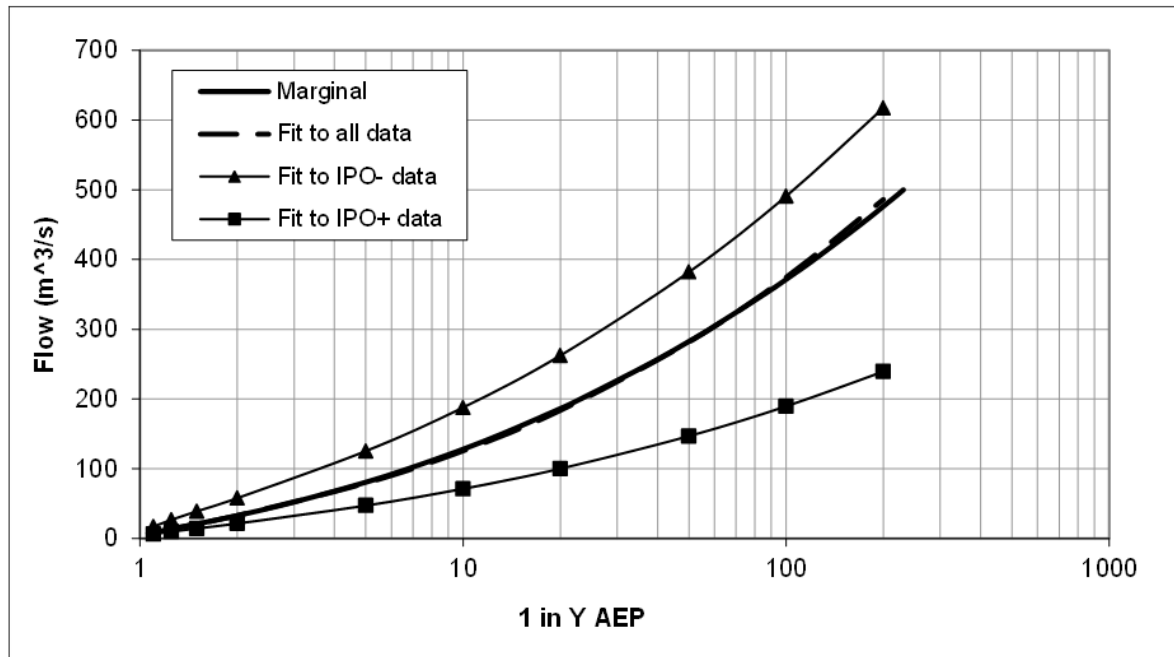


Figure 3.2.48. Marginal, IPO+ and IPO+ log-Normal distributions for the Clarence River at Lilydale

## 2.8.9. Example 9: L-moments fit to gauged data

This example illustrates fitting a GEV distribution to gauged data using L-moments. L-moments are a special case of LH-moments where there is no shift ( $H=0$ ). The procedure to use L-moments to fit a distribution is set out in [Book 3, Chapter 2, Section 6](#). In this example Annual Maximum flood data for the Styx River at Jeogla will be fitted using L-moments. The flood data are listed at the end of this example.

The procedure for fitting distributions by L-moments can be completed by hand, and also using TUFLOW Flike. Both of these techniques will be outlined in this example.

### 2.8.9.1. L-moments by Hand

The first four L-moments can be estimated by [Equation \(3.2.57\)](#) to [Equation \(3.2.60\)](#) and are reported in [Table 3.2.13](#). The GEV parameter estimates can be calculated by substituting the L-moment estimates into the equations in [Table 3.2.3](#) to estimate  $\tau$ ,  $K$  and  $\alpha$ . The standard deviation and correlation were derived from 5000 bootstrapped samples following the procedure described in [Book 3, Chapter 2, Section 6](#) and [Parametric bootstrap](#). Note standard deviation and correlation cannot be calculated by hand.

Table 3.2.13. L-moment and GEV Parameter Estimates

L-moment	L-moment Estimate	GEV Parameter	Parameter Estimate	Standard Deviation	Correlation	Correlation	Correlation
$\lambda_1$	189.238	$\tau$	100.660	17.657	1.000		
$\lambda_2$	92.476	$\alpha$	104.157	15.554	0.597	1.000	
$\lambda_3$	29.264	$\kappa$	-0.219	0.130	0.358	0.268	1.000

### 2.8.9.2. L-moments using TUFLOW Flike

L-moments and the distribution parameters can be estimated in TUFLOW Flike. To do this, create a new .fld file and import the Styx River at Jeogla data set. Return the **Flike Editor General** tab. Now set the Inference method to LH-moments fit to observed values with and check the H=0 radio box. This last option sets the shift to 0 (i.e. L-moments). The **Flike Editor** window should look like . Run TUFLOW Flike and examine the results file for the L-moments and GEV parameters.

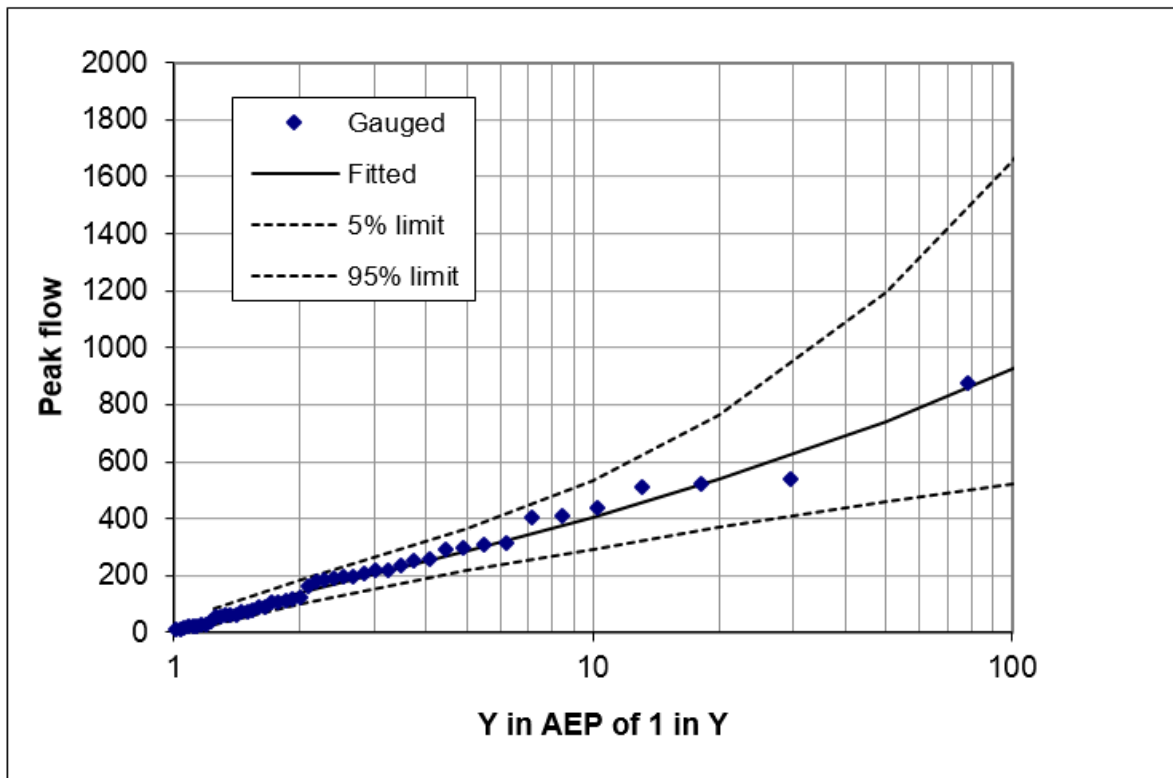


Figure 3.2.49. Flike Editor configured for L-moments

The following table lists 47 ranked flows for the Styx River at Jeogla.

878	541	521	513	436	411	405	315
309	300	294	258	255	235	221	220
206	196	194	190	186	177	164	126

At-Site Flood Frequency  
Analysis

117	111	108	105	92.2	88.6	79.9	74
71.9	62.6	61.2	60.3	58	53.5	39.1	26.7
26.1	23.8	22.4	22.1	18.6	13	8.18	

## 2.8.10. Example 10: Improving poor fits using LH-moments

In Example 5 the fit of the distribution to the Albert River flood series was improved by censoring low flows. In this example, LH-moments are used instead of censoring to improve the fit of the GEV distribution to the flood data.

### 2.8.10.1. Launch TUFLOW Flike

This example uses the same data as **Example 7** for the Albert River at Broomfleet, so the previous **Example 7.fld** file can be used. To do this, launch TUFLOW Flike and open **Example\_7.fld** and save the opened .fld as **Example\_10.fld**. Open the **Flike Editor** to configure the LH-moments fitting method. Note that the **Example\_7.fld** file was configured with a Bayesian inference method.

### 2.8.10.2. Configure Inference Method

In **Example 7**, a Bayesian inference method was used with censored low flows, so a number of changes are required to **Example\_7.fld** before the LH-moments inference method can be used. As low flows were censored in the previous example, these need to be included back into the analysis by:

- Removing the censoring threshold; and
- Including all the flood data.

Ensure that the **Bayesian with** button is still checked. If the **LH-moments fit to observed values with** radio button is checked the **Censoring of observed values** tab cannot be accessed.

To remove the censoring threshold, select the **Censoring of observed values** tab and select the **Clear all** button.

To include all the flood data, select the **Observed values** tab and select the **Include all** button. Scroll through the data to ensure that all the crosses (x) in the **Exclude** column have been removed.

### 2.8.10.3. Fit L-moments

To configure TUFLOW Flike to fit distributions using the LH-moments inference method, return to the **General** tab and check the **LH-moments fit to observed values with** radio button. In the first instance, select the **H=0** radio button. This will fit a distribution using L-moments, this is, LH-moments with no shift.

TUFLOW Flike will only fit LH-moments with  $H \geq 1$  for the GEV distribution, however it will fit L-moments ( $H = 0$ ) for all distributions. Ensure that the GEV probability model has been selected.

The configured **Flike Editor** should look like [Figure 3.2.50](#). Select OK and run TUFLOW Flike. As usual, a probability plot will appear together with the report file. Rescale the plot so it looks like [Figure 3.2.51](#).

# At-Site Flood Frequency Analysis

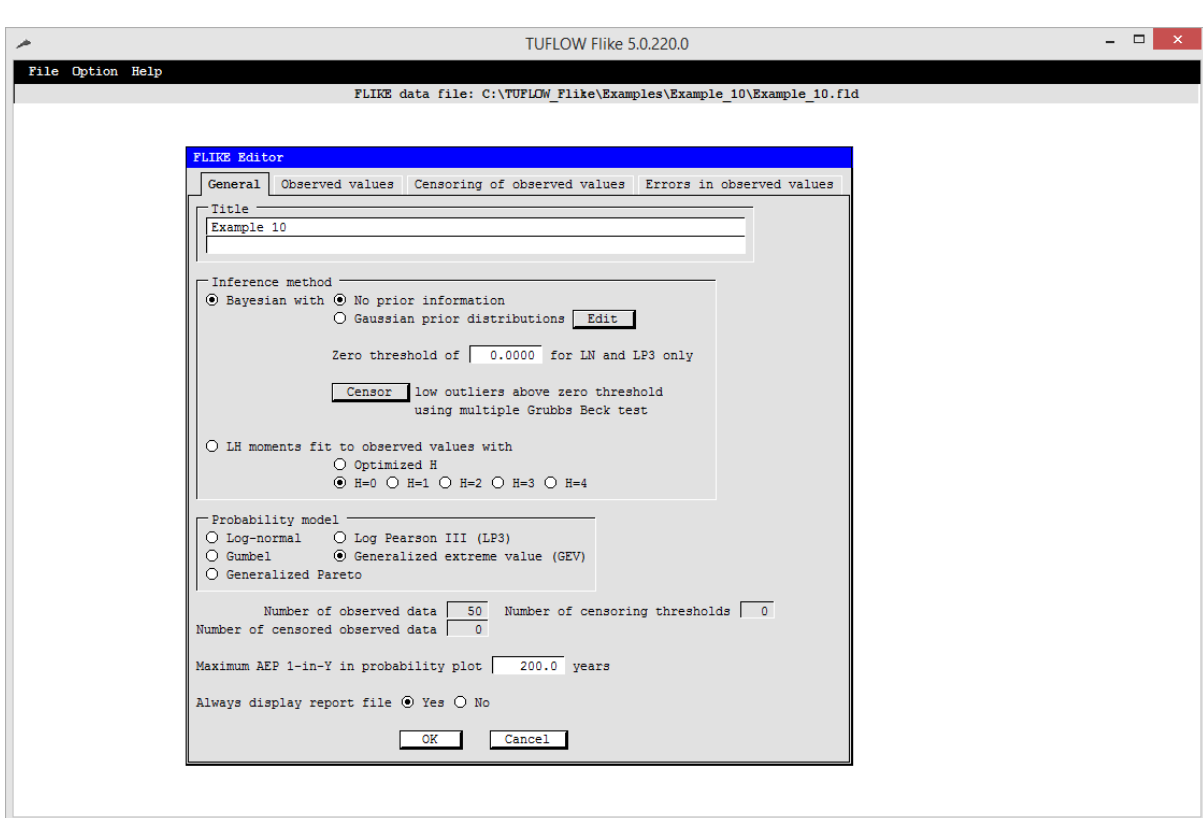


Figure 3.2.50. Configured Flike Editor



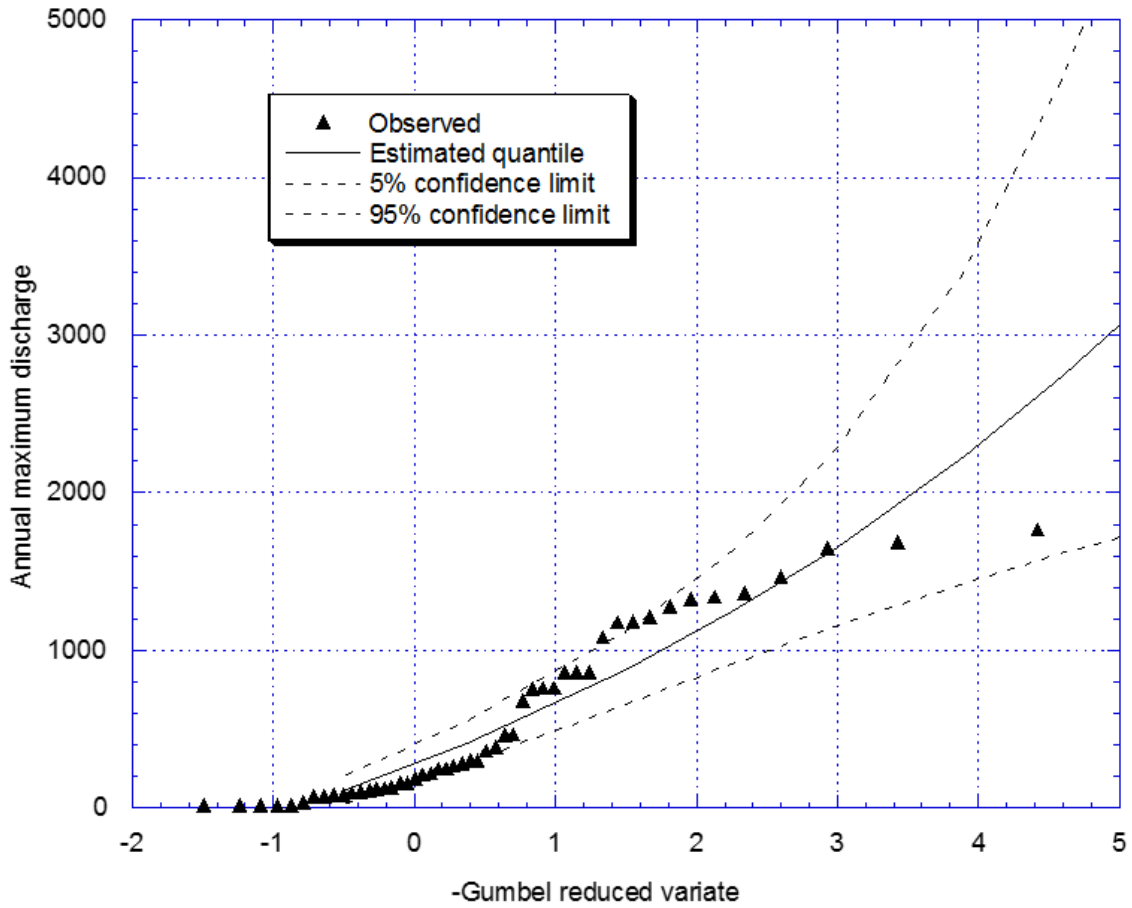


Figure 3.2.51. L-moment fit - Albert River at Broomfleet

Figure 3.2.51 displays the GEV L-moment fit on a Gumbel probability plot. Although the observed floods are largely contained within the 90% confidence limits, the fit, nonetheless, is poor with systematic departures from the data which exhibits reverse curvature.

#### 2.8.10.4. Fit LH-moments

To deal with this poor fit, a LH-moment search was conducted to find the optimal shift parameter using the procedure described in [Book 3, Chapter 2, Section 6](#). To do this in TUFLOW Flike check the **Optimized H** radio button and run TUFLOW Flike. The results file reveals that the optimal shift was found to be 4. [Figure 3.2.52](#) presents the LH-moment fit with shift equal to 4. The fit effectively disregards floods more frequent than the 50% AEP (around 350m<sup>3</sup>/s) and provides a very good fit to upper tail.

## At-Site Flood Frequency Analysis

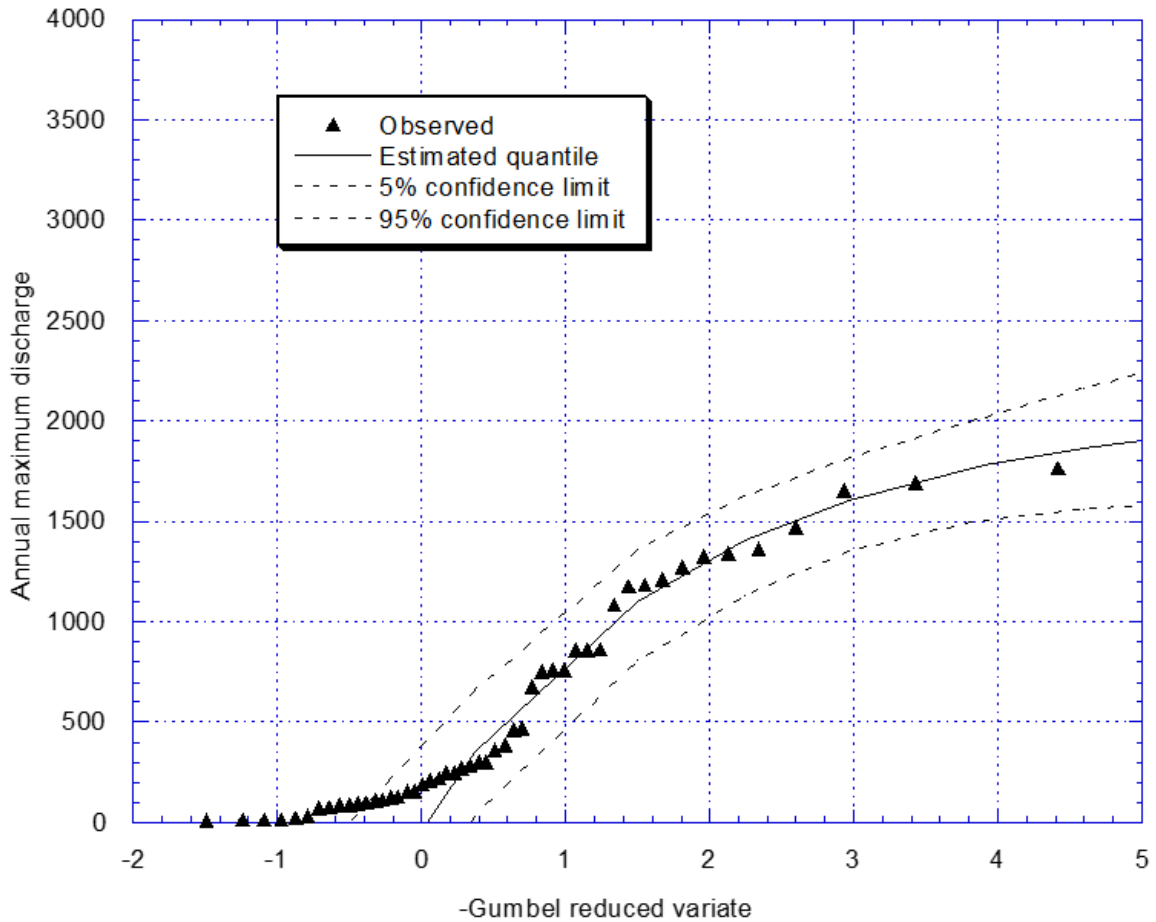


Figure 3.2.52. LH-moment fit with shift  $H=4$

The very significant reduction in the quantile confidence intervals is largely due to the shape parameter  $K$  changing from  $-0.17$  to  $0.50$ . The L-moment fit in Figure 2 was a compromise; most of the small and medium-sized floods suggested an upward curvature in the probability plot which resulted in a negative GEV shape parameter (to enable upward curvature). In contrast, the LH-moment fit favoured the large-sized floods which exhibit a downward curvature resulted in a positive shape parameter. For positive  $K$  the GEV has an upper bound. In this case the upper bound is about  $2070 \text{ m}^3/\text{s}$  which is only 17% greater than the largest observed flood.

A comparison of the quantile derived from the Bayesian inference method with censoring of PILFs and those determined using Optimised LH-moments is presented in Table 3.2.14. The two different inference methods produce similar results in terms of the calculated quantiles; however, the confidence limits are smaller using the Bayesian framework. This highlights how LH-moment results could be used to inform the selection of the censoring threshold for PILFs in the Bayesian framework.

Table 3.2.14. Comparison of Quantiles using a Bayesian and LH-moments Inference Methods

AEP (%)	Bayesian with removal of PILFS		Optimised LH-moments			
	Quantile Estimate $q_Y$	Quantile Confidence 5% Limit	Quantile Confidence 95% Limit	Quantile Estimate $q_Y$	Quantile Confidence 5% Limit	Quantile Confidence 95% Limit
10%	1400	1249	1590	1406	1133	1634
2%	1720	1605	1931	782	1492	2021
1%	1782	1675	2003	1868	1546	2168
0.2%	1854	1757	2111	1982	1,99	2482

### 2.8.11. Example 11: Fitting a probability model to POT data

This example is a continuation of Example 9 which considers the Styx River at Jeogla. It illustrates fitting an exponential distribution to POT data. The table lists all the independent peak flows recorded over a 47 year period that exceeded a threshold of 74 m<sup>3</sup>/s – the total number of peaks was 47. Comparison with the annual maximum flood peaks in Example 9 reveals that in 15 of the 47 years of record the annual maximum peak were below the threshold of 74 m<sup>3</sup>/s.

878	541	521	513	436	411	405	315
309	301	300	294	283	258	255	255
238	235	221	220	206	196	194	190
186	164	150	149	134	129	129	126
119	118	117	117	111	108	105	98
92.2	92.2	91.7	88.6	85.2	79.9	74	

The first two L-moments were estimated as 226.36 and 79.2. Noting that the exponential distribution is a special case of the generalised Pareto when  $\kappa = 0$ , it follows from [Table 3.2.3](#) that the exponential parameters are related to the L-moments by

$$\lambda_1 = q_* + \beta \quad \lambda_2 = \frac{\beta}{2} \quad (3.2.83)$$

which yields values for  $q_*$  and  $\beta$  of 68.11 and 158.24 respectively. Therefore the probability of the peak flow  $q$  exceeding  $w$  in any POT event is

$$P(q > w) = e^{\left(-\frac{w - q_*}{\beta}\right)} = e^{\left(-\frac{w - 68.11}{158.24}\right)} \quad (3.2.84)$$

The second step obtains the distribution of annual maximum peaks. Using [Equation \(3.2.11\)](#), the expected number of peaks that exceed  $w$  in a year is

At-Site Flood Frequency  
Analysis

---

$$EY(w) = \nu P(q > w) = \nu e^{\left(-\frac{w - q^*}{\beta}\right)} \quad (3.2.85)$$

where  $\nu$  is the average number of flood peaks above the threshold  $q^*$  per year.

For plotting purposes it is convenient to use a log transformation which yields

$$\log_e EY(w) = \log_e \nu + \frac{q^*}{\beta} - \frac{w}{\beta} \quad (3.2.86)$$

A plot of  $\log_e EY(w)$  versus  $w$  should follow a straight line if the underlying POT distribution is exponential.

Given that 47 peaks above the threshold occurred in 47 years,  $\nu$  equals 1.0. The following figure presents a plot of the fitted POT exponential model against the observed POT series.

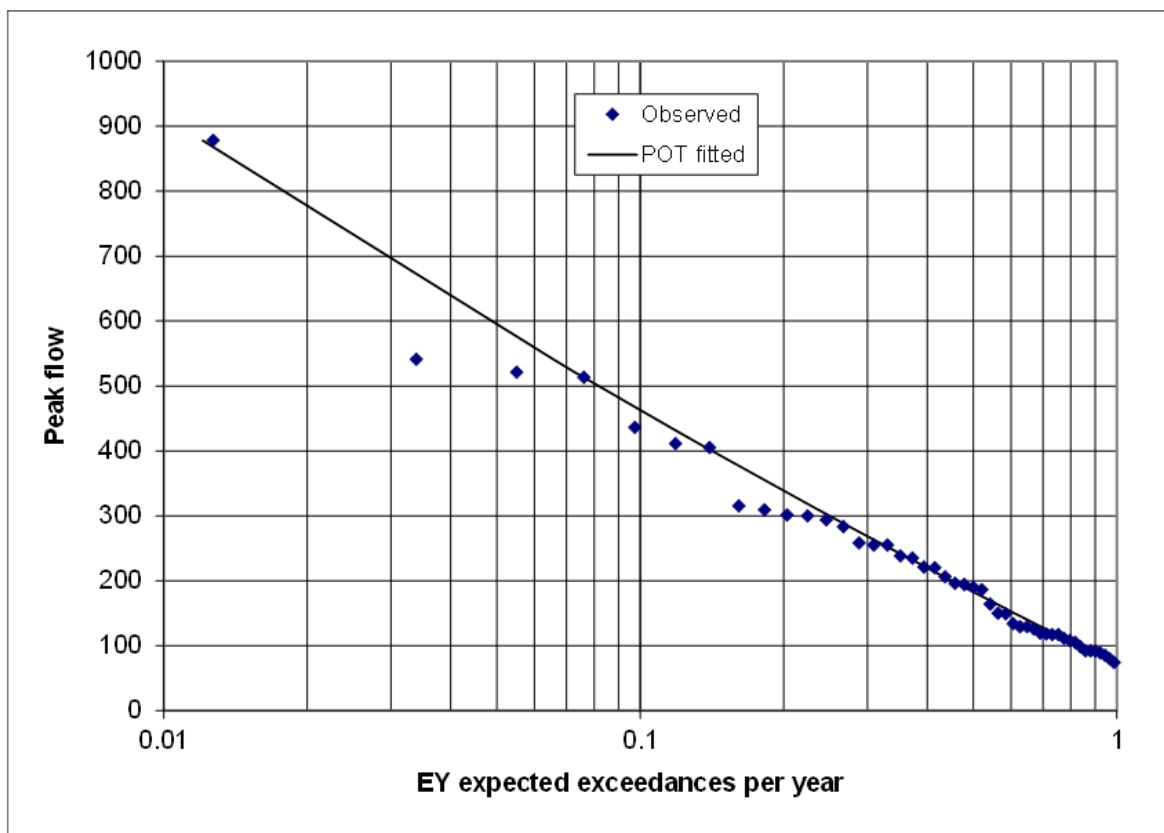


Figure 3.2.53. Plot of the fitted POT exponential model against the observed POT series

## 2.9. References

ASCE (American Society of Civil Engineers) (1949), Hydrology Handbook.

Adams, C.A. (1987), Design flood estimation for ungauged rural catchments in Victoria Road Construction Authority, Victoria. Draft Technical Bulletin.

Adams, C.A. and McMahon, T.A. (1985), Estimation of flood discharge for ungauged rural catchments in Victoria. Hydrol. and Water Resources Symposium 1985, Inst Engrs Aust., Natl Conf. Publ. No.85/2, pp: 86-90.

- Alexander, G.N. (1957), Flood flow estimation, probability and the return period. *Jour. Inst. Engrs Aust*, 29: 263-278.
- Allan, R.J. (2000), ENSO and climatic variability in the last 150 years, in *El Nino and the Southern Oscillation, Multi-scale variability, Global and Regional Impacts*, edited by H.F. Diaz and V. Markgraf, Cambridge University Press, Cambridge, uk, pp: 3-56.
- Ashkanasy, N.M. and Weeks, W.D. (1975), Flood frequency distribution in a catchment subject to two storm rainfall producing mechanisms. *Hydrol. Symposium 1975, Inst Engrs Aust, Natl Conf. Publ. (75/3)*, 153-157.
- Ashkar, F. and Rousselle, J. (1983) Some remarks on the truncation used in partial flood series models. *Water Resources Research*, 19: 477-480.
- Baker, V. (1984), Recent paleoflood hydrology studies in arid and semi-arid environments (abstract). *EOS Trans. Amer. Geophys. Union*, Volume 65, p: 893.
- Baker, V., Pickup, G. and Polach, H.A. (1983) ,Desert paleofloods in central Australia. *Nature*, 301: 502-504.
- Beard, L.R. (1974), Flood flow frequency techniques Univ. of Texas at Austin, Center for Research in Water Resources, Tech. Report CRWR119, October.
- Beran, M., Hosking, J.R.M. and Arnell, N. (1986), Comment on 'Two-component extreme value distribution for flood frequency analysis.' *Water Resources Research*, 22: 263-266.
- Blom, G. (1958), *Statistical Estimates and Transformed Beta-Variables*. Wiley, New York, p: 176.
- Clarke-Hafstad, K. (1942), Reliability of station-year rainfall-frequency determinations. *Trans. Amer. Soc. Civ. Engrs.*, 107(1), 633-652.
- Cohn, T.A., England, J.F., Berenbrock, C.E., Mason, R.R., Stedinger, J.R. and Lamontagne, J.R. (2013), A generalized Grubbs-Beck test statistic for detecting multiple potentially influential low outliers in flood series, *Water Resour. Res.*, 49(8), 5047-5058.
- Conway, K.M. (1970), Flood frequency analysis of some N.S.W. coastal rivers. Thesis (M.Eng Sc.), Univ.NSW.
- Costa, J.E. (1978), Holocene stratigraphy in flood frequency analysis. *Water Resources Research*, 4: 626-632.
- Costa, J.E. (1983), Palaeohydraulic reconstruction of flashflood peaks from boulder deposits in the Colorado Front Range. *Geol. Soc. America Bulletin*, 94(8), 986-1004.
- Costa, J.E. (1986), A history of paleoflood hydrology in the United States, 1800-1970. *EOS Trans. Aolier Geophysical Union*, 67(17), 425-430.
- Cunnane, C. (1985), Factors affecting choice of distribution for flood series. *Hydrological Sciences Journal*, 30: 25-36.
- Cunnane, C. (1978), Unbiased plotting positions - a review. *Jour. of Hydrology*, 37: 205-222.
- Dalrymple, T. (1960), Flood-frequency analyses. *Manual of Hydrology: Section 3. Flood-flow Techniques*. U.S. Geological Survey Water Supply Paper 1543-A, 79 p.

DeGroot, M.H. (1970) Optimal statistical decisions, McGraw-Hill

Doran, D.G. and Irish, J.L. (1980), On the nature and extent of bias in flood damage estimation. Hydrol. and Water Resources Symposium 1980, Inst. Engrs Aust, Natl Conf. Publ., (80/9), 135-139.

Duan, Q., Sorooshian, S. and Gupta, V. (1992), Effective and efficient global optimization for conceptual rainfall-runoff models, Water Resources Research, 28(4), 1015-1031.

Erskine, W. D. and Warner, R.F. (1988), Geomorphic effects of alternating flood and drought dominated regimes on a NSW coastal river, in Fluvial Geomorphology of Australia, edited by R.F. Warner, pp. 223-244, Academic Press, Sydney.

Fiering, M.B. (1963), Use of correlation to improve estimates of the mean and variance. U.S. Geological estimates of the mean and variance. U.S. Geological Survey Professional Paper 434-C.

Florentino, M., Versace, P. and Rossi, F. (1985), Regional flood frequency estimation using the two-component extreme value distribution. Hydrol. Sciences Jour., 30: 51-64.

Folland, C.K., Renwick, J.A., Salinger, M.J. and Mullan, A.B. (2002), Relative influences of the Interdecadal Pacific Oscillation and ENSO on the South Pacific Convergence Zone, Geophys. Res. Lett., 29(13), doi:10.1029/2001GL014201.

Franks, S.W. and Kuczera, G. (2002), Flood Frequency Analysis: Evidence and Implications of Secular Climate Variability, New South Wales, Water Resources Research, 38(5), 10.1029/2001WR000232.

Franks, S.W. (2002a), Identification of a change in climate state using regional flood data, Hydrol. Earth Sys. Sci., 6(1), 11-16.

Franks, S.W. (2002b), Assessing hydrological change: deterministic general circulation models or spurious solar correlation? Hydrol. Proc., 16: 559-564.

Gelman, A., Carlin, J.B., Stern, H.S. and Rubin, D.B. (1995), Bayesian data analysis, Chapman and Hall, p: 526.

Hosking, J.R.M. (1990), L-moments: Analysis and estimation of distributions using linear combinations of order statistics, J. Roy. Statist. Soc., Ser. B, 52(2), 105-124.

Hosking, J.R.M. and Wallis, J.R. (1986) Paleoflood hydrology and flood frequency analysis. Water Resources Research, 22: 543-550.

Houghton, J.C. (1978), Birth of a parent: The Wakeby distribution for modeling flood flows. Water Resources Research, 14: 1105-1109.

Interagency Advisory Committee on Water Data (1982), Guidelines for determining flood flow frequency. Bulletin 17B of the Hydrology Sub-committee, Office of Water Data Coordination, Geological Survey, U.S. Dept of the Interior.

Jayasuriya, M.D.A. and Mein, R.G. (1985), Frequency analysis using the partial series. Hydrol. and Water Resources Symposium 1985, Inst. Engrs Aust., Natl Conf. Publ. No. 85/2, pp: 81-85.

Kiem, A.S. and Franks, S.W. (2004), Multidecadal variability of drought risk - eastern Australia, Hydrol. Proc., 18, doi:10.1002/hyp.1460.

At-Site Flood Frequency  
Analysis

---

- Kiem, A.S., Franks, S.W. and Kuczera, G. (2003), Multi-decadal variability of flood risk, *Geophysical Research Letters*, 30(2), 1035, DOI:10.1029/2002GL015992.
- Kochel, R.C., Baker, V.R and Patton, P.C. (1982), Paleohydrology of southwestern Texas. *Water Resources Research*, 18: 1165-1183.
- Kopittke, R.A., Stewart, B.J. and Tickle, K.S. (1976), Frequency analysis of flood data in Queensland. *Hydrol. Symposium 1976, Inst Engrs Aust., Natl Conf. Publ. No. 76/2*, pp: 20-24.
- Kuczera, G. (1999), Comprehensive at-site flood frequency analysis using Monte Carlo Bayesian inference, *Water Resources Research*, 35(5), 1551-1558.
- Kuczera, G. (1996), Correlated rating curve error in flood frequency inference, *Water Resources Research*, 32(7), 2119-2128.
- Kuczera, G., Lambert, M.F., Heneker, T., Jennings, S., Frost, A. and Coombes, P. (2006), Joint probability and design storms at the crossroads, *Australian Journal of Water Resources*, 10(2), 5-21.
- Laurenson, E.M. (1987), Back to basics on flood frequency analysis. *Civ. Engg Trans., Inst Engrs Aust*, CE29: 47-53.
- Lee, P.M. (1989), *Bayesian statistics: An introduction*, Oxford University Press (NY).
- Mantua, N. J., Hare, S.R., Zhang, Y., Wallace, J.M. and Francis, R.C. (1997), A Pacific interdecadal climate oscillation with impacts on salmon production, *Bull. Amer. Meteorol. Soc.*, 78(6), 1069-1079.
- Matalas, N.C. and Jacobs, B. (1964), A correlation procedure for augmenting hydrologic data. *U.S. Geological Survey Professional Paper 434-E*.
- McDermott, G.E. and Pilgrim, D.H. (1982), Design flood estimation for small catchments in New South Wales. *Dept of National Development and Energy, Aust Water Resources Council Tech. Paper No.73*, p: 233
- McDermott, G.E. and Pilgrim, D.H. (1983), A design flood method for arid western New South Wales based on bankfull estimates. *Civ. Engg Trans., Inst Engrs Aust*, CE25: 114-120.
- McIlwraith, J.F. (1953), Rainfall intensity-frequency data for New South Wales stations. *Jour. Inst Engrs Aust*, 25: 133-139.
- McMahon, T.A. (1979), Hydrologic characteristics of Australian streams. *Civ. Engg Research Reports, Monash Univ., Report No.3/1979*.
- McMahon, T.A. and Srikanthan, R. (1981), Log Pearson III distribution- is it applicable to flood frequency analysis of Australian streams? *Jour. of Hydrology*, 52: 139-147.
- Micevski, T., Kiem, A.S., Franks, S.W. and Kuczera, G. (2003), Multidecadal Variability in New South Wales Flood Data, *Hydrology and Water Resources Symposium, Institution of Engineers, Australia, Wollongong*.
- Natural Environment Research Council (1975), *Flood Studies Report, Vol.1, Hydrological Studies*, London.

O'Connell, D.R., Ostemaa, D.A., Levish, D.R. and Klinger, R.E. (2002) Bayesian flood frequency analysis with paleohydrologic bound data, *Water Resources Research*, 38(5), 1058, DOI:10.1029/2000WRR000028.

Pedruco, P., Nielsen, C., Kuczera, G. and Rahman, A. (2014), Combining regional flood frequency estimates with an at site flood frequency analysis using a Bayesian framework: Practical considerations, *Hydrology and Water Resources Symp.*, Perth, Engineers Australia.

Pilgrim, DH (ed) (1987) *Australian Rainfall and Runoff - A Guide to Flood Estimation*, Institution of Engineers, Australia, Barton, ACT, 1987.

Pilgrim, D.H. and Doran, D.G. (1987), Flood frequency analysis, in *Australian Rainfall and Runoff: A guide to flood estimation*, Pilgrim, D.H. (ed), The Institution of Engineers, Australia, Canberra.

Pilgrim, D.H. and McDermott, G.E. (1982), Design floods for small rural catchments in eastern New South Wales. *Civ. Engg Trans., Inst Engrs Aust.*, CE24: 226-234.

Potter, D.J. and Pilgrim, D.H. (1971), Flood estimation using a regional flood frequency approach. Final Report, Vol.2, Report on Analysis Components. Aust. Water Resources Council, Research Project 68/1, Hydrology of Small Rural Catchments. Snowy Mountains Engg Corporation, April.

Potter, K.W. and Walker, J.F. (1981), A model of discontinuous measurement error and its effects on the probability distribution of flood discharge measurements, *Water Resources Research*, 17(5), 1505-1509.

Potter, K.W. and Walker, J.F. (1985), An empirical study of flood measurement error, *Water Resources. Research*, 21(3), 403-406.

Power, S., Tseitkin, F., Torok, S., Lavery, B., Dahni, R. and McAvaney, B. (1998), Australian temperature, Australian rainfall and the Southern Oscillation, 1910-1992: coherent variability and recent changes, *Aust. Met. Mag.*, 47(2), 85-101.

Power, S., Casey, T., Folland, C., Colman, A. and Mehta, V. (1999), Inter-decadal modulation of the impact of ENSO on Australia, *Climate Dynamics*, 15(5), 319-324.

Rossi, F., Fiorentino, M. and Versace, P. (1984), Two-component extreme value distribution for flood frequency analysis. *Water Resources Research*, 20: 847-856.

Slack, J.R., Wallis, J.R. and Matalas, N.C. (1975), On the value of information in flood frequency analysis, *Water Resources. Research*, 11(5), 629-648.

Stedinger, J.R. (1983), Design events with specified flood risk, *Water Resources Research*, 19(2), 511-522.

Stedinger, J.R. and Cohn, T.A. (1986), Flood frequency analysis with historical and paleoflood information. *Water Resources Research*, 22: 785-793.

Stedinger, J.R., Vogel, R.M. and Foufoula-Georgiou, E. (1993), Frequency analysis of extreme events in *Handbook of Hydrology*, Maidment, D.R. (ed.), McGraw-Hill, NY.

Tavares, L.V. and Da Silva, J.E. (1983), Partial series method revisited. *Jour. of Hydrology*, 64: 1-14.



Wallis, J.R. and Wood, E.F. (1985), Relative accuracy log Pearson III procedures. Proc. Amer. Soc. Civ. Engrs. J. of Hydraul. Eng., III(7), 1043-1056.

Wang, Q.J. (2001), A Bayesian joint probability approach for flood record augmentation, Water Resources Research, 37(6), 1707-1712.

Wang, Q.J. (1996), Direct sample estimators of L-moments, Water Resources Research, 32(12), 3617-3619.

Wang, Q.J. (1997), LH moments for statistical analysis of extreme events, Water Resources Research, 33(12), 2841-2848.

Wang, Q. J. (1998), Approximate goodness-of-fit tests of fitted generalized extreme value distributions using LH moments, Water Resources Research, 34(12), 3497-3502.

---

# Chapter 3. Regional Flood Methods

Ataur Rahman, Khaled Haddad, George Kuczera, Erwin Weinmann

Chapter Status	Final
Date last updated	14/5/2019

## 3.1. Introduction

Estimation of peak flows on small to medium sized rural catchments is required for the design of culverts, small to medium sized bridges, causeways, soil conservation works and for various planning and regulatory purposes. Typically, most design flood estimates for projects on small to medium sized catchments are on catchments that are ungauged or have little recorded streamflow data. In these cases, peak flow estimates can be obtained using a Regional Flood Frequency Estimation (RFFE) approach, which transfers flood frequency characteristics from a group of gauged catchments to the location of interest. Even in cases where there is recorded streamflow data it is beneficial to pool the information in the gauged record with the RFFE information. A RFFE technique is expected to be simple, requiring only readily accessible catchment data to obtain design flood estimates relatively quickly.

The RFFE method described in this chapter ensures that design flood discharge estimates are consistent with the gauged records and with results for other ungauged catchments in a region. It is recognised that there will be considerable uncertainty in estimates for ungauged catchments because of the limited number of gauged catchments available to develop the method and the wide range of catchment types that exist throughout Australia.

In developing the RFFE technique, a number of criteria had to be satisfied. These criteria included:

- National consistency in approach;
- Smooth interfacing at the boundaries between areas;
- Use readily accessible data; and
- Utilise as much of Australia's streamflow database as possible.

The basis for the development of the RFFE technique recommended herein, therefore, is a national database consisting of 853 gauged catchments. These data were used to develop and test the RFFE technique presented in this chapter. Further details of the development of the database and RFFE technique are provided by the references noted in [Book 3, Chapter 3, Section 16](#).

The following sections contain a description of the conceptual and statistical framework of the adopted RFFE technique, a computer-based application tool, referred to as 'RFFE Model 2015', that implements the adopted RFFE technique and a number of worked examples to demonstrate the application of the model.

Following the guidance provided in [Book 1](#) and [Book 3, Chapter 1](#), users of the RFFE technique are reminded that there are alternatives to the RFFE technique.

While the RFFE technique described in this chapter is regarded as a state-of-the-art approach for estimation of design flood peak discharges at ungauged catchments, the

limitations of the method must be recognised. The RFFE technique has been developed using the best available database of gauged catchments throughout Australia, but the fact remains that only a small number of gauged catchments were available to represent the wide range of conditions experienced over an area of about 7.5 million km<sup>2</sup>. Therefore, in accordance with the guidance in Book 1, Chapter 1 of ARR, designers and analysts have a duty to use an alternative technique if that technique can be shown to be superior to RFFE Model 2015 and to utilise any available local data, both formal and informal to assist in understanding local conditions and improve upon RFFE Model 2015 estimates. In comparing and selecting alternative methods, the uncertainty in the observed flood data due to factors such as limitations in record length and rating curve extrapolation should be recognised.

## 3.2. Conceptual Framework

### 3.2.1. Definition of Regional Flood Frequency Estimation

Regional Flood Frequency Estimation (RFFE) is a data-driven approach, which attempts to transfer flood characteristics from a group of gauged catchments to ungauged locations of interest (where design floods need to be estimated). A range of different methods are available to extract regional flood information from the pooled data and to transfer the relevant information to an individual ungauged catchment in the region (Sivapalan et al., 2013). All of these RFFE techniques use the results of at-site Flood Frequency Analysis (FFA, refer to Book 3, Chapter 2) as basic data. A RFFE technique essentially consists of two steps: (i) *Formation of Regions* - which involves identification of the regions for which flood data from the available streamflow gauging stations can be pooled for analysis; and (ii) *Development of Regional Estimation Equations* - which involves derivation of prediction equations to be used for design flood estimation within a region.

### 3.2.2. Formation of Regions

In RFFE techniques, the formation of regions can be based on geographic proximity or on similarity in catchment attributes. A region can be fixed, having a definite common boundary for all sites within it, or it can be formed around the ungauged catchment of interest (i.e. the location where flood quantile estimation is desired), using the nearest stations in geographic or catchment attributes space. Regions must satisfy explicitly or implicitly the assumption of 'regional homogeneity'. The decision on what constitutes a homogeneous region for the purposes of Regional Flood Frequency Estimation depends on the methods used, more specifically on the extent to which differences in flood characteristics can be expressed through parameters in the regionalisation method. There have been many techniques developed which attempt to establish homogenous regions. For example, the recommended RFFE model for eastern New South Wales (NSW) and Victoria in Australian Rainfall and Runoff 1987 (Pilgrim, 1987), namely the Probabilistic Rational Method, used geographical contiguity as an indication of homogeneity; in other words the catchments which are closer to each other should have similar runoff coefficients (Pilgrim, 1987).

There has been little success in the identification of 'acceptably homogeneous regions' in Australia using statistical measures such as those proposed by Hosking and Wallis (1993). A common approach to defining a fixed region has been to base the region on political boundaries. However, these fixed regions based on state borders and other geographical boundaries have often been found to be highly heterogeneous (Bates et al., 1998; Rahman, 1997; Haddad, 2008).

As an alternative to fixed regions, Burn (1990a), Burn (1990b), and Zrinji and Burn (1994) proposed the Region Of Influence (ROI) approach where a location of interest (i.e. the

catchment where flood quantiles are to be estimated) is allowed to form its own region by selecting a group of 'nearby catchments' in either a geographical or catchment attributes space (catchment attributes refer to the catchment characteristics that are influential in developing flood flows). The ROI approach attempts to reduce the degree of heterogeneity in a proposed region by excluding sites located remotely in geographical or catchment attributes space. The ROI approach often uses a statistical criterion to select the optimum size of the region, such as 'minimum model error variance' in the regression.

### 3.2.3. Development of Regional Flood Frequency Estimation Technique

According to [Bates \(1994\)](#), the most commonly adopted methods to develop Regional Flood Frequency Estimation techniques include various forms of the Rational Method, the Index Flood Method and regression based techniques. In ARR 1987, the Probabilistic Rational Method was recommended for general use in Victoria and eastern NSW ([Pilgrim, 1987](#)). The foundations of the Probabilistic Rational Method are presented by [Pilgrim and McDermott \(1982\)](#), [Mittelstadt et al. \(1987\)](#), and [Adams \(1984\)](#). The central component of the Probabilistic Rational Method, is the runoff coefficient and, in particular, the 10 year Average Recurrence Interval (ARI) runoff coefficient. It is worth noting that this runoff coefficient does not have a physical basis but rather is a parameter to ensure that the rainfall frequency is transferred to the flow frequency. Furthermore, this parameter has been assumed to vary smoothly over geographical space for purposes of extrapolating from known locations to locations for application. However, it has been found that the runoff coefficient may show sharp variation within a close proximity, reflecting discontinuities at many locations, particularly at catchment boundaries. Additionally, [French \(2002\)](#) noted that the isopleths of the runoff coefficient in ARR 1987 ignored the existence of watercourses.

Alternative methods to the Probabilistic Rational Method, such as the Index Flood Method heavily rely on the assumption of 'regional homogeneity', which as previously mentioned is satisfied poorly for Australian regional flood data. Studies on regression based RFFE techniques for Australia (e.g. ([Hackelbusch et al., 2009](#); [Haddad et al., 2008](#); [Haddad et al., 2009](#); [Haddad et al., 2011](#); [Haddad et al., 2012](#); [Haddad and Rahman, 2012](#); [Micevski et al., 2015](#); [Palmen and Weeks, 2009](#); [Palmen and Weeks, 2011](#); [Pirozzi et al., 2009](#); [Rahman, 2005](#); [Rahman et al., 2008](#); [Rahman et al., 2009](#); [Rahman et al., 2011a](#); [Rahman et al., 2011b](#); [Rahman et al., 2012](#); [Rahman et al., 2015a](#); [Rahman et al., 2015](#); [Rahman et al., 2015b](#); [Rahman et al., 2015c](#))) have demonstrated that these techniques are capable of providing quite accurate design flood estimates using only a few predictor variables. In particular, it has been found that the Generalised Least Squares (GLS) based regression technique offers a powerful statistical method which accounts for the inter-station correlation of annual maximum flood series and across-site variation in flood series record lengths in the estimation of the flood quantiles. Use of a GLS-based regression method also allows differentiation between sampling error and model error and thus provides a more realistic framework for error analysis. The GLS based quantile regression technique has been adopted in the US (see, for example, ([Stedinger and Tasker, 1985](#); [Tasker and Stedinger, 1989](#); [Griffis and Stedinger, 2007](#))).

As an alternative to the quantile regression technique, the parameters of a particular probability distribution can be regressed against the catchment characteristics to develop prediction equations for the parameters of interest. This method is referred to as Parameter Regression Technique (PRT). It is this approach that is the basis of the recommended technique for design flood estimation in Australia using the RFFE model. For development of a PRT, the Bayesian GLS regression method is used to develop prediction equations for the model parameters for the three-parameter Log Pearson III (LP III) distribution; these model

parameters are the mean, standard deviation and skewness of the natural logarithm of the annual maximum flood series. The PRT offers three significant advantages over the quantile regression technique:

1. It ensures flood quantiles increase smoothly with decreasing Annual Exceedance Probability (AEP), an outcome that may not always be achieved with quantile regression;
2. It is straightforward to combine any at-site flood information with regional estimates (see [Book 3, Chapter 2](#)) using the approach described by [Micevski and Kuczera \(2009\)](#) to produce more accurate quantile estimates; and
3. It permits quantiles to be estimated for any AEP in the range of interest.

### **3.2.4. Data Required to Develop Regional Flood Frequency Estimation Technique**

The success of a RFFE technique largely depends on the quantity and quality of the available data and the capability of the adopted statistical techniques to transfer information from gauged to ungauged sites within the region. There are two basic types of data required for the development and application of RFFE techniques:

1. Flood data at gauged sites; and
2. Catchment characteristics relevant to production of floods in both gauged and ungauged catchments.

The quality and representativeness of the flood data determine to a large degree the accuracy and reliability of regional flood estimates. The challenge in collating a database for RFFE lies in maximising the amount of useful flood information, while minimising the random and systematic error (or 'noise') that may be present in some flood data.

In RFFE, various sources of errors in data and their effects on final flood estimates need to be recognised. The accuracy of flood quantile estimates at each individual gauged site depends largely on rating curve accuracy and record length at the individual site. Thus, the selection of a minimum record length at an individual site in the region is a very important step in any RFFE technique; the record length should be as long as possible while retaining enough sites in the region to make the results of RFFE useful. Also, the flood data at each site should satisfy a number of basic assumptions e.g. homogeneity, independence and stationarity. In the case where these assumptions are violated, appropriate measures should be taken; suitable techniques include GLS regression to account for the inter-station correlation (e.g. ([Stedinger and Tasker, 1985](#); [Griffis and Stedinger, 2007](#))), and non-stationary Flood Frequency Analysis to account for the impacts of climate change and changes in catchment conditions during the period of record. The data preparation issues for a RFFE technique are discussed in more detail by [Haddad et al. \(2010\)](#) and ([Rahman et al., 2015a](#); [Rahman et al., 2015](#); [Rahman et al., 2015b](#); [Rahman et al., 2015c](#)). In addition to the consideration of the data available at individual gauging stations, it is important to also consider the representativeness of the gauged data. The available gauged catchments represent only a sample of the range of conditions that may occur throughout the regions where the RFFE method is developed and applied.

The transfer of flood information from gauged to ungauged catchments relies on the ability to identify a number of key catchment and climate characteristics which determine similarities and differences in the flood production of catchments. In the Probabilistic Rational Method similarity is assumed to exist on the basis of geographical proximity, but in other methods an

appropriately small but informative set of predictor variables needs to be identified. The accuracy of a RFFE technique does not necessarily increase with the number of adopted predictor variables. For example, [Rahman et al. \(1999\)](#) used 12 predictor variables in an L-moments based Index Flood Method for south-east Australia. A subsequent study by [Rahman \(2005\)](#) showed that use of only 2 to 3 predictor variables can provide a similar level of accuracy.

Because of the difficulty of obtaining a sufficiently large number of gauged catchments in developing and testing a RFFE method, there is a chance that the available gauged catchments do not fully represent the range of conditions encountered in the region. Therefore where a catchment is judged to be atypical in some critical characteristic, the regional method may not be directly applicable and further analysis may be needed to estimate design flood quantiles. This issue is discussed further below.

### **3.2.5. Accuracy Considerations**

All RFFE techniques are subject to uncertainty, which, generally, is likely to be greater than for at-site Flood Frequency Analysis when a good quality and long record of streamflow data set is available at the location of interest. A RFFE technique essentially represents a 'transfer function' that converts predictor variables to a flood quantile estimate. It is assumed that use of a limited number of predictor variables (e.g. catchment area and design rainfall intensity) combined with an optimised transfer function captures the general nature of the rainfall-runoff relationship for flood events and hence provides flood quantile estimates of 'acceptable' accuracy.

Because a RFFE technique typically has limited predictive power, design flood estimates produced by it are likely to have a lower degree of accuracy than those from a well calibrated catchment modelling system. From the investigations made by ([Rahman et al., 2009](#); [Rahman et al., 2012](#); [Rahman et al., 2015a](#); [Rahman et al., 2015](#)), it may be stated that the relative accuracy of regional flood estimates using the RFFE model presented in this chapter is likely to be within  $\pm 50\%$  of the true value; however, in a limited number of cases the estimation error may exceed the estimation by a factor of two or more (see [Book 3, Chapter 3, Section 7](#)). It is unlikely that any RFFE technique would be able to provide flood quantile estimates which are of much greater accuracy given the current availability of streamflow data (in terms of temporal and spatial coverage) and feasibility of the extraction of a greater number of catchment descriptors using simplified methods such as GIS based techniques. Because of the small sample of gauged catchments and limited availability of readily obtainable catchment descriptors, it is not possible to prepare an extremely detailed set of descriptor variables covering all possible conditions, so a sample must be selected that provides a suitable range to represent the critical parameters, but to limit the application of variables that do not contribute significantly to the overall performance of the RFFE technique.

For catchments having limited recorded streamflow data, the combination of at-site data with a RFFE technique is likely to provide more accurate flood quantile estimates than either the at-site or regional method alone. Details of how limited streamflow data can be combined with a RFFE technique are presented in [Book 3, Chapter 2](#). Testing has shown this improves estimates in many cases.

An important assumption in all RFFE techniques is that the small set of predictor variables used in the regression equations is able to explain the differences in flood producing characteristics of the catchments in a region. Not all ungauged catchments located in the region satisfy this basic homogeneity assumption; some catchments may have characteristics that are substantially different from the gauged catchments in the region.

[Book 3, Chapter 3, Section 13](#) contains further discussion on the limits of applicability of the RFFE technique, on what constitutes an atypical catchment and recommendations on how to derive flood estimates for such catchments.

### 3.3. Statistical Framework

#### 3.3.1. Region Of Influence (ROI) Approach

In the formation of regions, the Region Of Influence (ROI) approach has been adopted for the parts of Australia where there are adequate numbers of gauged stations within close proximity to form ROI sub-regions. In the absence of a proven technique for the use of catchment characteristics as the basis for the ROI, the adopted ROI approach uses the geographical distance between stations as the distance metric and sets a maximum distance for inclusion of stations in the ROI sub-region. More details regarding development of ROI sub-regions are provided by ([Rahman et al, 2015](#)). Nonetheless, a summary of the process is presented. In applying the ROI approach, in the first iteration, a ROI sub-region consisting of the ten nearest stations to the site of interest is formed, the regional prediction equation is developed and its prediction error variance noted. At each of the subsequent iterations, the radius of the ROI sub-region is increased by 10 km and new stations are added to the previously selected stations. The final ROI sub-region for the location of interest is then selected as the one exhibiting the lowest prediction error variance.

One of the apparent limitations of the ROI approach is that for each of the gauged sites in the region, the regional prediction equation has a different set of model parameters; hence a single regional prediction equation cannot be pre-specified. To overcome this problem, the parameters of the regional prediction equations for all the gauged catchment locations are pre-estimated and integrated with the RFFE Model 2015 (see [Book 3, Chapter 3, Section 14](#) for more details). To derive flood quantile estimates at an ungauged location of interest, the RFFE Model 2015 uses a natural neighbour interpolation method to derive quantile estimates based on up to the 15 nearest gauged catchment locations within a 300 km radius from the location of interest. This ensures a smooth variation of flood quantile estimates over the space.

#### 3.3.2. Parameter Regression Technique

In the adopted RFFE technique for the Humid Coastal areas of Australia (see [Book 3, Chapter 3, Section 4](#) for further details), the first three moments of the LP III distribution (i.e. the mean, standard deviation and skewness of the natural logarithms of the annual maximum flood series) were regionalised. This method is referred to as the Parameter Regression Technique (PRT). The LP III distribution is described by the following equation:

$$\ln Q_x = M + K_x S \quad (3.3.1)$$

where  $Q_x$  is the discharge having an AEP of X% (design flood or flood quantile),

M is the mean of the natural logarithms of the annual maximum flood series,

S is the standard deviation of the natural logarithms of the annual maximum flood series, and

$K_x$  is the frequency factor for the LP III distribution of X% AEP, which is a function of the AEP and the skewness (SK) of the natural logarithms of the annual maximum flood series.

The prediction equations for M, S and SK were developed for all the gauged catchment locations in the Humid Coastal areas using Bayesian GLS regression and model parameters were noted. These model parameters are then integrated with the RFFE Model 2015.

### 3.3.3. Generalised Least Squares Regression

In developing the prediction equations, for the Humid Coastal areas, the Bayesian Generalised Least Squares (GLS) regression was adopted. The GLS regression assumes that the variable of interest (e.g. a moment of the LP III distribution) denoted by  $y_i$  for a location  $i$  can be described by a function of catchment characteristics (explanatory variables) with an additive error (Griffis and Stedinger, 2007):

$$y_i = \beta_0 + \sum_{j=1}^k \beta_j X_{ij} + \delta_i, i = 1, 2, \dots, n \quad (3.3.2)$$

where  $X_{ij}$  ( $j = 1, \dots, k$ ) are explanatory variables,  $\beta_j$  are the regression coefficients,  $\delta_i$  is the model error which is assumed to be normally and independently distributed with model error variance  $\sigma_\delta^2$ , and  $n$  is the number of locations in the region. In all cases, an at-site estimate of  $y_i$  denoted as  $\hat{y}_i$  is available. To account for the error in the at-site estimate, a sampling error  $\eta_i$  must be introduced into the model so that:

$$\hat{y} = X\beta + \eta + \delta = X\beta + \varepsilon \text{ where } \hat{y}_i = y_i + \eta_i; i = 1, 2, \dots, n \quad (3.3.3)$$

Thus the observed regression model error  $\varepsilon$  is the sum of the model error  $\delta$  and the sampling error  $\eta$ . The total error vector has a mean of zero and a covariance matrix:

$$E[\varepsilon\varepsilon^T] = \Lambda(\sigma_\delta^2) = \sigma_\delta^2 I + \Sigma(\hat{y}) \quad (3.3.4)$$

where  $\Sigma(\hat{y})$  is the covariance matrix of the sampling error in the estimate of the flood quantile or the parameter of the LP III distribution and  $I$  is a  $(n \times n)$  identity matrix. The covariance matrix for  $\eta_i$  depends on the record length available at each location and the cross correlation among annual maximum floods at different locations. Therefore, the observed regression model error is a combination of time-sampling error  $\eta_i$  and an underlying model error  $\delta_i$ .

The GLS estimator of  $\beta$  and its covariance matrix for a known  $\sigma_\delta^2$  is given by:

$$\beta_{GLS} = [X^T \Lambda(\sigma_\delta^2)^{-1} X]^{-1} X^T \Lambda(\sigma_\delta^2)^{-1} \hat{y} \quad (3.3.5)$$

$$\Sigma[\beta_{GLS}] = [X^T \Lambda(\sigma_\delta^2)^{-1} X]^{-1} \quad (3.3.6)$$

The model error variance  $\sigma_\delta^2$  can be estimated by either generalised Method of Moments (MOM) or maximum likelihood estimators. The MOM estimator is determined by iteratively solving Equation (3.3.5) along with the generalised residual mean square error equation:

$$(\hat{y} - X\beta_i [\sigma_\delta^2 I + \Sigma(\hat{y})]^{-1}) (\hat{y} - X\beta_{GLS}) = n - (k + 1) \quad (3.3.7)$$

In some situations, the sampling covariance matrix explains all the variability observed in the data, which means the left-hand side of Equation (3.3.7) will be less than  $n - (k + 1)$  even if



$\sigma_\delta^2$  is zero. In these circumstances, the MOM estimator of the model error variance is generally taken to be zero.

With the adopted Bayesian approach, it was assumed that there was no prior information on any of the  $\beta$  parameters; thus a multivariate normal distribution with mean zero and a large variance (e.g. greater than 100) was used as a prior for the regression coefficient parameters. This prior was considered to be almost non-informative, which produced a probability distribution function that was generally flat in the region of interest. The prior information for the model error variance  $\sigma_\delta^2$  was represented by a one parameter exponential distribution. Further description of the adopted Bayesian GLS regression can be found in [Haddad et al. \(2011\)](#) and [Haddad and Rahman \(2012\)](#).

### **3.3.4. Development of Confidence Limits for the Estimated Flood Quantiles**

In developing the confidence limits for the estimated flood quantiles, a Monte Carlo simulation approach was adopted by assuming that the uncertainty in the first three parameters of the LP III distribution (i.e. the mean, standard deviation and skewness of the logarithms of the annual maximum flood series) can be specified by a multivariate normal distribution. Here the correlations among the three parameters for a given region were estimated from the residuals of the GLS regression models of the LP III parameters. The mean of the LP III parameter is given by its regional predicted value and the standard deviation of the LP III parameter is the square root of the average variance of prediction of the parameter at the nearest gauged location. Based on 10 000 simulated values of the LP III parameters from the multivariate normal distribution as defined above, 10 000  $Q_x$  values are estimated in the RFFE Model 2015, which are then used to develop the 90% confidence intervals.

## **3.4. RFFE Techniques for Humid Coastal Areas**

### **3.4.1. Data Used to Develop RFFE Technique**

#### **3.4.1.1. Flood data**

Humid Coast areas had a relatively large number of recorded streamflow stations, as shown in [Figure 3.3.1](#). An upper limit of catchment size of 1000 km<sup>2</sup> was generally adopted. However, in some states (such as the Northern Territory), a few larger catchments were included as the total number of catchments with areas less than 1000 km<sup>2</sup> was too small. The cut-off record length of 19 years was selected to maximise the number of eligible stations on the consideration that a higher cut-off would reduce that number.

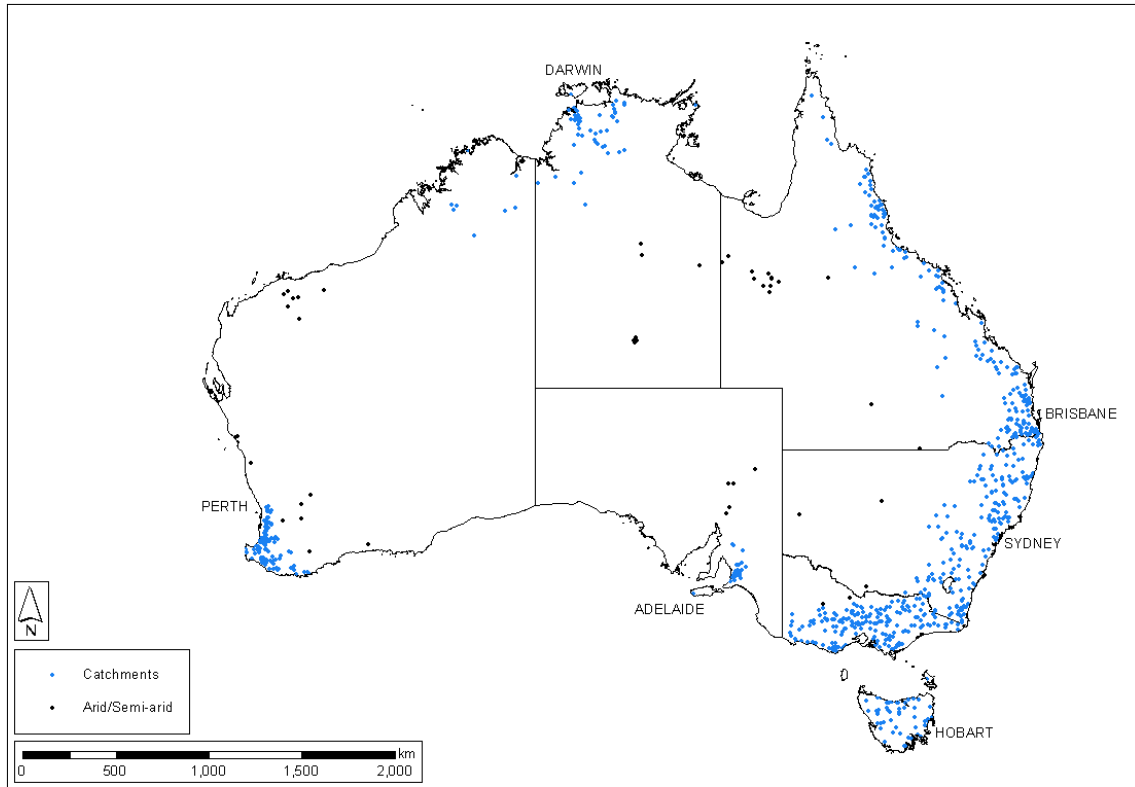


Figure 3.3.1. Geographical Distribution of the Adopted 798 Catchments from Humid Coastal Areas of Australia and 55 Catchments from Arid/Semi-arid Areas

The selected streams were unregulated since major regulation (e.g. a large dam on the stream) affects the rainfall-runoff relationship significantly by increasing storage effects. Streams with minor regulation, such as small farm dams and diversion weirs, were not excluded because this type of regulation is unlikely to have a significant effect on large annual floods. Gauging stations on streams subject to major upstream regulation were excluded from the data set. Catchments with more than 10% of the area affected by urbanisation were also excluded from the study data set. Catchments known to have undergone major land use changes, such as the clearing of forests or changing of agricultural practices over the period of streamflow records were excluded from the data set. Stations graded as 'poor quality' or with specific comments by the gauging authority regarding quality of the data were assessed in greater detail; if stations were deemed 'low quality' they were excluded.

The annual maximum flood series data may be affected by multi-decadal climate variability and climate change, which are not easy to deal with. The effects of multi-decadal climate variability can be accounted for by increasing the cut-off record length at an individual station. However, the impacts of climate change present a serious problem in terms of the applicability of the past data in predicting future flood frequency; this requires further research (Ishak et al., 2013). This is further discussed in [Book 3, Chapter 3, Section 10](#).

The data sets for the initially selected potential catchments are further examined, as detailed in [Haddad et al. \(2010\)](#), [Rahman et al. \(2015a\)](#), [Rahman et al. \(2015\)](#), and [Rahman et al. \(2015b\)](#): gaps in the annual maximum flood series was filled as far as could be justified, outliers were detected using the multiple Grubbs-Beck test ([Lamontagne et al., 2013](#); [Cohn et al., 2013](#)), errors associated with extrapolation of rating curves were investigated and the

presence of trends with the data were checked. From an initial number of approximately 1200 catchments, a total of 798 catchments were finally adopted from all over Australia (excluding catchments in the arid/semi-arid areas, where some of the above criteria were relaxed, as discussed in Section 5).

The record lengths of the annual maximum flood series of these 798 stations range from 19 to 102 years (median: 37 years). The catchment areas of the selected 798 catchments range from 0.5 km<sup>2</sup> to 4325 km<sup>2</sup> (median: 178 km<sup>2</sup>). [Table 3.3.1](#) provides summary of the selected catchments from Humid Coastal areas of Australia.

Table 3.3.1. Summary of Adopted Catchments from Humid Coastal Areas of Australia

State	No. of Stations	Streamflow Record Length (years) (range and median)	Catchment Size (km <sup>2</sup> ) (range and median)
New South Wales & Australian Capital Territory	176	20 – 82 (34)	1 – 1036 (204)
Victoria	186	20 – 60 (38)	3 – 997 (209)
South Australia	28	20 – 63 (37)	0.6 – 708 (62.6)
Tasmania	51	19 – 74 (28)	1.3 – 1900 (158.1)
Queensland	196	20 – 102 (42)	7– 963 (227)
Western Australia	111	20 – 60 (30)	0.5 – 1049.8 (49.2)
Northern Territory	50	19 – 57 (42)	1.4 – 4325 (352)
TOTAL	798	19 – 102 (37)	0.5 – 4325 (178)

The at-site Flood Frequency Analyses were conducted using the FLIKE software ([Kuczera, 1999](#)). The Potential Influential Low Flows (PILFs) were identified using multiple Grubbs-Beck test ([Lamontagne et al., 2013](#)) and were censored in the Flood Frequency Analysis. A Bayesian parameter estimation procedure with LP III distribution was used to estimate flood quantiles for each gauged site for AEPs of 50%, 20%, 10%, 5%, 2% and 1%.

### 3.4.1.2. Catchment Characteristics Data

As discussed by [Rahman et al. \(2009\)](#), [Rahman et al. \(2012\)](#), over ten predictor variables were selected initially; however, it was found that the accuracy of a RFFE technique does not necessarily increase with the number of adopted predictor variables. A total of five candidate predictor variables were adopted finally in the RFFE technique, as outlined below:

(i) catchment area in km<sup>2</sup> (*area*);

(ii) design rainfall intensity at catchment centroid (in mm/h) for the 6 hour duration and 50% AEP ( $^{50\%}I_{6h}$ );

(iii) design rainfall intensity at catchment centroid (in mm/h) for the 6 hour duration and 2% AEP ( $^{2\%}I_{6h}$ );

(iv) ratio of design rainfall intensities of AEPs of 2% and 50% for duration of 6 hour ( $^{2\%}I_{6h}/^{50\%}I_{6h}$ ); and

(v) *shape factor*, which is defined as the shortest distance between catchment outlet and centroid divided by the square root of catchment area.

Design rainfall values were extracted from the new Intensity Frequency Duration (IFD) data for Australia as discussed in Book 2, Chapter 3 of ARR. Table 3.3.2 provides the distribution of shape factors for the selected catchments.

Table 3.3.2. Distribution of Shape Factors for the Selected Catchments

Percentile	1%	10%	50%	90%	99%
Shape Factor	0.32	0.51	0.76	1.06	1.51

### 3.4.2. Adopted RFFE Regions

Australia is divided into seven regions. There are five Humid Coastal regions (Table 3.3.5) and two arid/semi-arid regions (Table 3.3.4), as shown in Figure 3.3.2. There are seven fringe zones that are the interface between two regions, as discussed in Book 3, Chapter 3, Section 6.

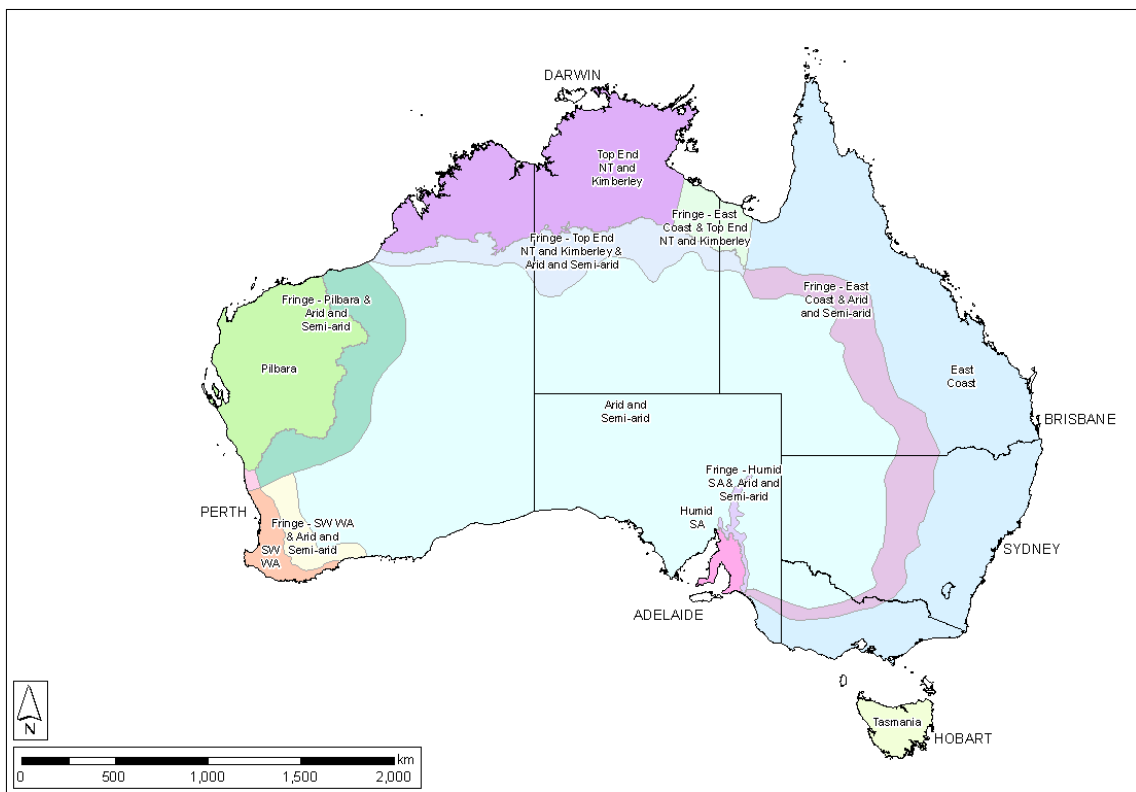


Figure 3.3.2. Adopted Regions for RFFE Technique in Australia

Table 3.3.3. Details of RFFE Technique for Humid Coastal Areas of Australia

Region	Method to form region	Number of stations	Estimation model
Region 1: East Coast	ROI (based on geographical proximity)	558	Bayesian GLS regression-PRT
Region 2: Tasmania		51	
Region 3: Humid SA		28	

Region	Method to form region	Number of stations	Estimation model
Region 4: Top End NT and Kimberley		58	
Region 5: SW WA		103	

### 3.4.3. Adopted Estimation Equations

For the five Humid Coastal regions described in [Table 3.3.3](#), the adopted estimation equations for M, S and SK for the regional LP III model ([Equation \(3.3.1\)](#)) have the following general form:

$$M = b_0 + b_1(\ln(\text{area})) + b_2(\ln(I_{6,50})) + b_3(\ln(\text{shape factor})) \quad (3.3.8)$$

$$S = c_0 + c_1 \ln\left(\frac{I_{6,2}}{I_{6,50}}\right) \quad (3.3.9)$$

$$SK = d_0 + d_1 \ln(\text{area}) + d_2 \ln\left(\frac{I_{6,2}}{I_{6,50}}\right) + d_3 \ln(I_{6,2}) \quad (3.3.10)$$

where, area is the catchment area (km<sup>2</sup>);

$I_{6,50}$  is the design rainfall intensity (mm/h) at catchment centroid for 6 hour duration and 50% AEP;

shape factor is the shortest distance between catchment outlet and centroid/area<sup>0.5</sup>; and

$I_{6,2}$  is the design rainfall intensity (mm/h) at catchment centroid for 6 hour duration and 2% AEP.

For Region 1 and 2, only the model intercepts were used in [Equation \(3.3.9\)](#) and [Equation \(3.3.10\)](#), which imply a regression equation without any predictor variable. Here, the weighted average values of S and SK were adopted, record lengths at the stations within the ROI sub-region were used as a basis for determining the weights.

The values of  $b_0$ ,  $b_1$ ,  $b_2$ ,  $b_3$ ,  $c_0$ ,  $c_1$ ,  $d_0$ ,  $d_1$ ,  $d_2$  and  $d_3$  at all the 798 individual gauged catchment locations (in the Humid Coastal areas) were estimated and embedded in the RFFE Model 2015. To derive flood quantile estimates at an ungauged location of interest, the RFFE Model 2015 uses a natural neighbour interpolation method to derive quantile estimates based on up to the 15 nearest gauged catchment locations within 300 km radius from the location of interest. This ensures a smooth variation of flood quantile estimates over space.

## 3.5. RFFE Techniques for Arid/Semi-Arid Areas

### 3.5.1. Data Used to Develop RFFE Technique

Most of Australia's interior falls into the arid/semi-arid areas, which are characterised by low mean annual rainfall in relation to mean annual potential evaporation. Rainfall events tend to be infrequent and their occurrence and severity are highly variable. Typically dry antecedent conditions may result in many rainfall events not producing any significant runoff. However, severe rainfall events can still result in significant flooding with serious consequences. Large

transmission losses (i.e. losses occurring from flow in rivers and other drainage channels) may also result in discharge reducing in a downstream direction, particularly in the lower river reaches of larger catchments in arid areas. The special flooding characteristics of catchments in arid/semi-arid areas make it desirable to treat them separately from catchments in more humid areas. In arid/semi-arid areas, annual maximum flood series generally contain many zero values; these values were censored in flood frequency analysis.

In ARR 1987 (Pilgrim, 1987), only a few catchments were used from arid/semi-arid areas to develop RFFE methods. Since the publication of ARR 1987, there has been little improvement in terms of streamflow data availability in most of the arid/semi-arid areas of Australia. There are a number of reasons for poor stream gauging coverage and quality in arid/semi-arid areas, as follows:

1. Poorly defined water course catchments, meaning that the water courses are hard to define and therefore gauge.
2. Large floods may be outside the water course, meaning that the cross-section may be hard to measure and the flow may be difficult to gauge.
3. Infrequent flood events, meaning that the gauge may be operating for extended periods of time without any flow.
4. Remote location, making it difficult to take velocity measurements during the flood events.
5. Little incentive to gauge flows because of the perceived limited water resources and the limited demand for development of these resources.

In the preparation of the Regional Flood Frequency Estimation database, only a handful of catchments from the arid/semi-arid areas satisfied the selection criteria. To increase the number of stations from the arid/semi-arid areas to develop a RFFE method, the selection criteria were relaxed i.e. the threshold streamflow record length was reduced to 10 years and the limit of catchment size was increased from 1000 km<sup>2</sup> to 6000 km<sup>2</sup>. These criteria resulted in the selection of 55 catchments from the arid/semi-arid areas of Australia (Figure 3.3.2 and Table 3.3.4). The selected catchments have average annual rainfall less than 500 mm. The catchment areas range from 0.1 to 5975 km<sup>2</sup> (median: 259 km<sup>2</sup>) and streamflow record lengths range from 10 to 46 years (median: 27 years).

Table 3.3.4. Summary of adopted stations from arid/semi-arid areas of Australia

Location	No. of stations	Streamflow record length (years) (range and median)	Catchment size (km <sup>2</sup> ) (range and median)
Pilbara	11	22 – 34 (28)	0.2 – 5975 (303)
Arid and Semi-arid	44	10 – 46 (27)	3 – 997 (209)
TOTAL	55	10 – 46 (27)	0.1 – 5975 (259)

### 3.5.2. Adopted Regions

The definition of regions in the arid/semi-arid areas in Australia is a difficult task, as there are only 55 catchments available over a vast area of Australia. There are two alternatives: (i) formation of one region with all the 55 stations; and (ii) formation of smaller sub-regions based on geographical proximity, noting that too small a region makes the developed RFFE technique of little statistical significance. Examination of a number of alternative sub-regions

led to the formation of two regions from the 55 arid/semi-arid catchments: Region 6 (11 catchments from the Pilbara area of WA) and Region 7 (44 catchments from all other arid areas except Pilbara) (see [Figure 3.3.2](#) for the extent of these two arid/semi-arid regions and [Table 3.3.5](#) for other details).

Table 3.3.5. Details of RFFE technique for arid/semi-arid regions

Region	Method to form region	Number of stations	Estimation model
Region 6: Pilbara	Fixed region	11	Index flood method with $Q_{10}$ as index variable
Region 7: Arid and Semi-arid		44	

### 3.5.3. Adopted Estimation Equations

Application of the ROI and PRT methods for arid/semi-arid regions was deemed inappropriate as the ROI due to an insufficient number of gauges. Hence a simpler RFFE method was considered more appropriate for the two arid/semi-arid regions. Here, an index type approach as suggested by [Farquharson et al. \(1992\)](#) is adopted. The 10% AEP flood quantile ( $Q_{10}$ ) was used as the index variable and a dimensionless Growth Factor for X% AEP ( $GF_x$ ) was used to estimate  $Q_x$ :

$$Q_x = Q_{10} \times GF_x \quad (3.3.11)$$

A prediction equation was developed for  $Q_{10}$  as a function of catchment characteristics, and regional growth factors were developed based on the estimated at-site flood quantile. In the arid areas, significant storm events do not typically occur every year, and some of these events do not produce significant floods. The at-site Flood Frequency Analyses for the arid catchments was conducted using the FLIKE software ([Kuczera, 1999](#)). The Potential Influential Low Flows (PILFs) were identified using multiple Grubbs-Beck test ([Lamontagne et al., 2013](#)) and were censored in the Flood Frequency Analysis. A Bayesian parameter estimation procedure with LP III distribution was used to estimate flood quantiles for each gauged site for AEPs of 50%, 20%, 10%, 5%, 2% and 1%. It should be noted that the Flood Frequency Analysis procedure adopted in the Humid Coastal and arid areas was the same.

The  $Q_x/Q_{10}$  values were estimated at individual stations; the weighted average of these values (weighting was done based on record length at individual stations) over all the stations in a region then defined the Growth Factors ( $GF_x$ ) for the region.

The adopted prediction equation for the index variable  $Q_{10}$  has the following form:

$$\log_{10} = b_0 + b_1 \log_{10}(\text{area}) + b_2 \log_{10}(I_{6,50}) \quad (3.3.12)$$

where  $b_0$ ,  $b_1$  and  $b_2$  are regression coefficients, estimated using ordinary least squares regression; area represents catchment area in  $\text{km}^2$ , and  $I_{6,50}$  is the design rainfall intensity (mm/h) at catchment centroid for 6 hour duration and 50% AEP. The values of  $b_0$ ,  $b_1$  and  $b_2$  and the regional Growth Factors ( $GF_x$ ) are embedded into the RFFE Model 2015.

## 3.6. Fringe Zones

The boundaries between the arid/semi-arid and Humid Coastal regions in [Figure 3.3.2](#) were drawn (as a smoothed line) approximately based on the 500 mm mean annual rainfall contour. To reduce the effects of sharp variation in flood estimates for the ungauged

catchments located close to these regional boundaries, seven fringe zones were delineated, as shown [Figure 3.3.2](#). The boundary of the fringe zone with the Humid Coastal region was approximately defined by the 500 mm mean annual rainfall isohyet, while the other side was defined by the 400 mm mean annual rainfall isohyet to establish a fringe zone. In drawing the boundary, some minor adjustment was made to make the boundary as smooth as possible.

For these fringe zones, the flood estimate at an ungauged catchment location is taken as the inverse distance weighted average value of the flood estimates based on the two nearest regions. The method is embedded into the RFFE Model 2015.

### **3.7. Relative Accuracy of the RFFE Technique**

The reliability and accuracy of the RFFE quantile estimates were assessed using leave-one-out (LOO) validation. In the LOO validation, one catchment was left out from the model data set and the RFFE technique is applied to the catchment that was left out. The flood quantiles estimated using the RFFE technique were then compared with the at-site flood frequency estimates obtained by FLIKE ([Kuczera, 1999](#)) as mentioned in [Book 3, Chapter 3, Section 5](#). The procedure was repeated for each catchment in the regional data set to provide an overall assessment of the performance of the RFFE technique.

The reliability of the RFFE flood quantile confidence limits described in [Book 3, Chapter 3, Section 3](#) was assessed empirically using standardised quantile residuals. The quantile residual is the difference between the logarithm of flood quantile estimates obtained using at-site Flood Frequency Analysis and the RFFE technique. The standardised quantile residual is the quantile residual divided by its standard deviation which is the square root of the sum of the RFFE predictive variance of the flood quantile and at-site quantile variance ([Haddad and Rahman, 2012](#); [Micevski et al., 2015](#)). This accounts for both the model error (e.g. inadequacy of the RFFE model) and the sampling error (e.g. due to limitations in streamflow record length). If the uncertainty in the log quantile estimates has been adequately described, the standardised quantile residuals should be consistent with a standard normal distribution.

[Figure 3.3.3](#) shows the plots of standardised residuals vs. normal scores for Region 1 for AEPs of 10% and 5% (the plots for other AEPs for Region 1 are provided in [Book 3, Chapter 3, Section 16](#)). Plots for other regions can be seen also in [Rahman et al \(2015\)](#). These residuals were estimated without bias correction (details of bias correction are provided in [Book 3, Chapter 3, Section 8](#) ). These plots include 558 catchments from Region 1 used in the RFFE model and some 28 catchments which were excluded from the final RFFE model data set based on the results of preliminary analysis and unusual characteristics such as significant natural floodplain storage. [Figure 3.3.3](#) reveals that most of the 558 catchments closely follow a 1:1 straight line indicating that the assumption of normality of the residuals was not inconsistent with the evidence; this is supported by the application of the Anderson-Darling and Kolmogorov-Smirnov tests which showed that the assumption of the normality of the residuals cannot be rejected at the 10% level of significance. Under the assumptions of normality, approximately 90% of the standardised quantile residuals should lie between  $\pm 2$ , which is largely satisfied. There were a few catchments with standardised residual values close to  $\pm 3$ . These correspond to instances where the RFFE confidence limits may not be reliable; an example of such a catchment is provided in [Book 3, Chapter 3, Section 15](#). The same conclusion applies to the other Humid Coastal regions.



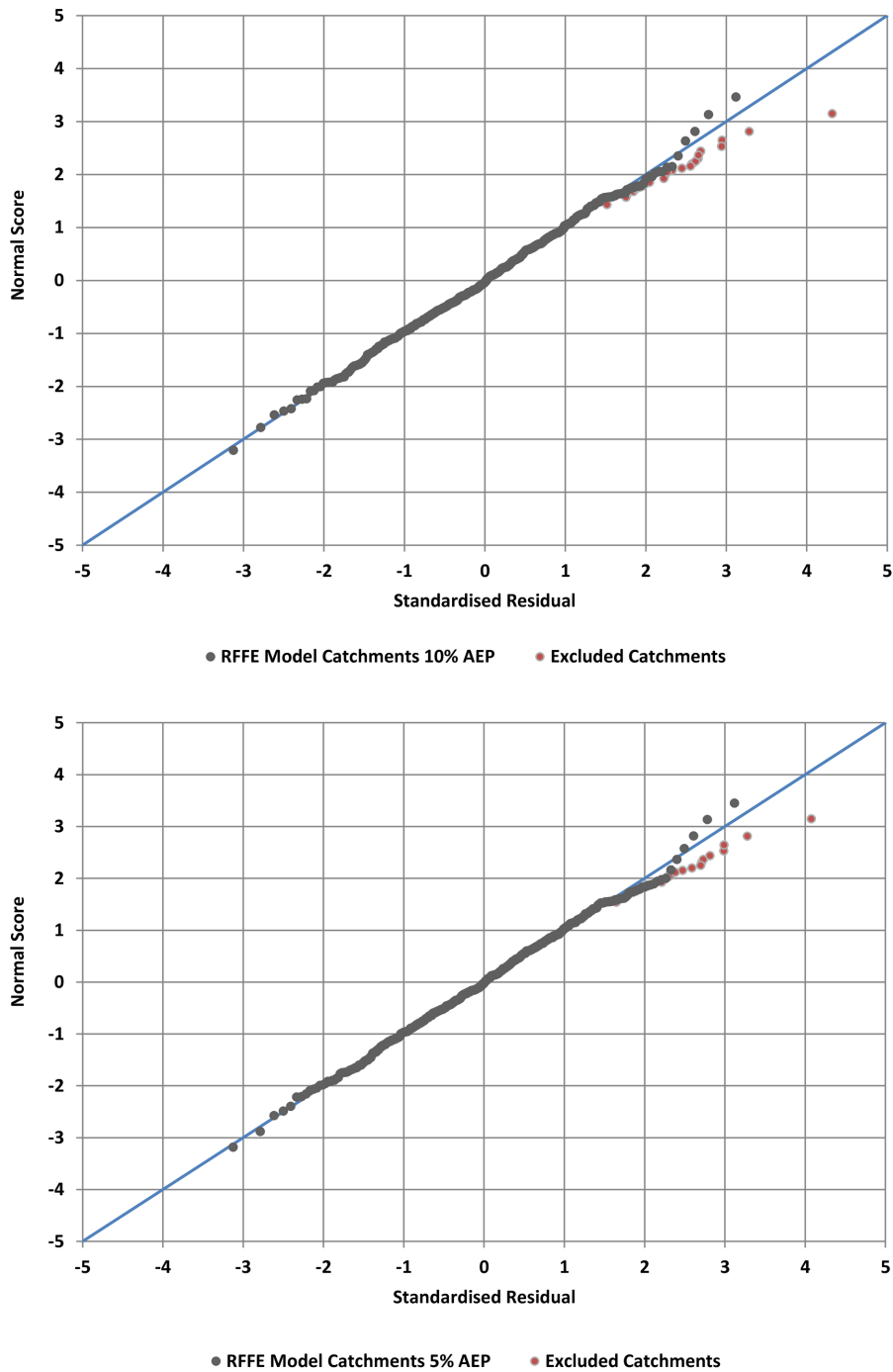


Figure 3.3.3. Standardised Residuals vs. Normal Scores for Region 1 Based on Leave One Out Validation for AEPs of 10% and 5%

The main conclusion from this analysis is that the quantification of uncertainty in the quantile estimates by the RFFE technique is reliable for the vast majority of the cases. [Figure 3.3.3](#) and [Book 3, Chapter 3, Section 15](#) serve as a reminder that some catchments may not be adequately represented by the catchments used in the RFFE analysis. Users of the RFFE Model 2015 should check that the catchment of interest is not atypical compared with the gauged catchments included in the ROI used to develop the RFFE estimate. To assist users in this regard the RFFE Model 2015 discussed in [Book 3, Chapter 3, Section 14](#) and [Book 3, Chapter 3, Section 13](#) lists the RFFE Model gauged catchments located nearest to the ungauged catchment of interest.

The accuracy of the flood quantile estimates provided by the RFFE technique is evaluated by using the Relative Error (RE) defined as:

$$RE(\%) = \frac{Q_{RFFE} - Q_{FFA}}{Q_{FFA}} \times 100 \quad (3.3.13)$$

where  $Q_{RFFE}$  is the flood quantile estimate for a given site for a given AEP by the RFFE technique; and  $Q_{FFA}$  is the flood quantile estimate from the at-site Flood Frequency Analysis (see Book 3, Chapter 3, Section 4 for details).

It should be noted that the Relative Error given by Equation (3.3.13) makes no allowance for the fact that the at-site flood frequency estimates are themselves subject to sampling error. Therefore, this error should be seen as an upper bound on the true relative error.

It should be noted here that LOO is a more rigorous validation technique compared with the split-sample validation where the model is tested on a smaller number of catchments (e.g. 10% of the total catchments). Hence, the relative error that is generated by LOO is expected to be higher than if split-sample validation were used. The medians of the absolute relative error values from the LOO validation for different regions are reported in Table 3.3.6. It can be seen that for the Humid Coastal regions, Region 5 (SW WA) has the highest relative error (59 to 69%) and Region 3 (Humid SA) has the smallest relative error (33 to 41%).

### 3.8. Bias Correction

In the spatial plots of the standardised residuals, a few cluster of notable underestimation and overestimation were detected. To overcome this problem, a bias correction was implemented, which attempted to provide estimates of  $M$  (for Humid Coastal areas) (Equation (3.3.8)) and  $Q_{10}$  (for arid/semi-arid areas) (Equation (3.3.12)) closer to the observed  $M$  or  $Q_{10}$  at the location of each of the 853 model gauged catchments. This correction was based on an additive bias correction factor  $M_{FFA} - M_{RFFE}$ , (obtained at each of the model 798 gauged catchments in the Humid Coastal areas) and  $Q_{10,FFA}/Q_{10,RFFE}$  (obtained at each of the model 55 catchments in arid/semi-arid areas). In practice, for an ungauged location of interest, an interpolated bias correction factor is calculated by the software using Natural Neighbour approach based on nearby 15 gauged catchments. It was found that this approach reduced the clusters of bias in the spatial plots of the standardised residuals and hence was adopted in the RFFE Model 2015.

Table 3.3.6. Upper bound on (absolute) median relative error (RE) from leave-one-out validation of the RFFE technique (without considering bias correction)

Median RE (%)						
	AEP					
Region	50%	20%	10%	5%	2%	1%
Region 1: East Coast	51	49	52	53	57	59
Region 2: Tasmania	53	46	46	46	46	45
Region 3: Humid SA	38	39	33	35	39	41

	Median RE (%)					
Region 4: Top End NT and Kimberley	33	36	36	38	39	47
Region 5: SW WA	61	59	66	68	68	69
Region 6: Pilbara	35	37	35	42	37	43
Region 7: Arid and Semi-arid	63	67	67	61	57	49

### 3.9. Combining Regional and At-Site Quantile Estimates

Unless a station has a very long annual maximum flood series data (e.g. greater than 100 years), it is desirable to combine at-site and regional flood frequency quantile estimates to achieve a more accurate estimate. The RFFE Model 2015 (see [Book 3, Chapter 3, Section 14](#) for the description of the model) provides the necessary parameter set and data in its output to combine the regional flood quantile estimates with the at-site data. This is discussed in more detail in [Book 3, Chapter 2](#).

### 3.10. Impact of Climate Change

The adopted regional estimation equations include design rainfall intensity as a key input variable. As a result the impact of climate change as reflected in changes in design rainfall estimates (which are expected to be upgraded regularly) can be propagated through the RFFE Model 2015 to provide a first order estimate of the impact of climate change on regional design flood estimates. This approach assumes that the contribution of the other catchment characteristics affecting flood production does not change with future climate state. Given that this assumption is unlikely to be valid ([Ball, 2014](#)) the use of potential future rainfall intensities in the RFFE Model 2015 will indicate the sensitivity of the design flood estimates with respect to climate change state. Further research on the impact of climate change on rainfall and flood in Australia will allow updating of the RFFE Model 2015 by incorporating the impact of climate change.

### 3.11. Progressive Improvement of RFFE Model 2015 v1

It is expected that the RFFE Model 2015 v1 will be updated in future when the streamflow record lengths at the selected 853 gauged catchments increase significantly and/or when additional catchments are available that satisfy the criteria of catchment selection ([Book 3, Chapter 3, Section 4](#)). Furthermore, additional predictor variables can potentially be included in the RFFE Model to enhance model accuracy, in particular if GIS based techniques can be adopted to more readily extract the additional predictor variables such as stream density and main stream slope.

## **3.12. RFFE Implementation and Limitations**

### **3.12.1. Overview of RFFE Accuracy**

#### **3.12.1.1. Data Coverage**

The RFFE Model has been developed from a detailed analysis of all appropriate streamflow gauging stations throughout Australia. The selected 853 gauges met the criteria for application to the development of the procedure.

It must be recognised however that this is a small number of gauges in the 7.7 million km<sup>2</sup> area of Australia. In addition to the sparse gauge coverage, there is a significant variation in catchment types across Australia. The RFFE Model must use the available data to develop a regional procedure that can estimate flood quantiles with the best possible accuracy. Relevant catchment characteristics therefore may not be represented sufficiently to allow inclusion in the regional relationship.

There are insufficient gauges to provide a representative coverage of all catchment types throughout Australia. This is a particular concern in the arid and semi-arid interior.

The regional relationship implemented in ARR has therefore used only characteristics that are sampled sufficiently. These characteristics are catchment area, rainfall intensity parameters and shape factor. Other factors, such as land use, slope, soils, geology or vegetation, are not sampled sufficiently to allow inclusion in the parameters used for the procedure, even though they are known to be important in the estimation of flood quantiles.

The RFFE Model therefore may be regarded as providing a “generic” estimate of flood quantiles for a range of typical catchment types. It may be expected that different flood estimates would be derived for other catchment types that have catchment characteristics that are dissimilar to those used in development of the method. If there were a larger sample of gauged catchments in Australia and they sampled a wider variety of catchment types, it is expected that the RFFE Model would incorporate a wider range of catchment characteristics and would therefore be capable of more reliable estimates for a wider range of catchments.

The procedure is based on the analysis of the selected catchment characteristics, but improvements in the procedure are possible with additional analysis.

#### **3.12.1.2. Data Accuracy**

While there is a relatively small and possibly unrepresentative distribution of gauged catchments used in the development of the procedure, it is also noted that there are inaccuracies in the base data used to develop the procedure. The gauges were selected to ensure at least a minimum quality standard. However all gauges have some level of inaccuracy, which could be caused by extrapolation of rating curves, variability with rating curves over time, effects of backwater at the gauge, changing catchment conditions, or flow diversions and overflows that affect flows. These factors particularly impact on the quality of flow records for the larger flows, which are the important records for Flood Frequency Analysis.

Imposing a higher data quality standard will reduce the number of gauges for analysis while lowering the standard will result in greater errors in the data used to develop the procedure.

For the development of the RFFE Model, the decision has been to impose a minimum data quality standard, to ensure a maximum number of gauges were included.

It must be noted though that such data inaccuracies were not be identified during the development of the RFFE Model as the analysis involved a large number of stations and detailed assessment of each of these was not feasible. The meta-data and other documentation provided by the water agencies was not sufficiently detailed to allow a routine assessment of data quality, and it was necessary to rely on local advice as to the suitability of the data used.

The inclusion of this data may impact on the quality of the regional results, but does improve the representativeness of the data. While it is impossible to quantify this impact, the possible impact needs to be borne in mind.

### **3.12.1.3. Representative Periods of Record**

The selection of the gauged catchments for analysis was based on the period of record with a minimum record length of 20 years. This record length could have been for the most recent period for stations that are still operating or it could have been for an earlier period for closed stations.

Longer periods of record are more likely to represent the variability in flood magnitude and also more likely to sample large floods that occur infrequently. However, even with a record length of more than 20 years, it is possible that the record may not sample a wide range of flood sizes and there is still a potential source of inaccuracy when extrapolating to larger floods. The samples from different time periods may also affect the flood quantiles since it is well known that there are longer term variations in the distribution of flood maxima due to inter-decadal variability in climate. This may result in differences in the design flood quantiles that are purely a result of the sample period rather than a real difference in flood probability.

### **3.12.2. RFFE Implementation**

The estimates of flood quantiles from the RFFE Model must be regarded as a first approximation of the required quantiles. In many cases, the estimates from the RFFE Model may provide an acceptable result for application.

However, given the accuracy considerations discussed above, some additional testing and review is recommended.

The additional testing and review can include the following processes:

- Review the catchment characteristics for the catchment being analysed and assess whether this catchment is typical for catchments that have been used in the development of the method: This review needs to consider the catchments in the local area, or elsewhere in Australia. The most relevant characteristics to review include the catchment shape, slope, soils and vegetation. The extent of floodplain storage, either natural or artificial needs to be reviewed. If the target catchment has features that are distinctly different from the range found in “typical” gauged catchments, the results from the RFFE Model can be either discarded or adjusted to allow for the local conditions.
- Review the nearby catchments listed in the RFFE Model: These are the nearest gauged catchments that have been used in the development of the procedure and are some gauges that will influence the results for the Region of Influence calculations.

This review will need to consider whether these nearby catchments are similar to the target catchment or if there are any apparent outliers in this group. As with the review of catchment characteristics, the review of the nearby catchments in the RFFE Model could

lead to an adjustment in the results, or the decision for the flood quantiles for the target catchment to be transposed directly (allowing for differences in catchment area) from a nearby catchment that is most similar to the target catchment.

- Consider an independent flood estimation procedure: such as the application of a runoff-routing model using regional parameter estimates that are appropriate for ungauged catchments in the local region. It must be remembered that these alternative procedures are still uncertain, but reconciliation of estimates from different sources provides valuable information with which to derive a “best estimate”. Consideration of catchment characteristics and similarities or differences need to be a part of this assessment. The RFFE Model results may be adjusted or neglected depending on the conclusions of this independent analysis.
- Review any local available data: This data may be as uncertain as a limited amount of anecdotal data, such as an observation of the frequency of overtopping of a bridge for example. Depending on the findings of the check of local observations, the RFFE Model results may need adjustment. The results of the RFFE Model calculation can be compared with the local observation to at least ensure that the calculated design flood quantiles are consistent with the local observations.

The conclusion of this additional analysis is that the calculated RFFE Model flood quantiles are not perfect, though they do provide the means to develop estimates that are consistent with a large body of gauged records. Further consideration of the results and possible adjustment will help to ensure a better estimate of the design flood quantiles needed for inclusion in the analysis.

### **3.13. Practical Considerations for Application of the RFFE Technique**

The basis of the RFFE Model 2015 has been the analysis of all available streamflow gauging stations that meet the selection criteria described in this chapter, primarily that the stream gauge has an adequate length of record and the streamflow data are of “reasonable” quality and relate to relatively natural catchments. Most selected streamflow gauges have a catchment area less than 1000 km<sup>2</sup>. The RFFE Model parameters were then developed based on regionalisation of the at-site flood quantiles for all of these gauges from a given region. All available and suitable streamflow data for all of Australia were adopted to develop the RFFE Model.

While the RFFE Model is appropriate for catchment types represented by the gauged catchments used to develop this model, there are catchments where the method either cannot be applied or where there may be gross error in the flood quantile estimates if the RFFE Model were applied without adjustments. These catchment types are described below.

#### **3.13.1. Urban Catchments**

One of the criteria for catchment selection in the development of the RFFE Model was that there should be essentially no urbanisation in the catchment, or at least such a small proportion that the Flood Frequency Analysis was not affected. It is well known that flooding is affected, sometimes significantly by urbanisation. There are insufficient gauged urban catchments to allow development of a RFFE Model for urban catchments.

Therefore, the RFFE Model 2015 cannot be applied for any catchment where urbanisation accounts for more than 10% of the catchment area, or where it is considered that there may

be an impact of urbanisation on rainfall runoff relationship. In these cases an alternative approach for estimating design floods is needed, as no equivalent regional method to the rural RFFE Model is available.

### **3.13.2. Catchments Containing Dams and Other Artificial Storage**

Dams or other artificial water storages will attenuate flood hydrographs and will therefore reduce the flood peak discharges at the catchment outlet. The selection of catchments used in the development of the RFFE Model excluded those with dams that were regarded as sufficiently significant to have an impact on flood discharges.

If a catchment has a dam where there will be an impact on flood discharges, the RFFE Model cannot be applied directly. In this case, the RFFE Model can be used to calculate design flood discharges for the “natural” catchment and then the effects of the dam can be included by the application of a runoff-routing model where the storage effects can be modelled directly.

### **3.13.3. Catchments Affected by Mining**

Catchments where mining activity has affected a significant portion of the catchment area have also been excluded from those used to develop the RFFE Model. Catchments where mining activities are significant may produce lower flood peak discharges than natural catchments due to the presence of water quality ponds, tailings dams and other water management infrastructure and the mine pit itself. In addition, the runoff response from mining areas that include waste dumps and rehabilitated areas will be quite distinct from natural catchments.

In cases where mining is judged to impact a significant proportion of a catchment, the RFFE Model can only be applied on the natural portions of the catchment. The area affected by mining activities should be modelled by an alternative method. Assessment of the water balance affecting the volume of runoff is needed to ensure that the effects of water control in ponds and mine pits and infiltration in highly modified catchments is represented correctly. The catchment response is also affected by drainage works and diversions. Calculation of runoff from mining areas is a complex and specialised exercise and detailed understanding of individual conditions is necessary. In general, a detailed runoff-routing model is needed as well as a good understanding of the water balance in these situations. However, direct calibration of runoff routing models on ungauged catchments is not possible, which may result in grossly inaccurate design flood estimates.

### **3.13.4. Catchments with Intensive Agricultural Activity**

While many of the catchments used in development of the RFFE Model have been located in agricultural regions, few are in areas of intensive agriculture, where the flood response may be affected by farm dams, soil conservation works or irrigation infrastructure. Many agricultural regions may be laser levelled to produce topography that is artificial and quite different from the natural catchments that are the primary catchment types used to develop the RFFE Model. The objectives of works on agricultural land is often to slow the rate of runoff and increase infiltration to the soil profile, thus the flood peak discharges will often be reduced on these catchment types as compared to the general catchment type as used to develop the RFFE Model.

Catchments affected by intense agricultural activities are similar to those affected by mining and similar analysis methods are needed to calculate flood discharges.

In this case the RFFE Model cannot be applied directly but additional analysis is needed to assess the catchment characteristics and then prepare a runoff-routing model to adjust the generic RFFE Model results using the catchment storage and channel characteristics.

### **3.13.5. Catchment Size**

The RFFE Model has been developed using all suitable gauged catchments throughout Australia with catchment areas generally less than 1000 km<sup>2</sup>.

The RFFE Model can be applied to small catchments with no lower limit though it is recognised that there are only a few gauged catchments smaller than 10 km<sup>2</sup> included in the database to develop the RFFE Model. Because of the limited available data, it is likely that there will be a greater degree of error in the quantile estimates for these smaller catchments.

The RFFE Model should not be applied for catchments larger than 1000 km<sup>2</sup> because these larger catchments were not generally used in the development of the method.

### **3.13.6. Catchment Shape**

The distribution of the shape factors of the selected catchments in developing the RFFE Model is shown in [Table 3.3.2](#). An ungauged catchment with shape factor beyond 10%-90% limit as shown in [Table 3.3.2](#) will have lower accuracy in the estimated flood quantiles.

### **3.13.7. Atypical Catchment Types**

The catchment characteristics adopted in the RFFE Model were limited to readily available/easily obtainable catchment variables. The catchment characteristics used to calculate model parameters are limited and testing did not determine that more complex characteristics provide significant benefit in the regional relationship.

It is known that there are many other catchment characteristics that influence catchment response and flood discharges. These include factors such as:

- Catchment land use including vegetation coverage: The extent of clearing or forest cover can have a significant impact, especially in the south-west of Western Australia, for example.
- Soils and geology: These factors influence the rainfall losses and catchment flood response.
- Slopes: Steeper catchments respond more rapidly and therefore produce larger flood peaks.
- Channel types and floodplain storage: Well defined channels and smaller floodplain storage extents produce faster response and therefore larger flood peaks.

In cases where the catchment requiring the design flood estimate is judged to have characteristics significantly different from those used in the development of the RFFE Model, further hydrology and hydraulic analyses may be needed to refine the results from the generic RFFE Model results.



The RFFE Model has been developed from the analysis of gauged catchments, but in reality all catchments exhibit some differences. Gauges need to be installed at locations where there is a sensitive and stable control and where the flow is well constrained within a defined stream channel. This means that larger catchments with extensive floodplain storage of widely distributed flow for example may not be well represented in the gauged dataset. These catchments may also have lower data quality but may well be required for design purposes.

### **3.13.8. Catchment Location**

Considering the large size of Australia and the relatively small number of gauged catchments used for the development of the RFFE Model, the average density of gauged catchments used in developing the model is quite low. In addition, it must be recognised that there are errors in the streamflow data (e.g. rating curve extrapolation error) used to develop the RFFE Model.

This means that catchments where design flood discharges are needed may be remote from the gauged catchments used to develop the RFFE Model and may have distinct differences from the adopted gauged catchments.

In these cases, the application of the RFFE Model may produce inaccurate results and hence additional review and checking are necessary to confirm that the catchment being analysed has similar characteristics to those used to develop the RFFE Model. Where there are significant differences, a similar assessment to that needed for atypical catchments should be considered, and an adjustment to the generic RFFE Model result may be needed.

### **3.13.9. Arid and Semi-arid Areas**

The arid and semi-arid areas of Australia pose a particular problem. The RFFE Model divides these areas into two regions, the Pilbara and Arid and semi-arid. There are few gauged catchments in these regions with only 55 gauged catchments to represent a total area of about 5 million km<sup>2</sup>.

The stream gauges in this region are often located at sites that may not be representative of the general area, since the gauge sites are selected because of access, confined channel and stable control, which may not be typical of the types of sites where design flood discharges are needed.

The Pilbara region is not as diverse as the remainder of arid and semi-arid areas and the RFFE Model estimates for catchments in the Pilbara can be adopted subject to the other limitations discussed here.

The general arid and semi-arid region though is more complex. The RFFE Model results for this region are based on the best available data from the gauges, but because of the diversity of conditions and the very low density of gauging, the RFFE Model results are very uncertain.

Because of this the recommended approach for the arid and semi-arid zone requires some additional analysis to refine the standard results. The RFFE Model data-base report ([Rahman et al., 2015a](#)) has a listing of all of the catchments that were used in the development of the method and the application of the RFFE Model software provides a map of the neighbouring catchments that were used in the development of the method.

### 3.13.10. Baseflow

The RFFE Model has been developed using at-site flood frequency analysis, so the estimated peak discharges include baseflow. This means that the results from the RFFE Model will not be consistent with those from runoff-routing models where only surface runoff is calculated. While baseflow is only a minor part of the total flood hydrograph in many areas of Australia, there are some areas where it is more significant and it becomes more important when considering smaller floods. When working with the two methods it is thus necessary to make appropriate allowance for baseflow contribution to the peak and volume of the design flood.

### 3.14. RFFE Model 2015

The RFFE technique presented in this chapter has been incorporated into a software tool referred to as RFFE Model 2015. The current version of the RFFE Model 2015 can be accessed from the ARR website<sup>1</sup>. [Figure 3.3.4](#) presents a screen shot of the RFFE Model 2015 software landing page. The model requires the following basic inputs (to be entered by the user in the interface shown in [Figure 3.3.5](#)) for the catchment of interest to generate design flood estimates for six AEPs (50%, 20%, 10%, 5%, 2% and 1%).

- i. Catchment name;
- ii. Catchment outlet latitude in decimal degrees;
- iii. Catchment outlet longitude in decimal degrees;
- iv. Catchment centroid latitude in decimal degrees;
- v. Catchment centroid longitude in decimal degrees; and
- vi. Catchment area in km<sup>2</sup>.

In the "Advanced" data input option, the user can also enter the following inputs:

- i. Region name (can be selected from the dropdown list, see [Table 3.3.7](#) for region name and [Figure 3.3.2](#) for the extent of the regions);

Table 3.3.7. Region Names for Application of the RFFE Model 2015 (see [Figure 3.3.2](#) for the Extent of the Regions)

Region name	Region code
Region 1: East Coast	1
Region 2: Tasmania	2
Region 3: Humid SA	3
Region 4: Top End NT and Kimberley	4
Region 5: SW WA	5
Region 6: Pilbara	6
Region 7: Arid and Semi-arid	7

- ii. Design rainfall intensity at catchment centroid for 50% AEP and duration of 6 hour in mm/h; and

<sup>1</sup>[www.arr.org.au](http://www.arr.org.au)

iii. Design rainfall intensity at catchment centroid for 2% AEP and duration of 6 hour in mm/h.

The RFFE Model 2015 output contains the following principal information (see [Figure 3.3.6](#) as an example).

RFFE About Limitations Publications Acknowledgments Changelog Logged in as arr

### Regional Flood Frequency Estimation Model (DRAFT)

Draft Version of the Regional Flood Frequency Estimation Model for the 4th edition of Australian Rainfall and Runoff.

Australian Rainfall & Runoff

#### Input Data

Basic  Advanced

**Catchment Name**

**Catchment Outlet Latitude**

**Catchment Outlet Longitude**

**Catchment Centroid Latitude**

**Catchment Centroid Longitude**

**Catchment Area (km<sup>2</sup>)**

Outlet Location

Method by Dr Alaur Rahman and Dr Khalid Haddad from Western Sydney University for the Australian

Figure 3.3.4. Screen Shot of RFFE Model 2015 (Landing Page)

**Regional Flood Frequency Estimation Model (DRAFT)**

Draft Version of the Regional Flood Frequency Estimation Model for the 4th edition of Australian Rainfall and Runoff.



**Input Data**

Basic
Advanced

**Catchment Name**

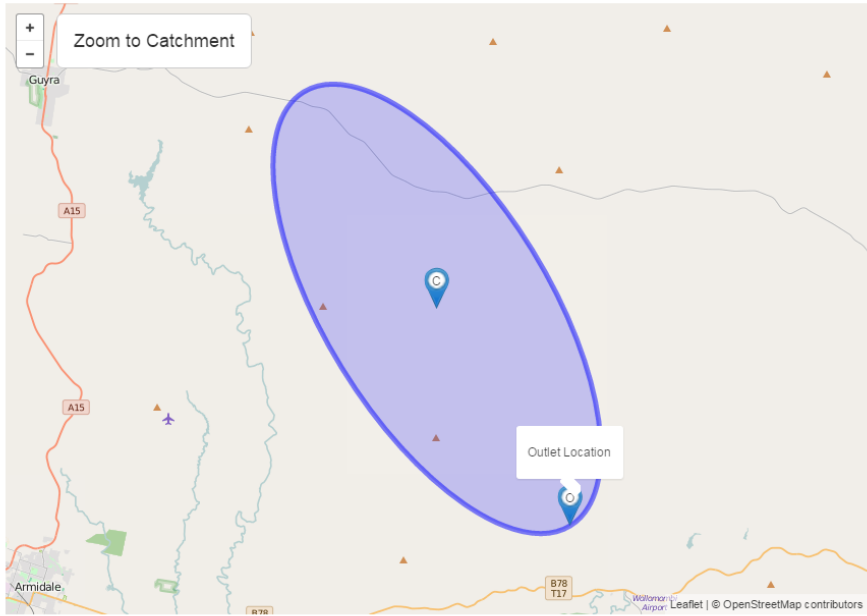
**Catchment Outlet Latitude**

**Catchment Outlet Longitude**

**Catchment Centroid Latitude**

**Catchment Centroid Longitude**

**Catchment Area (km<sup>2</sup>)**



Method by Dr Ataur Rahman and Dr Khaled Haddad from Western Sydney University for the Australian Rainfall and Runoff Project. Full description of the project can be found at the [project page](#) on the ARR website. Send any questions regarding the method or project [here](#).

Made possible by the Australian government.

Website by Peter Stensmyr at WMA Water.



Figure 3.3.5. RFFE Model 2015 Screen Shot for Data Input for the Wollomombi River at Coinside, NSW

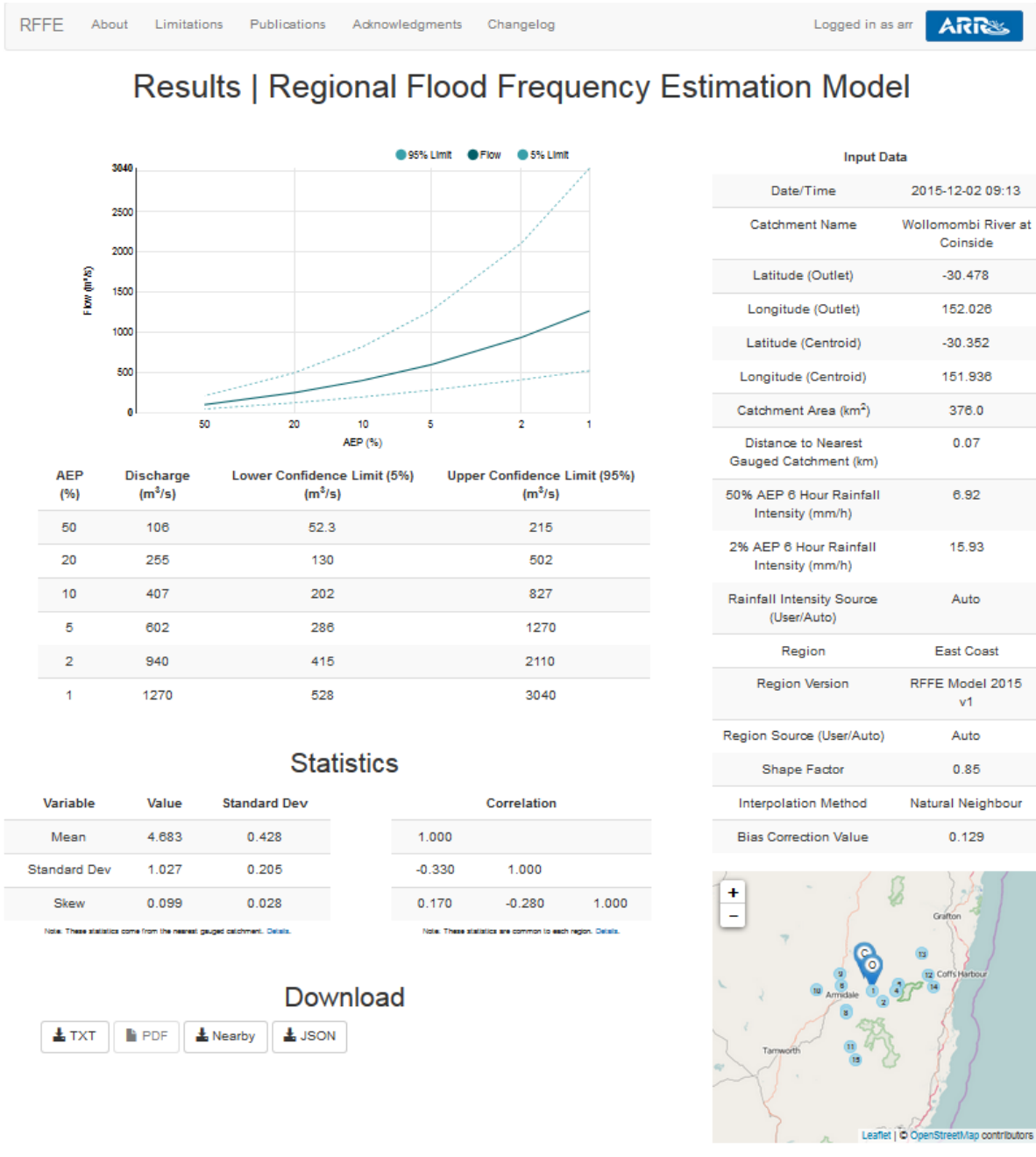


Figure 3.3.6. RFFE Model 2015 Screen Shot for Model Output for the Wollomombi River at Coinside, NSW (Region 1)

- i. A table of AEP (in the first column), estimated flood quantiles labelled as discharge (m<sup>3</sup>/s) in the second column, lower confidence limit (5%) (third column) and upper confidence limit (95%) (fourth column). The confidence limits represent the overall uncertainty with the estimated flood quantiles by the RFFE Model 2015.
- ii. A second table labelled "Statistics", which shows the statistics for the regional LP III model at the catchment of interest, which are particularly useful to combine at-site and

regional information to enhance the accuracy of flood quantile estimates (for details see [Book 3, Chapter 2](#)).

- iii. A graph that shows estimated flood quantiles and confidence limits against AEPs.
- iv. A graph that shows the catchment of interest with outlet and centroid locations and nearby gauged catchments that were included in the database to develop RFFE technique.
- v. A download menu that allows the user to save the results and additional outputs generated by the model.

Three worked examples are provided in [Book 3, Chapter 3, Section 15](#) to illustrate the use of RFFE Model 2015. The first two examples relate to catchments with no major regulation, no major natural or artificial storage and no major land use changes over time where the RFFE Model 2015 is directly applicable.

The third example relates to a catchment which has significant natural floodplain storage where RFFE Model 2015 is not directly applicable. For this case, the RFFE Model significantly overestimates the flood quantiles (as compared to at-site Flood Frequency Analysis). Here, the RFFE Model estimates need to be adjusted to account for the storage effect of the catchment by applying an appropriate technique (see [Book 3, Chapter 3, Section 13](#) for further details).

## **3.15. Worked Examples**

### **3.15.1. Application of RFFE Model 2015 to the Wollomombi River at Coinside, NSW (Region 1) (A Catchment Having No Major Regulation, No Major Natural or Artificial Storage and No Major Land Use Change)**

The basic input data for the Wollomombi River at Coinside, NSW are provided in [Table 3.3.8](#). The model screen shot for the data input is provided in [Figure 3.3.5](#). The flood quantiles generated by the RFFE Model 2015 are provided in [Figure 3.3.6](#). [Figure 3.3.7](#) compares the RFFE Model and at-site FFA estimates, which shows that the RFFE Model estimates match the at-site FFA estimates well except for rarer AEPs where the RFFE Model estimates are higher compared with the at-site FFA estimates. [Figure 3.3.7](#) also shows that the confidence band of the RFFE Model 2015 is much wider compared with at-site FFA confidence band, which is expected.

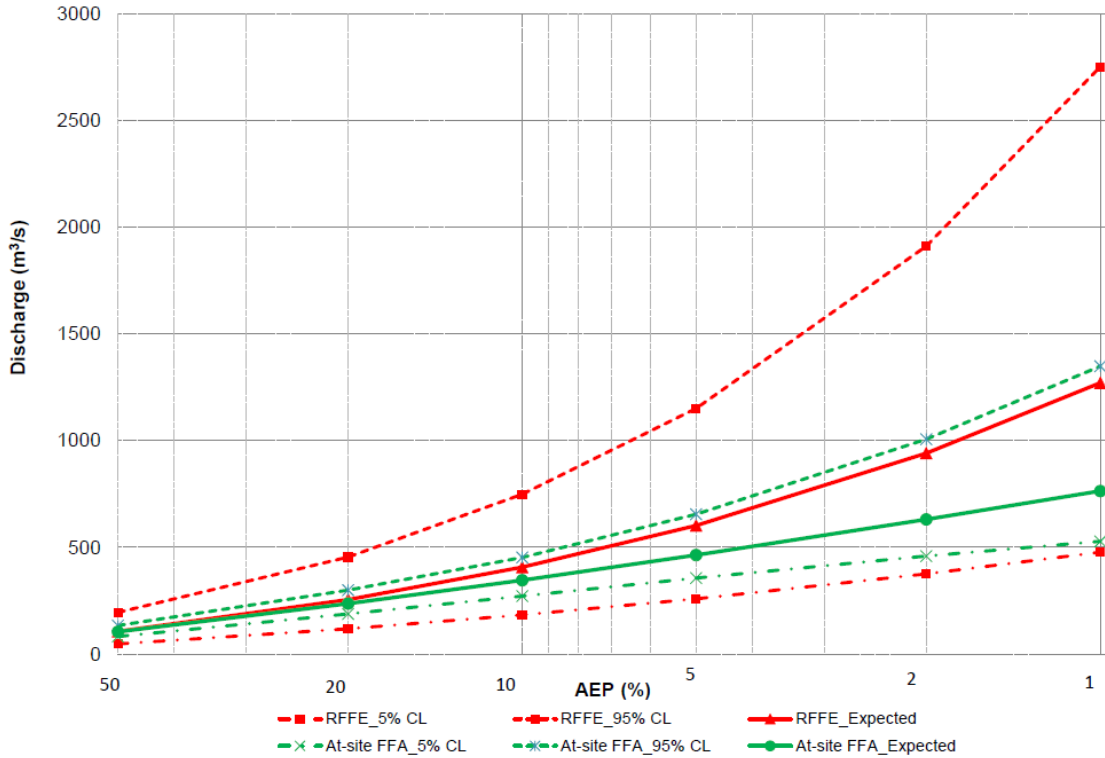


Figure 3.3.7. RFFE Model 2015 vs. At-site FFA Flood Estimates for the Wollomombi River at Coinside, NSW (Region 1)

Table 3.3.8. Application Data for the Wollomombi River at Coinside, NSW (Region 1) (Basic Input Data)

Menu	Input
Catchment Name	Wollomombi River at Coinside
Catchment Outlet Latitude in decimal degrees	-30.478
Catchment Outlet Longitude in decimal degrees	152.026
Catchment Centroid Latitude in decimal degrees	-30.352
Catchment Centroid Longitude in decimal degrees	151.936
Catchment Area in km <sup>2</sup>	376

Table 3.3.9 shows a list of 15 gauged catchments, which is generated as part of the RFFE Model output. In this example, these gauged catchments are located closest to the Wollomombi River at Coinside, NSW and were used in the development of the RFFE model. The user should compare the characteristics of the ungauged catchment of interest with those of the nearest gauged catchments (as in Table 3.3.9) to ensure that the ungauged catchment is not atypical.

Table 3.3.9. Fifteen Gauged Catchments (Used in the Development of RFFE Model 2015)  
Located Closest to Wollomombi River at Coinside, NSW

Site ID	Dist. (km)	Area km <sup>2</sup>	Lat. (outlet)	Long. (outlet)	Lat. (centroid)	Long. (centroid)	Record Length (years)	Mean Annual Rainfall (mm)	Shape Factor
206014	0.07	376	-30.478	152.0267	-30.352	151.936	57	871	0.8786
206001	18	163	-30.59	152.1617	-30.5244	152.279	33	1167	1.082
204030	24.29	200	-30.26	152.01	-30.1904	151.828	34	940	1.3946
206017	28.01	22	-30.478	152.3183	-30.4632	152.352	24	1167	0.8005
204008	31.64	31	-30.405	152.345	-30.4139	152.382	29	1249	0.6824
206026	35.67	8	-30.42	151.66	-30.4201	151.639	37	789	0.734
206025	37.68	594	-30.68	151.71	-30.6802	151.557	39	945	0.6194
206034	39.29	117	-30.7	151.7067	-30.7666	151.648	26	758	0.8859
418034	41.98	14	-30.3	151.64	-30.2758	151.65	29	818	0.7876
418014	63.83	855	-30.47	151.36	-30.5063	151.476	37	725	0.4171
206018	68.38	894	-31.051	151.7683	-30.9996	151.634	51	711	0.4846
204017	68.62	82	-30.306	152.7133	-30.3529	152.698	40	1995	0.6086
204037	72.28	62	-30.09	152.63	-30.1082	152.576	40	1586	0.7302
205002	72.50	433	-30.426	152.78	30.4537	152.566	29	1570	1.0277
206009	81.35	261	-31.19	151.83	-31.2597	151.757	57	910	0.6642

### 3.15.2. Application for the Four Mile Brook at Netic Rd, SW Western Australia (Region 5) (a Catchment Having No Major Regulation, No Major Natural or Artificial Storage and no Major Land Use Change)

The basic input data for the Four Mile Brook at Netic Rd, SW WA is provided in [Table 3.3.10](#). The model screen shot for the data input is provided in [Figure 3.3.8](#). The flood quantiles generated by the RFFE Model 2015 are provided in [Figure 3.3.9](#). [Figure 3.3.10](#) compares the RFFE Model and at-site FFA flood estimates which shows that RFFE Model estimates match the at-site FFA estimates quite well for all the six AEPs. [Figure 3.3.10](#) also shows that the confidence band by the RFFE Model 2015 is much wider compared with at-site FFA confidence band, which is as expected.



**Regional Flood Frequency Estimation Model (DRAFT)**  
 Draft Version of the Regional Flood Frequency Estimation Model for the 4th edition of Australian Rainfall and Runoff.

**ARR**  
 Australian Rainfall & Runoff

**Input Data**

Basic **Advanced**

Catchment Name: Four Mile Brook at Netic Rd

Catchment Outlet Latitude: -34.30

Catchment Outlet Longitude: 116.00

Catchment Centroid Latitude: -34.318

Catchment Centroid Longitude: 116.021

Catchment Area (km<sup>2</sup>): 13.1

Submit

Zoom to Catchment

Outlet Location

Solar forest block

Cassiana Valley Orchards

Shannybearup forest block

Leaflet | © OpenStreetMap contributors

Method by Dr Ataur Rahman and Dr Khaled Haddad from Western Sydney University for the Australian Rainfall and Runoff Project. Full description of the project can be found at the [project page](#) on the ARR website. Send any questions regarding the method or project here.

Made possible by the Australian government.

Website by Peter Stensmyr at WMA Water.

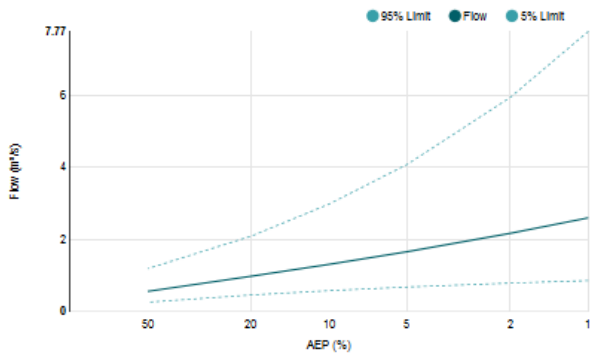


Figure 3.3.8. RFFE Model 2015 Screen Shot for Data Input for Four Mile Brook at Netic Rd, SW WA (Region 5)

Table 3.3.10. Application Data for Four Mile Brook at Netic Rd, SW Western Australia (Region 5) (Basic Input Data)

Menu	Input
Catchment Name	Four Mile Brook at Netic Rd
Catchment Outlet Latitude in decimal degrees	-34.30
Catchment Outlet Longitude in decimal degrees	116.00
Catchment Centroid Latitude in decimal degrees	-34.318
Catchment Centroid Longitude in decimal degrees	116.021
Catchment Area in (km <sup>2</sup> )	13.1

## Results | Regional Flood Frequency Estimation Model



AEP (%)	Discharge (m³/s)	Lower Confidence Limit (5%) (m³/s)	Upper Confidence Limit (95%) (m³/s)
50	0.580	0.280	1.19
20	0.980	0.460	2.09
10	1.31	0.580	2.98
5	1.66	0.680	4.08
2	2.17	0.790	5.94
1	2.80	0.880	7.77

Input Data	
Date/Time	2015-12-02 09:16
Catchment Name	Four Mile Brook at Netic Road
Latitude (Outlet)	-34.3
Longitude (Outlet)	116.0
Latitude (Centroid)	-34.318
Longitude (Centroid)	116.021
Catchment Area (km²)	13.1
Distance to Nearest Gauged Catchment (km)	0.0
50% AEP 6 Hour Rainfall Intensity (mm/h)	5.27
2% AEP 6 Hour Rainfall Intensity (mm/h)	10.3
Rainfall Intensity Source (User/Auto)	Auto
Region	SW WA
Region Version	RFFE Model 2015 v1
Region Source (User/Auto)	Auto
Shape Factor	0.77
Interpolation Method	Natural Neighbour
Bias Correction Value	-0.031

### Statistics

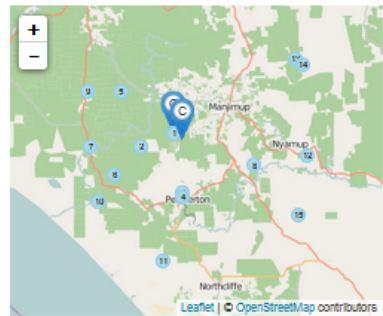
Variable	Value	Standard Dev	Correlation		
Mean	-0.587	0.461	1.000		
Standard Dev	0.670	0.277	-0.280	1.000	
Skew	-0.036	0.092	-0.050	-0.070	1.000

Note: These statistics come from the nearest gauged catchment. Details.

Note: These statistics are common to each region. Details.

### Download

-  TXT
-  PDF
-  Nearby
-  JSON



Method by Dr Ataur Rahman and Dr Khalid Haddad from Western Sydney University for the Australian Rainfall and Runoff Project. Full description of the project can be found at the [project page](#) on the ARR website. Send any questions regarding the method or project [here](#).  
Made possible by the Australian government.



Figure 3.3.9. RFFE Model 2015 Screen Shot for Model Output for Four Mile Brook at Netic Rd, SW WA (Region 5)

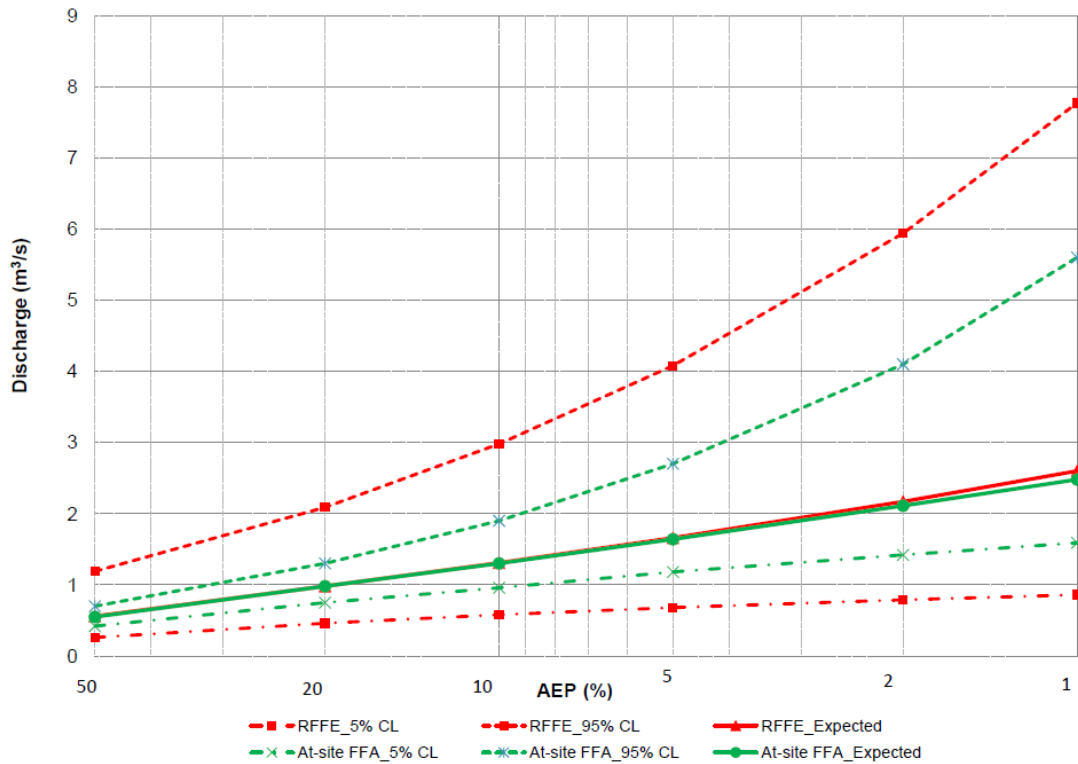


Figure 3.3.10. RFFE Model 2015 vs. At-site FFA Flood Estimates for Four Mile Brook at Netic Rd, SW WA (Region 5)


### 3.15.3. Application for the Morass Creek at Uplands, VIC (Region 1) (a Catchment Having Significant Natural Floodplain Storage Where RFFE Model 2015 Output is Not Directly Applicable)

This example (Morass Creek at Uplands, VIC) illustrates a catchment type where the RFFE Model is not applicable. The basic input data for this catchment is provided in [Table 3.3.11](#). The model screen shot for the data input is provided in [Figure 3.3.11](#). The flood quantiles generated by the RFFE Model 2015 are provided in [Figure 3.3.12](#). [Figure 3.3.13](#) compares the RFFE Model and at-site FFA flood estimates, which shows that RFFE Model estimates are much higher compared with at-site FFA estimates. This catchment has significant natural floodplain storage which is not typical for other catchments in the Region of Influence (ROI) on which the RFFE Model 2015 estimates are based. The RFFE Model 2015 estimates are thus not directly applicable. Here, the RFFE Model estimates would need to be adjusted downwards to account for the floodplain storage effect by applying an appropriate technique.

Table 3.3.11. Application Data for the Morass Creek at Uplands, VIC (Region 1) (Basic Input Data)


Menu	Input
Catchment Name	Morass Creek at Uplands
Catchment Outlet Latitude in decimal degrees	-36.87

Menu	Input
Catchment Outlet Longitude in decimal degrees	147.70
Catchment Centroid Latitude in decimal degrees	-36.88
Catchment Centroid Longitude in decimal degrees	147.84
Catchment Area in (km <sup>2</sup> )	471

RFFE About Limitations Publications Acknowledgments Changelog Logged in as arr 

### Regional Flood Frequency Estimation Model (DRAFT)

Draft Version of the Regional Flood Frequency Estimation Model for the 4th edition of Australian Rainfall and Runoff.



#### Input Data

Basic  Advanced

Catchment Name

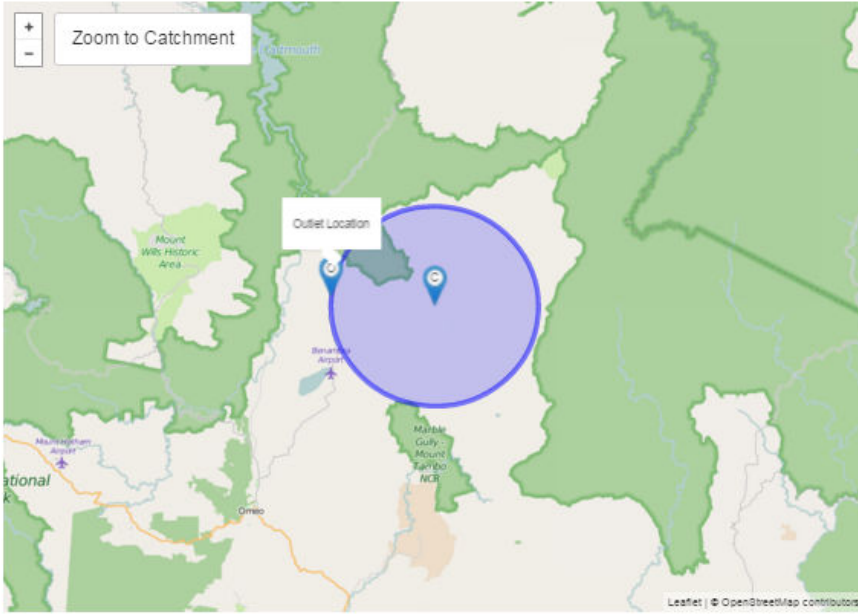
Catchment Outlet Latitude

Catchment Outlet Longitude

Catchment Centroid Latitude

Catchment Centroid Longitude

Catchment Area (km<sup>2</sup>)



Method by Dr Alour Mahman and Dr Khaled Mattedd from Western Sydney University for the Australian Rainfall and Runoff Project. Full description of the project can be found at the [project page](#) on the ARR website. Send any questions regarding the method or project here.

Made possible by the Australian government.

Website by Peter Stanbury at WWSA Water.



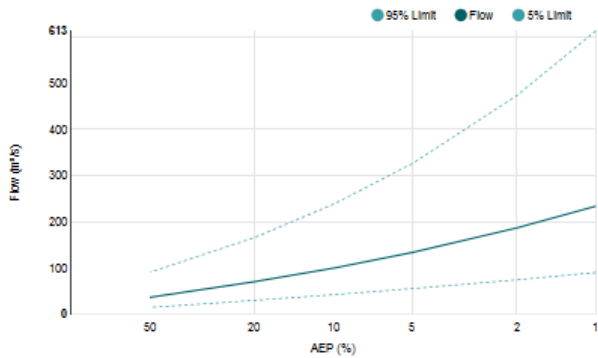



Figure 3.3.11. RFFE Model 2015 Screen Shot for Data Input for the Morass Creek at Uplands, VIC (Region 1)

## Results | Regional Flood Frequency Estimation Model



AEP (%)	Discharge (m³/s)	Lower Confidence Limit (5%) (m³/s)	Upper Confidence Limit (95%) (m³/s)
50	37.0	15.0	91.0
20	70.8	30.4	166
10	100	42.6	238
5	134	55.9	326
2	187	74.8	473
1	234	90.6	613

Input Data	
Date/Time	2015-12-02 09:19
Catchment Name	Morass Creek at Uplands
Latitude (Outlet)	-36.87
Longitude (Outlet)	147.7
Latitude (Centroid)	-36.88
Longitude (Centroid)	147.84
Catchment Area (km²)	471.0
Distance to Nearest Gauged Catchment (km)	13.37
50% AEP 6 Hour Rainfall Intensity (mm/h)	5.35
2% AEP 6 Hour Rainfall Intensity (mm/h)	10.96
Rainfall Intensity Source (User/Auto)	Auto
Region	East Coast
Region Version	RFFE Model 2015 v1
Region Source (User/Auto)	Auto
Shape Factor	0.58
Interpolation Method	Natural Neighbour
Bias Correction Value	-0.01



### Statistics

Variable	Value	Standard Dev	Correlation		
Mean	3.644	0.576	1.000		
Standard Dev	0.711	0.197	-0.330	1.000	
Skew	0.093	0.027	0.170	-0.280	1.000

Note: These statistics come from the nearest gauged catchment. [Details.](#)

Note: These statistics are common to each region. [Details.](#)

### Download

-  TXT
-  PDF
-  Nearby
-  JSON



Method by Dr Atsar Rahman and Dr Khaled Haddad from Western Sydney University for the Australian Rainfall and Runoff Project. Full description of the project can be found at the [project page](#) on the ARR website. Send any questions regarding the method or project [here](#).  
Made possible by the Australian government.



Figure 3.3.12. RFFE Model 2015 Screen Shot for Model Output for the Morass Creek at Uplands, VIC (Region 1)

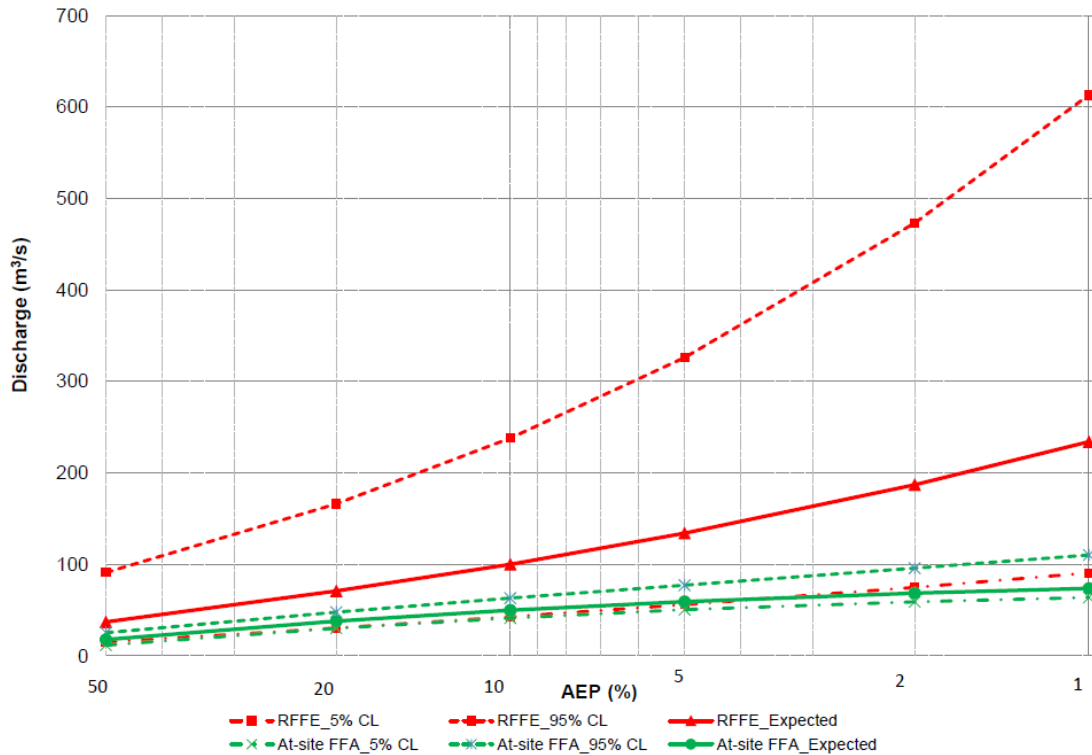


Figure 3.3.13. RFFE Model 2015 vs. At-site FFA Flood Estimates (for the Morass Creek at Uplands, VIC) (Region 1)

### 3.16. Further Information on the Development and Testing of RFFE Technique 2015

Table 3.3.12. Further Information on the Development and Testing of RFFE Technique 2015

Information	Source
Database consisting of 853 gauged catchments used to develop RFFE Technique 2015	<a href="#">Rahman et al. (2015a)</a>
Aspects of streamflow data preparation	<a href="#">Haddad et al. (2010)</a>
Comparison of Probabilistic Rational Method and quantile regression technique	<a href="#">Rahman et al. (2011b)</a>
Comparison of ordinary and generalised least squares regression techniques	<a href="#">Haddad et al. (2011)</a>
Comparison of fixed region and region-of-influence approaches for quantile and parameter regression techniques	<a href="#">Haddad and Rahman (2012)</a>
Regionalisation of the parameters of the LP3 distribution	<a href="#">(Haddad et al., 2012; Micevski et al., 2015)</a>
Development and testing of the RFFE technique	<a href="#">(Rahman et al., 2009; Rahman et al., 2012; Rahman et al, 2015)</a>

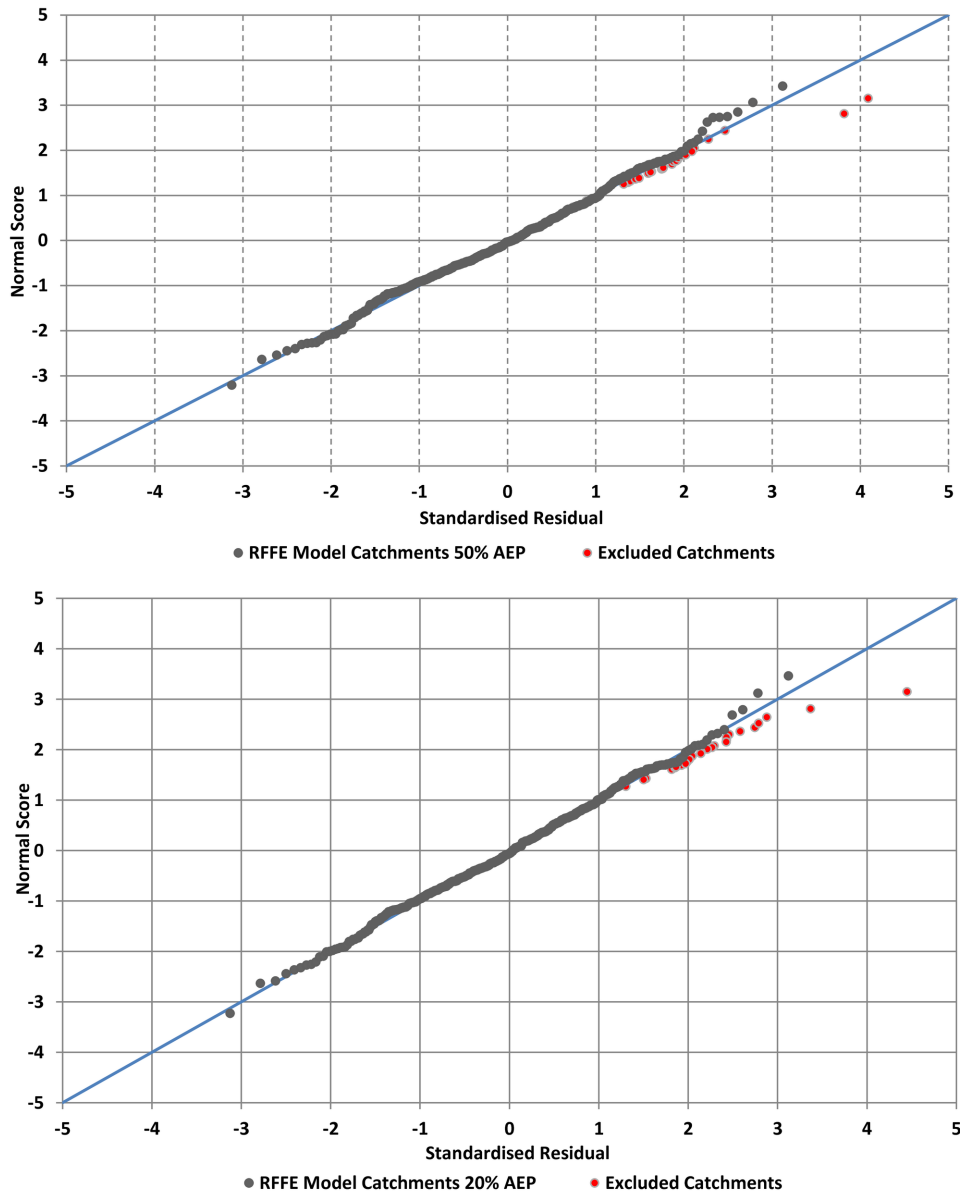


Figure 3.3.14. Standardised Residuals vs. Normal Scores for Region 1 Based on Leave-one-out Validation for AEPs of 50%, 20%, 2% and 1%

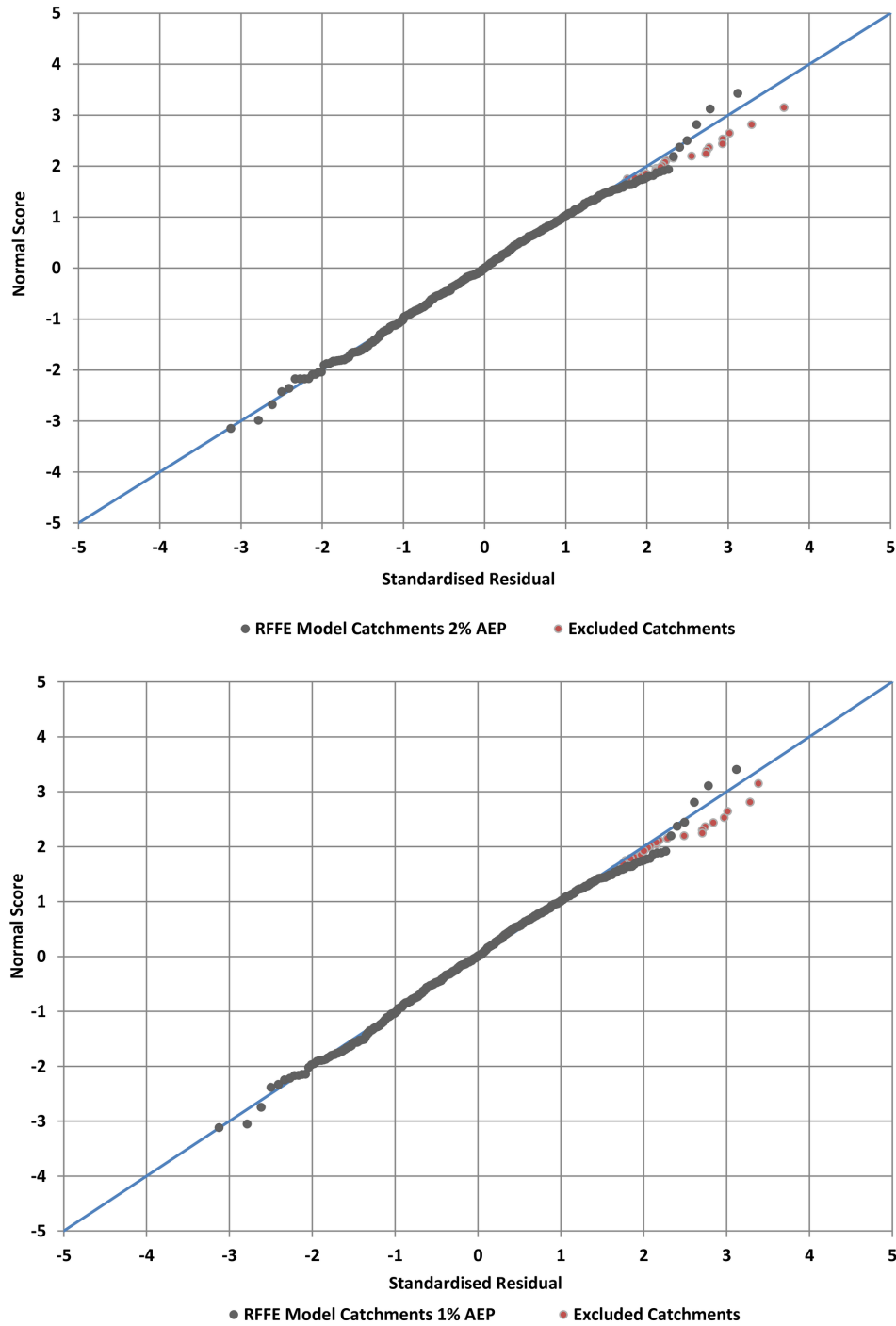


Figure 3.3.15. Standardised Residuals vs. Normal Scores for Region 1 Based on Leave-one-out Validation for AEPs of 2% and 1%

### 3.17. References

Adams, C.A. (1984), 'Regional flood estimation for ungauged rural catchments in Victoria', MEngSc Thesis, The University of Melbourne.

Ball, J.E. (2014), 'Flood estimation under climate change', 19th IAHR-APD Congress, Hanoi, Vietnam.



- Bates, B.C. (1994), 'Regionalisation of hydrological data: A review', Report 94/5, CRC for Catchment Hydrology, Monash University.
- Bates, B.C., Rahman, A., Mein, R.G. and Weinmann, P.E. (1998), Climatic and physical factors that influence the homogeneity of regional floods in south-eastern Australia, *Water Resources Research*, 34(12), 3369-3382.
- Burn, D.H. (1990a), An appraisal of the region of influence approach to Flood Frequency Analysis, *Hydrological Sciences Journal*, 35(2), 149-165.
- Burn, D.H. (1990b), Evaluation of regional Flood Frequency Analysis with a region of influence approach, *Water Resources Research*, 26(10), 2257-2265.
- Cohn, T.A., England, J.F., Berenbrock, C.E., Mason, R.R., Stedinger, J.R. and Lamontagne, J.R. (2013), A generalized Grubbs-Beck test statistic for detecting multiple potentially influential low outliers in flood series, *Water Resour. Res.*, 49(8), 5047-5058.
- Farquharson, F.A.K., Meigh, J.R. and Sutcliffe, J.V. (1992), Regional Flood Frequency Analysis in arid and semi-arid areas, *Journal of Hydrology*, 138: 487-501.
- French, R. (2002), 'Flaws in the rational method', Proc. 27th National Hydrology and Water Resources Symp., Melbourne.
- Griffis, V.W. and Stedinger, J.R. (2007), The use of GLS regression in regional hydrologic analyses, *Journal of Hydrology*, 344: 82-95.
- Hackelbusch, A., Micevski, T., Kuczera, G., Rahman, A. and Haddad, K. (2009), 'Regional Flood Frequency Analysis for eastern New South Wales: a region of influence approach using generalised least squares based parameter regression', Proc. 31st Hydrology and Water Resources Symp., Newcastle, pp: 603-615.
- Haddad, K. (2008), 'Design flood estimation in ungauged catchments using a quantile regression technique: ordinary and generalised least squares methods compared for Victoria', Masters (Honours) thesis, School of Engineering, University of Western Sydney, New South Wales.
- Haddad, K. and Rahman, A. (2012), Regional Flood Frequency Analysis in eastern Australia: Bayesian GLS regression-based methods within fixed region and ROI framework - quantile regression vs. parameter regression technique, *Journal of Hydrology*, pp: 430-431, 142-161.
- Haddad, K., Rahman, A. and Weinmann, P.E. (2008), 'Development of a generalised least squares based quantile regression technique for design flood estimation in Victoria', Proc. 31st Hydrology and Water Resources Symp., Adelaide, pp: 2546-2557.
- Haddad, K., Pirozzi, J., McPherson, G., Rahman, A. and Kuczera, G. (2009), 'Regional flood estimation technique for NSW: application of generalised least squares quantile regression technique', Proc. 32nd Hydrology and Water Resources Symp., Newcastle, pp: 829-840.
- Haddad, K., Rahman, A. and Kuczera, G. (2011), Comparison of ordinary and generalised least squares regression models in regional Flood Frequency Analysis: A case study for New South Wales, *Australian Journal of Water Resources*, 15(2), 59-70.
- Haddad, K., Rahman, A. and Stedinger, J.R. (2012), Regional Flood Frequency Analysis using Bayesian generalised least squares: A comparison between quantile and parameter regression techniques, *Hydrological Processes*, 26: 1008-1021.

Haddad, K., Rahman, A., Weinmann, P.E., Kuczera, G. and Ball, J.E. (2010), Streamflow data preparation for regional Flood Frequency Analysis: Lessons from south-east Australia, *Australian Journal of Water Resources*, 14(1), 17-32.

Hosking, J.R.M. and Wallis, J.R. (1993), Some statistics useful in regional frequency analysis, *Water Resources Research*, 29(2), 71-281.

Ishak, E., Rahman, A., Westra, S., Sharma, A. and Kuczera, G. (2013), Evaluating the non-stationarity of Australian annual maximum floods, *Journal of Hydrology*, 494: 134-145.

Kuczera, G. (1999), Comprehensive at-site Flood Frequency Analysis using Monte Carlo Bayesian inference. *Water Resources Research*, 35(5), 1551-1557.

Lamontagne, J.R., Stedinger, J.R., Cohn, T.A. and Barth, N.A. (2013), 'Robust national flood frequency guidelines: What is an outlier?', *Proc. World Environmental and Water Resources Congress, ASCE*, pp: 2454-2466.

Micevski, T. and Kuczera, G. (2009), Combining site and regional flood information using a Bayesian Monte Carlo approach, *Water Resources Research*, 45, W04405, doi: 10.1029/2008WR007173.

Micevski, T., Hackelbusch, A., Haddad, K., Kuczera, G. and Rahman, A. (2015), Regionalisation of the parameters of the log-Pearson 3 distribution: a case study for New South Wales, Australia, *Hydrological Processes*, 29(2), 250-260.

Mittelstadt, G.E., McDermott, G.E. and Pilgrim, D.H. (1987), Revised flood data and catchment characteristics for small to medium sized catchments in New South Wales. University of New South Wales, Department of Water Engineering, unpublished report.

Palmen, L.B. and Weeks, W.D. (2009), 'Regional flood frequency for Queensland using the Quantile Regression Technique', *Proc. 32nd Hydrology and Water Resources Symp.*, Newcastle.

Palmen, L.B. and Weeks, W.D. (2011), Regional flood frequency for Queensland using the quantile regression technique, *Australian Journal of Water Resources*, 15(1), 47-57.

Pilgrim, DH (ed) (1987) *Australian Rainfall and Runoff - A Guide to Flood Estimation*, Institution of Engineers, Australia, Barton, ACT, 1987.

Pilgrim, D.H. and McDermott, G. (1982), Design floods for small rural catchments in eastern New South Wales, *Civil Engineering Transactions*, I. E. Aust., CE24: 226-234.

Pirozzi, J., Ashraf, M., Rahman, A., and Haddad, K. (2009), 'Design flood estimation for ungauged catchments in eastern NSW: evaluation of the Probabilistic Rational Method', *Proc. 32nd Hydrology and Water Resources Symp.*, Newcastle, pp: 805-816.

Rahman, A. (1997), 'Flood estimation for ungauged catchments: a regional approach using flood and catchment characteristics', PhD thesis, Department of Civil Engineering, Monash University.

Rahman, A. (2005), A Quantile Regression Technique to Estimate Design Floods for Ungauged Catchments in South-East Australia, *Australian Journal of Water Resources*, 9(1), 81-89.

Rahman, A., Haddad, K., Rahman, A.S., Haque, M.M., Kuczera, G. and Weinmann, P.E. (2015) Australian Rainfall and Runoff Revision Project 5: Regional Flood Methods: Stage 3, ARR Report Number P5/S3/025, ISBN 978-0-85825-869-3.

Rahman, A., Rima, K. and Weeks, W.D. (2008), 'Development of Regional Flood Frequency Estimation methods using Quantile Regression Technique: a case study for north-eastern part of Queensland', Proc. 31st Hydrology and Water Resources Symp., Adelaide, pp: 329-340.

Rahman, A., Haddad, K., Kuczera, G. and Weinmann, P.E. (2009), 'Australian Rainfall and Runoff Revision Projects, Project 5 Regional Flood Methods, Stage 1 Report', No.P5/S1/003, Nov 2009, Engineers Australia, Water Engineering, pp: 181.

Rahman, A., Haddad, K., Zaman, M., Ishak, E., Kuczera, G. and Weinmann, P.E. (2012), 'Australian Rainfall and Runoff Revision Projects, Project 5 Regional flood methods, Stage 2 Report', No.P5/S2/015, Engineers Australia, Water Engineering, pp: 319.

Rahman, A., Bates, B.C., Mein, R.G. and Weinmann, P.E. (1999), Regional Flood Frequency Analysis for ungauged basins in south - eastern Australia, Australian Journal of Water Resources, 3(2), 199-207.

Rahman, A., Haddad, K., Zaman, M., Kuczera, G. and Weinmann, P.E. (2011a), Design flood estimation in ungauged catchments: a comparison between the Probabilistic Rational Method and Quantile Regression Technique for NSW, Australian Journal of Water Resources, 14(2), 127-139.

Rahman, A., Haddad, K., Rahman, A.S. and Haque, M.M. (2015a), 'Australian Rainfall and Runoff Revision Projects, Project 5 Regional flood methods, Database used to develop ARR RFFE Model 2015', Engineers Australia, Water Engineering.

Rahman, A., Zaman, M., Fotos, M., Haddad, K., Rajaratnam, L. and Weeks, W.D. (2011b), 'Towards a new Regional Flood Frequency Estimation method for the Northern Territory', Proc. 34th IAHR World Congress, Brisbane, pp: 364-371.

Rahman, A., Haddad, K., Haque, M.M., Kuczera, G., Weinmann, P.E., Stensmyr, P., Babister, M., Weeks, W.D. (2015b), 'The New Regional Flood Frequency Estimation Model for Australia: RFFE Model 2015', 36th Hydrology and Water Resources Symp., 7-10 Dec, 2015, Hobart.

Rahman, A., Haque, M., Haddad, K., Rahman, A.S., Caballero, W.L. (2015c), 'Database Underpinning the RFFE 2015 Model in the new Australian Rainfall and Runoff', 36th Hydrology and Water Resources Symposium, 7-10 Dec, 2015, Hobart.

Sivapalan, M., Blöschl, G. and Wagener, T. (2013), 'Runoff Prediction in Ungauged Basins: Synthesis across Processes, Places and Scales', Cambridge University Press.

Stedinger, J.R. and Tasker, G.D. (1985), Regional hydrologic analysis 1 Ordinary, weighted, and generalised least squares compared, Water Resources Research, 21(9), 1421-1432.

Tasker, G.D. and Stedinger, J.R. (1989), An operational GLS model for hydrologic regression, Journal of Hydrology, 111(1-4), 361-375.

Zrinji, Z. and Burn, D.H. (1994), Flood frequency analysis for ungauged sites using a region of influence approach. Journal of Hydrology, 153: 1-21.



11 national Circuit  
BARTON ACT 2600

[www.arr.org.au](http://www.arr.org.au)

